Modifications de la paroi au cours de la maturation et de la germination des conidies de Scedosporium boydii

Sarah Ghamrawi

Thèse de Doctorat

Sarah GHAMRAWI

Mémoire présenté en vue de l'obtention du
grade de Docteur de l'Université d'Angers
sous le label de L'Université Nantes Angers Le Mans

École doctorale : Biologie - Santé

Discipline : Biologie Cellulaire (CNU : Groupe X – section 65)
Spécialité : Microbiologie moléculaire
Unité de recherche : Groupe d'Etude des Interactions Hôte-Pathogène (GEIHP), UPRES EA 3142

Soutenue le 17 Novembre 2014
Thèse N° : 1422

Modifications de la paroi au cours de la maturation et de la germination des conidies de *Scedosporium boydii*

A multifaceted study of the cell wall changes during maturation and germination of the conidia in *Scedosporium boydii*

JURY

Rapporteurs :	**Jean-Paul LATGE,** Professeur, Institut Pasteur de Paris, France **Jean-Pierre GANGNEUX**, Professeur des Universités – Praticien Hospitalier, Université de Rennes I, France
Examinateurs :	**Nicolas PAPON,** Maître de Conférences, Université de Tours, France **Stéphane CUENOT**, Maître de Conférences, Université de Nantes, France
Directeur de Thèse :	**Jean-Philippe BOUCHARA**, Professeur des Universités – Praticien Hospitalier, Université d'Angers, France

2013-2014

Microbiologie
Microbiologie moléculaire

Modifications de la paroi au cours de la maturation et de la germination des conidies de *Scedosporium boydii*

Sarah GHAMRAWI

Sous la direction de M.
Jean-Philippe BOUCHARA

Membres du jury
Jean-Paule LATGE | Professeur
Jean-Pierre GANGNEUX | Professeur
Nicolas PAPON | Maître de Conférences
Stéphane CUENOT | Maître de Conférences
Jean-Philippe BOUCHARA | Professeur

Soutenu publiquement le :
17 Novembre 2014

université angers

ACKNOWLEDGEMENTS

This Ph.D has been a remarkable experience that could not have been completed without the invaluable support and contribution of many people. Foremost, I would like to express my deepest gratitude to my supervisor Professor Jean-Philippe Bouchara, whose leadership, large scientific background, attention to detail and ability to keep a broader view throughout my research has given a whole new dimension to my learning experience. I would also like to thank you for your support and genuine caring and concern that facilitated communication and created a pleasant working environment.

To all members of my thesis committee I would like to express my sincere appreciation for doing me the honor of judging this work. I would also like to thank you for your intellectual contributions to my development as a scientist. The outstanding research of Professor Jean-Paul Latgé on *Aspergillus* and particularly on fungal cell walls was of great importance to this work. The opportunity given by Professor Jean-Pierre Gangneux, President of the French Society for Medical Mycology (SFMM), to Ph.D students during SFMM meetings is greatly appreciated as it improves their research and visibility. I am grateful to Dr. Stéphane Cuenot for the valuable discussions about force and chemical microscopy and for the financial support through Région Pays de la Loire within the Myco-AFM research program. I am also indebted to Dr Nicolas Papon for patiently teaching me some of his techniques in molecular biology in Tours, thank you.

To Dr. Thomas Guillemette, I would like to say that it was a pleasure collaborating with you; thank you for your advice and support. My gratitude is also extended to Dr. Agatha Zykwinska for her efforts and for having constantly answered my questions concerning force and chemical microscopy.

I must also acknowledge members of the "Service Commun d'Imageries et Analyses Microscopiques" (SCIAM) group for teaching me their methods in electron microscopy experiments and for their assistance throughout my Ph.D.

A very special thanks goes out to members of the Host-Pathogen Interaction Study Group (GEIHP) and particularly to Marc, Amandine Gastebois, Gilles, Patrick and Agnes for their advice and their willingness to share their bright thoughts with me, which were very fruitful for shaping up my ideas and research. I also thank Gaelle who was always ready to lend a helping hand especially during the last phase of my thesis. Many thanks go to other members of the GEIHP and in particular to Tram, Rayane, Gaelle, Charlotte, Abdel, Sara, Amandine Rougeron, Julia, Maxime and Sandrine for giving me such a pleasant time during and outside work. I never forget the nice time we spent together in Berlin that allowed me to get to know some of you better.

My most heartfelt thanks go to my parents and parents-in-law for instilling in me confidence and the drive for pursuing my PhD and for constantly reminding me of how proud they were of me. I convey special acknowledgement to my brother Dr. Wissam who shares my enthusiasm to science and who always inspired me.

Words fail me to express my appreciation to my husband Imad whose love and encouragement were central to the completion of this work. There are no words that can express my gratitude for the patience you had with my weekly absence over years and for the numerous surprises you prepared on many occasions to cheer me up.

Finally, I hope that this thesis would be a good contribution to our understanding of the cell wall dynamics in *Scedosporium boydii* and that it would support more research on this fungus.

TABLE OF CONTENTS

LIST OF ABBREVIATIONS

AHB	Alanyl-hydroxy-benzothiazine
ADHDB	Alanyl 5,6 dihydro-di-benzothiazine
AFM	Atomic force microscopy
ANA	Accession number Not Available yet
BAA	Benzoquinone acetic acid
CDC	Center for Disease Control and Prevention
CDS	Coding sequences
CF	Cystic fibrosis
CFEM	Common in fungal extracellular and membrane
CFS	Chemical force spectroscopy
CMH	Ceramide monohexoside
CNS	Central nervous system
ConA	Concanavalin A
CSH	Cell surface hydrophobicity
CWP	Cell wall protein
DCT	DOPAchrome tautomerase
DCE	DOPAchrome conversion enzyme
DHI	5,6-dihydroxyindole
DHICA	DHI-2-carboxylic acid
DHN	1,8-dihydroxynaphtalene
DOPA	3,4-dihydroxyphenylalanine
DOPA-Q	DOPA-quinone
EC	Enzyme commission number
ECMM	European Confederation of Medical Mycology
EPR	Electron paramagnetic resonance
ER	Endoplasmic reticulum
ESI	Electrospray ionization
FITC	Fluorescein isothiocyanate
FSC	Forward scatter
GC	Gas chromatography
GlcNac	N-acetyl glucosamine
GRAVY	Grand Average of Hydropathy
HGA	Homogentisic acid
4HNR	Tetrahydroxynaphtalene reductase

HPLC	High performance liquid chromatography
HPP	4-hydroxyphenyl pyruvate
HPQ	1,4,6,7,9,12-hexahydroxyperylene-3,10-quinone
HPTLC	High performance thin layer chromatography
IL	Interleukin
ISHAM	International Society for Human and Animal Mycology
LC	Liquid chromatography
MAb	Monoclonal antibody
MALDI-TOF	Matrix Assisted Laser Desorption/Ionization-Time of Flight
MDM	Monocyte derived macrophage
MNC	Mononuclear leukocyte
MS	Mass spectrometry
Man*p*	Mannopyranose
NMR	Nuclear magnetic resonance
ORF	Open reading frame
PAMP	Pathogen associated molecular pattern
Pir	protein with internal repeats
PKS	Polyketide synthase
PKS-1	Polyketide synthase type 1
PMN	Polymorphonuclear leukocyte
PMP	Plasma membrane protein
PNA	Peanut agglutinin
PPO	Polyphenol oxidase
PRM	Peptidorhamnomannannes
Rha*p*	Rhamnopyranose residues
ROS	Reactive oxygen species
SCD	Scytalone dehydratase
SDS	Sodium dodecyl sulfate
SEM	Scanning electron microscopy
SSC	Side scatter
TEM	Transmission electron microscopy
THN	1,3,6,8-tetrahydroxynaphtalene
THR	Tetrahydroxynaphtalene reductase
TLR	Toll-like receptor
Trp	Tyrosinase-related proteins
TYR	Tyrosinase
TYRP	Tyrosinase-related protein

TYDC	Tyrosine decarboxylase
WGA	Weat Germ Agglutinin
WHO	World Health Organization
YPD	Yeast extract - peptone – dextrose

LIST OF FIGURES

LIST OF TABLES

RESUME DE LA THESE

Introduction générale

En 1991, la diversité fongique sur la terre était estimée à 1,5 M espèces, mais dix ans plus tard était rapporté un nombre d'espèces fongiques trois fois plus important, Disease Control and Prevention" (CDC), seulement 300 d'entre elles sont pathogènes pour l'homme **[4**, **5]**. Même si quelques espèces seulement sont responsables de la plupart des cas de mycoses, le nombre de champignons pathogènes émergents à l'origine des infections invasives augmente régulièrement. Par exemple, les espèces du genre *Scedosporium* (mentionnés précédemment sous une autre nomenclature) qui ont été découvertes en 1889 en tant qu'agents d'otite humaine, n'ont été reconnues comme pathogènes humains qu'à la fin des années 1980, période où la fréquence des maladies attribuées à ces champignons a commencé à augmenter et où ces pathologies ont commencé à se diversifier **[6]**.

Les infections superficielles de la peau et des ongles causées par des champignons sont estimées affecter 20 à 25% de la population mondiale **[7]**. Par ailleurs, on estime entre autres à 10 millions le nombre de cas annuels de candidose orale chez les patients atteints du VIH et à 2 millions le nombre de cas annuels d'infections de l'œsophage **[8]**. Même si les infections fongiques invasives sont beaucoup moins fréquentes que les infections superficielles, le nombre de décès causés par les infections invasives est au moins égal, sinon supérieur, au nombre de décès causés par *Plasmodium falciparum* ou par *Mycobacterium tuberculosis* selon Brown *et al*. **[8]**. En dépit de leur importance en terme de morbidité et de mortalité, les infections fongiques ne sont pas reconnues, et il n'existe aujourd'hui encore pas de plan établi par des organismes comme l'Organisation mondiale de la Santé pour lutter contre ces infections **[8**, **9]**.

Au cours des dernières décennies, l'incidence des infections fongiques a augmenté considérablement, notamment en raison de l'incidence croissante de nombreux cancers et hémopathies malignes, du développement des soins intensifs et des techniques de réanimation médicale et chirurgicale impliquant le recours à des procédures de plus en plus agressives, du nombre croissant de patients immunodéprimés avec l'émergence de l'épidémie de SIDA et le développement des greffes de moelle osseuse et transplantation d'organes solides, de l'amélioration de la prise en charge de certaines pathologies chroniques comme la mucoviscidose, de l'émergence de phénomènes de résistance des agents de mycoses aux antifongiques ainsi que des changements climatiques **[5**, **10**, **11**, **12**, **13]**. Cette multitude de facteurs augmentant le nombre et la gravité des infections fongiques montre la complexité de la situation. Une meilleure compréhension des mécanismes

pathogéniques des champignons est donc nécessaire pour identifier de nouvelles cibles thérapeutiques.

Le complexe *Scedosporium apiospermum* comprend les agents étiologiques les plus courants de mycétome cutanés et sous-cutanés. Mais ces champignons provoquent aussi des infections disséminées chez des patients infectés par le VIH à un stade avancé, des patients atteints d'hémopathies malignes ou ayant subit une transplantation, mais aussi des atteintes des voies respiratoires supérieures et des infections pulmonaires. Ainsi, le complexe *S. apiospermum* se situe au deuxième rang parmi les champignons les plus fréquemment isolés dans les voies respiratoires des patients atteints de mucoviscidose. Ces espèces sont réfractaires au traitement et à l'heure actuelle elles sont considérées comme un défi diagnostique et thérapeutique **[14]**.

Aujourd'hui, nos connaissances sur les mécanismes pathogéniques de ces champignons sont encore très limitées. Au cours de ce travail, nous avons donc étudié la paroi cellulaire de *Scedosporium boydii*, l'une des deux espèces majeures de ce complexe, puisque le paroi joue un rôle essentiel pour la survie du champignon dans le milieu extérieur et sa pathogénicité, conditionnant en effet l'adhérence du champignon aux tissus de l'hôte et son échappement vis-à-vis des mécanismes de défense de l'hôte. Les modifications qui se produisent dans la paroi cellulaire ont été étudiées au cours de la maturation et la germination des conidies en utilisant diverses approches pour tenter d'identifier les facteurs potentiels de virulence (mélanine, hydrophobines, protéines à ancre GPI pour glycosylphosphatidylinositol). Le premier génome séquencé pour l'un des membres de ce complexe d'espèces (*Scedosporium apiospermum*) est également décrit. Un certain nombre de voies métaboliques ont été identifiées dans le génome concernant le potentiel biotechnologique de ces champignons dans la bioremédiation, ce qui corrobore un grand nombre d'études expérimentales dans ce domaine. De plus, la connaissance du génome de ces champignons facilitera la recherche fondamentale sur les mécanismes pathogéniques des champignons du genre *Scedosporium*.

Etude I

Scedosporium boydii et *S. apiospermum sensu stricto* sont les deux espèces majeures du complexe *S. apiospermum* en pathologie humaine. Ce sont notamment les deux espèces les plus fréquemment isolées des sécrétions respiratoires chez les patients atteints de mucoviscidose **[15]**. Les mécanismes d'adhérence des conidies de ces champignons au niveau des voies respiratoires sont encore inconnus. Bien que non démontré expérimentalement, il est hautement probable que l'infection respiratoire débute par l'inhalation de conidies aéroportées, suivie de l'adhérence des conidies aux cellules

épithéliales ou aux composants du mucus bronchique, et de leur différenciation en hyphes. Toutes ces étapes sont régies par la paroi sporale qui constitue la première structure fongique au contact des tissus de l'hôte, ou de composants de l'hôte.

L'adhérence est régie par deux types de mécanismes, des interactions spécifiques de type récepteur-ligand et des interactions non spécifiques, électrostatiques ou hydrophobes **[16]**. En fonction du champignon, les interactions spécifiques peuvent impliquer des polysaccharides (mannanes **[17]**, glucanes ou galactosaminogalactannes **[18]**), des glycoprotéines liées à la paroi cellulaire par le biais de liaisons covalentes ou non (par exemple des hydrophobines **[19**, **20]** ou des protéines à ancre GPI comme les adhésines Pwp7p et Aed1p de *Candida glabrata* **[21]** et la CSPA d'*Aspergillus fumigatus* **[22]**). Les interactions non spécifiques sont déterminées par les propriétés physiques de la surface cellulaire telles que l'hydrophobicité et la charge électrostatique qui reflètent la composition biochimique de la paroi **[23]**. L'importance de ces interactions non spécifiques a été prouvée dans plusieurs modèles fongiques y compris des levures **[24**, **25]** et des champignons filamenteux. La délétion du gène *medA* chez *A. fumigatus*, par exemple, entraîne une modification des propriétés physiques de la surface ainsi qu'une réduction de l'adhérence aux cellules épithéliales et de la virulence **[26]**.

Échapper à la reconnaissance par le système immunitaire et à la lyse qui en résulte est un autre défi pour les agents pathogènes. Chez *A. fumigatus*, l'hydrophobine rodA contribue à la viabilité du champignon *in vivo* en masquant certaines molécules immunogènes de paroi (PAMPs), empêchant ainsi la reconnaissance par Dectine-1 et Dectine-2 **[27]**. Des études sur d'autres agents pathogènes fongiques, *Pneumocystis jirovecii* et *Cryptococcus neoformans,* ont montré leur capacité à échapper à l'immunosurveillance respectivement par modification de l'expression des glycoprotéines majeures de surface **[28]** ou par l'intermédiaire d'une capsule qui recouvre les composants antigéniques des propagules infectieuses et module la réponse immunitaire **[29]**. La mélanine est un autre facteur de virulence utilisé par de nombreux champignons afin de résister à la phagocytose et à l'action des espèces radicalaires dérivées de l'azote ou de l'oxygène. La mélanine fongique est connue pour limiter l'activation du complément, et pour conférer une résistance aux agents antimicrobiens **[30]**. En outre, la modification ou l'inhibition de l'expression de la mélanine ou de l'hydrophobine rodA a des répercussions sur les propriétés physiques de la surface cellulaire.

Chez *S. boydii*, seul un nombre limité de constituants de la paroi ont été caractérisés à ce jour, notamment des peptidorhamnomannannes (PRM) et des alpha-glucanes **[31]**. Il a notamment été démontré que les PRM jouent un rôle dans l'adhérence de conidies aux cellules épithéliales HEp2 *in vitro* **[32]**, ainsi que dans l'activation des récepteurs de type

Toll (TLR) 4 qui sont à l'origine de la sécrétion de cytokines par les macrophages **[33]**. D'autre part, les alpha-glucanes pourraient susciter la phagocytose et induire la sécrétion de cytokines inflammatoires dans un mécanisme impliquant CD14, TLR 2 et MyD88 **[34]**. Des activités phosphatase acide et phosphatase alcaline ont également été détectées dans la paroi de *S. boydii* **[35]**. De même, il a été mis en évidence la présence de céramides monohexosides qui seraient essentiels dans la différenciation hyphale **[36]**.

Dans cette première étude, nous avons donc examiné les changements temporels dans les propriétés physiques de la paroi des conidies de *S. boydii* au cours de leur maturation, et recherché la présence d'hydrophobines et de mélanine en tant que facteurs potentiels de virulence.

Cette étude a été initiée devant l'hétérogénéité du marquage d'une spore à l'autre après incubation des conidies d'une même culture avec de la concanavaline A (Con A), une lectine spécifique du mannose et du glucose couplée à l'isothiocyanate de fluorescéine (FITC). Chez *A. fumigatus*, la germination des conidies est précédée d'une étape de "swelling" qui se traduit par une augmentation importante de la taille des spores, un amincissement de la paroi avec disparition de la couche pariétale externe, et une vacuolisation du cytoplasme. L'étude morphologique et ulturastructurale des conidies au cours de la germination montre que ce phénomène n'existe pas chez *S. boydii*. La paroi des spores dormantes est tout à fait comparable à celle des cellules mères de tubes germinatifs, et aucune vacuolisation n'a été observée dans le cytoplasme; en outre, les conidies intensément marquées par la Con A-FITC étaient d'une taille comparable à celle des conidies non marquées. Une autre hypothèse a donc été explorée pour expliquer l'hétérogénéité du marquage après incubation avec la Con A : l'existence d'un processus de maturation des conidies. Pour tester cette hypothèse, nous avons étudié les variations des propriétés de la surface des conidies provenant de cultures d'âge variable (5, 9 et 14 jours). Les propriétés physiques de surface reflètent la composition biochimique de la paroi, et leurs variations mettent en évidence les changements dans le taux ou l'accessibilité de ses composants. La comparaison des conidies provenant de cultures âgées de 5, 9 et 14 jours a montré des variations importantes de l'hydrophobicité et la charge électronégative de surface avec un maximum pour des spores provenant de cultures âgées de 9 jours. Bien que l'ensemble des composants de la paroi cellulaire participent aux propriétés physiques de surface des spores, un rôle plus prononcé de certains composants comme la mélanine a déjà été démontré dans d'autres espèces fongiques comme *A. fumigatus* **[37]** et *C. neoformans* **[38**, **39]**. Wang *et al.* **[40]** ont montré que la mélanisation de *C. neoformans* augmente de manière linéaire pendant 14 jours. Nosanchuk et Casadevall **[38]** ont également analysé la charge de surface des conidies en fonction de l'âge des cultures et corrélé ses variations avec la mélanisation

des spores. Ils ont constaté que l'augmentation de la charge électronégative en fin de phase stationnaire était corrélée avec la mélanisation progressive des blastospores de *C. neoformans*. De même, certaines espèces du genre *Trichoderma* ont été étudiées par Pokorny *et al.* **[41]**; leurs résultats montrent une variation de l'activité des laccases dans les conidies en fonction de l'âge de cultures, les laccases étant des enzymes responsables de la dernière étape dans la synthèse de la mélanine. En effet, cette activité atteint un maximum dans les conidies provenant de cultures âgées de 14 jours. Pour *S. boydii*, aucune étude n'avait été réalisée sur la synthèse de mélanine. Nous avons donc précisé dans un premier temps la voie de synthèse de la mélanine produite par les conidies en incorporant des inhibiteurs de la dihydroxynaphtalène (DHN) ou de la dihydroxyphénylalanine (DOPA)-mélanine dans le milieu de culture. Une nette différence a été observée dans la couleur des conidies provenant de cultures réalisées en présence d'inhibiteurs de la DHN-mélanine, suggérant que la synthèse de la mélanine chez *S. boydii* s'effectue majoritairement par la voie de la DHN-mélanine ce qui est confirmée par l'analyse par spectrophotométrie UV-visible d'extraits de mélanine. La voie de synthèse de la DHN-mélanine est une voie métabolique complexe, qui fait intervenir chez *A. fumigatus* 6 gènes organisés en cluster. Nous avons pu identifier chez *S. boydii* deux de ces gènes, codant respectivement une polyketide synthase de type I (*PKSI*) et la tétrahydroxynaphtalène réductase (*4HNR*). L'analyse bioinformatique a montré une forte homologie des séquences nucléotidiques de ces deux gènes et des séquences en acides aminés prédites pour les protéines correspondantes entre *S. boydii* et d'autres champignons proches qui synthétisent également de la DHN-mélanine. L'expression de ces gènes a également été démontrée dans des extraits d'ARN obtenus à partir de cultures d'âge variable, mais nous n'avons pas trouvé de gène de ménage dont l'expression soit stable dans nos conditions expérimentales, de sorte que nous n'avons pas pu évaluer l'évolution de l'expression de ces deux gènes avec l'âge des cultures. Néanmoins, deux autres techniques nous ont permis de démontrer l'accumulation de la mélanine avec l'âge des cultures. Dans un premier temps, nous avons isolé des spores provenant de cultures d'âge variable, extrait la mélanine présente dans la paroi sporale et les extraits ont été analysés par spectrophotométrie UV/visible, technique qui a montré une augmentation de la quantité de mélanine avec l'âge des cultures. Parallèlement, nous avons analysé par résonance paramagnétique électronique (RPE) des cellules entières provenant de cultures d'âge variable pour estimer les radicaux libres dont le taux reflète les intermédiaires de synthèse. Les intermédiaires de synthèse de la mélanine génèrent naturellement des radicaux libres qui peuvent être détectés par un signal RPE **[42]**. De nombreuses études ont déjà associé les dommages exercés sur les spores *in vitro*, par exemple par exposition à un rayonnement ionisant (UV), à la production de radicaux libres et donc à une augmentation

de l'intensité du signal RPE, suggérant un événement de dépolymérisation de la mélanine. De même, la mélanine est également connue pour ses propriétés anti-oxydantes. Elle piège les espèces oxygénées réactives (ROS, reactive oxygen species), tels que les singulets d'oxygène O^{2*}, le peroxyde d'hydrogène H_2O_2 et les anions superoxyde O^{2-}, protégeant ainsi les spores inhalées des réactions de défense de l'hôte. L'équilibre entre les propriétés anti-oxydantes et pro-oxydantes intrinsèques de la mélanine détermine l'état d'oxydo-réduction et le degré de polymérisation de la mélanine et donc son poids moléculaire **[43**, **44]**. Dans cette étude, nous avons démontré que l'augmentation de la quantité de mélanine avec l'âge des cultures chez *S. boydii* est accompagnée d'une diminution de l'intensité du signal RPE de conidies, ce qui implique une polymérisation progressive de la mélanine avec la maturation des conidies et l'acquisition d'une plus grande activité anti-oxydante.

Nos expériences ont par ailleurs montré le lien entre la teneur en mélanine et la charge électronégative de surface. L'incorporation d'inhibiteurs de synthèse de la DHN-mélanine se traduit par une diminution importante de la charge électronégative de surface, alors qu'elle est inchangée en présence d'inhibiteurs de synthèse de la DOPA-mélanine. De même, l'examen des conidies en microscopie éléctronique à transmission montre que l'épaisseur de la paroi sporale, qui est composée de deux couches superposées, une couche interne transparente aux électrons et une couche externe dense aux électrons, n'est pas affectée par l'incorporation d'inhibiteurs de synthèse de la DOPA-mélanine dans le milieu de culture. Par contre, la couche pariétale externe est plus fine, voire absente par endroits, si l'on utilise un inhibiteur de synthèse de la DHN-mélanine.

La maturation des conidies se traduit également par une augmentation de la teneur en glycoconjugués riches en résidus mannose dans la paroi, mais ces glycoconjugués sont masqués par la mélanine. En effet, l'analyse par cytométrie en flux de conidies incubées en présence de Con A-FITC, ne montre pas de variations significatives de l'intensité moyenne de fluorescence de surface des spores avec l'âge des cultures. Néanmoins, l'intensité moyenne de fluorescence et le nombre des conidies fluorescentes augmentent progressivement avec l'âge des cultures pour des spores provenant de cultures réalisées en présence d'inhibiteurs de synthèse de la DHN-mélanine.

La mélanine et les hydrophobines de la paroi sporale constituent des systèmes de défense très efficaces pour échapper à la reconnaissance par le système immunitaire et lutter contre l'effet délétère des espèces oxygénées réactives. Chez *S. boydii* et indépendamment de l'âge des cultures, nous n'avons pas observé en microscopie de force atomique (AFM) la présence d'hydrophobines organisées sous forme de rodlets (ou bâtonnets), contrairement à ce qui est décrit pour les spores d'*A. fumigatus* pour lesquelles

les hydrophobines se déposent en surface des spores sous forme de batonnets disposés parallèlement les uns aux autres et organisés en faisceaux.

En conclusion, les changements dans les propriétés de surface et la composition biochimique de la paroi des conidies avec l'âge de la culture mettent en évidence l'existence d'un processus de maturation des conidies. L'ensemble de ces résultats démontre qu'il y a polymérisation et accumulation progressive de la mélanine dans les spores avec l'âge des cultures, ce qui est corrélé avec une augmentation de la charge électronégative de surface. La DHN-mélanine est connue pour permettre l'échappement du champignon aux défenses immunitaires de l'hôte en raison de ses propriétés anti-oxydantes. De plus, son accumulation masque progressivement les glycoconjugués riches en résidus mannoses qui sont impliqués dans la reconnaissance immunitaire, ce qui conforte le rôle de la mélanine dans l'établissement de la colonisation des voies respiratoires et le développement ultérieur de l'infection.

Etude II

La germination des conidies inhalées et l'élongation progressive des filaments mycéliens constituent des étapes essentielles dans la colonisation des voies respiratoires. En tant qu'interface avec les structures de l'hôte, la paroi joue là aussi un rôle majeur et une meilleure connaissance des modifications structurales et biochimiques de la paroi au cours de la germination constitue un préalable indispensable pour l'identification des mécanismes pathogéniques du champignon. Le second volet de notre thèse a donc porté sur l'étude des modifications pariétales au cours de la germination des conidies de *S. boydii*. Ces changements de la paroi cellulaire ont été mis en évidence à l'aide de différentes techniques de microscopie (microscopie électronique à balayage ou à transmission, microscopie de force atomique). Parallèlement, nous avons analysé l'évolution des propriétés physiques de surface (hydrophobicité de la surface cellulaire et charge électronégative, évaluation de la fixation de la ferritine cationisée), et recherché des modifications de la composition biochimique de la surface cellulaire par des méthodes indirectes (spectroscopie de force chimique, cytométrie en flux après marquage des éléments fongiques avec des lectines fluorescentes) ou directes (analyse protéomique après extraction des protéines à ancre GPI). Ainsi, nous avons montré que la paroi cellulaire de *S. boydii* subit des modifications importantes au cours de la germination. Sur le plan ultrastructural, on assiste à un remaniement de la couche externe dense aux électrons qui est compacte et d'épaisseur régulière pour les conidies dormantes et les cellules mère de tubes germinatifs, alors qu'elle apparaît irrégulière et plus lache pour la portion hyphale des tubes germinatifs. Par contre, à la différence d'*A. fumigatus* pour lequel le processus de germination comprend une étape

initale de gonflement, aucun changement majeur dans la taille des cellules n'est observé. De même, il n'y a pas de vacuolisation dans le cytoplasme.

Les propriétés physiques de la surface cellulaire sont également affectées par le processus de germination. Les conidies sont plus hydrophobes et plus électronégatives que les tubes germinatifs, comme en témoignent les techniques de partition de phase dans un système eau/hexadécane et de microélectrophorèse. La diminution de la charge électronégative est confirmée par l'examen de tubes germinatifs en microscopie électronique après marquage par la ferritine cationisée. Le marquage concerne essentiellement la surface de la cellule mère des tubes germinatifs. Par ailleurs, aucun marquage n'est observé en présence de ferritine native, ce qui confirme l'importance des charges électronégatives de surface dans la fixation de la ferritine cationisée à la surface des cellules mères. Enfin, la présence des acides sialiques a été recherchée car ils pourraient affecter la charge de surface compte tenu de leur caractère électronégatif. De plus, il a été suggéré que les acides sialiques contribuaient à la pathogénicité **[45]** et à l'adhérence des conidies aux cellules épithéliales de l'hôte dans d'autres modèles fongiques **[46]**. Pour *S. boydii*, la dégradation de ces molécules par la neuraminidase ne réduit pas l'intensité du marquage par la ferritine cationisée suggérant que les acides sialiques ne sont pas impliqués dans la charge électronégative de surface révélée dans ces expériences. A l'inverse, comme nous l'avons vu précédemment, l'inhibition de la synthèse de la DHN-mélanine se traduit par une réduction importante de la charge électronégative en surface des spores. Or *S. boydii* est un hyphomycète produisant des filaments mycéliens hyalins (non pigmentés). Il est donc probable que la mélanine joue un rôle majeur dans le caractère électronégatif de surface des conidies et son absence en surface des hyphes, contrairement à la surface des spores dormantes, serait à l'origine de la diminution de la charge et de l'hydrophobicité de la surface cellulaire.

Précédemment, nous avons montré que la teneur de la paroi en glycoconjugués riches en résidus mannose augmente avec la maturation des conidies **[47]**, et que leur accessibilité à la Con A était cependant entravée par l'accumulation de mélanine **[47]**. Avec la germination des conidies, l'absence de mélanine dans la paroi des filaments produits permet l'accessibilité de ces glycoconjugués riches en mannose ainsi que des polymères de GlcNac, ce qui se traduit par une augmentation très importante des capacités de fixation des lectines fluorescentes Con A et wheat germ agglutinin (WGA).

Les interactions CH3/CH3 (forces d'adhésion hydrophobes dues aux glycoprotéines) enregistrées en surface des conidies de *S. boydii* (1,8 ± 0,3 nN) sont significativement plus faibles que celles enregistrées par Dague *et al.* **[48]** pour les conidies d'*A. fumigatus* (3 ± 0,4 nN). Comme nous l'avons vu précédemment, les spores de *S. boydii* ne présentent pas

de rodlets à leur surface, à la différence des conidies d'*A. fumigatus* pour lesquelles l'agencement de la protéine rodA en batonnets disposés parallèlement les uns aux autres procure à la surface des spores une hydrophobicité homogène **[49]**. L'évaluation des interactions CH3/CH3 (hydrophobes) et OH/OH (hydrophiles) montre que la surface des éléments fongiques comprend un mélange de composants hydrophobes et de composants hydrophiles. Néanmoins, après germination, on constate une diminution des interactions hydrophobes (CH3/CH3). L'inhibition de la synthèse de la DHN-mélanine n'affecte pas ces forces d'adhérence hydrophobes (données non présentées), suggérant que les interactions ici mesurées ne sont pas liées à la mélanine. A l'inverse, l'intensité des interactions hydrophiles (OH/OH) n'est pas modifiée par la germination.

Les changements dans la paroi cellulaire au cours de la germination ont également été illustrés au niveau moléculaire par l'analyse des protéines à ancre GPI. Les protéines à ancre GPI sont les principales protéines intégrales de la paroi des champignons et diverses études ont montré qu'elles jouent un rôle clé dans la morphologie et la virulence dans d'autres modèles fongiques. L'analyse des extraits protéiques de la paroi des conidies et des hyphes de *S. boydii* a révélé un total de 250 protéines, parmi lesquelles seulement 20 présentaient une ancre GPI prédite, et ceci en dépit de l'utilisation de protocoles déjà éprouvés pour la réalisation de la phase d'extraction. Néanmoins, la présence de protéines dépourvues d'ancre GPI est également signalée dans de nombreuses études sur *C. albicans* **[50**, **51**, **52]** pour lequel de telles protéines atypiques sont systématiquement rencontrées dans les extraits de paroi, excepté dans les travaux de Groot *et al*. **[53**, **54]**.

Chez les levures et les champignons filamenteux, les protéines à ancre GPI peuvent avoir deux localisations cellulaires différentes, puisqu'on distingue des protéines ancrées dans la membrane plasmique (GPI-PMP) et des protéines localisées dans la paroi (GPI-CWP). Les protéines de paroi sont caractérisées par un degré important de glycosylation (*N*- et *O*-glycosylation), un peptide signal **[55]**, et l'absence d'hélices transmembranaires, ce qui était le cas pour 19 des 20 protéines à ancre GPI que nous avons identifiées. En outre, selon Pittet et Conzelmann **[56]**, les GPI-CWP ont des pIs de 4,87 ± 0,22 alors que les GPI-PMP ont des pIs significativement plus élevés (pI de 6.67±0.95). Toutefois, une étude récente réalisée sur *Pichia pastoris* n'a pas montré de différence dans leur pI entre les protéines à ancre GPI de la paroi cellulaire et celles de la membrane plasmique **[57]**. Dix-neuf des 20 protéines à ancre GPI que nous avons identifiées, avaient un pI prédit inférieur à 5.

Il existe de plus en plus de preuves que les acides aminés à proximité du site d'attachement de l'ancre GPI (appelé site ω) exercent un effet important sur la localisation finale de la protéine. La présence d'une forte proportion de sérine (S) et thréonine (T) en amont du site ω est largement reconnue comme une caractéristique importante des GPI-

CWP **[58**, **59]** car elle peut outrepasser l'influence des acides aminés dibasiques arginine (R), histidine (H) et lysine (K) localisés en position ω-1 et ω-2, qui habituellement adressent les protéines à ancre GPI à la membrane plasmique **[60]**. Pour les 20 protéines à ancre GPI que nous avons identifiées, le contenu en S/T était supérieur à 10% après exclusion des séquences N- et C-terminales. En outre, nous n'avons pas retrouvé d'acides aminés dibasiques simultanément en position ω-1 et ω-2. Par ailleurs, la présence de valine (V), isoleucine (I) ou leucine (L) en position ω-4 et ω-5, ainsi que la présence de tyrosine (Y) ou d'asparagine (N) en position ω-2, a également été suggérée pour orienter l'adressage vers la paroi selon Hamada *et al.* **[61]**. De tels acides aminés ne sont cependant pas rencontrés aux positions correspondantes dans la séquence des protéines à ancre GPI que nous avons identifiées. Toutefois, ces règles ne semblent pas s'appliquer pour les champignons filamenteux, comme en témoigne la séquence de la protéine Mp1p d'*A. fumigatus* **[62]**.

Toutes ces données suggèrent une localisation pariétale pour 19 des protéines à ancre GPI que nous avons détectées. Néanmoins, le rôle des acides aminés voisins du site ω dans l'adressage des protéines à la paroi ou à la membrane plasmique demeure un sujet de débat, d'autant qu'une même protéine à ancre GPI peut être présente à la fois dans les deux compartiments cellulaires.

Enfin, les différentes familles auxquelles ces protéines appartiennent ont également été recherchées. Parmi les 20 protéines à ancre GPI que nous avons identifiées, une n'a été retrouvée que dans des extraits de conidies et 12 dans les extraits de tubes germinatifs seulement, alors que les 7 autres protéines étaient présentes dans les deux extraits. La protéine à ancre GPI détectée seulement dans les extraits de conidies (KEZ44265.1) a été identifiée comme une Cu/Zn superoxyde dismutase. Les superoxide dismutases (SOD) sont des enzymes anti-oxydantes impliquées dans la dégradation des anions super-oxyde. Douze protéines à ancre GPI n'ont été détectées que dans des extraits de tubes germinatifs ; parmi celles-ci, 4 appartiennent à des familles de protéines à ancre GPI connues pour intervenir dans la synthèse de la paroi cellulaire, une avait un domaine CFEM (Common in Fungal Extracellular and Membrane) et les autres n'avaient aucune fonction connue. Le premier groupe comprend une protéine similaire à des protéines Crhp (KEZ42985.1) dont on pense qu'elles sont impliquées dans la liaison entre les polysaccharides de la paroi cellulaire β (1-6) glucanes et chitine et qui appartiennent à la famille des glycoside hydrolases 16 (GH16) selon la base de données CAZy (http://www.cazy.org/) **[63**, **64**, **65]**. Deux des autres protéines à ancre GPI détectées dans l'extrait pariétal de tubes germinatifs sont similaires à des protéines de la famille Gelp/Gasp (KEZ466191.1, KEZ46098.1). Il s'agit de protéines de la famille des glycoside hydrolases 72 (GH72) qui seraient impliquées dans l'allongement du polymère de β(1-3) glucane. Dans l'extrait pariétal préparé à partir de tubes germinatifs,

une protéine similaire à des protéines de la famille Bgtp/Bglp a également été identifiée. Ces protéines de la famille des glycoside hydrolases 17 (GH17) ont été étudiées chez *S. cerevisiae* et *A. fumigatus*. Dans la paroi cellulaire, AfBgt2p est impliquée dans la ramification des chaînes de β-glucane, puisque cette enzyme catalyse le clivage de chaînes de β(1-3) glucane et le transfert à d'autres chaînes de β(1-3) glucane avec une liaison β(1-6) **[66]**. Une protéine ayant un domaine prédit CFEM a également été détectée dans l'extrait fongique. Ce domaine comprend environ 60 acides aminés, majoritairement hydrophobe, et huit résidus cystéine avec un espacement conservé **[67]**. De tels domaines se rencontrent principalement dans les GPI-CWP et de nombreuses protéines contenant ce domaine sont impliquées dans les interactions hôte-pathogène et la virulence.

Parmi les sept protéines communes aux deux extraits étudiés (conidies et tubes germinatifs), 3 n'avaient aucune fonction ou domaine connu, 3 autres avaient un domaine CFEM et la dernière était semblable à AfBgt2p.

Aucune hydrophobine n'a été identifiée dans nos extraits en utilisant le logiciel proFasta pour detecter la séquence consensus constituée de 8 résidus cystéines. Plusieurs hydrophobines sont décrites chez *A. fumigatus*, dont la protéine RodAp dont l'expression en surface des spores est corrélée avec l'intensité des interactions CH3/CH3 (interactions hydrophobes). RodAp est une protéine modérément hydrophobe avec une valeur GRAVY de 0,245 (*A. fumigatus* Af293, numéro d'accession P41746.2) et une ancre GPI prédite **[68]**. Parmi les protéines à ancre GPI que nous avons identifiées, une seule provenant de l'extrait de conidies présentait un caractère hydrophobe (GRAVY > 0). Fait intéressant, cette protéine apparaît deux fois plus hydrophobe que RodAp (GRAVY = 0,453) et elle présente un domaine CFEM (numéro d'accession KEZ44163.1). Comme mentionné précédemment, le domaine CFEM est un motif composé de huit résidus cystéine conservés, mais distinct du motif caractérisant les hydrophobines. Des domaines CFEM sont communément identifiés dans les protéines à ancre GPI extraites de la paroi, et les protéines de cette famille présentent une forte proportion de résidus d'acides aminés hydrophobes dans leur séquence (32 à 45% des acides aminés totaux) **[67]**. La protéine à domaine CFEM que nous avons identifiée (numéro d'accession KEZ44163.1), était présente à la fois dans les extraits de conidies et de tubes germinatifs, mais sa quantité relative par rapport à l'ensemble des protéines à ancre GPI que nous avons détectées était deux fois plus élevée dans l'extrait de conidies (2.05%) que dans l'extrait de tubes germinatifs (1.06 %). Ces résultats pourraient donc expliquer l'hydrophobicité plus marquée de la surface des conidies face aux tubes germinatifs et la diminution des interactions CH3/CH3 avec la germination.

Nous avons donc montré que la paroi chez *S. boydii* subit des changements structurels avec la germination accompagnés d'une diminution du caractère hydrophobe, de

la charge électrostatique de surface et du marquage par la ferritine cationisée. La germination s'accompagne également d'une plus grande accessibilité des polysaccharides de paroi aux lectines, et d'une diminution de l'intensité des interactions hydrophobes. Nous avons également extrait et identifié 20 protéines à ancre GPI, dont 12 sont présentes uniquement dans la paroi des filaments contre une détectée seulement dans l'extrait de conidies. Les protéines identifiées comprenaient des protéines similaires à des protéines pariétales appartenant à des familles déjà étudiées chez certaines levures et champignons filamenteux comme les protéines Gelp/Gasp, les protéines Crhp ou celles de la famille Bglp/Bgtp, ainsi qu'une superoxyde dismutase à ancre GPI.

Ces résultats mettent en évidence le remodelage de la paroi cellulaire pendant la germination chez *S. boydii.* Il s'agit donc, comme pour d'autres modèles fongiques, d'une structure hautement dynamique. Par ailleurs, avec l'identification d'un nombre important de protéines pariétales à ancre GPI dont certaines sont exprimées spécifiquement par la phase filamenteuse, nos résultats fournissent une base pour étudier le rôle de ces molécules dans les interactions du champignon avec l'hôte et sa virulence. L'obtention de mutants invalidés pour les gènes codant ces protéines à ancre GPI et le couplage des données moléculaires à la cartographie des interactions de surface pourraient s'avérer très utiles pour la compréhension de la pathogénèse.

Etude III

Au cours de ce travail, le séquençage du génome est apparu une étape indispensable puisque le séquençage des gènes *PKS1* et *4HNR* en vue de fournir un support génétique pour l'étude de la synthèse de la DHN-mélanine chez *S. boydii* s'est révélé une tâche difficile. En outre, les premiers essais d'analyse protéomique se sont avérés infructueux compte tenu de l'absence de données génomiques pour notre champignon, et du fait qu'aucun champignon suffisamment proche de *S. boydii* n'avait été séquencé jusqu'à présent. Un programme de séquençage a donc été initié au sein du réseau international sur les infections respiratoires fongiques au cours de la mucoviscidose (ECMM/ISHAM Working group *Fungal respiratory infections in Cystic Fibrosis*) puisque le Pr. Wieland Meyer (Sydney, Australie), le Dr. Laurence Delhaès (Lille, France) et le Dr. Christopher Thornton (Exeter, Royaume-Uni) ont entrepris de séquencer le génome de *S. aurantiacum*, *S. minutisporum* et *S. boydii*, respectivement. Nous nous sommes donc intéressés à *S. apiospermum* qui constitue avec *S. boydii* l'une des deux espèces majeures de ce complexe en pathologie humaine en Europe. La souche IHEM 14462 isolée en 1998 à partir d'un produit d'expectoration d'un patient atteint de mucoviscidose suivi dans le centre hospitalier de Tours (France) a été choisie.

Le séquençage du génome a produit, après assemblage des données, 3744 contigs formant 176 scaffolds avec une taille moyenne de 246 804 paires de bases représentant une longueur totale de 43,4 Mbps. Une fonction a été assignée à 8 818 des 10 919 CDS identifiés (80,75%).

Enfin, l'analyse des voies métaboliques prédites dans le génome de *S. apiospermum* à l'aide de la base de données KEGG (http://www.genome.jp/kegg/) a permis d'identifier un grand nombre d'enzymes potentiellement impliquées dans la dégradation de divers polluants. Cet équipement enzymatique pourrait expliquer la capacité des espèces du complexe *S. apiospermum* à s'adapter à différents environnements impactés par les activités humaines, notamment les sols pollués par des hydrocarbures et les eaux fortement contaminées **[69]** qui constituent des environnements particulièrement favorables à la prolifération de ces champignons et une source potentielle de contamination.

Les espèces du genre *Scedosporium* sont capables d'utiliser le benzoate de phényle et du pétrole brut comme seules sources de carbone et d'énergie **[70**, **71]**. Par ailleurs, il a été montré qu'elles étaient capables de dégrader les hydrocarbures saturés **[72]**, le phénol et le *p*-crésol **[73]**, ainsi que la dioxine **[74**, **75]**.

Après annotation du génome, il apparaît que 23, 22 et 3 cadres de lecture ouverts (ORF, open reading frame) codent pour des enzymes impliquées dans les voies de dégradation du benzoate, de l'aminobenzoate et du fluorobenzoate, respectivement. Trente-quatre ORFs codent pour des enzymes impliquées dans le métabolisme du méthane, 13 ORFs ont été identifiés pour coder des enzymes impliquées dans la dégradation de toluène, deux ORFs pour la dégradation du xylène, 11 pour la dégradation du styrène, 13 pour la dégradation du chlorohexane et du chlorobenzène et 2 pour la dégradation des polychlorobiphényles.

Claussen et Schmidt **[73]** ont montré que la dégradation du phénol par *S. apiospermum* implique deux voies distinctes d'après la mesure des activités enzymatiques correspondantes à chaque voie : les voies catéchol et hydroquinone. Nous avons pu identifier dans le génome de *S. apiospermum*, les ORF codant pour des enzymes impliquées dans ces deux voies métaboliques. Trois ORFs ont été identifiés pour la voie du catéchol, codant pour des catéchol 1,2-dioxygénases (Enzyme Commission number (EC) 1.13.11.1) et trois autres pour la voie de l'hydroquinone, codant l'une pour une 1,2-hydroxyquinol dioxygénase (EC 1.13.11.37) et les deux autres pour la maléylacétate réductase (EC 1.3.1.32). En outre, deux gènes ont été identifiés, codant pour deux phénol monooxygénases (EC 1.14.13.7), enzymes impliquées dans l'étape d'hydroxylation commune aux deux voies **[76]**.

En outre, de nombreuses enzymes fongiques non spécifiques sont connues pour cataboliser les polluants organiques **[77]**. A titre d'exemple, le génome de *S. apiospermum*

comprend 2 gènes codant pour des laccases (EC 1.10.3.2), un gène codant une tyrosinase (EC 1.14.18.1), ainsi que trois gènes codant une chlorure peroxydase (EC 1.11.1.10), une nitroréductase putative et une quinone réductase (EC 1.6.5.2). Enfin, parmi les 98 gènes identifiés codant pour des cytochromes P450, nous avons recherché des gènes impliqués dans la dégradation des polluants appartenant notamment aux familles CYP52, CYP53 et CYP504. Deux gènes appartenant à la famille des cytochromes CYP53, connus pour dégrader le benzoate et ses dérivés, ont été identifiés dans le génome de *S. apiospermum* (EC 1.14.13.12 et EC 1.14.14.1).

La disponibilité de ces données génomiques fournit donc un support moléculaire pour les travaux en cours visant à utiliser des souches atténuées du champignon à des fins de bioremédiation. En outre, elle ouvre la voie pour préciser les facteurs de pathogénicité des espèces du complexe *S. apiospermum*, et notamment pour réaliser des expériences d'invalidation de gènes et étudier les répercussions phénotypiques *in vitro* ou dans un modèle animal de scédosporiose disséminée.

Conclusion

La paroi fongique est une structure très dynamique qui est soumise à des changements et des modifications. Les résultats que nous avons obtenus pour *S. boydii*, illustrent les modifications ultratructurales et biochimiques de la paroi démontrées dans d'autres modèles fongiques au cours de la maturation des conidies et de leur germination. Ils auront des conséquences biologiques importantes puisque que l'équilibre entre les composants de surface a des implications directes sur la pathogénicité, ainsi que sur la résistance à des conditions environnementales défavorables. En outre, les données obtenues sur le génome de *S. apiospermum* faciliteront l'annotation des données de séquence des autres espèces du complexe, et ainsi la progression des connaissances sur les mécanismes pathogéniques de ces champignons en permettant des approches de génomique comparative, ainsi que des approches transcriptomiques, protéomiques et métabolomiques.

References

1. **Hawksworth DL** (1991) The fungal dimension of biodiversity: magnitude, significance, and conservation. Mycol Res **95**: 641–655.

2. **O'Brien HE, Parrent JL, Jackson JA, Moncalvo J-M, Vilgalys R** (2005) Fungal community analysis by large-scale sequencing of environmental samples. Appl Environ Microbiol **71**: 5544–5550.

3. **Blackwell M** (2011) The fungi: 1, 2, 3 … 5.1 million species? Am J Bot **98**: 426–438.

4. Types of Fungal Diseases | Fungal | CDC (n.d.). Available: http://www.cdc.gov/fungal/diseases/index.html/. Accessed 21 August 2014.

5. **Garcia-Solache MA, Casadevall A** (2010) Global warming will bring new fungal diseases for mammals. mBio **1**: e00061–10.

6. **Cortez KJ, Roilides E, Quiroz-Telles F, Meletiadis J, Antachopoulos C, *et al*.** (2008) Infections caused by *Scedosporium* spp. Clin Microbiol Rev **21**: 157–197.

7. **Havlickova B, Czaika VA, Friedrich M** (2008) Epidemiological trends in skin mycoses worldwide. Mycoses **51** Suppl 4: 2–15.

8. **Brown GD, Denning DW, Gow NAR, Levitz SM, Netea MG,** *et al.* (2012) Hidden killers: human fungal infections. Sci Transl Med **4**: 165rv13–rv165rv13.

9. Global Plague : How 150 people die every hour from fungal infection while the world turns a blind eye | Gaffi - Global Action Fund for Fungal Infections (n.d.). Available: http://www.gaffi.org/global-plague-how-150-people-die-every-hour-from-fungal-infection-while-the-world-turns-a-blind-eye/. Accessed 21 August 2014.

10. **Maertens J, Vrebos M, Boogaerts M** (2001) Assessing risk factors for systemic fungal infections. Eur J Cancer Care **10**: 56–62.

11. **Cornely OA, Böhme A, Reichert D, Reuter S, Maschmeyer G, *et al.*** (2008) Risk factors for breakthrough invasive fungal infection during secondary prophylaxis. J Antimicrob Chemother **61**: 939–946.

12. **Puel A, Cypowyj S, Bustamante J, Wright JF, Liu L, *et al.*** (2011) Chronic mucocutaneous candidiasis in humans with inborn errors of interleukin-17 immunity. Science **332**: 65–68.

13. **Ferwerda B, Ferwerda G, Plantinga TS, Willment JA, van Spriel AB,** *et al.* (2009) Human dectin-1 deficiency and mucocutaneous fungal infections. New Engl J Med **361**: 1760–1767.

14. **Guarro J, Kantarcioglu AS, Horré R, Luis Rodriguez-Tudela J, Cuenca Estrella M, *et al.*** (2006) *Scedosporium apiospermum*: changing clinical spectrum of a therapy-refractory opportunist. Med Mycol **44**: 295–327.

15. **Zouhair R, Rougeron A, Razafimandimby B, Kobi A, Bouchara J-P, *et al.*** (2013) Distribution of the different species of the *Pseudallescheria boydii/Scedosporium apiospermum* complex in french patients with cystic fibrosis. Med Mycol **51**: 603–613.

16. **Tronchin G, Pihet M, Lopes-Bezerra LM, Bouchara J-P** (2008) Adherence mechanisms in human pathogenic fungi. Med Mycol **46**: 749–772.

17. **Dalle F, Jouault T, Trinel PA, Esnault J, Mallet JM, *et al.*** (2003) β-1,2- and α-1,2-Linked oligomannosides mediate adherence of *Candida albicans* blastospores to human enterocytes *in vitro.* Infect Immun **71**: 7061–7068.

18. **Gravelat FN, Beauvais A, Liu H, Lee MJ, Snarr BD, *et al.*** (2013) *Aspergillus* galactosaminogalactan mediates adherence to host constituents and conceals hyphal β-glucan from the immune system. PLoS Pathog **9**: e1003575.

19. **Dubey MK, Jensen DF, Karlsson M** (2014) Hydrophobins are required for conidial hydrophobicity and plant root colonization in the fungal biocontrol agent *Clonostachys rosea*. BMC Microbiol **14**: 18.

20. **Kim S, Ahn I-P, Rho H-S, Lee Y-H** (2005) *MHP1*, a *Magnaporthe grisea* hydrophobin gene, is required for fungal development and plant colonization. Mol Microbiol **57**: 1224–1237.

21. **Desai C, Mavrianos J, Chauhan N** (2011) *Candida glabrata* Pwp7p and Aed1p are required for adherence to human endothelial cells. FEMS Yeast Res **11**: 595–601.

22. **Levdansky E, Kashi O, Sharon H, Shadkchan Y, Osherov N** (2010) The *Aspergillus fumigatus cspA* gene encoding a repeat-rich cell wall protein is important for normal conidial cell wall architecture and interaction with host cells. Eukaryot Cell **9**: 1403–1415.

23. **Masuoka J, Hazen KC** (1997) Cell wall protein mannosylation determines *Candida albicans* cell surface hydrophobicity. Microbiology **143**: 3015–3021.

24. **Masuoka J, Wu G, Glee PM, Hazen KC** (1999) Inhibition of *Candida albicans* attachment to extracellular matrix by antibodies which recognize hydrophobic cell wall proteins. FEMS Immunol Med Microbiol **24**: 421–429.

25. **Kriznik A, Bouillot M, Coulon J, Gaboriaud F** (2005) Morphological specificity of yeast and filamentous *Candida albicans* forms on surface properties. C. R. Biologies **328**: 928–935.

26. **Gravelat FN, Ejzykowicz DE, Chiang LY, Chabot JC, Urb M, *et al.*** (2010) *Aspergillus fumigatus MedA* governs adherence, host cell interactions and virulence. Cell Microbiol **12**: 473–488.

27. **Carrion S de J, Leal SM, Ghannoum MA, Aimanianda V, Latgé J-P, *et al.*** (2013) The rodA hydrophobin on *Aspergillus fumigatus* spores masks dectin-1– and dectin-2–dependent responses and enhances fungal survival *in vivo*. J Immunol **191**: 2581–2588.

28. **Stringer JR** (2007) Antigenic variation in *Pneumocystis*. J Eukaryot Microbiol 54: 8–13.

29. **Voelz K, May RC** (2010) *Cryptococcal* interactions with the host immune system. Eukaryot Cell **9**: 835–846.

30. **Nosanchuk JD, Casadevall A** (2006) Impact of melanin on microbial virulence and clinical resistance to antimicrobial compounds. Antimicrob Agents Chemother **50**: 3519–3528.

31. **Santos ALS, Santos ALS, Bittencourt VCB, Pinto MR, Silva BA, *et al.*** (2009) Biochemical characterization of potential virulence markers in the human fungal pathogen *Pseudallescheria boydii*. Med Mycol **47**: 375–386.

32. **Pinto MR, de Sá ACM, Limongi CL, Rozental S, Santos ALS, *et al.*** (2004) Involvement of peptidorhamnomannan in the interaction of *Pseudallescheria boydii* and HEp2 cells. Microbes Infect **6**: 1259–1267.

33. **Figueiredo RT, Fernandez PL, Dutra FF, González Y, Lopes LC, *et al.*** (2010) TLR4 recognizes *Pseudallescheria boydii* conidia and purified rhamnomannans. J Biol Chem **285**: 40714–40723.

34. **Bittencourt VCB, Figueiredo RT, Silva RB da, Mourão-Sá DS, Fernandez PL, *et al.*** (2006) An α-Glucan of *Pseudallescheria boydii* is involved in fungal phagocytosis and toll-like receptor activation. J Biol Chem **281**: 22614–22623.

35. **Kiffer-Moreira T, Pinheiro AAS, Pinto MR, Esteves FF, Souto-Padrón T, *et al.*** (2007) Mycelial forms of *Pseudallescheria boydii* present ectophosphatase activities. Arch Microbiol **188**: 159–166.

36. **Pinto MR, Rodrigues ML, Travassos LR, Haido RMT, Wait R, *et al.*** (2002) Characterization of glucosylceramides in *Pseudallescheria boydii* and their involvement in fungal differentiation. Glycobiology **12**: 251–260.

37. **Pihet M, Vandeputte P, Tronchin G, Renier G, Saulnier P, *et al.*** (2009) Melanin is an essential component for the integrity of the cell wall of *Aspergillus fumigatus* conidia. BMC Microbiol **9**: 177.

38. **Nosanchuk JD, Casadevall A** (1997) Cellular charge of *Cryptococcus neoformans*: contributions from the capsular polysaccharide, melanin, and monoclonal antibody binding. Infect Immun **65**: 1836.

39. **Frases S, Salazar A, Dadachova E, Casadevall A** (2007) *Cryptococcus neoformans* can utilize the bacterial melanin precursor homogentisic acid for fungal melanogenesis. Appl Environ Microbiol **73**: 615–621.

40. **Wang Y, Aisen P, Casadevall A** (1996) Melanin, melanin "ghosts," and melanin composition in *Cryptococcus neoformans.* Infect Immun **64**: 2420–2424.

41. **Pokorný R, Vargovič P, Hölker U, Janssen M, Bend J, *et al.*** (2005) Developmental changes in *Trichoderma viride* enzymes abundant in conidia and the light-induced conidiation signalling pathway. J. Basic Microbiol **45**: 219–229.

42. **Enochs WS** (1993) A standardized test for the identification and characterization of melanins using electron paramagnetic resonance (EPR) spectroscopy. Pigment Cell Res **6**: 91–99.

43. **Sarangarajan R, Apte SP** (2006) The polymerization of melanin: a poorly understood phenomenon with egregious biological implications. Melanoma Res **16**: 3–10.

44. **Khajo A, Bryan RA, Friedman M, Burger RM, Levitsky Y, *et al.*** (2011) Protection of melanized *Cryptococcus neoformans* from lethal dose gamma irradiation involves changes in melanin's chemical structure and paramagnetism. PLoS ONE **6**(9): e25092.

45. **Wasylnka JA, Simmer MI, Moore MM**. 2001. Differences in sialic acid density in pathogenic and non-pathogenic *Aspergillus* species. Microbiology **147**:869–877.

46. **Wasylnka JA, Moore MM**. 2000. Adhesion of *Aspergillus* species to extracellular matrix proteins: evidence for involvement of negatively charged carbohydrates on the conidial surface. Infect. Immun. **68**:3377–3384.

47. **Ghamrawi S, Renier G, Saulnier P, Cuenot S, Zykwinska A, Dutilh BE, Thornton C, Faure S, Bouchara J-P**. 2014. Cell wall modifications during conidial maturation of the human pathogenic fungus *Pseudallescheria boydii*. PLoS ONE **9**:e100290.

48. **Dague E, Alsteens D, Latgé J-P, Dufrene YF**. 2008. High-resolution cell surface dynamics of germinating *Aspergillus fumigatus* conidia. Biophys. J. **94**:656–660.

49. **Dague E, Alsteens D, Latgé J-P, Verbelen C, Raze D, Baulard AR, Dufrêne YF**. 2007. Chemical force microscopy of single live cells. Nano Lett. **7**:3026–3030.

50. **Castillo L, Calvo E, Martínez AI, Ruiz-Herrera J, Valentín E, Lopez JA, Sentandreu R**. 2008. A study of the *Candida albicans* cell wall proteome. Proteomics **8**:3871–3881.

51. **Ebanks RO, Chisholm K, McKinnon S, Whiteway M, Pinto DM**. 2006. Proteomic analysis of *Candida albicans* yeast and hyphal cell wall and associated proteins. Proteomics **6**:2147–2156.

52. **Nombela C, Gil C, Chaffin WL**. 2006. Non-conventional protein secretionin yeast. Trends Microbiol. **14**:15–21.

53. **De Groot PWJ, de Boer AD, Cunningham J, Dekker HL, de Jong L, Hellingwerf KJ, de Koster C, Klis FM**. 2004. Proteomic analysis of *Candida albicans* cell walls reveals covalently bound carbohydrate-active enzymes and adhesins. Eukaryot Cell **3**:955–965.

54. **De Groot PWJ, Brandt BW, Horiuchi H, Ram AFJ, de Koster CG, Klis FM**. 2009. Comprehensive genomic analysis of cell wall genes in *Aspergillus nidulans*. Fungal Genet. Biol. **46 Suppl 1**:S72–81.

55. **Bowman SM, Free SJ** (2006) The structure and synthesis of the fungal cell wall. BioEssays 28: 799–808.

56. **Pittet M, Conzelmann A**. 2007. Biosynthesis and function of GPI proteins in the yeast *Saccharomyces cerevisiae*. Biochim. Biophys. Acta **1771**:405–420.

57. **Zhang L, Liang S, Zhou X, Jin Z, Jiang F, Han S, Zheng S, Lin Y**. 2013. Screening for glycosylphosphatidylinositol-modified cell wall proteins in *Pichia pastoris* and their recombinant expression on the cell surface. Appl. Environ. Microbiol. **79**:5519–5526.

58. **Frieman MB, Cormack BP**. 2004. Multiple sequence signals determine the distribution of glycosylphosphatidylinositol proteins between the plasma membrane and cell wall in *Saccharomyces cerevisiae*. Microbiology **150**:3105–3114.

59. **De Groot PWJ, Brandt BW**. 2012. ProFASTA: A pipeline web server for fungal protein scanning with integration of cell surface prediction software. Fungal Genet. Biol. **49**:173–179.

60. **Eisenhaber B, Schneider G, Wildpaner M, Eisenhaber F**. 2004. A sensitive predictor for potential GPI lipid modification sites in fungal protein sequences and its application to genome-wide studies for *Aspergillus nidulans, Candida albicans Neurospora crassa*, *Saccharomyces cerevisiae* and *Schizosaccharomyces pombe*. J. Mol. Biol. **337**:243–253.

61. **Hamada K, Terashima H, Arisawa M, Yabuki N, Kitada K**. 1999. Amino acid residues in the ω-minus region participate in cellular localization of yeast glycosylphosphatidylinositol-attached proteins. J. Bacteriol. **181**:3886–3889.

62. **Ouyang H, Chen X, Lu Y, Wilson IBH, Tang G, Wang A, Jin C**. 2013. One single basic amino acid at the ω-1 or ω-2 site is a signal that retains glycosylphosphatidylinositol-anchored protein in the plasma membrane of *Aspergillus fumigatus*. Eukaryot. Cell **12**:889–899.

63. **Cabib E, Blanco N, Grau C, Rodriguez-Pena JM, Arroyo J**. 2007. Crh1p and Crh2p are required for the cross-linking of chitin to beta(1-6)glucan in the *Saccharomyces cerevisiae* cell wall. Mol Microbiol **63**:921–935.

64. **Cabib E, Farkas V, Kosik O, Blanco N, Arroyo J, McPhie P**. 2008. Assembly of the yeast cell wall. Crh1p and Crh2p act as transglycosylases *in vivo* and *in vitro*. J. Biol. Chem. **283**:29859–29872.

65. **Cabib E**. 2009. Two novel techniques for determination of polysaccharide cross-links show that Crh1p and Crh2p attach chitin to both beta(1-6)- and beta(1-3)glucan in the *Saccharomyces cerevisiae* cell wall. Eukaryot Cell **8**:1626–1636.

66. **Gastebois A, Mouyna I, Simenel C, Clavaud C, Coddeville B, Delepierre M, Latgé J-P, Fontaine T**. 2010. Characterization of a new beta(1-3)-glucan branching activity of *Aspergillus fumigatus*. J. Biol. Chem. **285**:2386–2396

67. **Kulkarni RD, Kelkar HS, Dean RA**. 2003. An eight-cysteine-containing CFEM domain unique to a group of fungal membrane proteins. Trends Biochem. Sci. **28**:118–121.

68. **Aimanianda V, Bayry J, Bozza S, Kniemeyer O, Perruccio K, Elluru SR, Clavaud C, Paris S, Brakhage AA, Kaveri SV, Romani L, Latgé J-P.** (2009) Surface hydrophobin prevents immune recognition of airborne fungal spores. Nature **460**: 1117–1121.

69. **Rougeron A, Schuliar G, Leto J, Sitterle E, Landry D, *et al.*** (2014) Human-impacted areas of France are environmental reservoirs of the *Pseudallescheria boydii* / *Scedosporium apiospermum* species complex. Environ Microbiol doi:10.1111/1462-2920.12472.

70. **April TM, Abbott SP, Foght JM, Currah RS** (1998) Degradation of hydrocarbons in crude oil by the ascomycete *Pseudallescheria boydii* (Microascaceae). Can J Microbiol **44**: 270–278.

71. **Claußen M, Schmidt S** (1999) Biodegradation of phenylbenzoate and some of its derivatives by *Scedosporium apiospermum*. Res Microbiol **150**: 413–420.

72. **Onodera M, Endo Y, Ogasawara N** (1989) Utilization of short-chain hydrocarbons and accumulation of methylketones by a gaseous hydrocarbon assimilating mold, *Scedosporium* sp. A-4. Agricultur Biol Chem **53**: 1431–1432.

73. **Claußen M, Schmidt S** (1998) Biodegradation of phenol and *p*-cresol by the hyphomycete *Scedosporium apiospermum*. Res Microbiol **149**: 399–406.

74. **Ishii K, Furuichi T** (2007) Development of bioreactor system for treatment of dioxin-contaminated soil using *Pseudallescheria boydii.* J Hazard Mater **148**: 693–700.

75. **Ishii K, Furuichi T, Tanikawa N, Kuboshima M** (2009) Estimation of the biodegradation rate of 2,3,7,8-tetrachlorodibenzo-*p*-dioxin by using dioxin-degrading fungus, *Pseudallescheria boydii*. J Hazard Mater **162**: 328–332.

76. **Enguita FJ, Leitã**o AL (2013) Hydroquinone: environmental pollution, toxicity, and microbial answers. BioMed Res Int **2013**: e542168.

77. **Harms H, Schlosser D, Wick LY** (2011) Untapped potential: exploiting fungi in bioremediation of hazardous chemicals. Nat Rev Micro **9**: 177–192.

INTRODUCTION

By 1991 the estimates for fungal diversity on earth were 1.5 M species but later in 2011 studies advocated numbers up to 5.1 M different fungal species **[1**, **2**, **3]**. According to the Centers for Disease Control and Prevention (CDC), only 300 of these species are pathogenic for humans **[4**, **5]**. Even though few species are responsible for most cases of mycoses, the number of emerging pathogenic fungi causing invasive infections that are difficult to treat is increasing. *Scedosporium* species (previously mentioned as *Pseudallescheria* species) were first discovered in the 1889 as agents of human otitis, but were not recognized as human pathogens until the 1980s when the diseases ascribed to these fungi started to increase and diversify **[6]**.

Superficial infections (skin and nail) caused by fungi are estimated to affect 20 to 25% of the world population **[7]**. Add to this, 10 million cases of oral thrush in HIV/AIDS patients and 2 million cases of esophageal infections, among others, occur on an annual basis **[8]**. Even though invasive fungal diseases are far less frequent than superficial infections, the number of deaths caused by invasive fungal diseases is at least the same if not higher than the number of deaths due to malaria or tuberculosis according to Brown *et al.* **[8]**. Despite all this, fungal infections are still not widely recognized, as no plans are yet implemented by organizations like the World Health Organization (WHO) in this regard **[8]**, **[9]**.

Over the past several decades, the incidence of fungal infections has been increasing and the factors responsible for this include the increasing incidence of many cancers and hematological malignancies, the development of intensive care for critically ill patients and the use of more and more aggressive procedures, the increasing number of immunosuppressed patients in relation with the emergence of the AIDS epidemics and the development of bone marrow and solid organ transplantation, the increase in life expectancy in some chronic diseases like cystic fibrosis, genetic predisposition, the emergence of antifungal resistance as well as climate changes **[5**, **10**, **11**, **12**, **13]**. This multitude of factors that are boosting the number and gravity of fungal infections shows how complicated the situation is. A better understanding of fungal pathogenesis is necessary to identify new therapeutic targets and therefore limit the damages caused by these microorganisms.

Species of the *Scedosporium apiospermum* (*S. apiospermum*) complex are the most common etiologic agents of cutaneous and subcutaneous mycetoma. They commonly cause disseminated infections in patients with advanced human immunodeficiency virus (HIV) infection, hematological malignancies, stem cell transplantation and others, but more importantly they cause infections in the lung and upper respiratory tract. They are the second most frequently isolated fungi from the respiratory tract of patients with cystic

fibrosis. These species are refractory to therapy and at present they are considered as a diagnostic and theurapeutic challenge **[14]**.

Today, our knowledge about the pathogenic mechanisms of these fungi is still at its infancy. This work aims to study the cell wall of *Scedosporium boydii* (*S. boydii*), one of the two major species of the *S. apiospermum* complex, since this structure is essential for the survival and pathogenesis of the fungus. Modifications occurring in the cell wall are investigated during maturation and germination of conidia using various approaches in an attempt to identify potential virulence factors (melanins, hydrophobins, GPI-anchored proteins). The first published genome of a member of this species-complex (*S. apiospermum sensu stricto*) is also reported. A number of interesting metabolic pathways were identified in the genome regarding the biotechnological potential of these fungi in bioremediation, which corroborates the bulk of previous experimental studies. Finally, this work is aimed at accelerating fundamental research on *Scedosporium* species using molecular approaches.

I. Biology and pathogenicity of *Scedosporium boydii*

I.1. Morphology and reproductive modes

Scedosporium boydii is a saprophytic filamentous fungus that can be readily isolated from a variety of environmental sources. The fungus can grow on all culture media used for mycological examination. On poor media like Malt agar it conidiates faster and more frequently than on rich media like yeast extract-peptone-dextrose (YPD) agar. *Scedosporium boydii* tolerates temperatures up to 40°C **[15]**. Colonies are floccose and initially white on the upper side (up to 3-4 days of culture), becoming progressively dark grey or smoky brown with sporulation (**Figure I.1**). The reverse side is pale to brownish with black zones.

Figure I.1. *Scedosporium boydii* IHEM 15155 on YPD agar (14 days, 37°C). Surface (left) and reverse (right) sides of the colony.

Two modes of reproduction can be observed, sexual and asexual reproduction. In the sexual reproduction (teleomorph), yellow-brown to black cleistothecia (100 to 300 µm in diameter) can be seen toward the periphery of colonies especially on nutrient-poor media like cornmeal agar, potato dextrose agar, pea agar, potato-carrot agar or plain water agar (**Figure I.2**). However such structures are rarely produced by clinical isolates and an incubation of two to three weeks is necessary for their formation. The ascocarp has a thin, single layered, membranaceous wall composed of jigsaw-shaped brown cells. When mature, the ascocarp bursts releasing globose asci that contain eight ascospores. Ascospores are ovoid to ellipsoidal with a golden brown color. The presence of an internal oil droplet and the absence of a truncated base are indicators of the sexual origin of spores with respect to those produced asexually **[6]**.

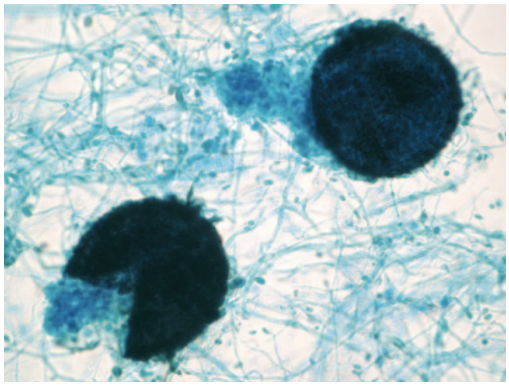

Figure I.2. *Scedosporium boydii* cleistothecia liberating ascospores (X100). Cortez *et al.* **[6]**.

In asexual reproduction, two anamorphic states (synanamorphs) are described, one called *Graphium* state that may or may not be produced depending on strains, and the other that is a major type, invariably present and consisting of septate hyaline filaments with lateral or terminal cylindrical conidiogenous cells (**Figure I.3**). Conidiogenesis occurs through the solitary type of the thallic mode in which a young conidium starts to develop only after being delimited from the filament with a septum **[6]**. Conidia are thick walled, globose to subglobose, brown and sticky **[16]**. On the other hand, the *Graphium* state may be produced at a later stage at the edge of colonies but is less commonly seen; it consists of a bundle of hyphae cemented together forming a stiff erect olive-brown synnema that terminates in a brush of conidiogenous cells (**Figure I.3**). The conidia of both forms are typically truncated at their base (3 to 7 by 5 to 12 µm), oval for the major type, more cylindrical for the *Graphium* state. The conidia of the major type are often formed singly whereas those of the *Graphium* state are arranged in clusters at the apex of synnemata **[6]**.

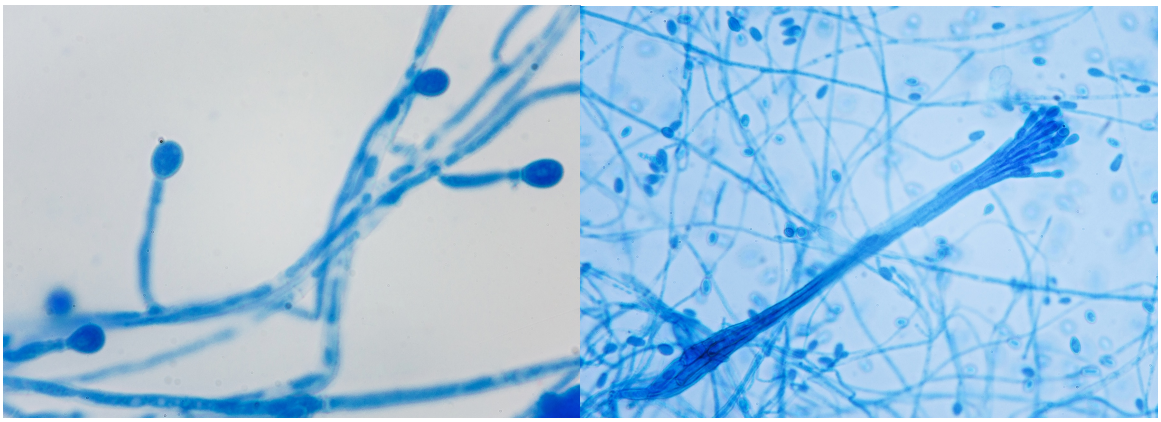

Figure I.3. Asexual reproduction of *S. boydii* IHEM 15155 (14 days, YPD agar, 37°C). Lactic blue stain was used. Conidiophore of the major type (left, X400) that is commonly seen in culture. Synnema of the *Graphium* state, a rare image for this species (right, X100).

I.2. Taxonomy

The history of taxonomy of the *S. apiospermum* complex is quite complicated. It dates back to 1911 where Saccardo described the first isolate of the genus, obtained from a patient with mycetoma that reproduced only asexually and called it *Monosporium apiospermum*. In 1919, Castellani and Chalmers formally proposed the name *Scedosporium* giving rise to the name *S. aspiospermum*. In 1922, Shear isolated from a mycetoma a new fungus that produced cleistothecia and called it *Allescheria boydii*. At the time both entities were considered different fungi causing the same disease, until 1944 when Emmons reported that *S. apiospermum* was the anamorph of *A. boydii*. In 1970, Malloch proposed the name *Petriellidium boydii* for the teleomorph but later on the genus *Pseudallescheria* was considered synonymous to *Petriellidium* and the name *Pseudallescheria boydii* was finally adopted for the teleomorph **[6]**.

Until 2008, the anamorph (*S. apiospermum*) and the teleomorph (*P. boydii*) were considered as two reproductive forms of the same fungus, therefore both names were considered synonymous. In 2008, with the advent of molecular phylogeny, Gilgado *et al.* **[16]** demonstrated after molecular and phenotypic comparisons of a large number of isoaltes that *S. apiospermum* should be considered a different taxon from *P. boydii*. However, the genus name (*Pseudallescheria*/*Scedosporium*) remained interchangeable to indicate the teleomorph or the anamorph forms. Hereby, the *Scedosporium*/*Pseudallescheria* complex comprised at least five distinct species: *P. boydii* (anamorph: *S. boydii*), *Pseudallescheria apiosperma* (anamorph: *S. apiospermum*), *Scedosporium aurantiacum*, *Scedosporium dehoogii* and *Pseudallescheria minutispora*. *Scedosporium prolificans* was clearly distinct from the others and was not included in the complex **[15**, **16]**. The classification of smaller taxonomic entities (like *Pseudallescheria ellipsoidea*, *Pseudallescheria fusoidea*, *Pseudallescheria angusta*, *Pseudallescheria desertorum*, and *Scedosporium deficiens*) into separate species was not yet settled though.

In July 2014, the ECMM/ISHAM working group on *Pseudallecheria*/*Scedosporium* infections published a new nomenclature due to the major changes in the International Code of Nomenclature on the use of different names for sexual and asexual stages of fungi **[17]**. The new nomenclature suggested in 2011 (Amesterdam Declaration on Fungal Nomenclature) is based on molecular phylogeny rather than on morphological and culture techniques or sexual types of reproduction as in the old system **[18]**. In the new nomenclature, the genus name "*Pseudallescheria*" was abandoned since "*Scedosporium*" name is the oldest valid generic name, this implies, for example, the transfer of *Pseudallescheria boydii* to *Scedosporium boydii*. The fungus *S. boydii* now belongs to the order *Microascales*, family *Microascaceae* and genus *Scedosporium. Scedosporium*

apiospermum and *S. boydii* are considered completely two different species but in terms of pathology and antifungal susceptibility these two species have no medically significant difference. Therefore in routine identification in the clinical laboratory these two closely related siblings can be considered belonging to the "*S. apiospermum* complex" that now comprises: *S. apiospermum*, *S. boydii*, *S. aurantiacum*, *S. minutisporum* and *S. dehoogii.* However, the taxonomic status of the subgroups of *S. boydii*, *Pseudallescheria angusta* and *Pseudallescheria ellipsoidea* is not yet resolved. Likewise, the taxonomic status of *Scedosporium deficiens* that is very close to *S. dehoogii* is still debated. Finally, *S. prolificans* was unambiguously separated from the other *Scedosporium* species. Therefore it now belongs to a different genus named *Lomentospora prolificans* (Refer to **Figure I.4** for the phylogenetic tree and to **Table I.1** for the old and new nomenclatures as well as the different structures formed by each specie).

Since this new nomenclature appeared only recently in july 2014 most of the studies published so far were available under synonymous names (**Table I.1**) according to the nomenclature prior 2014 (including the study by Ghamrawi *et al.* **[19]** presented in study I of the experimental part of this thesis. Add to this, many studies even after 2008 used *P. boydii* as synonymous to *S. apiospermum* especially in case reports. Therefore the information included in this book may not always distinguish between the different species and therefore "*Scedosporium* species" is often mentioned regrouping *S. apiospermum*, *S. boydii*, *S. aurantiacum*, *S. dehoogi* and *S. minutisporum* (**Table I. 1**).

I.3. Ecology and epidemiology

Scedosporium species are commonly found in temperate climates, less frequently in tropical areas. These species have properties permitting their survival in polluted areas where there is poor aeration and high osmotic pressure since they are thermo-tolerant and capable of surviving in anaerobic conditions and at high salt concentrations (5% NaCl in liquid cultures) **[20]**. They are ubiquitous eutrophic fungi commonly isolated from polluted soil and water, agricultural areas, potted plants and human-impacted areas but extremely infrequent in the air and indoor environment **[14**, **21**, **22]**.

Ecological studies demonstrated variability in the abundance of the *Scedosporium* species according to geographical areas and types of environments. In Austria, the most frequent species in the environment was *S. apiospermum* followed by *S. dehoogii* and the largest number of *Scedosporium* isolates was found in industrial areas, followed by urban playgrounds and agricultural areas. In this study, a positive correlation was established between the presence of *Scedosporium* species in Austria and the nitrogen concentration in the soil as well as a pH range of 6.1 to 7.5 **[23]**.

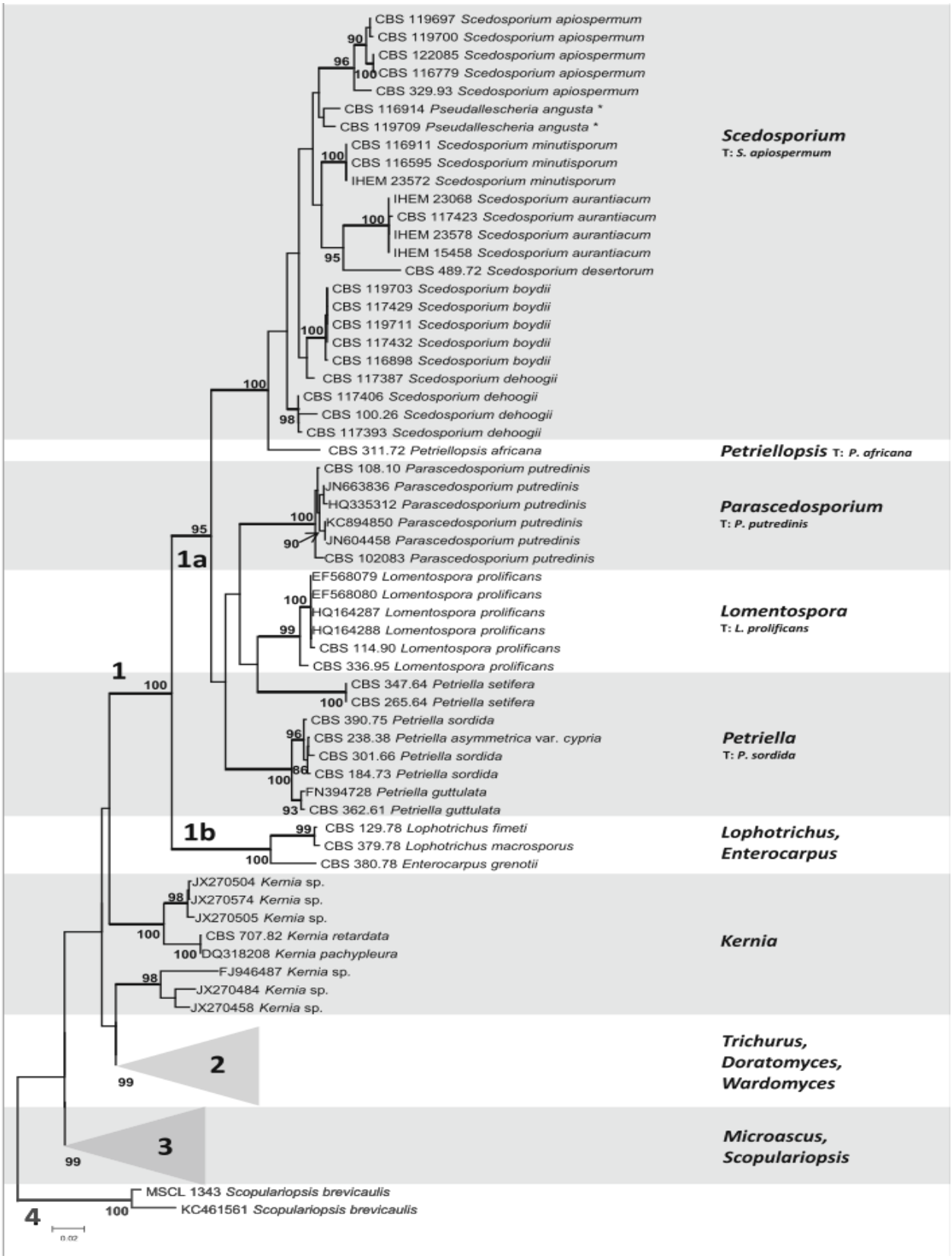

Figure I.4. Phylogenetic overview of *Microascaceae* family using the Internal Transcribed Spacer (ITS) region of rDNA for classification (Lackner *et al.* **[17]**)

Table I.1. Newly proposed nomenclature for *Scedosporium*/*Pseudallescheria* and the type of reproductive structures identified for each species.
(ISHAM/ECMM 2014, adapted from Lackner *et al.* **[17]**)

Order/ family	Genus name	Epithet	Commonly used synonymous names	Synanamorphs/Teleomorph +/–
Microascales/ Microascaceae	*Lomentospora*	*prolificans*	*Scedosporium prolificans, Scedosporium inflatum*	*Scedosporium*-like/–
	Scedosporium	*apiospermum*	*Pseudallescheria apiosperma*	*Scedosporium*, 'Graphium'/+
		aurantiacum	–	*Scedosporium*/–
		boydii	*Allescheria boydii, Petriellidium boydii, Pseudallescheria boydii, Polycytella hominis*	*Scedosporium*, 'Graphium'/+
		dehoogii	–	*Scedosporium*
		minutisporum	*Pseudallescheria minutispora*	*Scedosporium*/+
		desertorum	*Pseudallescheria desertorum*	arthroconidia

In Australia*, S. aurantiacum* was found to be the most frequent species followed by *S. boydii* and *S. dehoogii* (the last two species were isolated in low frequencies) and the highest number of *Scedosporium* isolates was found associated with areas of high human activity. Sampling at different times of the year showed no significant variations **[24]**.

In France, the most abundant species was *S. dehoogii* (39%) followed *S. boydii*, *S. apiospermum* and *S. aurantiacum* at equal frequencies (18 - 22% each). The highest densities for the *Scedosporium* species in France were found in human-impacted areas (agricultural areas, waste water treatment plants, playgrounds and industrial areas); no isolates were found in acidic (forest soils) or basic pH (higher than 8.27) nor were they found in enriched soil (high ammonium content) **[25]**.

All these studies point out to the abundance of these species in human-impacted areas which raises the question to whether there is a link between the high prevalence in certain areas and *Scedosporium* epidemiology. Most species within the *S. apiospermum* complex are considered to have a « dual ecology », as described by Lackner, since they can develop in polluted areas acting as efficient agents of bioremediation and also in human hosts leading to various diseases notably respiratory infections in cystic fibrosis (CF) patients **[26**, **27**,

28]. While the environmental factors fortify the high frequencies of *S. apiospermum* and *S. aurantiacum* in CF patients in Austria **[23]** and Australia **[29]** respectively, it fails to explain the results seen with CF patients in France. Zouhair *et al.* **[30]** showed that the most frequently isolated species from CF patients in France was *S. boydii* (62%), followed by *S. apiospermum* (24%), *S. aurantiacum* (10%) and *S. minutisporum* (4%). Despite the fact that *S. dehoogii* was highly abundant in French soils and was shown to be one of the most virulent species in animal models **[31]**, it was not recovered in a CF context in this study **[30]**. This indicates that the geographical settings are not sufficient to explain the frequencies of *Scedosporium* species in clinical cases and especially in the CF context. Therefore a better understanding of how infection is established in different clinical settings and the inherent virulence factors employed by each of these species is required.

I.4. The importance of studying *S. boydii*

I.4.1. Pathogenesis: From infection to treatment

a) Infections caused by *Scedosporium* species

Scedosporium species (particularly *S. boydii*, *S. apiospermum* and *S. aurantiacum*) stand behind various infections in immunocompromised as well as immunocompetent individuals (**Figure I.5**). These fungi are typical opportunists, in which the appearance of clinical symptoms widely depends on the portal of entry and the patient's clinical status but no clinical syndromes are fully characteristic for the species. Infections caused by *Scedosporium* can be localized after a trauma, in the form of symptomatic or asymptomatic colonization of cavities or disseminated **[14]**.

In the case of **traumatic inoculations**, the vast majority of infections are mycetomas that occur in otherwise healthy individuals. Mycetoma is a chronic, progressive, destructive morbid inflammatory disease usually involving the foot or the hand, but any part of the body can also be affected. There exists two types of mycetoma infection. **Actinomycetoma** is caused by microaerophilic gram-positive branching actinomycetes bacteria. This form represents 60% of cases worldwide with the major causative agent being *Nocardia brasiliensis*. The second type is **eumycetoma** caused by fungal organisms with the most common causative agent being *Madurella mycetomatis*. At the site of inoculation, nodules form and usually increase in size with time and can rupture and form secondary nodules with fungal or bacterial granular drainage. Grains vary in color, depending on the etiologic agent and type of infection. White grains indicate that the causative agent is *S. apiospermum* complex, *Aspergillus nidulans*, or *Acremonium kiliense,* while black grains indicate *Curvularia lunata*, *Exophiala jeanselmei*, *Pyrenochaeta romeroi*, *Leptosphaeria senegalensis*, *Madurella*

grisea, or *Madurella mycetomatis* **[32]**. Of note, *Scedosporium* species are the most prevalent agent of mycetoma in temperate, moist climate zones **[33]**.

Other types of traumatic infections are cutaneous or subcutaneous or lymphocutaneous and they include infections of the eye, skin, ear, nails, lungs, bones, muscle and joints **[6**, **14]**.

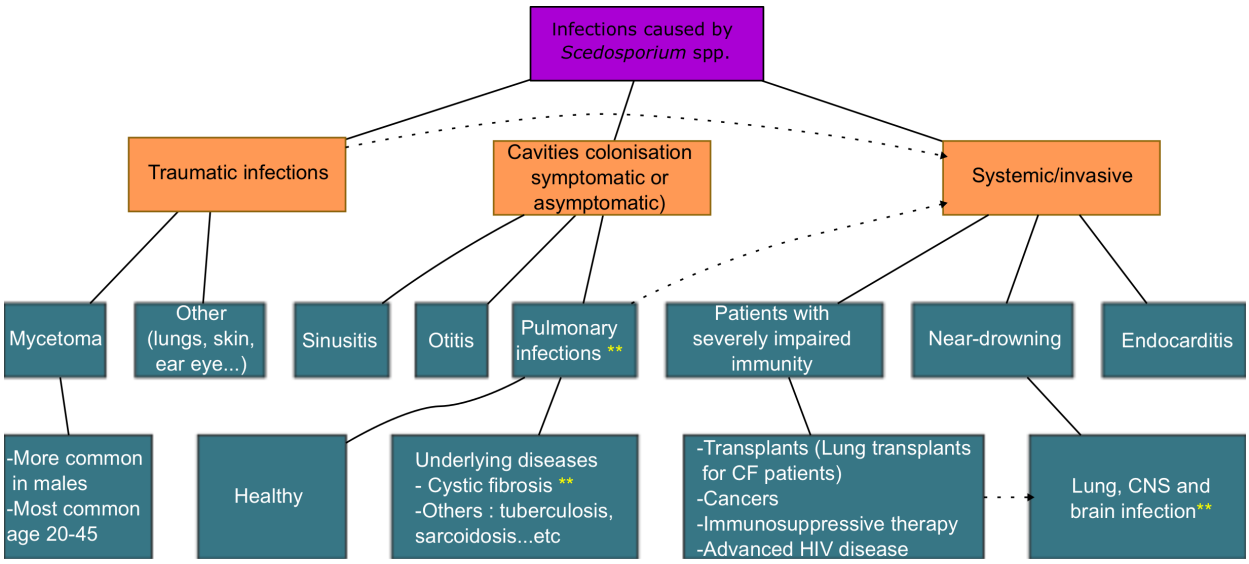

Figure I.5. Infections caused by *Scedosporium* species.
Stars indicate important disease entities. Dashed lines indicate possible routes for disease progression **[6, 34, 28]**.

Symptomatic or asymptomatic colonization of cavities is frequently caused by *Scedosporium* species. The nasal septum or the ear might act as a portal of entry causing sinusitis or otitis respectively, but such occurrences remain infrequent. The most frequent infections with *Scedosporium* species are pulmonary diseases. Kantarcioglu *et al.* **[35]** analysed all case reports of pulmonary pseudallescheriasis from 1955 to 2010; for 189 cases studied, they found that the main clinical manifestations were pneumonia (47.0%), followed by fungal balls (13.7%) and chest abscesses (9.5%). Invasive pulmonary pseudallescheriasis was mostly related to patients with impaired immunity resulting in mortality rates of 57.2%. Although colonization of the lungs of patients suffering from cystic fibrosis was underestimated in the past **[27**, **28]**, CF is now recognised as the most common underlying disease among pulmonary infections or colonization with *Scedosporium* species. Cystic fibrosis is an autosomal recessive disease caused by a mutation in the *Cystic Fibrosis Transmembrane conductance Regulator* (*CFTR*) gene; more than 1900 *CFTR* mutations leading to a disease phenotype have been identified so far **[36]**. The gene codes for a cAMP/PKA-dependent, ATP-requiring, membrane chloride ion channel that is generally found

in the apical membranes of cells in many secreting epithelia. In the lungs, the key role of this ion channel is to maintain homoeostasis of the airway surface liquid layer. The major clinical characteristics of CF are progressive lung disease caused by thick dehydrated airway mucus that entraps inhaled microorganisms, more oftenly bacteria (like *Pseudomonas* and *Staphylococcus*) than fungi (like *Candida*, *Aspergillus* and *Scedosporium, Exophiala*). Recent advances have lead to improved prevention and treatment of bacterial infections and thus to a marked increase in life expectancy, however fungal infections remain problematic. Cystic fibrosis is the most common autosomal recessive disease in Europe, it affects approximately 1 in 2500 live births among Caucasians and the significance of infections by *Scedosporium* species in CF patients has gained these fungi their worldwide recognition in the last two decades. *Scedosporium apiospermum* species are the second most frequently isolated fungi from the respiratory tract of CF patients with a frequency ranging from 3.4% to 17.4% **[25]**. *Scedosporium apiospermum* complex can chronically colonize the respiratory tract of CF patients. A recent study analysing *S. apiospermum* complex seroprevalence revealed that 9.4% of patients produced antibodies against the fungal complex **[37]**. It is important to mention here that despite the high frequency of respiratory infections with *S. apiospermum* species, these fungi are rarely isolated from air since they rank 49th over 52 detected fungal genera in the air **[21]**.

Systemic invasive infections. Both traumatic and pulmonary routes of infection with *Scedosporium* species may ultimately lead to dissemination to the central nervous system but morbidity increases when patients are immunocompromised or come from near drowning incidents. Near-drowning is a term used to describe survival or temporary survival after experiencing respiratory impairment from submersion/immersion in liquid (< 24 h survival is considered drowning rather than near-drowning **[38]**). According to the latest updates by the World Health Organisation (WHO, April 2014, **[39]**), there is an estimated 359,000 annual drowning deaths worldwide which accounts for nearly 10% of total global mortality due to injuries. According to WHO, the real magnitude of the problem goes beyond that especially that data reports are not uniformly collected from all countries. According to Ender and Dolan **[40]**, near-drowning cases should be 2 to 20 times higher than reported drowning cases. *Scedosporium apiospermum* complex are recognized as the fungi the most commonly implicated in invasive disease after near-drowning in polluted waters **[6]** and are considered as main agents of near-drowning-related brain infection **[38]**. Near-drowning related infections were much less reported with *Aspergillus* species and have not been associated to *Lomentospora prolificans* (previously *S. prolificans*) **[6**, **42]** . Buzina *et al.* **[42]** indicated that a comatose period following aspiration of contaminated water is a syndrome unique to the *S. apiospermum* complex **[23**, **42**, **43]**. The incubation period of

these infections is 1 to 4 weeks before the appearance of symptoms **[40]**. Today**,** the pathogenic mechanisms by which *Scedosporium* penetrates deep tissues and neurons remain unknown.

Scedosporium species have a particular tropism for the central nervous system but the majority of CNS infections was only seen in cases of patients with immunodeficiencies or in the case of near drowning for otherwise healthy individuals. Karioglu *et al.* **[44]** reviewed all reports of CNS infections from 1948 to mid-2007. For a total 99 case reports comprising similar percentages of healthy and immunocompromised patients, he found that the main clinical symptoms were brain abscess (69%), co-infection of brain tissue and /or spinal cord with meninges (10%) and meningitis (9%) and the total mortality rate was 74%. In the case of immunocompetent patients, CNS infection was preceded by near drowning or trauma and had a 76% fatality rate. Invasive infections due to *S. apiospermum* complex were rarely reported in CF patients after lung transplantation, nevertheless examples of therapeutic failure do exist even with the use of voriconazole treatment **[45**, **46]**.

Dissemination and CNS implication in patients with advanced immunodeficiencies such as acute lymphocytic or myelogenous leukemia, solid cancer, chronic granulomatous disease, bone marrow or solid organ transplantation, or advanced HIV disease remain problematic with poor prognosis **[44**, **47**, **48]**.

b) Virulence factors

Even though extremely rare in the air, *Scedosporium* spp. are believed to disseminate through conidia that enter into the respiratory tract and adhere to the host cells. After incubation of *Scedosporium* cells with HEp2 epithelial cells for 2 h, conidia were shown to germinate and penetrate the HEp2 epithelial cell membrane. This interaction was shown to be partially mediated by the carbohydrate moiety of the major cell wall molecule **peptidorhamnomannan** (PRM) that bound to a 25-kDa molecule on HEp2 epithelial cells **[48]**. Unlike proteinase K treatment, the mannose treatment and de-*O*-glycosylation of PRM were shown to inhibit the adherence. Thereafter, enzymes secreted by *Scedosporium* species and capable of degrading the basement membrane molecules were also extracted from mycelial supernatants. A 33-kDa **serine proteinase** belonging to the subtilisin family was purified and characterized by Larcher *et al.* **[49]**. The enzyme resembled in its biochemical and physical properties the major alkaline proteinase from *Aspergillus fumigatus* (*A. fumigatus*)*;* it was extracellular, non-glycosylated and able to degrade human fibrinogen. Moreover, Silva *et al.* **[50]** also extracted from mycelial supernatants two **metallopeptidases** with a mass of 28 kDa and 35 kDa. These enzymes showed a high activity at acidic pH (5.5) and were able to cleave extracellular matrix proteins including

laminin and fibronectin, IgG, mucins, fetuins and albumin. The ensemble of these peptidases may act as an aggravating factor for chronic bronchopulmonary inflammation that CF patients suffer from and therefore can help fungal cells to migrate into adjacent tissues.

During tissue invasion, the fungal cells are exposed to oxidative stresses generated by immune cells which can alter membrane bound and other macromolecules leading to fungal death. Gil-Lamaignere *et al.* **[51]** studied the phagocytosis of *Scedosporium* conidia by polymorphonuclear leukocytes (PMNs), mononuclear leukocytes (MNCs) and monocyte derived macrophages (MDMs). Two fungal isolates were subjected to phagocytosis by the immune cells, one isolated from a fatal disseminated infection was resistant to amphotericin B and the other isolated from a successfully treated localized subcutaneous infection was susceptible to amphotericin B. Unlike the amphotericin B-susceptible strain, serum opsonisation of the hyphae of the amphotericin B-resistant strain resulted in a higher level of superoxide ($O_2^{\bullet -}$) ion release by PMNs but lower hyphal damage by PMNs and MNCs. On the contrary, MDMs phagocytic activities were unchanged towards both isolates. This showed that the survival of the amphotericin B-resistant strain was maintaind through redox homeostasis after being subjected to phagocytosis **[51]**.

Furthermore, a study on interleukin (IL)-15, a cytokine similar to IL-2 known to activate key cells of the innate immune system, showed that this molecule (IL-15) failed to enhance damage and oxidative burst of *S. apiospermum* hyphae by PMN contrary to other pathogenic fungi like *Fusarium solani, Fusarium oxysporum, A. fumigatus, Aspergillus flavus* and *L. prolificans* **[52]**. Lima *et al.* **[53]** also purified a scavenger protein, the **Cu,Zn superoxide dismutase**, that might protect mycelial cells during the oxidative burst. The purified protein had an optimum pH activity at 7.0, a 72% identity rate with the Cu,Zn-SOD from *A. fumigatus* and its synthesis was stimulated by iron starvation **[53]**.

Scedosporium cell wall components and particularly the **α-glucan** were shown to play a role in conidial phagocytosis by macrophages that was not the case of β-glucans. Alpha-glucans were shown to stimulate the secretion of inflammatory cytokines by macrophages and dendritic cells in a mechanism involving Toll-like receptor 2 (TLR2), CD14 and MyD88 that finally led to the Tumor Necrosis Factor-alpha (TNF-α) secretion **[55**, **56]**. Moreover, **rhamnomannans** that were previously shown to allow the adherence of conidia to epithelial cells were also shown to play a role in the activation of TLR4 **[56]** as shown in **Figure I.6**.

Conidia and hyphae of *Scedosporium* spp. did not have the same induction pathways for macrophages. While conidial recognition involved only TLR4, hyphal recognition was dependent on both TLR2 and TLR4 pathway channels **[57]**. Other cell wall molecules, the **glucosyl ceramides** (GlcCer), which belong to ceramide monohexosides (CMH), were shown to interfere with the fungal phagocytosis by marcrophages since the addition of anti-

CMH monoclonal antibody (MAb) significantly increased phagocytosis **[58]**. **Ectophosphatases** were also found on the cell walls that might hypothetically play a role in the protection against acidic conditions, allow adhesion to host cells and be involved in the endocytosis by vascular endothelial cells **[59]**.

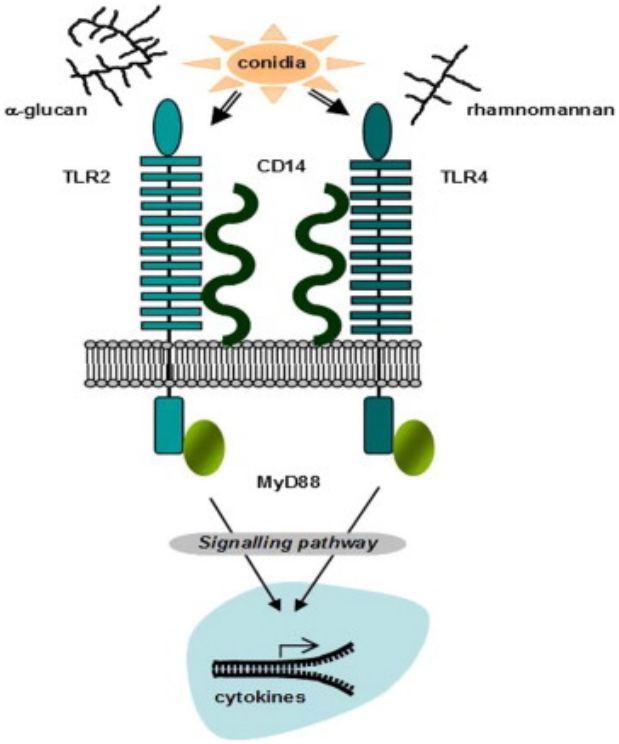

Figure I.6. Recognition of alpha-glucans and rhamnomannans of *S. boydii* by TLR2 and TLR4, respectively.
From Figueiredo *et al*. **[57]**.

The accessibility to iron during pathogenesis is primordial for pathogenic microorganisms since it is involved in many cellular processes such as ergosterol synthesis, respiration and detoxification of free radicals. In human hosts, iron is not easily accessible; therefore microorganisms have developed numerous mechanisms to scavenge iron. For this, Bertrand *et al.* **[60]** identified two hydroxamate siderophores from expectorations of patients colonized by (or infected with) *Scedosporium* species and these are the **dimerumic acid** and **N*α*-methyl coprogen B**.

Another factor contributing to the pathogenesis of *Scedosporium* species was described by Raggam *et al*. **[61]** who studied the expression of a heat shock protein-60 (HSP-60). This protein is considered as an immunodominant antigen involved in humoral and cellular responses and in the induction of regulatory T cells by interaction with cells of the innate immune system.

The various elements contributing to the virulence of *Scedosporium* species are summarized in **Table I.2**.

Table I.2. Summary of virulence factors produced by *Scedosporium* species.

Name	Location	Role during pathogenesis	Ref
33-kDa serine proteinase	Extracellular, secreted	Degradation of human fibrinogen	[49]
28 and 35 kDa metallopeptidases	Extracellular, secreted	Cleavage of laminin and fibronectin extracellular matrix proteins	[50]
Cu,Zn-SOD	Cytoplasmic	Scavenging and protection during oxidative burst	[53]
α-glucans	Cell wall	TLR2 activation	[54]
Rhamnomannans	Cell wall	Epithelial cell adhesion, activation of TLR4	[49, 57]
Glucosyl ceramides	Cell wall	Interfere against phagocytosis	[58]
Siderophores: Dimerumic acid and N*α*-methyl coprogen B	Extracellular, secreted	Iron scavenging	[60]
HSP-60	Mitochondrial *	Immunomodulation, induction of T_{reg} *	[61]
Ectophosphatases	Cell wall	Protection against acidic conditions, adhesion to host cells and endocytosis by vascular endothelial cells *	[59]

* Hypothetical

c) Diagnosis

Scedosporium species are fungi of increasing clinical importance, but their diagnosis at present remains challenging mainly because of the similarities of clinical features and histopathology with other relatively common hyaline hyphomycetes like *Aspergillus* or *Fusarium* species. Today the detection of these species mainly relies on cultural methods, but these techniques present many inconveniences since the type of culture medium used, the temperature and duration of incubation might greatly affect the growth of fungi, thus favoring the growth of some fast-growing fungi over others. Therefore, the use of semi-selective media, like SceSel+, Scedo-Select III or others, is essential for the proper detection in respiratory secretions **[62]**.

Other diagnostic techniques include histochemical staining, but again this technique has its inconveniences since the cytopathology and/or histopathology in infections caused by *Scedosporium* spp., *Aspergillus* spp., *Fusarium* spp., *Petriella* spp. and other hyaline hyphomycetes are very similar. *Scedosporium* species may present hyphae with branching at acute angles, dichotomous branching or more irregular branching. *Scedosporium* species may also present terminal or intercalary chlamydospores that can be confused with yeasts **[6]**.

More efficient diagnostic techniques include serology, biochemical techniques and molecular techniques. For serology, an interesting study by Thornton **[63]** described the development of MAbs that bound an immunodominant 120 kDa carbohydrate epitope present on the conidial and hyphal cell walls of *S. boydii* and closely related species. More importantly, these MAbs did not react with *L. prolificans*, *S. dehoogii*, *A. fumigatus, Candida albicans, Cryptococcus neoformans, F. solani* and *Rhizopus oryzae.* Further investment in the development of such molecules can be a turning point for the detection of *S. apiospermum* complex infections. Other studies also presented potential interesting antigens for the development of specific antibodies like peptidorhamnomannans or pseudacyclins **[65**, **66**, **67]**.

As an alternative to cultures, Bertrand *et al.* **[67]** described a potential biomarker of the airway colonization by the *S. apiospermum* complex. This marker was a siderophore named N^{α}-methyl coprogen B, exclusively identified for the *S. apiospermum* complex. It was identified in expectorations after being analysed with High Performance Liquid Chromatography (HPLC) followed by positive electrospray ionization-mass spectrometry **[67]**.

Molecular techniques are particularly important for epidemiological studies, hereof there exist two techniques for *Scedosporium* species detection in expectorations: PCR amplification of internal transcribed spacer (ITS) sequences **[68]** or β-tubulin sequences from total DNA extracts **[69]** and an oligonucleotide array using species-specific probes **[70]**.

Finally the unexpected diversification of pathogenic *Scedosporium* species and the number of other pathogenic fungal agents that can complicate fungal identification, necessitate early and specific diagnosis in order to improve treatments.

d) Treatment

Meletiadis *et al.* **[71]** investigated the susceptibilities of 13 clinical isolates of *Scedosporium* species to a range of new and conventional antifungal agents belonging to three classes of antifungals: the azoles (miconazole, itraconazole, voriconazole,

posaconazole and UR-9825 which is now called albaconazole), polyenes (amphotericin B, nystatin and liposomal nystatin), and allylamines (terbinafine). This study showed that the highest growth-inhibitory activity was for voriconazole (MIC_{90} 0.5 µg/ml), followed by miconazole (MIC_{90} 1 µg/ml), posaconazole (MIC_{90} 2 µg/ml), UR-9825 (MIC_{90} 2 µg/ml), itraconazole (MIC_{90} 4 µg/ml) and amphotericin B (MIC_{90} 16 µg/ml) **[71]**. No statistically significant difference in the antifungal activities after 48 h or 72 h of incubation was seen for any of the drugs. These results were further confirmed by a recent study that compared the antifungal susceptibilities of the different *Scedosporium* species (332 isolates) to itraconazole, voriconazole, posaconazole, isavuconazole, caspofungin, micafungin, anidulafungin and amphotericin B **[72]**. The study found that voriconazole and posaconazole were the most promising drugs against all *Scedosporium* species whereas micafungin was very promising if *S. aurantiacum* was excluded.

Despite the promising antifungal activity of voriconazole on *Scedosporium* species based on MIC values, a recent study on 43 patients treated with voriconazole for a *S. apiospermum* complex infection showed only 54% successful response rates in patients **[73]**. Response rate was either lower in one study where 2 out of 6 patients (33%) infected with *S. apiospermum* complex responded to voriconazole treatment **[74]**, or higher in another study where 5 patients out of 6 (83%) responded to voriconazole treatment **[75]**. Hereby, the mortality rates from infections with *S. apiospermum* complex after treatment with voriconazole, our best antifungal so far, ranges between 17% and 67%. However such values seem to resemble the worldwide mortality rates by other fungi like *C. neoformans* (20–70%), *C. albicans* (46–75%) and *A. fumigatus* (30–95%) **[8]**. The resemblance of mortality ranges incites the need for better antifungal drugs.

A novel orally active antifungal molecule named E1210 that targets glycosylphosphatidylinositol (GPI)-linked protein biosynthesis seems to hold promise for the treatment of a wide range of medically relevant yeasts and molds like *Candida* spp. (MIC_{90} of < 0.008 to 0.06 µg/ml; except *C. kruzei*), *A. fumigatus* (MIC_{90} 0.13 µg/ml), *S. boydii* (MIC 0.03 to 0.13 µg/ml) and *L. prolificans* (MIC 0.03 µg/ml) and *C. neoformans* (MIC 0.13 to 0.5 µg/ml) among others. Antifungal activity of E1210 was generally either higher or comparable to that of voriconazole. Cytotoxicity assays using human HK-2 cells showed low toxicities as low as that of fluconazole. E1210 also demonstrated a consistent efficacy in murine models of oropharyngeal and disseminated candidiasis, pulmonary aspergillosis, and disseminated fusariosis, its efficacy *in vivo* with other fungal infections remains to be determined. However based on these results, E1210, which is first-in-class, is likely to be a promising antifungal agent for the treatment of invasive fungal infections **[77**, **78]**. Interestingly, another novel molecule also inhibiting GPI anchor biosynthesis named gepinacin (for GPI acylation

inhibitor) showed an increased immunogenicity of *C. albicans*, by disrupting the mannoprotein outer layer of the cell wall and therefore unmasking the more immunogenic inner β-glucan layer which might also explain the mechanism of action of E1210 **[78]**. Finally, GPI-linked mannoproteins components of the fungal cell wall remain interesting targets for antifungal drugs.

I.4.2. Biotechnological applications

Despite the pathogenic nature of some of them, fungi have great benefits since early historic times. The intricate and unique metabolic processing makes them one of the most important groups of organisms in modern technology, where food and various metabolites such as antibiotics, steroids, enzymes and alkaloids are produced on an industrial scale. Moreover, fungi have a remarkable degradation capacity that helps in pollution control and recycling.

In this context, a number of molecules have been discovered in *Scedosporium* species as summarized in **Table I.3**; their discovery will be henceforth explained in a chronological order. The first molecules date back to 1985 where Maebayashi *et al.* **[79]** extracted two metabolites from the fungus *S. boydii* IFM 4642 named **Pseurotin A** and **PB-4** that had an inhibitory effect on monoamine oxidase. Pseurotin A is produced also by other fungi like *Pseudeurotium ovalis* or some aspergilli and it is already commercialized as an inhibitor of IgE production, as a nematicidal molecule and a stimulator of neuritogenic activity (neuritogenesis is the outgrowth of dendrites and axons from neuron cells which is important for neuronal maturation during the development of CNS) **[80]**.

In 1993, Kuroda *et al.* **[81]** extracted from *Scedosporium* sp. SPC 15549 a novel inhibitor of acyl-CoA:cholesterol acyltransferase (ACAT) named AS-183. ACAT is responsible for cholesterol ester formation in atherogenesis and in cholesterol absorption from the intestines. Therefore, inhibitors of ACAT are effective for the treatment of atherosclerosis and hypercholesterolemia.

Tyroscherin and tyroscherin analogues were extracted in several *Scedosporium* species in several studies. In 2004, there were two studies, the first one by Hayakawa *et al.* **[82]** who extracted a **tyroscherin** molecule from *Scedosporium* sp., this molecule had an inhibitory effect on insulin-like growth factor-1 (IGF-1) that is a receptor known to be significant for tumor cell growth and survival. The second study was by Kamigri *et al.* **[83]** who extracted a tyroscherin-analogue named **YM-193221** from the fungus *P. ellipsoidea* CBS 128.78 that presented a potent antifungal activity against *C. albicans* by the inhibition of mannan synthesis. Later on, these two molecules were studied again by Katsuta *et al* **[84]** to improve extraction methods. In 2013, Nirma *et al.* **[85]** also identified two molecules named Tyroscherin and N-methyltyroscherin from *S. boydii* SNB-CN73, both

molecules presented antifungal activities against *C. albicans* and *Trichophyton rubrum* (*T. rubrum*).

Table I.3. Summary of molecules produced by *Scedosporium* species with a biotechnological application

Name	Activity	Application	Fungus	Ref
Pseurotin A	Inhibitory of monoamine oxidase	Inhibition of IgE production Nematicidal activity Stimulation of neuritogenic activity	*S. boydii* IFM 4642	[79]
PB-4	Inhibitory of monoamine oxidase	NS	*S. boydii* IFM 4642	[79]
AS-183	Inhibitor of ACAT	Treatment of atherosclerosis and hypercholesterolemia	*Scedosporium* sp. SPC 15549	[81]
Tyroscherin	Inhibits insulin-like growth factor-1 (IGF-1)	Antitumor activity against IGF-1 dependent cells	*Scedosporium* sp.	[82]
YM-193221 (Tyroscherin analogue)	Inhibition of mannan synthesis	Antifungal against *C. albicans*	*P. ellipsoidea* CBS 128.78	[83]
Tyroscherin and N-methyl tyroscherin	NS	Antifungals against *C. albicans* and *T. rubrum*	*S. boydii* SNB-CN73	[85]
Gliotoxins (1), (2) and (3)	NS	Antibacterial activity against MRSA and MDRSA	*Scedosporium* sp. (MFB165)	[86]
Pseudallin	Inhibit A. brassicicola	Antitumor activity against IGF-1 dependent cells Control black leaf spot disease of cabbage plants	*S. boydii* TKF-4	[87] [88]
Ligninolytic enzymes	Biological treatment of wood fibres	Improve the production of wood-based composites	*P. angusta* MF4	[89]
Botryorhodine F and C	NS	Antitumor activity against A549 non-small-cell lung cancer cell line	*S. boydii* NTOU2362	[90]
Pseudaboydin A	Moderate cytotoxic activity	Moderate antitumor activity against 3 cancer cell lines	*S. boydii* (marine strain)	[91]

NS: Not specified

In 2006, three other metabolites were extracted from the strain *Scedosporium* sp. MFB165 by Li *et al*. **[86]**, the dioxopiperazine, dehydroxybisdethiobis(methylthio)gliotoxin (1), the bisdethiobis(methylthio)gliotoxin (2) and gliotoxin (3) and these molecules presented a potent antibacterial activity against the methicillin-resistant and multidrug-resistant *Staphylococcus aureus*. Gliotoxin (3) had a significant radical scavenging activity.

In 2010, Ko *et al.* **[87]** isolated from the soil four *S. boydii* strains capable of inhibiting the germination of *Alternaria brassicicola* and thus reducing the disease incidence of black leaf spot of spoon cabbage caused by *A. brassicicola.* The potent fungistatic molecule was then identified to be 6-6'-bis (2 *H*-pyran-3-carbaldehyde) ether that was named pseudallin **[88]**.

Later on, Guisado *et al.* **[89]** discovered a strain with high ligninolytic activity named *P. angusta* MF4. The strain had a high production rate of ligninolytic enzymes in the presence of inducers. Unlike *A. flavus* MF 20, this strain was capable of achieving the highest values of growth after 21 days of incubation on sawdust without any additional nutrients. The transformation of residual lignocellulosic materials into added-value products using microorganisms is considered an environmentally friendly alternative to chemical treatments for the manufacturing of composites.

Last year, Chang *et al.* **[90]** extracted nine molecules from a *S. boydii* strain NTOU2362; among these molecules two of them, botryorhodine F and C, exhibited moderate to potent growth inhibition activity on A549 non-small-cell lung cancer cell line with GI_{50} values of 41.3 and 4.1 µM, respectively, in comparison with fluorouracil (GI_{50} = 3.6 µM).

Finally, few months ago, Lan *et al.* **[91]** extracted from a marine strain of *S. boydii*, associated with the starfish *Acanthaster planci* two novel isobenzofuranone derivatives, pseudaboydins A and B along with 5 other molecules. Pseudaboydin A showed moderate cytotoxic against human nasopharyngeal carcinoma cells HONE1, human nasopharyngeal carcinoma cells SUNE1 and human glandular lung cancer cells GLC82 with IC50 values of 37.1, 46.5 and 87.2 µM, respectively.

Other biotechnological applications were also proposed for *Scedosporium* species concerning bioremediation, especially that these fungi are mainly isolated from polluted soil and water. The first study on the growth of *Scedosporium* species on known pollutants dates back to 1988 by Onodera *et al.* **[92]**. However, this topic will be discussed in detail in another section of this thesis (General Discussion).

II. The fungal cell wall

The discovery of the fungal cell wall dates back to the early 18th century. This structure remained virtually ignored by researchers and was assumed to act merely as a backbone that held together the internal organelles **[93]**. In the beginning of the 20th century, research on cell walls, mainly in plants and bacteria, started to expand and later on, the biotechnological industry employing fungi intensified the progress of scientific investigations on fungal cell walls. This shift was a turning point for scientific research on fungi since major classes of antifungal drugs currently in use or still under investigation target the fungal cell wall components or biosynthesis (ergosterol, chitin, β 1,3 glucan β 1,6-glucan and GPI-anchored proteins) **[77**, **95]**.

Our understanding of the fungal cell wall underwent major changes; it is now viewed as a dynamic structure that evolves to fit vital needs while providing the fungal cell structure. It acts like a modular gateway that protects the fungus from harmful chemical, physical and biological aggressions. It maintains internal homeostasis, senses the external stimuli and recognizes the external biological and inert surfaces. It also provides selective permeability for molecules allowing the accumulation of those necessary for fungal survival or those to be secreted to the outer medium **[95]**. This wide panel of functions provided by the cell wall highlights the role of its components for the development of antifungal drugs, the diagnosis of fungal infections and also for various biotechnological applications.

II.1. Components of the fungal cell walls and their functions

The general organization of the cell wall may vary between fungi or even in the same fungal species during diverse morphological stages as revealed by electron microscopy techniques.

The fungal cell wall is mainly composed of polysaccharides, proteins, melanin and lipids that are cross-linked together, which renders it challenging to study. However the development and the combination of microscopic (atomic force microscopy, electron microscopy,…), immunological and molecular techniques provided critical information about the location of different components within the wall, giving a picture of a carbohydrate-rich inner cell wall layer and a protein-rich outer layer. The development of mass spectrometry techniques (gas chromatography-mass spectrometry, GC-MS; nano liquid chromatography with MS/MS, nano LC-MS/MS;…), nuclear magnetic resonance (NMR) and chromatography techniques also allowed the identification and characterization of various cell wall components. The different cell wall constituents and their functions will be a major focus of this part.

II.1.1. Polysaccharides

Polysaccharides are the most abundant cell wall components in fungi, they make at least 90% and 85% of the cell wall dry weight in *A. fumigatus* **[96]** and *Saccharomyces cerevisiae* **[97]**, respectively. The richness of fungal cell walls with polysaccharides is mainly due to glucans and mannan-containing polymers.

a) Glucans

Glucans is a name given to a number of polysaccharides made solely of glucose residues, but different types of linkages may occur; thus alpha glucans with α-1,3 bonds and beta glucans with β-1,3, β-1,6 or β-1,4 bonds may be distinguished **[96**, **99]**.

β-1,3-Glucans constitute the major class of glucans found in the fungal cell walls with a mass ranging from 30% in *C. albicans* to 87% in *Neurospora crassa* **[96**, **100**, **101]**. β-1,3-Glucan is a branched polymer with β-1,6 inter-chain links and a coiled spring–like structure that confers elasticity and tensile strength to the cell wall **[97]**. The glucan is synthesized by β-1,3-glucan synthase. In *A. fumigatus, C. neoformans, N. crassa*, and *C. albicans* there is one β-1,3-glucan synthase, called *FKS1*, while in *S. cerevisiae* and *Schizosaccharomyces pombe* (*S. pombe*) there are 3 and 4 β-1,3-glucan synthases, respectively **[99]**. *FKS1* mutations dramatically affect fungal morphology and growth, therefore such enzymes form major targets for antifungal agents like drugs belonging to the echinocandin family that induce cell swelling and lysis **[100**, **102]**. Following synthesis, β-1,3-glucans undergo remodeling inorder to be incorporated in the preexisting cell wall. An array of enzymes is responsible for such remodeling in *A. fumigatus* including exoβ(1-3)glucanases (*EXG1* to *EXG10*), endoβ(1-3)glucanases (*ENGL1* to *ENGL8*), other exo-β-glucanases (*EXG12* to *EXG21*), branching enzymes (*BGT1* to *BGT3*, *SCW4* and *SCW11*), elongation enzymes (*GEL1* to *GEL7*) and cross linking enzymes (*CRH1* to *CRH5*) **[102]**. β-1,3-Glucans are well known pathogen associated molecular pattern (PAMPS) molecules that can be recognized by Dectin-1 and that induce strong pro-inflammatory responses by the innate immune system **[103]**.

β-1,6-Glucan polymers are found in *S. cerevisiae* (10-15% of cell wall dry weight), *C. albicans* (43-53% of cell wall dry weight) and *C. neoformans* but are absent in *A. fumigatus, N. crassa* and *S. pombe* **[99]**. β-1,6-polymer is shorter than β-1,3-glucan, it is amorphous in structure and forms covalent bonds with β-1,3-glucan, chitin, and cell wall mannoproteins, which gives flexibility to the cell wall structures **[98**, **105]**. In *C. albicans,* mutations in *KRE5,* a gene involved in β-1,6-glucan synthesis, lead to mutants with severe cell wall defects : mutants were unable to form hyphae on solid medium even in the presence of serum, they showed 50% reduction in adhesion to human epithelial cells and were completely avirulent in mouse models **[105]**.

The mixed β-1,3-/β-1,4-glucans were first discovered in *A. fumigatus* **[106]**. Chitin, galactomannan and the linear β1-3/1-4 glucan were found covalently linked to the non-reducing end of β-1,3-glucan side chains. Later on, 1,4-linked glucose was identified as one of the major sugars in *N. crassa* suggesting presence of such mixed polymer **[100]**. However, the synthesis and function of this type of β-1,3-/β-1,4-glucans remain unknown **[99]**.

α-1,3-Glucans have been found in a number of fungal cell walls, in *A. fumigatus* (35-46% of cell wall dry weight), *S. pombe* (18–28% of cell wall dry weight), *C. neoformans* where they are necessary for anchoring the capsule to the cell wall and in the conidial wall of *N. crassa* **[99]**. α-1,3-Glucans were found to be linked to virulence in many fungi. In *A. fumigatus*, they were indirectly linked to virulence since the deletion of an α-1,3-glucan synthase gene, *AGS3*, led to a hypervirulent mutant strain due to a compensation mechanism consisting of an increased amount of melanin in the conidial cell wall which resulted in a higher resistance to reactive oxygen species **[107]**.

b) Mannose-containing polymers

Mannose polymers in the fungal cell wall are mostly in the form of carbohydrate moiety of glycoproteins in *C. albicans* and *S. cerevisiae*. Mannan polymers also exist in the form of heteropolysaccharides as galactomannans in *A. fumigatus* (20-25% of cell wall), *N. crassa* (12% of cell wall), *S. pombe* (9-14% of cell wall) and *C. neoformans* or as rhamnomannans in *Sporothrix schenckii*, *Ceratocystis stenoceras, Ceratocystis ulmi* and *L. prolificans* **[65**, **100**, **109]**. The majority of the cell wall mannan-containing polymers are found on cell wall proteins as post-translational modifications, but in *A. fumigatus* galactomannan has also been found linked to lipids. Synthesis of homo- or heteropolymers occurs through mannosyltransferases, but other enzymes responsible for the addition of galatofuranose side chains for example are yet to be identified **[99]**.

Two types of linkages exist in mannoproteins between the mannan-containing chains and the protein core, the *O*-glycosidic linkage between mannose and the hydroxyl group of the amino acids serine and threonine, and the *N*-glycosidic bond. In this last case, a high molecular weight and highly branched mannan chain is linked to the protein moiety at the asparagine residues found in the context of Asn-X-Ser/Thr within the amino acid sequence of the protein (X is any amino acid except proline) **[99]**.

Mutational analysis shows that *O*-linked oligosaccharides are essential for growth, morphology, and virulence of *C. neoformans, C. albicans, A. fumigatus* and *N. crassa* **[100**, **102**, **110]**. Given the fact that almost all cell wall proteins are extensively *O*-glycosylated,

one might suspect that tempering with *O*-linkages would compromise the activity of attached proteins or render them vulnerable to degradation.

Finally, mannoproteins are generally more abundant on the external leaflet of the cell wall, thus covering both glucans and chitin **[111**, **112]** and in *C. albicans* mannosides were shown to have adhesive and immunomodulatory properties during infections which is essential during the early stages of colonization as well as during the host tissue invasion **[112]**.

c) Chitin

Chitin is a linear polymer of β-(1,4)-linked *N*-acetylglucosamine. This polymer is less abundant in fungal cells walls than β-glucans since it forms only 1-2% of the total cell wall dry weight in *S. cerevisiae*, 2-6% in *C. albicans*, 7-15% in *A. fumigatus*, and 4% in *N. crassa* **[99]**. The chains of chitin associate by hydrogen bonds to form microfibrils arranged in different forms. Among the 3 structures known so far in nature, only the α-chitin has been found in fungal cell walls where the sugar chains run antiparallel to each other. This ribbon-like structure accounts for the extreme insolubility and great rigidity of these molecules, which confers stretching resistance to fungal cell wall. In fact chitin has a tensile strength higher than that of steel (4000 MPa *vs.* 2800 MPa) and is said to be the toughest molecule found in nature **[113]**. Chitin deposition in the fungal cell wall is controlled spatially and temporally **[97]**. Until now, seven different classes of chitin synthases are known in fungi **[114]**. Even thought the functional significance of all these classes remains unknown, it is believed they perform redundant roles in cell wall synthesis with class II enzymes being the most consequential on cell viability. Chitin chains are covalently cross-linked to β(1,3)-glucans. Immunogenicity of chitin seems to be dependent on the size of the molecule with small ones being most immunogenic. Chitin provokes allergic immune responses by chitin-degrading enzymes released by human host cells resulting in the accumulation of IL-4 expressing basophils, eosinophils and neutrophils in tissues and induces alternative macrophage activation **[114]**. Immune responses to chitin are mediated by RegIIIg, a C-type lectin that is expressed in neutrophil-like Paneth cells **[114]**.

d) Chitosan

Chitosan is a deacetylated form of chitin; it is a polymer of glucosamine that is produced enzymatically by chitin deacetylases (EC 3.5.1.41) **[115]**. Chitosan is more flexible and soluble than chitin allowing cell wall plasticity in response to various environmental stimuli and during fungal growth. In *C. albicans* less than 5% of chitin is deacetylated into chitosan while in *C. neoformans* more than two thirds of chitin is

deacetylated and it can exceed the chitin content of the cell wall by ten folds **[117**, **118]**. Mutations in chitin deacetylases in *S. cerevisiae* were not lethal while in *C. neoformans* such deletions resulted in a "leaky melanin" where melanin molecules could no more be fully retained in the cell wall. Of note, *S. cerevisiae* is a non-melanized fungus and the amount of chitosan present in its cell wall is lower than that in *C. neoformans* which would explain the difference in the associated phenotype **[115]**. Chitosan can activate dendritic cells via a TLR4-dependent mechanism but this does not lead to T-cells stimulation since no cytokine production occurs. However, co-stimulation with other microbial PAMPS can override this partial activation **[118]**.

II.1.2. Proteins

From a quantitative point of view, proteins are much less abundant than cell wall polysaccharides forming about 3% to 20% of the cell wall dry weight only. Nevertheless, they have extremely important roles in maintaining the cell shape, mediating adhesion for cell migration and fusion, protecting the cell against foreign substances, mediating the absorption of molecules, transmitting intracellular signals from external stimuli and synthesizing and remodeling cell wall components **[96**, **120]**. There exist two types of fungal cell wall proteins: integral and non-integral proteins. Integral proteins are found cross-linked to the fibrillar meshwork of polysaccharides (chitin and glucans) in the cell wall while the non-integral proteins are found associated to the cell wall and can have important functions like many hydrophobins.

Hydrophobins form amphiphatic layers on the surface of specific cells giving a protective hydrophobic coating to filamentous fungi. They play a role in fungal growth, aerial growth in particular, in the interaction of fungi with their environment and attachment to solid supports as well as adherence to the host tissues **[120]**. By 2005, there were at least 70 unique hydrophobin gene sequences identified in fungi **[120]**. Hydrophobins are moderately hydrophobic proteins with hydrophobicity indices (Grand Average of Hydropathy, GRAVY) that vary between 0.01 and 0.6, but less than 20% of hydrophobins in Ascomycota have hydrophobicities higher than 0.5 GRAVY values **[121**, **122]**. Hydrophobins are all secreted proteins with signal peptides; they have poor nucleotide sequence homology but a conserved spacing of eight cystein residues and can be generally divided into two classes (**Figure I.7**). However it is important to mention that a recent study on 9 genome sequences of *Aspergillus* species showed that among 50 identified hydrophobins, 26 could not be classified in either classes and showed intermediate forms **[122]**. Class I hydrophobins show a considerable cysteine-spacing variation unlike to Class II **[123]**, they form highly insoluble membranes in water, organic solvents and 2% SDS **[121]** and they are present in both Basidiomycetes and Ascomycetes **[120]**. Class II hydrophobins can be

dissolved in aqueous ethanol (60%) or SDS 2%, they lack the rodlet morphology of class I hydrophobins **[124]** and they have only been identified in Ascomycetes. Hydrophobins have been correlated to fungal pathogenicity, for example a class I hydrophobin, mpg1 protein identified in *Magnaporthe grisea* (*M. grisea*) has been shown to play a role during rice blast disease symptom development and in the perception of inductive surfaces for the initiation of appresorium development suggesting that it functions in the intimate association between fungi and surfaces on which they are living on **[125]**. On the other hand, the deletion of the class II hydrophobin cerato-ulmin in *Ophiostoma novo-ulmi* showed no reduction in pathogenicity of this fungus during Dutch elm disease **[126]**. In *A. fumigatus,* 8 hydrophobins have been detected in the genome of multiple strains **[127]**, the expression of 6 of which, named rodAp through rodFp, was reported by Beauvais *et al.* **[128]**. All 6 proteins belong to class I hydrophobins, but only one, rodAp, seems to be responsible for the rodlet layer structure found on the surface of conidia **[129]**. RodAp plays a key role in rendering conidia immunologically inert but it has a predicted GPI anchor which makes it an integral cell wall protein.

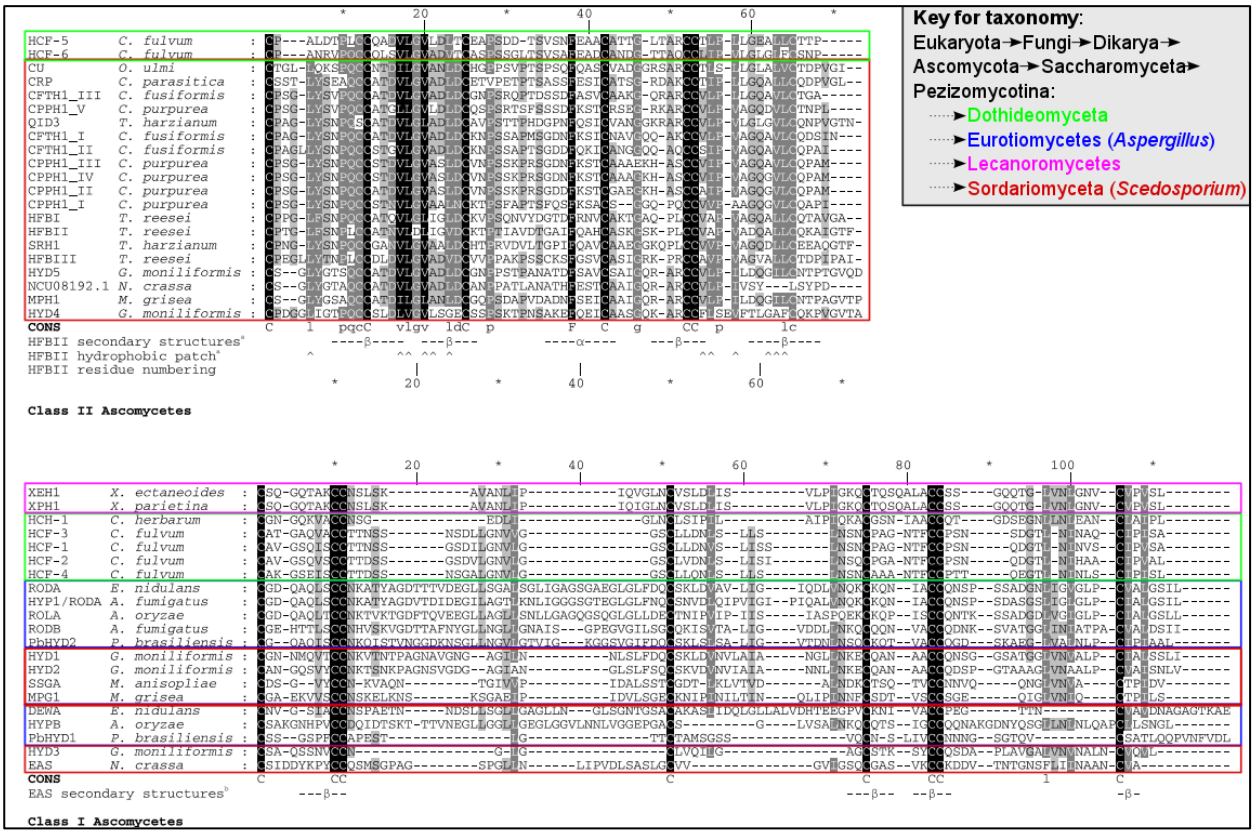

Figure I.7. Regrouping hydrophobin (Class I and Class II) sequence alignments from Ascomycota according to the taxonomical classifications (adapted from Linder *et al.* **[120]**).

The second type of cell wall proteins are those covalently linked to the cell wall polysaccharide components and these are also divided into two classes. The first are Pir (*p*roteins with *i*nternal *r*epeats) proteins and the second class that is more abundant, is anchored to the cell wall through a glycosylphosphatidyl inositol (GPI) moiety.

Regarding the GPI-anchored proteins, it is important to note that they may be targeted to the plasma membrane and/or to the cell wall. However it is not always easy to determine the fate of these proteins since some proteins might be found in both compartments while others might be restricted to one **[130]** and the categorization of these proteins to the cell wall or plasma membrane remains a matter of ongoing research. Cell wall GPI-anchored proteins play a role during pseudohyphal and invasive growth, iron and water retention, sterol uptake, cell wall porosity, flocculation, recognition of mating partners, cell wall maintenance, protection against environmental stressess, cell wall repair, adhesiveness and hydrophobicity, cell-cell interactions, virulence, biofilm formation, antigenicity, iron uptake, and various enzymatic functions **[131]**. The GPI anchor is added to proteins through a transamidase complex, located at the lumenal side of the endoplasmic reticulum (ER). This enzymatic complex recognizes a C-terminal signal in substrate proteins, cleaves the C-terminal propeptide from the proprotein substrate and attaches a GPI moiety (a composite structure including an inositol phospholipid and an oligosaccharide with, at least, one phosphoethanolamine substitution) at the attachment site called ω-site **[132]**.

In 2003, de Groot, Hellingwerf and Klis **[133]** proposed an update to the consensus sequence described by Caro *et al.* **[134]** in 1997 for the GPI attachment site and its downstream region. The new algorithm based on analysis of 4 genomes was as follows: [NSGDAC]–[GASVIETKDLF]–[GASV]–X(4,19)–[FILMVAGPSTCYWN](10)>, where > indicates the C-terminal end of the protein and X denotes any amino acid, and the first brackets correspond to the ω-site, the second brackets correspond to the ω+1, the third to ω+2 and the last brackets correspond to the hydrophobic tail that is necessary to retain the protein on the membrane until GPI modification. However in 2004, a new software named "Big-PI fungal predictor" (accessible at: http://mendel.imp.ac.at/gpi/fungi_server.html) was proposed by Eisenhaber *et al.* **[132]** for genome-wide GPI-anchor detection and the analysis was based on more additional features. The new criteria permitted a more precise detection of GPI-anchored proteins. Therefore the canonical sequence motif for the C-terminus of proproteins was described as consisting of four necessary subsegments: (1) a polar, flexible linker (ω - 11... ω - 1) without intrinsic secondary structural preference; (2) the volume-constrained ω-site region (ω - 1... ω + 2); (3) a moderately polar spacer (ω + 3... ω + 9); and (4) a hydrophobic tail beginning with ω + 9 or ω + 10 up to the C-terminal end. It is noteworthy that the algorithm in this software, although highly precise, has a less optimal

sensitivity resulting in a false negative rate as high as 20% as suggested by de Groot and Brandt **[127]**. Later on, a new software was also proposed, called proFasta (accessible at: http://www.bioinformatics.nl/tools/profasta/) that allows pipeline filtering through composition or pattern recognition and pI values. These and other filters can also be applied on results obtained from Big PI, TMHMM (for the detection of transmembranal helixes) and Signal IP (for the detection of signal peptides) and this software seems to be very promising **[127]**.

Finally, data currently available on many yeast and mycelial genomes indicate that members belonging to the Gas/Gel, Crh and other GPI-cell wall protein families are widespread among the ascomycetous fungi, which is consistent with their specific roles. For example Gas/Gel family members are involved in elongating β-1,3-glucan, a widespread cell wall polysaccharide, while Crh family members are transglycosylases believed to be involved in attaching chitin to β-glucan **[103**, **136]**. Interestingly, this Crh family was not found in the fission yeast *S. pombe* which is in agreement with the absence of chitin in its cell wall **[135]**.

As for the other less abundant class of integral cell wall proteins, the Pir proteins, they consist of a putative N-terminal signal peptide, followed by a Kex2 endoprotease cleavage site, an internal repeat region with a variable number of repeats of Q-[IV]-X-D-G-Q-[IVP]-Q (Prosite format), and a C-terminal cysteine-based motif **[98**, **128]**. Genome database search allowed the detection of 76, 11, 5, 3 and 1 Pir proteins with two or more repeat units in *S. cerevisiae, C. glabrata, C. albicans, N. crassa* and aspergillar species, respectively **[127]**. In *S. cerevisiae,* Pir proteins are linked to β-1,3-glucan chains through a yet unidentified mild-alkali-sensitive linkage, whereas GPI-anchored proteins can be released by hydrofluoric acid treatment that cleaves the phosphodiester bond **[136]**. Current lines of evidence in *S. cerevisiae* and *Candida* species indicate that the expression of these proteins changes in response to environmental conditions suggesting a protective role **[98**, **138]**.

Finally, researchers working on cell wall protein extraction almost invariably find a set of "cytosolic" proteins, even when the preparations are rigorously treated with alkali, high salts, and boiling SDS solutions **[138**, **139**, **140**, **141**, **142]**. In *S. cerevisiae*, these proteins were also found in the extracellular medium which suggests that they are released by the cells and their detection is not due to contamination during cell lysis and isolation of the cell wall **[141]**. These proteins are often referred to as "noncanonical" or "nonconventional" cell wall proteins. The mechanism by which these proteins get cross-linked to the cell wall remains enigmatic, as well as whether they are true cell wall proteins or not, and whether they have cell wall-specific functions. For now, most studies on the cell wall largely disregard these proteins **[99]**.

II.1.3. Melanins

The term "melanin" originates from the Greek word *melanos*- meaning black. Melanins are high molecular weight pigments with a variety of biological functions. For more than 50 years, fungi were known to produce this pigment, but unlike other components of the fungal cell wall, its molecular structure remains elusive **[142]**. Melanins are macromolecules formed by oxidative polymerization of phenolic and/or indolic compounds. These pigments are usually black or brown but other colors do exist. Melanins are generally defined based on their properties since they are (i) insoluble in water and organic solvents, (ii) resistant to concentrated acids and to bleaching by oxidizing agents as hydrogen peroxide and hypochlorite ions and (iii) soluble in hot alkaline solutions, criteria that are useful for melanin extraction. Nowadays, more advanced techniques are also used as the UV-visible spectrophotometry (melanin absorbs in the UV region) and electron paramagnetic resonance. Elemental analysis can be performed through Infra Red spectra and High Performance Liquid Chromatography (HPLC) analysis after chemical degradation **[143]** as well as Matrix Assisted Laser Desorption/Ionization-Time of Flight (MALDI-TOF) mass spectrophotometry **[144]**.

Dihydroxyphenylalanine (DOPA)-melanin and dihydroxynaphthalene (DHN)-melanin are the predominant types of melanin in fungi (**Figure I.8**). DOPA-melanin is particularly well studied in the pathogenic yeast *C. neoformans,* where it is found in the cell wall under the capsule, next to the plasma membrane **[145]**. Melanin in *C. neoformans* is in the form of granular particles of approximately 40- 130 nm in diameter based on NMR cryoporometry and arranged in multiple concentric layers **[145]**. The synthesis of DOPA-melanin starts with the hydroxylation or oxidation of L-tyrosine or L-DOPA, respectively, to dopaquinone (DOPA-Q). This latter is a highly reactive intermediate; therefore in the absence of thiols, DOPA-Q forms leucodopachrome which is then oxidized to dopachrome. Hydroxylation (and decarboxylation) yields dihydroxyindoles that polymerize to form DOPA-melanin. Unlike mammalian cells, no evidence of pheomelanins has been found in *C. neoformans*, nor were the enzymes tyrosinase-related proteins 1 (trp1) and 2 (trp2) found **[146]**. The synthesis of DOPA-melanin can be inhibited by kojic acid and tropolone that have a strong inhibitory effect on the tyrosinase acitivity **[147]** as well as glyphosate that interferes with the shikimate pathway by inhibiting the enzyme 5-enolpyruvoylshikimate 3-phosphatesynthase **[148]**.

DHN-melanins are negatively charged hydrophobic molecules that are synthesized through a complex metabolic pathway, the polyketide synthesis pathway **[149]**. DHN-melanin synthesis involves a number of enzymes encoded by an equal number of genes organized in clusters, there are 3 genes in *Alternaria alternata* **[150]** whereas 6 genes in *A.*

fumigatus **[149]**. The 1,8-DHN-melanin pigment is synthesized from acetyl-CoA or malonyl-CoA, and formation of 1,3,6,8-tetrahydroxynaphthalene (1,3,6,8-THN) is catalysed by a polyketide synthase (PKSp). Two successive reduction and dehydration reactions follow this step to produce 1,8-DHN. The reduction of 1,3,6,8-tetrahydroxynaphthalene and 1,3,8-trihydroxynaphthalene is catalyzed by 1,3,6,8-tetrahydroxynaphthalene reductase and 1,3,8-trihydroxynaphthalene reductase. Dehydration of scytalone and vermelone is efficiently catalyzed by scytalone dehydratase (SCD). The enzymes catalyzing the reduction steps can be inhibited by tricyclazole and pyroquilone, whereas the enzyme involved in dehydration steps can be inhibited by carpropamid.

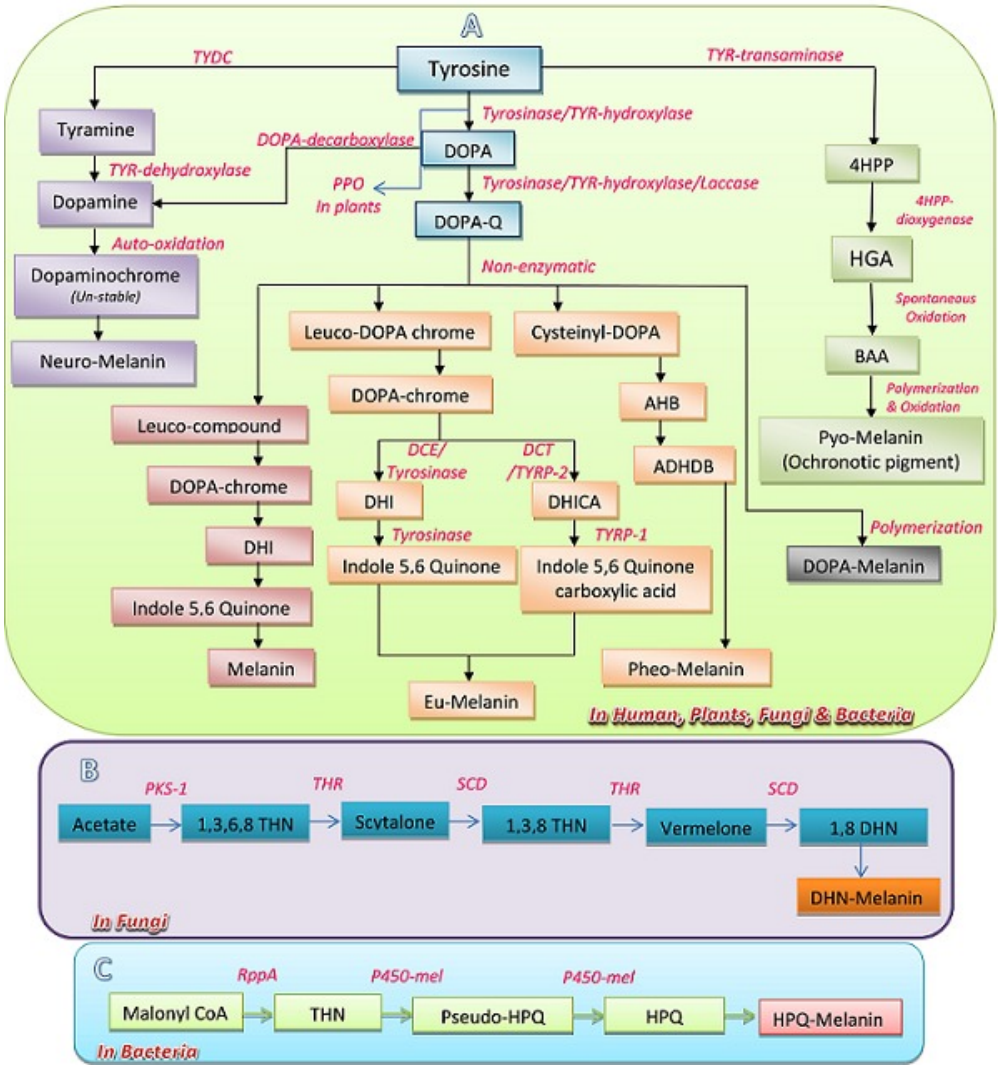

Figure I.8. Melanin synthesis pathways in humans (A) plants (A) fungi (A and B) and bacteria (A and C).

TYDC: Tyrosine decarboxylase; **TYR**: Tyrosinase; **HPP**: 4-Hydroxyphenyl pyruvate; **HGA**: Homogentisic acid; **BAA**: Benzoquinone acetic acid; **DOPA**: 3,4-Dihydroxyphenylalanine; **DOPA-Q**: DOPA-quinone ; **PPO**: Polyphenol oxidase; **AHB**: Alanyl-hydroxy-benzothiazine;

ADHDB: Alanyl 5,6 dihydro-di-benzothiazine; **DHI**: 5,6-Dihydroxyindole ; **DHICA**: DHI-2-carboxylic acid; **DCT**: DOPAchrome tautomerase ; **DCE**: DOPAchrome conversion enzyme; **TYRP**: Tyrosinase-related protein; **PKS-1**: Polyketide synthase type 1; **THN**: 1,3,6,8-Tetrahydroxynaphtalene; **THR**: Tetrahydroxynaphtalene reductase; **SCD**: Scytalone dehydratase; **DHN**: 1,8-Dihydroxynaphtalene; **HPQ**: 1,4,6,7,9,12-Hexahydroxyperylene-3,10-quinone (Source: Singh *et al.* **[151]**).

Melanins can be found either enmeshed within the cell wall or restricted to the outer layer and they play an important role in protecting fungi against adverse conditions in the environment, including toxic products like heavy metals **[152]**, radiation (UV, gamma and solar radiation), enzymatic degradation and heat **[154**, **155]**. Eventhough melanins are ubiquitous in nature, pathogenic fungi do employ these molecules to infect plants and subjugate the human host defense mechanisms. In phytopathogenic fungi such as *M. grisea* and *Colletotrichum lagenarium*, DHN-melanin plays an essential role in generating turgor for plant appressoria to penetrate plant leaves **[155]**. The absence of melanin in human pathogenic fungi often leads to a decrease in virulence. In *S. schenkii*, unmelanized conidia were less resistant to phagocytosis and killing by human monocytes and murine macrophages than were the wild-type strains showing that melanization protects against oxidative antimicrobial compounds and killing during phagocytosis **[156]**. In *Penicillium marneffei,* deletion of the *PKS* gene (*ALB1*) involved in the first step of melanin synthesis led to strains of a significantly reduced virulence in a mouse model **[157]**. Other examples include *A. fumigatus* where conidia having an *ALB1* gene deletion were readily ingested by human neutrophils, which was not the case for wild-type strain or *ALB1*-complemented strains. Likewise, *ALB1*-disruptants were significantly less virulent in a murine model **[158]**. Taken together, these studies reinforce conclusions that melanins are effective in quenching free radicals and enzymes, they aid in antifungal resistance, act as chelators for transition metals, possibly compensate the decrease in superoxide dismutase and act as a redox buffers. Finally, the radical concentration in melanin is known to respond to effectors like pH, temperature and UV which alter the equilibrium between reduced and oxidized species. The degree of polymerization or the molecular weight of the molecule would determine the ratio of its pro-oxidant to anti-oxidant properties **[159]**.

II.1.4. Lipids

Lipids are the least studied molecules of the fungal cell wall as they have been long been considered to be contaminants arising from the cell membrane. Lipids are generally present in minor quantities in the fungal cell walls ranging from 1-10% of its dry weight **[95]**. Cell wall lipids may be readily extractable with solvents, but some require primary step

of hydrolysis, which suggests covalent linkage of these molecules to cell wall components. Several types of lipids were identified in cell wall: free fatty acids, triglycerides, sterol, sterol esters and phospholipids. Even though the role of lipids in the cell wall is still unknown, there are some suggestions that they might be involved in growth, signaling, protection from desiccation **[95]**. The presence of more complex lipid molecules has recently gained the attention of researchers. Cerebrosides or ceramide monohexoside (CMH) seem to be present in all fungal species studied so far except *C. glabrata* and *S. cerevisiae* **[160]**. CMHs are neutral glycosphingolipids that usually contain glucose or galactose with β-glycosidic linkages to the primary alcohol of an *N*-acyl sphingolipid base (ceramide) containing 9-methyl-4,8-sphingadienine with amidic linkage to 16 or 18 carbon atom fatty acids (2-hydroxyhexadecanoic or 2-hydroxyoctadecanoic acids). These molecules can be structurally analysed using high-performance thin layer chromatography (HPTLC) and column chromatography coupled to mass spectrometry (MS) techniques and NMR **[161]**. CMHs appear to be involved in morphological transitions and fungal growth **[162]**. Recently, a glucosyl ceramide was identified in *S. apiospermum* and treatment of conidia with the monoclonal antibodies targetting this molecule significantly reduced fungal growth and enhanced phagocytosis and killing of *S. apiospermum* by murine cells **[163]**.

II.2. The cell wall composition of *Scedosporium boydii*

The first study on the chemical composition of *S. boydii* cell wall was in 2001 by Pinto *et al.* **[64]**, who demonstrated that it was predominantly made up of rhamnopyranose (Rha*p*) and mannopyranose (Man*p*) residues and traces of galactose and glucose. Further analysis of peptidopolysaccharide extracts by NMR revealed a branched structure of α-Rha*p*-(1→3)-α-Rha*p*- side chain epitope linked (1→3) to a (1→6)-linked α-Man*p* core as depicted in **Figure I.9-A**. The carbohydrate content of these molecules was shown to be 70% and the protein content was 15%. Among the other human pathogenic fungi, the presence of peptidorhamnomannans was described only in the dimorphic fungus *S. schenckii* with a high carbohydrate to protein ratio (90.5% carbohydrates and 14.2% protein) **[164]** and lately in *L. prolificans* (62% carbohydrate, 35% protein in PRM) **[108]**. Rhamnose-containing structures appear to be the immunodominant epitopes in the rhamnomannans of *S. boydii, L. prolificans, S. schenckii* and *C. stenoceras*, particularly if they are present as (1→3)-linked α-Rha*p* side-chain units **[56]**. The *O*-glycosidically terminated oligosaccharides may account for a significant part (70–80%) of the PRM antigenicity similar to that of peptidogalactomannans (50%) in *A. fumigatus* **[165]**.

Another cell wall component was described in *S. boydii*, the α-glucans that consist of linear 4-linked α-D-Glc*p* residues substituted at position 6 with α-D-Glc*p* branches (**Figure**

I.9-B). Infact, NMR analysis unravelled three types of residues (→4-αGlc*p*-(1→4)-), (terminal αGlc*p*-(1→4)-), and (→4-αGlc*p*-(1→6)-), however the length of chains formed by these residues as well as the extent of branching and whether there exists one backbone remains unknown **[54]**. Paradoxically, *S. schenckii* that shares the peptidorhamnomannan component with *S. boydii* does not have any α-glucans detected so far **[164]**.

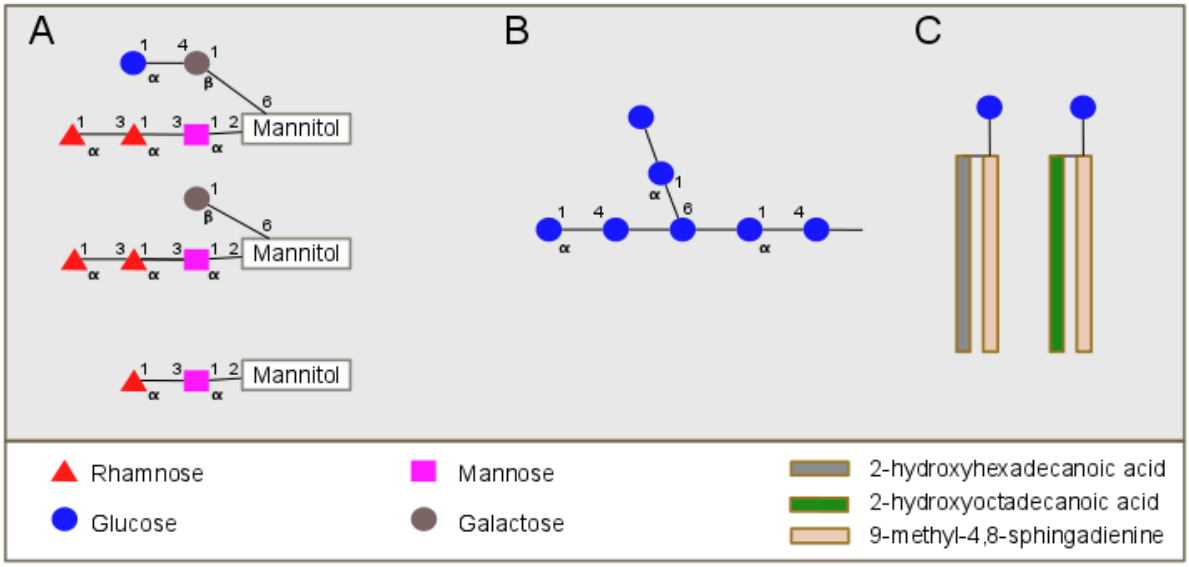

Figure I.9. Cell wall components of *S. boydii.*

A: Structures of *O*-linked rhamnomannans B: Simplified structural diagram of α-glucans showing three types of residues (→4-αGlc*p*-(1→4)-), (terminal αGlc*p*-(1→4)-) and (→4-αGlc*p*-(1→6)-). C: Structure of ceramide monohexosides (Diagrams are based on Lopes *et al.* **[56]**, Bittencourt *et al.* **[54]** and Pinto *et al.* **[166]**)

Finally a glucosylceramide molecule was also characterized using a combination of techniques: HPTLC, GC/MS, fast atom bombardment–mass spectrometry, and NMR. Analysis of the extracted ceramide monohexosides allowed the identification of the molecule (depicted in **Figure I.9-C**) as a glucose residue attached to 9-methyl-4,8-sphingadienine in amidic linkage to 2-hydroxyhexadecanoic or 2-hydroxyoctadecanoic acids **[166]**. An ectophosphatase activity was detected on *S. boydii* cell wall but no molecules in particular were identified **[59]**.

EXPERIMENTAL PART

Study I

Cell wall modifications during conidial maturation of the human pathogenic fungus *Scedosporium boydii*

Remark: The fungal name was changed to meet the latest recommendations for nomenclature. The title and the text were originally published under the name *Pseudallescheria boydii* which was changed here to *Scedosporium boydii.*

Study II

A multifaceted study of *Scedosporium boydii* cell wall during germination and identification of some GPI-anchored proteins

Study III

Draft genome sequence of the pathogenic fungus *Scedosporium apiospermum*

I. Study I: Cell wall modifications during maturation of *S. boydii*

Cell wall modifications during conidial maturation of the human pathogenic fungus *Scedosporium boydii*

Sarah Ghamrawi[1], Gilles Renier[1,2], Patrick Saulnier[3], Stéphane Cuenot[4], Agata Zykwinska[4], Bas E. Dutilh[5,6], Christopher Thornton[7], Sébastien Faure[8], Jean-Philippe Bouchara[1,2]

1 L'UNAM Université, Université d'Angers, Groupe d'Etude des Interactions Hôte-Pathogène EA 3142, Angers, France
2 Laboratoire de Parasitologie-Mycologie, Centre Hospitalier Universitaire, Angers, France
3 L'UNAM Université, University d'Angers, INSERM U646, Angers, France
4 L'UNAM Université, Université de Nantes, Institut des Matériaux Jean Rouxel, Nantes, France
5 Center for Molecular and Biomolecular Informatics, Radboud University Medical Centre, Nijmegen, The Netherlands
6 Department of Marine Biology, Institute of Biology, Federal University of Rio de Janeiro, Rio de Janeiro, Brazil
7 Department of Biosciences, University of Exeter, Biosciences, Exeter, United Kingdom
8 L'UNAM Université, INSERM U1063, Angers, France

Published in **Plos One** (2014, 9: e100290)

Remark: The fungal name was changed to meet the latest recommendations for nomenclature. The title and the text were originally published under the name *Pseudallescheria boydii* which was changed here to *Scedosporium boydii.*

I.1. Abstract

Progress in extending the life expectancy of cystic fibrosis (CF) patients remains jeopardized by the increasing incidence of fungal respiratory infections. *Scedosporium boydii* (*S. boydii*), an emerging pathogen of humans, is a filamentous fungus frequently isolated from the respiratory secretions of CF patients. It is commonly believed that infection by this fungus occurs through inhalation of airborne conidia, but the mechanisms allowing the adherence of *Scedosporium* to the host epithelial cells and its escape from the host immune defenses remain largely unknown. Given that the cell wall orchestrates all these processes, we were interested in studying its dynamic changes in conidia as function of the age of cultures. We found that the surface hydrophobicity and electronegative charge of conidia increased with the age of culture. Melanin that can influence the cell surface properties was extracted from conidia and estimated using UV-visible spectrophotometry. Cells were also directly examined and compared using electron paramagnetic resonance (EPR) that determines the production of free radicals. Consistent with the increased amount of melanin, the EPR signal intensity decreased suggesting polymerization of melanin. These results were confirmed by flow cytometry after studying the effect of melanin polymerization on the surface accessibility of mannose-containing glycoconjugates to fluorescent concanavalin A. In the absence of melanin, conidia showed a marked increase in fluorescence intensity as the age of culture increased. Using atomic force microscopy, we were unable to find rodlet-forming hydrophobins, molecules that can also affect conidial surface properties. In conclusion, the changes in surface properties and biochemical composition of the conidial wall with the age of culture highlight the process of conidial maturation. Mannose-containing glycoconjugates that are involved in immune recognition, are progressively masked by polymerization of melanin, an antioxidant that is commonly thought to allow fungal escape from the host immune defenses.

I.2. Introduction

There has been an increase in the incidence of human infections due to fungi in the *Scedosporium* species (*S. boydii*, *S. apiospermum*, *S. aurantiacum*, *S. dehoogii* and *S. minutispora*) over recent years **[1**, **2**, **3**, **4]**. Infections range from localized, such as subcutaneous mycetoma in immunocompetent individuals, to disseminated infections in immunocompromised patients.

In addition, *S. boydii* and the closely related species *S. apiospermum* are the most common species recovered from the respiratory tract of patients with cystic fibrosis **[5]**. The mechanisms of adherence and establishment of an infection by these fungi in the lung are still largely unknown. It is thought that the infection process in the respiratory tract starts by inhalation and adhesion of airborne conidia that differentiate into hyphae, with both processes mediated by the spore cell wall since that acts as the interface between the fungus and lung tissues.

Adherence is governed by two types of mechanisms, specific receptor-ligand and/or non-specific cellular interactions **[6]**. Depending on the fungus, specific interactions can involve polysaccharides (mannose polymers **[7]**, glucans or galactosaminogalactan **[8]**), proteins or glycoproteins bound to the cell wall through covalent or non-covalent bonds (ex. hydrophobins **[9**, **10]** or glycosylphosphatidylinositol-anchored proteins like Pwp7p and Aed1p adhesins of *Candida glabrata* **[11]** and *CspA* of *Aspergillus fumigatus*). Non-specific interactions involve cell surface properties such as electrostatic charge and surface hydrophobicity which reflect the biochemical composition of the cell wall **[12]**. The importance of such properties has been demonstrated in several fungal models including yeasts **[13**, **14]** and filamentous fungi. Deletion of the *medA* gene in *A. fumigatus,* for example*,* leads to a modification in the surface physical properties along with impaired adherence to epithelial cells and reduced virulence **[15]**.

Escaping recognition and destruction by the immune system is another challenge for fungal pathogens. In *A. fumigatus,* rodA hydrophobin contributes to fungal viability *in vivo* by masking fungal pathogen-associated molecular patterns (PAMPs), thus preventing recognition by Dectin-1 and Dectin-2 **[16]**. Other fungal pathogens, like *Pneumocystis jirovecii* or *Cryptococcus neoformans* have been shown to evade immunosurveillance either by changing the expression of major surface glycoproteins **[17]** or by means of a capsule that cover the antigenic components of infective propagules and modulate the immune response respectively **[18]**. Melanin is an additional virulence factor employed by many fungi in order to resist phagocytosis and cellular damage secondary to nitrogen- or oxygen-derived radical attack. Fungal melanin has been reported to limit complement activation, and confer resistance to antimicrobial agents **[19]**. Modification or inhibition of the expression of

melanin or rodA hydrophobins has repercussions on the cell surface physical properties in fungi.

In *S. boydii*, only a limited number of cell wall constituents have been characterized so far including peptidorhamnomannans (PRM) and alpha-glucans **[20]**. PRMs were demonstrated to play a role in the adhesion of conidia to HEp2 epithelial cells *in vitro* **[21]** as well as activation of Toll-like receptor (TLR) 4, responsible for cytokine induction in macrophages **[22]**. Alpha-glucans were shown to partially elicit phagocytosis and to induce secretion of inflammatory cytokines in a mechanism involving CD14, TLR 2 and MyD88 **[23]**. On the hyphal wall, an acid and alkaline phosphatase activity was also detected **[24]**, as well as ceramide monohexosides suggested to be critical for fungal differentiation **[25]**.

In this study, we investigate temporal changes in the physical properties of the conidial wall of *S. boydii*, and we study the presence of rodlet structures and melanin as putative virulence factors in the pathogen.

I.3. Materials and Methods

Strain and culture conditions

The filamentous fungus *Scedosporium boydii* IHEM 15155 (subgroup *P. ellipsoidea*), isolated in 1990 from a bronchial aspirate in Angers University Hospital, was used throughout this study. According to the classification of Gilgado *et al.* **[3**, **4**, **18]**, this strain was identified after sequencing the internal transcribed spacer (ITS) regions 1 and 2 of ribosomal RNA genes (NCBI accession number EF441725) and the TUB region of the beta tubulin gene (KJ566742).

The strain was routinely maintained on YPD (0.5% w/v yeast extract, 2% w/v glucose, 1% w/v peptone, 0.05% w/v chloramphenicol) agar plates. Conidia were harvested from cultures grown for 5, 9 or 14 days at 37°C by flooding the agar surface with sterile water followed by filtration on a 20-µm pore size nylon filter. Conidia were washed twice with Milli-Q™ water, centrifuged at 5000 g for 5 min at 4°C, and finally counted with a hemocytometer.

For some experiments, the fungus was grown in the presence of 1,8-dihydroxynaphthalene (DHN) melanin inhibitors (tricyclazol, pyroquilon or carpropamid) or 3,4-dihydroxyphenylalanin (DOPA) melanin inhibitors (tropolone, kojic acid or glyphosate). Inhibitors were diluted in ethanol and incorporated into YPD agar to a final concentration of 20 µg/ml, according to Cunha *et al.* **[26]**. All inhibitors were purchased from Sigma-Aldrich (St. Louis, MI, USA).

Fluorescence studies

Freshly harvested conidia (10^8) were washed once with Tris buffer (0.5 mM Tris, 100 mM NaCl, 1 mM $CaCl_2$, 1 mM $MgCl_2$, pH 7.0), pelleted by centrifugation, and then resuspended in fluorescein isothiocyanate (FITC)-labeled lectins (Sigma): concanavalin A (Con A), Wheat Germ Agglutinin (WGA), or Peanut Agglutinin (PNA) at a final concentration of 100 µg/ml in Tris buffer. After 30 min of incubation at 37°C with continuous agitation, conidia were washed three times in Tris buffer and then fixed in 1% formaldehyde (v/v) in phosphate buffered saline 0.15 M pH 7.2 (PBS). For controls the fluorescent lectin was omitted or the condia were incubated in the presence of an excess (0.2 M) of methyl α-D-mannopyranoside, N-acetyl glucosamine (GlcNac) or galactose for Con A, WGA and PNA respectively, prior to the addition of the FITC-conjugated lectin. Samples were observed with a fluorescence microscope (Leica DMR) using immersion oil at 1000x.

After labeling with FITC-Con A, fluorescence intensity was also quantified by flow cytometry on a FACSCanto™ II cytofluorometer driven by the FACSDiva™ software (BD Biosciences, Pont de Clay, France). The conidia were gated on the forward scatter/side scatter (FSC/SSC) plots. Fifty thousand cells per sample were analyzed and the mean fluorescence intensity was recorded. Flow-Jo software was used for histograms overlays.

Transmission electron microscopy (TEM)

Conidia were washed once in cacodylate buffer (0.1 M) and pelleted at 5000 g for 5 min at 4°C. After incubation in fixative solution (2.5% (w/v) glutaraldehyde, 2% (w/v) paraformaldehyde, 0.1 M cacodylate buffer) for 24 hours at room temperature under vacuum, they were washed with cacodylate buffer, and incubated for 24 hours in 2% $KMnO_4$ in cacodylate buffer at 4°C. After washing, fixed conidia were incubated for 2 hours at room temperature in 2% osmium tetroxide, washed in Milli-Q™ water, and finally dehydrated through a series of ethanol-water solutions (50, 70, 95% ethanol, 2 x 30 min each) followed by 100% ethanol (3 x 20 min). The ethanol was finally substituted with propylene oxide (3 x 20 min). Conidia were impregnated overnight in a propylene oxide-Epon mixture (1:1 v/v), then embedded in pure Epon for 16 hours and 8 hours. Polymerization was performed at 37°C for 24 hours, then at 45°C for 24 hours and finally at 60°C for 48 hours. Thin sections were counter stained with uranyl acetate and lead citrate in the case of melanin inhibition experiments, otherwise they were directly examined on a JEM-1400 transmission electron microscope (Jeol, Paris, France) operating at 120 kV.

For gold-conjugated Con A labeling, conidia (10^8) were incubated for 30 min at 37°C with continuous shaking in the presence of 5 nm gold-conjugated Con A (Biovalley, Marne la Vallée, France) diluted 1:50 in Tris buffer. Then conidia were washed three times in Tris buffer. Two controls were also prepared, by omission of the lectin, or the inclusion of 0.2 M

methyl α-D-mannopyranoside in Tris buffer added just prior to the addition of the gold-conjugated lectin. Samples were prepared for TEM as previously indicated without contrasting.

Surface physical properties

Zeta-potential. Conidia were washed once in Milli-QTM water containing 1 mM NaCl, then resuspended in the same solution to a density of 106 conidia /ml. The electrophoretic mobility of cells was measured with a zeta potential analyzer (Zetasizer Nano ZS; Malvern Instruments Ltd, Malvern, UK) before being converted to zeta potentials using the Smoluchowski equation. The measurements, performed at 25°C, were repeated three times with ten to thirty cycles for each measurement. Experiments were repeated three times.

Two-phase partitioning. Cell surface hydrophobicity (CSH) was determined essentially as described by Pihet *et al.* **[27]** with some modifications. Hexadecane (0.5 ml) was dispensed onto a spore suspension (2.5 ml) prepared in PBS (5 x 107 conidia /ml). A control of 1 ml conidia suspension without hexadecane was prepared and the test samples were prepared in duplicates. Tubes were vortexed for 2 min, allowed to stand at room temperature for 3 min before carefully transferring 1 ml of the aqueous phase (bottom) into a new tube using a Pasteur pipette. The transferred material was vortexed again for 2 min, and the optical density (OD) was read at 405 nm in triplicate on 200-µl aliquots. The hydrophobic index (percentage of conidia that were excluded from the aqueous phase) was calculated using the following equation:

$$\frac{(OD_{control} - OD_{test}) * 100}{OD_{control}}$$

Atomic force microscopy (AFM) measurements

Conidial suspensions of *S. boydii* with different cell densities were prepared in PBS and 500 µl were added per well in a 24-well plate containing poly-L-lysine (0.1% (w/v) in distilled water, Sigma-Aldrich)-coated 12 mm-diameter glass cover slips prepared according to the manufacturer's recommendations. Cells were incubated with the coated cover slips for 30 min at 37°C with gentle agitation. Afterwards, the cover slips were washed twice with PBS (5 min each with agitation), then left to dry at ambient temperature and conserved at 4°C before analysis.

The surface of *S. boydii* conidia was imaged using a NanoWizard atomic force microscope (JPK, Berlin, Germany) operating in intermittent contact mode under ambient conditions. A standard rectangular cantilever (Nanosensors NCL-W) was used for imaging,

with a free resonance frequency of 165 kHz and a typical spring constant of about 40 N/m. The radius curvature of the tip was ~10 nm.

PCR conditions and gene sequencing

Genomic DNA extraction. Mycelium from 10 day-old culture in YPD broth was harvested and ground in liquid nitrogen with a mortar and pestle. Intact genomic DNA was obtained by the method of Moller *et al.* **[28]**. Briefly, the ground mycelium (150-300 mg) was washed three times with methanol containing 0.1% β-mercaptoethanol. Dried pellet was resuspended in 500 µl TES (100 mM Tris pH 8.0, 10 mM EDTA, 2% SDS) containing 5 µl proteinase K (100 µg). After incubation for 1 hour at 60°C, 140 µl NaCl (5 M) and 65 µl of 10% CTAB (cetyltrimethylammoniumbromide) were added to the mixture which was then incubated for 10 min at 65°C. An equal volume of chloroform: isoamylic alcool (24:1, v/v) was then added. After incubation for 30 min on ice and centrifugation at 20,000 g for 10 min at 4°C, the upper phase was transferred and gently mixed with 0.215 vol (approximately 130 µl) ammonium acetate. After a further 30-min incubation on ice and centrifugation, DNA was precipitated by mixing the supernatant with 0.55 vol isopropanol and immediate cooling on ice before centrifugation for 10 min at 20000 g. The pellet was washed twice with cold 70% ethanol, dried, and resuspended in 50 µl Tris-EDTA (10 mM Tris pH 8.0, 0.1 mM EDTA). The DNA extract was finally treated with RNase.

Gene sequencing. The polyketide synthase type I (*PKSI*) and tetrahydroxynaphthalene reductase (*4HNR*) genes were sequenced using degenerate primers listed in **Table E.4**. Primers for *PKSI* were designed from the alignment of *Colletotrichum lagenarium* polyketide synthase (Accession no. D83643) and a homologue of *PKSI* in the genomic sequence database of *S. boydii* (C.R. Thornton, unpublished) using the Multalin program **[4]** (http://multalin.toulouse.inra.fr/multalin/). Similarly, primers for PCR amplification of an internal fragment of *4HNR* gene were designed from the multi-alignment of four fungal ortholog sequences or their corresponding cDNA: *T4HR1* gene of *Colletotrichum orbiculare* (Accession no. AB661336), *4HNR* gene of *Lomentospora prolificans* strain 3.1 (Accession no. JX861395), 1,3,6,8-tetrahydroxynaphthalene reductase gene of *Magnaporthe grisea* (Accession no. AY846877) and hydroxynaphthalene reductase gene of *Ophiostoma floccosum* (Accession no. AF285781).

The upstream and downstream regions of the amplified *4HNR* gene fragment were obtained by walking-PCR as described by Siebert *et al.* **[29]**. Briefly, genomic DNA (2.5 µg) of *S. boydii* IHEM 15155 was digested overnight at 37°C with restriction enzymes *Eco*RV, *Nru*I or *PvU*II according to the supplier's recommendations (New England Biolabs, Evry, France). Then 10 µl of the obtained fragments (250 ng) were ligated to adaptors (1 pmol) overnight at 14°C; afterwards the ligated products were used as template to amplify by

nested PCR the flanking regions of the known gene fragment using outer primers directed towards the adaptor AP1 and the end of the known fragment (indicated by F1 for downstream sequence or R1 for upstream sequence in **Table E.4**). The second step of the nested PCR was then performed using adaptor primer AP2 and inner primers also targeting the known gene fragment (indicated by F2 or R2 in **Table E.4**).

PCR conditions were as follows: 5 min of denaturation at 95°C, followed by 30 cycles of 30 s at 95°C for denaturation, 30 s at 55-60°C for annealing and 1 min at 72°C for elongation, with a final elongation step of 10 min at 72°C. For walking-PCR, the first round was performed as follows: 94°C for 3 min, then 35 cycles (94°C for 30 s, 55°C for 1 min, 72°C for 4 min) and finally 72°C for 15 min. For the second round, PCR conditions were the same except for the number of cycles (25 instead of 35) and duration of final denaturation (30 min instead of 15 min). Amplicons were excised from the gels and purified using NucleoSpin Gel and PCR Clean-up kit (Macherey-Nagel, Hoerdt, France), and then sent for bidirectional Sanger sequencing at GATC Biotech Platform (GATC Biotech AG, Köln, Germany). Sequence analysis was performed using the Translation tool in ExPASy SIB Bioinformatics Resource Portal (http://web.expasy.org/translate/) and The Basic Local Alignment Search Tool (BLAST) in NCBI.

Table E.4. Primers for sequencing genes involved in the melanin synthesis pathway.

Primers*	Primer sequence 5'→3'(**)	Tm
***PKSI* gene sequencing**		
F PKSI.29	ACMAACCAYTCTGCYGA	49°C
R PKSI.29	TAGATWGTATCGCTKGC	
F PKSI.31	GTCGTTTGGGAATGCCTCA	55°C
R PKSI.31	GAGGATCAACGCCAGCCT	
F PKSI.32	GTTATTGTTCAGCTCGGTCTTTG	55°C
R PKSI.32	GTGCTCCGTTGACAACATG	
F PKSI.39	GAACTGATGAAGGCTTGCGGATGTA	60°C
R PKSI.39	GTAGAAGHAATGGCGGAGGCGGC	
F PKSI.40	GCTTAACGAGAAATATCACGCCCAAG	60°C
R PKSI.40	GCTCTCCTTGTGGATTCTGAGGCTC	
F PKSI.41	CTCAGTACCTGCGGCAATCATG	60°C
R PKSI.41	CAGTAGCAGTGGTCGGTCTTCT	

F PKSI.42	CATGTTGTCAACGGAGCACCAC	60°C
R PKSI.42	CTCCTCCCTCAGTCGCCCA	
F PKSI.43	GGCGTTGTGGGTCAAATTAAGTTCC	60°C
R PKSI.43	GTAAGGTCCAGTTGGCTGTCGGCGT	
F PKSI.44	CGCCACCAGCTATACCGAAATCG	60°C
R PKSI.44	CCAAGCGAGCCAAAAGACTAAGAC	
F PKSI.50	CCTCACATACTTCTGTCGGGAG	55°C
R PKSI.50	GGAGCTAAAGTTGGAGAATGCTC	
F PKSI.51	CTCATATTTCAGGTCTGCGGAGAG	55°C
R PKSI.51	GGAATCCATGTGTGTCCAACGA	
***4HNR* gene sequencing**		
F 4HNR.70	GCCGAYATCAGCAAGCC	57°C
R 4HNR.70	CGTAGTGCCASGAGTTCTCG	
***4HNR* primers and adaptor primers for Walking-PCR**		
F1.4HNR.74	CCGCATCATCCTCACCTCTTCC	60°C
F2.4HNR.74	CCACAATCATGCTCTCTACGCCG	60°C
F1.4HNR.83	AGCAGGTTACCGTCAACGCCATC	60°C
F2.4HNR.83	GATCATTGACCAGGGTCTTGCCAAC	60°C
R1.4HNR.75	GGAAGAGGTGAGGATGATGCGG	60°C
R2.4HNR.75	GGACCACACCTCAGTACCCGA	60°C
AP1	GGATCCTAATACGACTCACTATAGGGC	60°C
AP2	AATAGGGCTCGAGCGG	60°C

*Primers carrying the same number represent forward and reverse primers included in the same amplification reaction. Tm of each amplification reaction is indicated in the same row next to the forward primers.

**IUPAC-IUB symbols for nucleotide nomenclature: M = A or C; Y = C or T; W = A or T; K = G or T; and H = A, C or T.

Nucleotide sequences accession number. The sequences of the *PKSI* and *4HNR* genes of *S. boydii* IHEM 15155 were deposited in the GenBank database (Accession no. KC440182 and KJ549637 respectively).

Melanin extraction and quantification

Electron paramagnetic resonance (EPR). Freshly harvested conidia were washed and resuspended in PBS (150 mM) to a final density of 1.0 x109 conidia/ml. Fungal suspensions were aspired in 1 ml syringes and frozen by immersion in liquid nitrogen. EPR spectra were recorded using a MiniScope MS200 EPR spectrometer (Magnettech, Berlin, Germany) operating at X-band. Samples were held in a quartz immersion finger Dewar filled with liquid nitrogen. Experimental parameters were as follows: modulation amplitude 1 G, microwave power 0.1 mW, modulation frequency 100 kHz, microwave frequency 9.5 GHz, number of scans averaged 3. Images were treated using Multiplot 2.0 **[30]**.

Melanin extraction. Melanin was extracted according to the method of Gadd **[31]**. *Scedosporium boydii* conidia (5 x 109) were washed once with MilliQTM water, then with NaOH (1 M) and centrifuged at 4500 g for 5 min at 4°C. The pellet was mixed with 5 ml NaOH (1 M) and the pigments were extracted by boiling for 20 min followed by autoclaving for 20 min at 115°C. Cell debris were removed by centrifugation at 12000 g for 5 min and the supernatant was acidified to pH 2 with concentrated HCl. Melanin was precipitated after centrifugation at 12000 g for 5 min, then the pellet was washed with MilliQTM water and finally lyophilized.

UV-visible spectrum. Melanin pellets were reconstituted in 1 ml of NaOH 1 M, then diluted to avoid saturation. A standard curve was designed based on the absorption spectra of synthetic DOPA melanin (Sigma) that was solubilized in NaOH 1 M at different concentrations ranging from 0.01 mg/ml to 1 mg/ml. Spectra for extracted and synthetic melanin were recorded in the wavelength range 190-900 nm using a UV-visible spectrophotometer (UV-2600; Shimadzu Scientific Instruments, Columbia, USA).

Statistical analysis

Statistical analysis was conducted using a non-parametric test Kruskal–Wallis one-way analysis of variance (ANOVA) or two-way ANOVA with Bonferroni post-hoc test using GraphPad Prism V5.0 software (GraphPad Software, San Diego, CA, USA). *P*-values were considered significant if lower than 0.05.

I.4. Results

Surface accessibility of cell wall polysaccharides to fluorescent lectins

Spores from 5-day-old cultures were incubated with fluorescent lectins (Con A, WGA and PNA) in order to detect mannose/glucose, GlcNAc and galactose residues, respectively. No fluorescence was observed at the cell wall surface after incubation with FITC-WGA, which only bound to the scar region that appears at the basis of the conidia after their release (data not shown). In contrast, fluorescence of conidia labeled with Con A-FITC was highly

heterogeneous. While a few conidia were intensely labeled (asterisks) and some others faintly marked (arrows), the majority exhibited labeling exclusively on their release scar (**Figure E.10.A** and **B**). Inhibition assays with methyl α-D-mannopyranoside confirmed the specificity of labeling (**Figure E.10.C** and **D**). No fluorescence was observed after incubation with FITC-PNA (results not shown).

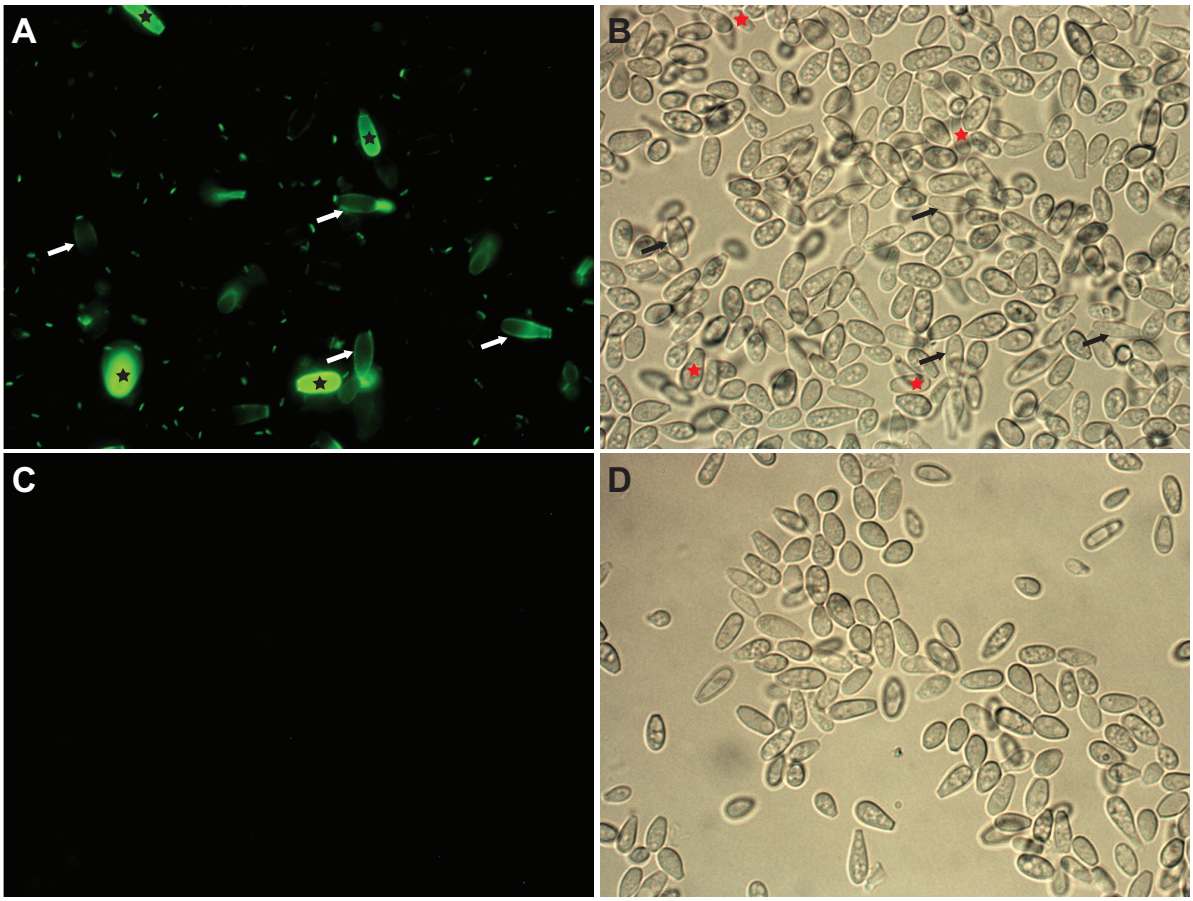

Figure E.10. Fluorescence labeling of cell wall mannan groups in *S. boydii* conidia.
Conidia recovered from 5-day-old cultures were incubated with concanavalin A conjugated to fluorescein isothiocyanate (Con A-FITC), and examined under fluorescence microscopy. Whereas a few conidia were highly fluorescent (asterisks) and some others were faintly labeled (arrows), the majority exhibited labeling exclusively on their release scar (A) as demonstrated by examination of the same field by phase-contrast microscopy (B). In (C) and (D), conidia incubated with a large excess of the inhibitor methyl α-D-mannopyranoside prior labeling with FITC-Con A showed no fluorescence, thus attesting the specificity of the labeling.

Effect of the age of culture on cell surface properties of conidia

Heterogeneity of the labeling with Con A-FITC suggested maturation of the conidia with the ageing culture. To confirm this hypothesis, we first studied the impact of age of

culture on the cell surface properties which reflects the entire composition of the cell wall. Conidia were thus recovered from 5-, 9- and 14-day-old cultures and their surface hydrophobicity and electrostatic charge were measured (**Figure E.11**). Conidia exhibited a high electronegative charge that increased overtime, from - 39.0 mV on day 5 to - 49.3 mV on day 14 ($P < 0.05$). Similarly, the surface hydrophobicity of spores markedly increased after 5 days of culture as shown in **Figure E.11.B** ($P < 0.001$). The difference in CSH between conidia from 9- and 14-day-old cultures was not significant according to Dunn's post-hoc test.

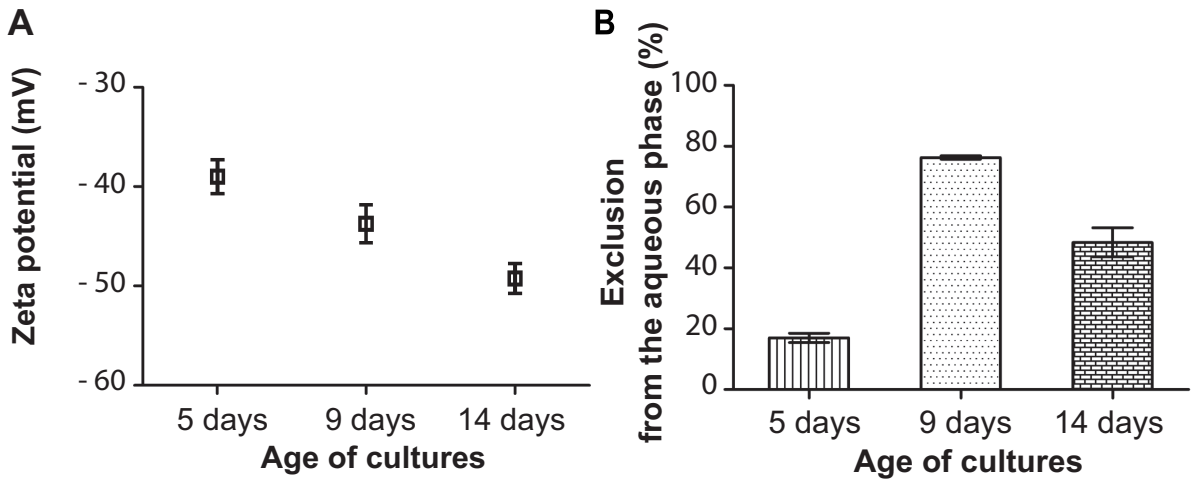

Figure E.11. Influence of the age of the cultures on the physical surface properties of conidia.

Surface electrostatic charge (A) and cell surface hydrophobicity (B) of conidia recovered from 5-, 9-, and 14-day-old cultures were significantly different among the three groups with a $P < 0.01$ for (A) and $P < 0.001$ for (B).

Melanin detection and changes in the melanin content of the conidial wall with the age of cultures.

DHN-melanin in *S. boydii*. In order to identify the type of melanin synthesized in *S. boydii*, inhibitors of DOPA- (tropolone, kojic acid and glyphosate) or DHN- (tricyclazol, pyroquilon and carpropamid) melanin synthesis pathways were added to the culture medium and melanin was extracted from conidia after 9 days of incubation of the cultures. Melanin content in these extracts was investigated by UV-visible spectrophotometry over a wide range of wavelengths from 190 nm to 900 nm (**Figure E.12**). Strong absorption was detected in the UV region for conidia taken from cultures grown with or without DOPA-melanin inhibitors, with an absorption maximum at about 226 nm, the same wavelength at which maximum absorption of synthetic melanin occurs. Conversely, extracts of conidia taken from cultures grown in the presence of DHN-melanin inhibitors had no detectable

absorption in the UV region, which indicates that only DHN-inhibitors were able to suppress the synthesis of melanin. These results were in accordance with the color of conidia that turned from dark brown to cream color upon incubation with DHN-melanin inhibitors.

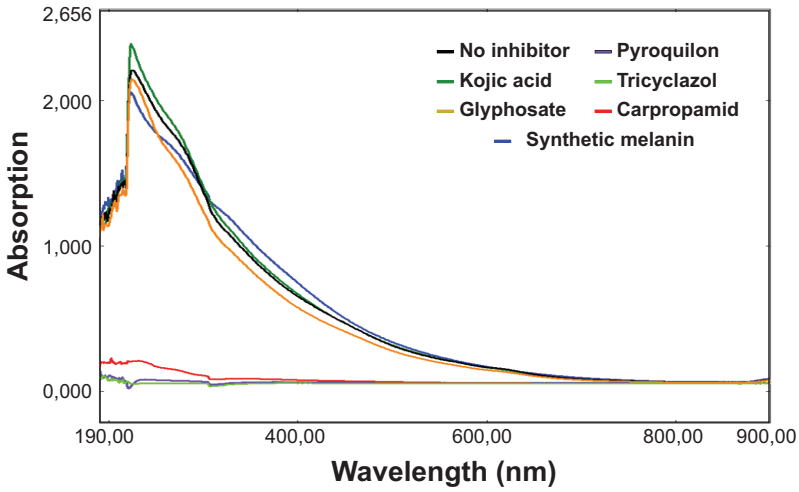

Figure E.12. UV-visible spectrophotometry of melanin extracts.
Melanin extracts from control conidia or conidia recovered from cultures grown in the presence of DOPA-melanin (kojic acid or glyphosate) or DHN-melanin (pyroquilon, tricyclazol or carpropamid) inhibitors were examined under UV-visible spectrophotometry. A spectrum similar to synthetic melanin (0.05 mg/ml) was obtained only for extracts from control conidia or conidia produced with DOPA-melanin inhibitors.

The effect of melanin inhibitors on the structure of the cell wall in conidia was also examined in TEM (**Figure E.13**). The outer electron-dense cell wall layer became markedly thinner, fragmented and sometimes detached for conidia recovered from cultures grown in the presence of pyroquilon in comparison to the thick uniform outer cell wall layer of control spores or spores recovered from cultures with glyphosate.

Sequencing of genes involved in the DHN-melanin biosynthesis pathway. The search for enzymes in the synthesis pathway of DHN-melanin lead to the identification of genes encoding polyketide synthase type I (*PKSI*) and tetrahydroxynaphtalene reductase (*4HNR*) (**Figure E.14**). Genes were sequenced after multiple sequence alignment of homologous genes in other taxonomically close fungi. Function of the corresponding proteins was confirmed by identification of predicted functional domains after translation. Similarly to *Colletotrichum lagenaria* and *Ophiostoma piceae*, *PKSI* gene in *S. boydii* had 2 introns, while homologous genes in *Verticillium dahliae* and *Magnaporthe oryzae* had 3 introns. As for the *4HNR* gene, *S. boydii*, *C. orbiculare*, *O. floccosum* and *M. grisea* all shared one short intron unlike *L. prolificans* that lacked any. Expression of these genes has also been confirmed by analysis of mRNA extracts from conidia (results not shown), however attempts to perform

quantitative real time-PCR failed due to the incapacity to normalize the expression of *PKSI* and *4HNR* genes in our experimental conditions. Four reference genes were chosen based on the work of Fang and Bidochka **[32]** and Raggam *et al.* **[33]**, *i.e.* beta-tubulin, tryptophan biosynthesis enzyme, actin and glyceraldehyde 3-phosphate dehydrogenase, but all showed high delta Ct values when conidia from 5-day-old cultures were taken as reference.

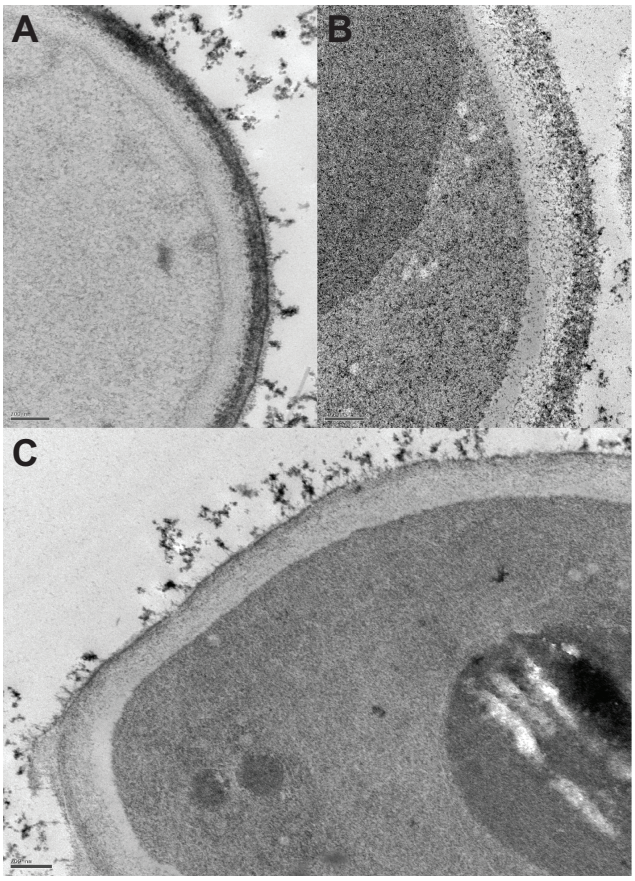

Figure E.13. Transmission electron microscopy examination of conidia from cultures grown with or without melanin inhibitors.

Control conidia (A) or conidia recovered from cultures grown with the melanin inhibitors glyphosate (B) or pyroquilon (C) examined by transmission electron microscopy (scale bar = 200 nm).

Comparison of melanin extracts with UV-visible spectrophotometry. Melanin was extracted from conidia recovered from 5-, 9- and 14-day-old cultures, and the maximum absorbance at 226 nm was recorded for all samples analyzed in triplicate (**Figure E.15.A**). The mean ranks of absorption were significantly different among the three groups of conidia: melanin content in extracts from conidia increased after 5 days of culture ($P < 0.05$). The mean absorbance values obtained for melanin extracts of conidia taken from 9-

and 14-day-old cultures were not significantly different according to Dunn's comparison test (post-hoc analysis).

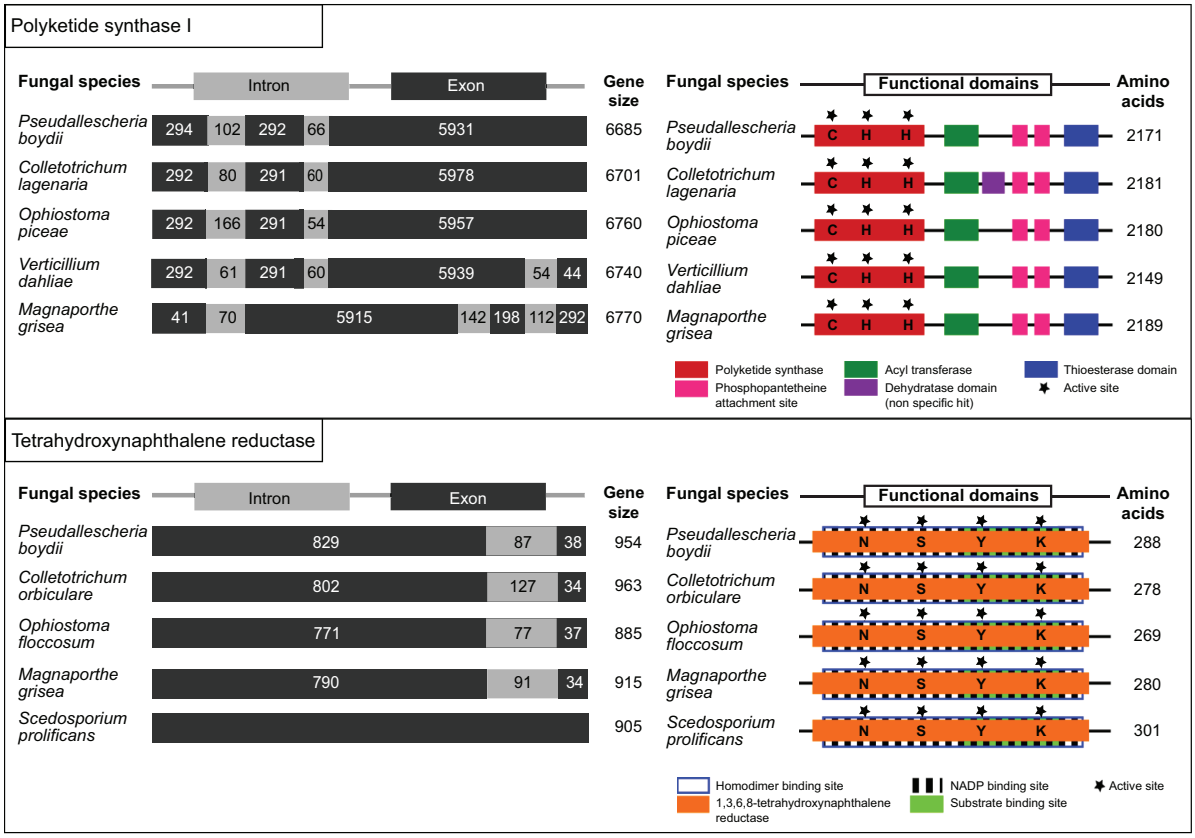

Figure E.14. Analysis of *PKSI* and *4HNR* gene sequences and predicted protein sequences.

Alignment of protein and nucleotide sequences for polyketide synthase type I of the fungi (Accession number): *Scedosporium boydii* (KC440182, this work), *Colletotrichum lagenaria* (BAA18956.1), *Verticillium dahliae* (EGY13508.1), *Magnaporthe oryzae* (ELQ39536.1), *Ophiostoma piceae* (ABD47522.2). Alignment of protein and nucleotide sequences for tetrahydroxynaphtalene reductase of the fungi (Accession number): *Scedosporium boydii* (KJ549637, this study, previously *P. boydii*), *Colletotrichum orbiculare* (AB661336), *Ophiostoma floccosum* (AF285781), *Magnaporthe grisea* (AY846877), and *Lomentospora prolificans* (previously *S. prolificans*) strain 3.1 (JX861395). Protein functional domains were predicted by conserved domain search in NCBI.

EPR spectroscopy comparison of *S. boydii* conidia taken from cultures of different age. Conidia taken from cultures of different age showed a diminishing EPR signal intensity as the age of culture increased (**Figure E.15.B**). Experiments were repeated three times and similar regressions were obtained each time. A decrease in the EPR signal intensity was also found with a wild-type strain of *A. fumigatus* (CBS 113.26) when conidia

isolated from 3- or 8-day-old cultures were compared (data not shown). No EPR signal was observed for PBS buffer alone, or with conidia from a mutant strain of *A. fumigatus* (strain IHEM 9860) blocked in the early steps of melanin synthesis **[27]**.

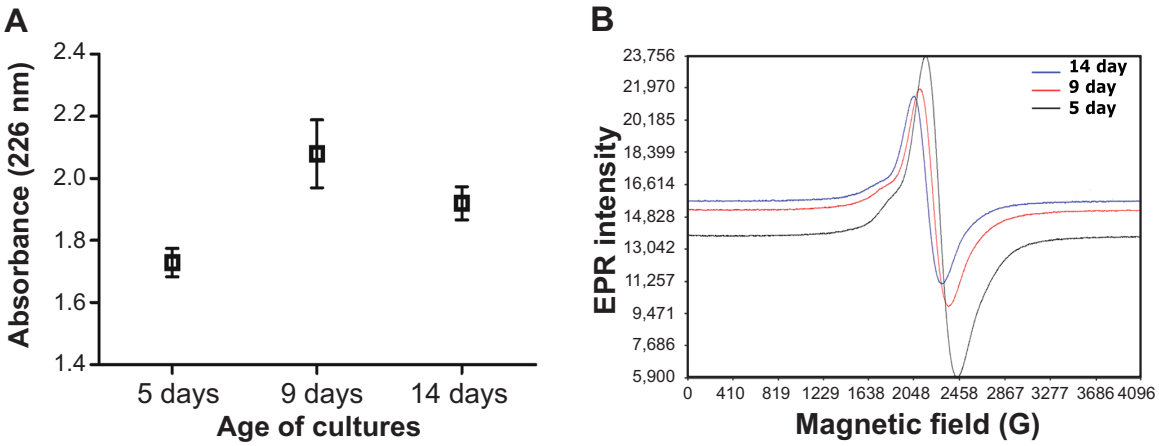

Figure E.15. Changes in melanin amount in conidia as the age of culture progresses. Melanin amount in the conidial wall changed with the age of culture as revealed by UV-visible spectrophotometry (A) or electron paramagnetic resonance (B). (A) The mean rank of the quantity of melanin extracted from conidia was significantly different among cultures of different age ($P < 0.05$). (B) EPR spectra of *S. boydii* conidia taken from cultures of different age (5, 9 and 14 days). The spectra were recorded at a microwave power of 30 db. Spectra are representative of three independent experiments.

Melanin masks mannose-containing glycoconjugates and affects the electrostatic charge of the conidial surface. Conidia recovered from cultures containing the DOPA-melanin inhibitor glyphosate were incubated with FITC-conjugated Con A. No significant changes were observed by flow cytometry in the mean fluorescence intensity of these conidia compared to cells from control cultures of the same age ($P > 0.05$). In contrast, conidia recovered from cultures grown in the presence of pyroquilon showed a significant increase ($P < 0.001$) in fluorescence intensity as the age of culture progressed suggesting an increase in the amount of mannose-containing glycoconjugates in the conidial wall (**Figure E.16**).

The presence of melanin is commonly known to affect the surface electrostatic charge in fungi **[34]**. In order to test this, conidia were recovered from 9-day-old cultures with or without melanin inhibitors. Conidia taken from cultures with pyroquilon showed a marked decrease ($P = 0.001$) in the surface electronegative charge with respect to conidia taken from cultures with glyphosate or control cultures without any inhibitor (**Figure E.17**).

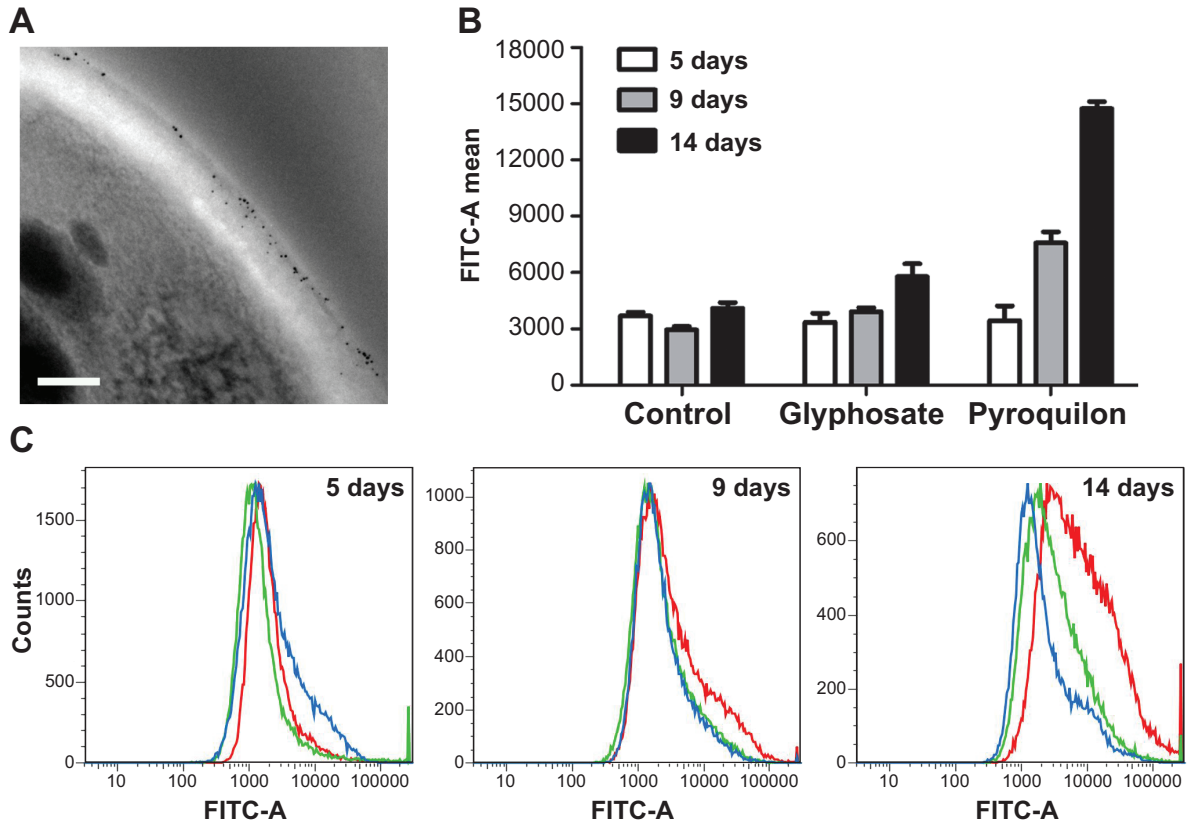

Figure E.16. Repercussion of the increased melanin synthesis on the surface labeling of conidia with concanavalin A.

(A) Trasmission electron microscopy showing conidia labeled with gold-conjugated concanavalin A (Con A; 5-nm gold particle). Scale bar = 200 nm. (B, C) Quantitative analysis by flow cytometry of fluorescence at the surface of conidia treated with fluorescein isothiocyanate (FITC)-ConA. (B) Comparison of mean specific fluorescence intensity of conidia recovered from 5-, 9-, or 14-day-old cultures grown with or without glyphosate or pyroquilon. Contrary to conidia with glyphosate treatment, conidia with pyroquilon treatment showed a significant increase in labelling with respect to their counterparts from 9- or 14-day-old control cultures grown without any melanin inhibitor ($P < 0.001$). Specific fluorescence was obtained after normalizing against the fluorescence in conidia untreated with FITC-ConA or conidia treated with methyl α-D-mannopyranoside prior to the addition of FITC-Con A. (C) Fluorescence frequency distribution histograms: the blue-lined histogram represents the relative signal of conidia from cultures grown without any melanin inhibitor, whereas the red- or green-lined histograms represent the relative signal of conidia treated with pyroquilon or glyphosate, respectively (number of fungal cells in the y-axis versus relative fluorescence intensity in the x-axis expressed as arbitrary units on a logarithmic scale).

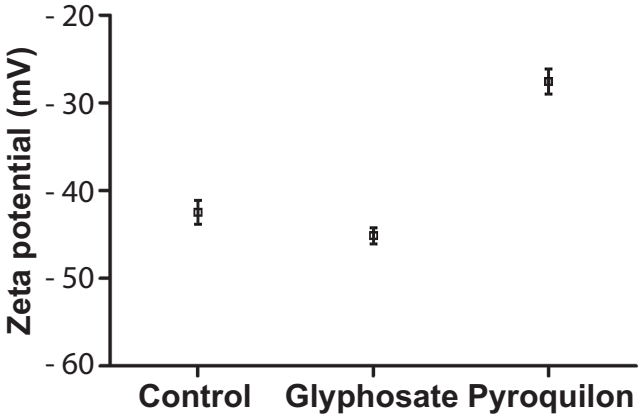

Figure E.17. Changes in the physical properties of the conidial surface induced by melanin inhibition.

The surface electronegativity of conidia recovered from cultures grown with pyroquilon was markedly reduced with respect to conidia recovered from control cultures or cultures grown with glyphosate (P = 0.0010).

Absence of rodlets on conidia of *S. boydii*.

As illustrated in **Figure E.18** for conidia taken from 9-day-old cultures, AFM analysis of conidia from 5-, 9- or 14-day-old cultures showed the absence of rodlet layer at the cell surface whatever the age of culture was (data not shown).

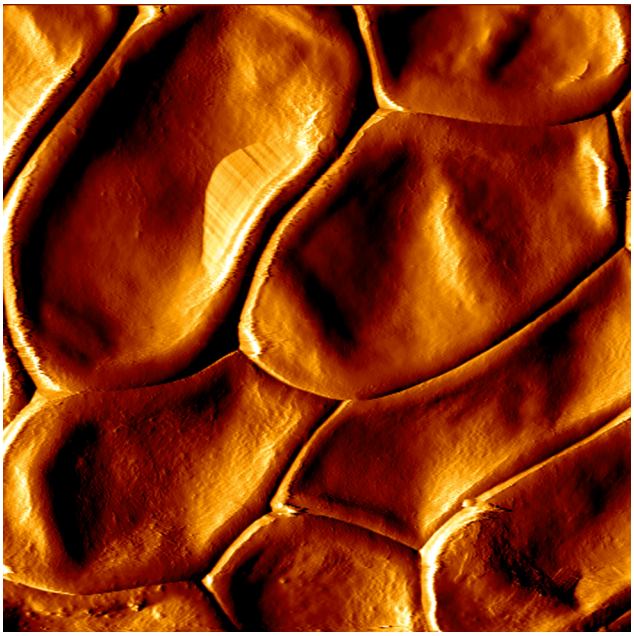

Figure E.18. Atomic force microscopy image of the surface of *S. boydii* conidia.

Conidia recovered from 9-day-old cultures examined by AFM in the tapping mode showed a smooth surface without any rodlet layer of hydrophobins (10 µm x 10 µm image).

I.5. Discussion

Knowledge of the chemical composition and structural modifications of the fungal cell wall is crucial to understanding how infectious propagules interface with host tissues during early the stages of morphogenesis and pathogen establishment. To date, our knowledge of *S. boydii* is largely restricted to taxonomical studies and medical case reports. Interest in the molecular genetics, biochemistry and cellular physiology of this fungus is still in its infancy and so the present study set out to investigate cell wall modifications during maturation of the *S. boydii* conidium, the infectious propagule of this emerging human pathogen. Our interest in studying conidial maturation came from the observation that conidia from the same culture labeled with mannose/glucose-specific lectin Con A showed an unexpected heterogeneity in the surface fluorescence intensity from one spore to another. It is well known that the cell wall in *S. boydii* comprises peptidorhamnomannan as the main structural component, and this molecule was shown to activate TLR4 and to mediate adherence to HEp2 epithelial cells **[21**, **22]**. The observed variability of fluorescence between cells could not be explained by swelling, as is the case with *A. fumigatus*, since conidia that were intensely labeled with FITC-conjugated Con A were of a similar size to unstained conidia. Likewise, thickness of the outer cell wall layer was unaltered and no cytoplasm vacuolization was observed. Therefore, to explain the variability among conidia taken from the same culture, we hypothesised that they were undergoing maturation. To test this, we investigated variations in cell surface physical properties in conidia taken from 5-, 9- and 14-day-old cultures. Examining surface physical properties provides a general overview of the cell surface reflecting the properties of its components and highlights the changes in the biochemical composition of the cell wall. Comparison of conidia showed a marked increase after day 5 in both CSH and the surface electronegative charge. Although the ensemble of cell wall components are implicated in giving conidia their surface physical property signature, a prominent role of certain components, such as melanin on the surface electrostatic charge for example, has previously been demonstrated in other fungal species like *A. fumigatus* **[27]** and *C. neoformans* **[35**, **36]**. Wang *et al.* **[37]** showed that melanization of *C. neoformans* increases in an approximately linear rate over the course of a 14-day growth period. Nosanchuk and Casadevall **[35]** also performed a time course analysis of melanization and modification in the surface charge of conidia. They found that an increase in the electronegative charge in late stationary phase paralleled a progressive melanization in *C. neoformans* cells. Similarly, in *Trichoderma* species, Pokorny *et al.* **[38]** found that the activity of laccase, an enzyme responsible for the final step of DOPA-melanin synthesis, varied in conidia according to the age of cultures. Indeed, this activity reached a maximum in conidia taken from ≈14-day-old cultures. In *S. boydii*, no previous studies were

available about melanin synthesis. Therefore we investigated the type of melanin produced by conidia by incorporating DHN- or DOPA-melanin inhibitors in the culture medium. A clear difference could be seen in the color of conidia isolated from cultures grown in the presence of DHN-melanin inhibitors after 9 days of incubation. UV-visible spectrophotometry analysis of melanin extracts confirmed that DHN-melanin is a major pathway for the production of melanin in *S. boydii*. Enzymes involved in the DHN-melanin synthesis pathway were also found in mRNA extracts. Melanin amount in extracts from conidia progressively increased after day 5. Our experiments demonstrated that melanin synthesis influences the ultrastructure of the condial wall and that its presence affects the zeta potential of cells. Inhibition of melanin synthesis by the addition of pyroquilon led to a marked decrease in the electronegative charge of the conidial surface.

Melanins naturally contain unpaired electrons that can be detected by EPR as a free radical signal **[39]**. Synthesis intermediates, capable of generating free radicals through a reversible reaction, polymerize to form melanin polymers. Although phenolic subunits have in some instances been discovered in melanin polymers, the exact arrangement of these subunits in the polymer remains unknown **[40]**. Numerous studies have previously associated damage to melanin, by ionizing radiation for example, to the production/liberation of free radicals and an increase in the EPR signal intensity suggesting a depolymerization event. On the other hand, melanin is also known for its antioxidant properties. Melanin scavenges reactive oxygen species (ROS), such as singlet oxygen hydroxyl radicals and superoxide anions, thus conferring protection against oxidative stress inside human host cells. The balance between the intrinsic anti-oxidant and pro-oxidant properties of melanin determines it redox status and its degree of polymerization or the molecular weight of the melanin polymer **[41**, **30]**. In this study we demonstrated that the increasing quantity of melanin in *S. boydii* is accompanied by a decrease in EPR signal intensity in conidia, which implies that melanin tends to polymerize with time and potentially gains a higher antioxidant activity.

Finally, to conclude on our primary observation that conidia did not show a homogeneous labeling with fluorescent Con-A lectin, we demonstrated in this study that the time-dependent increase in melanin amount at the conidial surface during maturation of the spores progressively masks the cell wall mannose-containing glycoconjugates, thus diminishing the accessibility of the conidial surface components to the lectin.

Melanin and hydrophobins provide efficient systems to evade recognition by the immune system and counteract the deleterious effect of reactive oxygen species. In *S. boydii*, we didn't find any rodlet layer on the surface of conidia with AFM analysis irrespective of culture age. However, the absence of such structures does not mean that hydrophobins

are absent at the cell surface. In *A. fumigatus* there are different class I hydrophobins but unlike rodAp, rodBp does not form rodlets. Furthermore class II hydrophobins, which are frequent in the order *Sordariomycetes* (to which *S. boydii* belongs), were never seen to form rodlets at the surface of fungal entities **[42]**. Identifying and sequencing hydrophobins by nucleotide homology was not possible since protein sequences in fungi have very poor homology except for eight cystein residues and few other amino acid residues characteristic of class I or class II hydrophobins.

I.6. Conclusion

The conidial wall is a highly dynamic structure and is subject to changes and modifications with culture age. These findings have important biological consequences since the fine balance between immunogenic molecules at the cell surface, such as cell wall carbohydrates, versus molecules that mask these such as DHN-melanin, needs to be taken into consideration for future studies aimed to understand fungal pathogenicity. All these components conspire to influence the adherence process and the evasion from host immune defenses. Culture conditions should be strictly standardized for all studies concerned with the adherence mechanisms, evasion from host immune defenses or virulence in animal models. Moreover, elucidation of the melanin biosynthesis pathway in *S. boydii* and identification of two of the genes involved offer new opportunities to establish the role of melanin in protecting the fungus against stresses it may be exposed to in the host or in the natural environment. For instance, species of the *S. boydii/S. apiospermum* complex are ubiquitous fungi that are particularly common in highly polluted soils and waters, and melanin at the conidial surface would likely be required to protect spores against toxic agents such as aromatic compounds or heavy metals. Fungicides targeting the synthesis of DHN-melanin may be useful to reduce the dispersal of these pathogens.

I.7. Acknowledgements

We thank Dr. Thomas Guillemette (Institut de Recherche en Horticulture et Semences, Angers University, Angers, France) for his help in the Walking-PCR experiments, and Dr. Guillaume Mabilleau (Service Commun d'Imageries et Analyses microscopiques, Angers University, Angers, France) for helping in electron microscopy experiments.

I.8. References

1. **O'Bryan TA** (2005) Pseudallescheriasis in the 21st century. Expert Rev. Anti Infect. Ther **3**: 765–773.

2. **Cortez KJ, Roilides E, Quiroz-Telles F, Meletiadis J, Antachopoulos C, *et al.*** (2008) Infections caused by *Scedosporium* spp. Clin Microbiol Rev 21: 157–197.

3. **Gilgado F, Cano J, Gené J, Guarro J** (2005) Molecular phylogeny of the *Pseudallescheria boydii* species complex: proposal of two new species. J Clin Microbiol **43**: 4930–4942.

4. **Gilgado F, Cano J, Gené J, Sutton DA, Guarro J** (2008) Molecular and phenotypic data supporting distinct species statuses for *Scedosporium apiospermum* and *Pseudallescheria boydii* and the proposed new species *Scedosporium dehoogii*. J Clin Microbiol **46**: 766–771.

5. **Zouhair R, Rougeron A, Razafimandimby B, Kobi A, Bouchara J-P, *et al.*** (2013) Distribution of the different species of the *Pseudallescheria boydii/Scedosporium apiospermum* complex in french patients with cystic fibrosis. Med Mycol **51**: 603–613.

6. **Tronchin G, Pihet M, Lopes-Bezerra LM, Bouchara J-P** (2008) Adherence mechanisms in human pathogenic fungi. Med Mycol **46**: 749–772.

7. **Dalle F, Jouault T, Trinel PA, Esnault J, Mallet JM, *et al.*** (2003) β-1,2- and α-1,2-Linked oligomannosides mediate adherence of *Candida albicans* blastospores to human enterocytes *in vitro.* Infect Immun **71**: 7061–7068.

8. **Gravelat FN, Beauvais A, Liu H, Lee MJ, Snarr BD, *et al.*** (2013) *Aspergillus* galactosaminogalactan mediates adherence to host constituents and conceals hyphal β-glucan from the immune system. PLoS Pathog **9**: e1003575.

9. **Dubey MK, Jensen DF, Karlsson M** (2014) Hydrophobins are required for conidial hydrophobicity and plant root colonization in the fungal biocontrol agent *Clonostachys rosea*. BMC Microbiol **14**: 18.

10. **Kim S, Ahn I-P, Rho H-S, Lee Y-H** (2005) *MHP1*, a *Magnaporthe grisea* hydrophobin gene, is required for fungal development and plant colonization. Mol Microbiol **57**: 1224–1237.

11. **Desai C, Mavrianos J, Chauhan N** (2011) *Candida glabrata* Pwp7p and Aed1p are required for adherence to human endothelial cells. FEMS Yeast Res **11**: 595–601.

12. **Masuoka J, Hazen KC** (1997) Cell wall protein mannosylation determines *Candida albicans* cell surface hydrophobicity. Microbiology **143**: 3015–3021.

13. **Masuoka J, Wu G, Glee PM, Hazen KC** (1999) Inhibition of *Candida albicans* attachment to extracellular matrix by antibodies which recognize hydrophobic cell wall proteins. FEMS Immunol Med Microbiol **24**: 421–429.

14. **Kriznik A, Bouillot M, Coulon J, Gaboriaud F** (2005) Morphological specificity of yeast and filamentous *Candida albicans* forms on surface properties. C. R. Biologies **328**: 928–935.

15. **Gravelat FN, Ejzykowicz DE, Chiang LY, Chabot JC, Urb M, *et al.*** (2010) *Aspergillus fumigatus MedA* governs adherence, host cell interactions and virulence. Cell Microbiol **12**: 473–488.

16. **Carrion S de J, Leal SM, Ghannoum MA, Aimanianda V, Latgé J-P, *et al.*** (2013) The rodA hydrophobin on *Aspergillus fumigatus* spores masks dectin-1– and dectin-2–

dependent responses and enhances fungal survival *in vivo*. J Immunol **191**: 2581–2588.

17. **Stringer JR** (2007) Antigenic variation in *Pneumocystis*. J Eukaryot Microbiol 54: 8–13.

18. **Voelz K, May RC** (2010) *Cryptococcal* interactions with the host immune system. Eukaryot Cell **9**: 835–846.

19. **Nosanchuk JD, Casadevall A** (2006) Impact of melanin on microbial virulence and clinical resistance to antimicrobial compounds. Antimicrob Agents Chemother **50**: 3519–3528.

20. **Santos ALS, Santos ALS, Bittencourt VCB, Pinto MR, Silva BA, *et al.*** (2009) Biochemical characterization of potential virulence markers in the human fungal pathogen *Pseudallescheria boydii*. Med Mycol **47**: 375–386.

21. **Pinto MR, de Sá ACM, Limongi CL, Rozental S, Santos ALS, *et al.*** (2004) Involvement of peptidorhamnomannan in the interaction of *Pseudallescheria boydii* and HEp2 cells. Microbes Infect **6**: 1259–1267.

22. **Figueiredo RT, Fernandez PL, Dutra FF, González Y, Lopes LC, *et al.*** (2010) TLR4 recognizes *Pseudallescheria boydii* conidia and purified rhamnomannans. J Biol Chem **285**: 40714–40723.

23. **Bittencourt VCB, Figueiredo RT, Silva RB da, Mourão-Sá DS, Fernandez PL, *et al.*** (2006) An α-Glucan of *Pseudallescheria boydii* is involved in fungal phagocytosis and toll-like receptor activation. J Biol Chem **281**: 22614–22623.

24. **Kiffer-Moreira T, Pinheiro AAS, Pinto MR, Esteves FF, Souto-Padrón T, *et al.*** (2007) Mycelial forms of *Pseudallescheria boydii* present ectophosphatase activities. Arch Microbiol **188**: 159–166.

25. **Pinto MR, Rodrigues ML, Travassos LR, Haido RMT, Wait R, *et al.*** (2002) Characterization of glucosylceramides in *Pseudallescheria boydii* and their involvement in fungal differentiation. Glycobiology **12**: 251–260.

26. **Cunha MML, Franzen AJ, Alviano DS, Zanardi E, Alviano CS, *et al.*** (2005) Inhibition of melanin synthesis pathway by tricyclazole increases susceptibility of *Fonsecaea pedrosoi* against mouse macrophages. Microsc Res Tech **68**: 377–384.

27. **Pihet M, Vandeputte P, Tronchin G, Renier G, Saulnier P, *et al.*** (2009) Melanin is an essential component for the integrity of the cell wall of *Aspergillus fumigatus* conidia. BMC Microbiol **9**: 177.

28. **Möller EM, Bahnweg G, Sandermann H, Geiger HH** (1992) A simple and efficient protocol for isolation of high molecular weight DNA from filamentous fungi, fruit bodies, and infected plant tissues. Nucleic Acids Res. **20**: 6115.

29. **Gilgado F, Serena C, Cano J, Gene J, Guarro J** (2006) Antifungal susceptibilities of the species of the *Pseudallescheria boydii* complex. Antimicrob Agents Chemother **50**: 4211–4213.

30. **Khajo A, Bryan RA, Friedman M, Burger RM, Levitsky Y, *et al.*** (2011) Protection of melanized *Cryptococcus neoformans* from lethal dose gamma irradiation involves changes in melanin's chemical structure and paramagnetism. PLoS ONE **6**(9): e25092.

31. **Gadd GM** (1982) Effects of media composition and light on colony differentiation and melanin synthesis in *Microdochium bolleyi*. Trans Br Mycol Soc **78**: 115–122.

32. **Fang W, Bidochka MJ** (2006) Expression of genes involved in germination, conidiogenesis and pathogenesis in *Metarhizium anisopliae* using quantitative real-time RT-PCR. Mycol Res **110**: 1165–1171.

33. **Raggam RB, Salzer HJF, Marth E, Heiling B, Paulitsch AH, *et al.*** (2011) Molecular detection and characterisation of fungal heat shock protein 60. Mycoses **54**: e394–e399.

34. **Wargenau A, Fleißner A, Bolten CJ, Rohde M, Kampen I, *et al.*** (2011) On the origin of the electrostatic surface potential of *Aspergillus niger* spores in acidic environments. Res. Microbiology **162**: 1011–1017.

35. **Nosanchuk JD, Casadevall A** (1997) Cellular charge of *Cryptococcus neoformans*: contributions from the capsular polysaccharide, melanin, and monoclonal antibody binding. Infect Immun **65**: 1836.

36. **Frases S, Salazar A, Dadachova E, Casadevall A** (2007) *Cryptococcus neoformans* can utilize the bacterial melanin precursor homogentisic acid for fungal melanogenesis. Appl Environ Microbiol **73**: 615–621.

37. **Wang Y, Aisen P, Casadevall A** (1996) Melanin, melanin "ghosts," and melanin composition in *Cryptococcus neoformans.* Infect Immun **64**: 2420–2424.

38. **Pokorný R, Vargovič P, Hölker U, Janssen M, Bend J, *et al.*** (2005) Developmental changes in *Trichoderma viride* enzymes abundant in conidia and the light-induced conidiation signalling pathway. J. Basic Microbiol **45**: 219–229.

39. **Enochs WS** (1993) A standardized test for the identification and characterization of melanins using electron paramagnetic resonance (EPR) spectroscopy. Pigment Cell Res **6**: 91–99.

40. **Wakamatsu K, Ito S** (2002) Advanced chemical methods in melanin determination. Pigment Cell Res **15**: 174–183.

41. **Sarangarajan R, Apte SP** (2006) The polymerization of melanin: a poorly understood phenomenon with egregious biological implications. Melanoma Res **16**: 3–10.

42. **Linder MB, Szilvay GR, Nakari-Setälä T, Penttilä ME** (2005) Hydrophobins: the protein-amphiphiles of filamentous fungi. FEMS Microbiol Rev **29**: 877–896.

II. Study II: Cell wall changes during germination of *S. boydii*

A multifaceted study of *Scedosporium boydii* cell wall changes during germination and identification of GPI-anchored proteins

Sarah Ghamrawi[1,*], Amandine Gastebois[1], Agata Zykwinska[2], Agnès Marot[1], Guillaume Mabilleau[3], Stéphane Cuenot[2], Jean-Philippe Bouchara [1,4]

1 L'UNAM Université, Université d'Angers, Groupe d'Etude des Interactions Hôte-Pathogène, EA 3142, France

2 L'UNAM Université, Université de Nantes, Institut des Matériaux Jean Rouxel, Nantes, France

3 L'UNAM Université, Service Commun d'Imageries et Analyses microscopiques, Angers, France

4 Laboratoire de Parasitologie-Mycologie, Centre Hospitalier Universitaire, Angers, France

II.1. Abstract

Scedosporium boydii is a filamentous fungus of increasing clinical importance in individuals with underlying diseases like cystic fibrosis. The development of new therapeutic strategies targeting this fungus necessitates a better understanding of its physiology and the identification of new molecular targets. Here we studied the ultrastructural and biochemical cell wall modifications during conidium to germ tube transition using a variety of microscopic (scanning and transmission electron and atomic force microscopy), physical (two-phase partitioning, microelectrophoresis, and cationized ferritin labeling), chemical (chemical force spectroscopy, lectin labeling), and molecular (extraction and identification of cell wall glycosylphosphatidylinositol (GPI)-anchored proteins) techniques. We demonstrated that the cell wall undergoes structural changes with germination accompanied with a lower hydrophobicity, electrostatic charge and binding capacity to cationized ferritin. Changes during germination also included a higher accessibility of some cell wall polysaccharides to lectins, less CH_3/CH_3 interactions (hydrophobic adhesion forces mainly due to some glycoproteins). We also extracted and identified 20 GPI-anchored proteins from the cell wall of *S. boydii*, among which one was detected only in the conidial wall extract and 12 only in the mycelial wall extract. The identified proteins included some proteins similar to cell wall proteins belonging to families already studied in some yeast and filamentous fungal species like Gelp/Gasp, Crhp, Bglp/Bgtp families and also one extracellular GPI-anchored superoxide dismutase. These results highlighted the cell wall remodeling during germination in *S. boydii* with the identification of a substantial number of cell wall GPI-anchored proteins in conidial and hyphal forms, which provides a basis to investigate the role of these molecules in the host-pathogen interaction and fungal virulence.

II.2. Introduction

Scedosporium boydii is a pathogenic filamentous fungus that causes a wide range of human infections, notably respiratory complications in patients with cystic fibrosis **[1]**. The increasing frequency of these infections and their high mortality rate in immunocompromised patients such as lung transplant recipients call for a better understanding of the fungal biology in order to define new strategies for the improvement of treatments. One of the most attractive targets for antifungal agents is the cell wall, mainly because of the uniqueness of many of its components with respect to mammalian cells **[2]**. The cell wall plays a critical role during morphogenesis and fungal growth since it changes accordingly to fit survival needs **[3]**. It protects the fungus from a wide range of environmental stresses such as desiccation, osmotic stresses and temperature variations. In pathogenic fungi it also provides the means to sustain fungal presence inside the human host by allowing adherence to the host tissues and evasion from the host immune response.

In *S. boydii*, the conidial and mycelial cell walls were shown to contain *N*- and *O*-linked peptidorhamnomannans (PRM) having a branched structure of α-Rha*p*-(1→3)-α-Rha*p*-side chain epitope linked (1→3) to a (1→6)-linked α-Man*p* core **[4]**. Unlike alpha-glucans, isolated from both conidial and hyphal cell walls of *S. boydii*, glucosylceramides could only be obtained from mycelial samples **[5]**, **[6]**. However a more recent study again showed that glucosylceramides were also detectable on the conidial surface of the fungus **[7]**.

We previously demonstrated that the conidial cell wall of *S. boydii* contains dihydroxynaphtalene (DHN)- melanin and that the cell wall content in melanin and mannose-rich glycoconjugates increased during maturation of conidia along with the cell surface physical properties **[8]**. In this study, we track the cell wall changes during the germination process using various approaches, including investigation, at the molecular level, of glycosylphosphatidylinositol (GPI)-anchored proteins in conidial and hyphal walls as these integral cell wall proteins (CWPs) play a major role in normal morphology and virulence in other fungal models **[9**, **10**, **11]**.

II.3. Materials and methods

Strain and culture conditions

The fungal strain *S. boydii* IHEM 15155 (subgroup *P. ellipsoidea,* previously named *Pseudallescheria boydii*) was used throughout this study. It was maintained on YPD (0.5% w/v yeast extract, 2% w/v glucose, 1% w/v peptone, 0.05% w/v chloramphenicol) agar plates.

Cultures were incubated for 7 days at 37°C, then conidia were harvested by flooding the agar surface with sterile Milli-Q™ water and filtered through a 20-µm pore size nylon filter. Conidia were washed twice, pelleted at 5000 X g for 5 min at 4°C, resuspended in 10 ml sterile water and finally counted with a hemocytometer.

Kinetics of germination

To study the kinetics of germination, three conditions were tested: the effect of age of cultures, culture medium and incubation temperature. First, cultures on YPD agar medium were incubated at 37°C for 5, 9 and 14 days, afterwards conidia were isolated and resuspended in YPD liquid medium (20 ml per Petri dish) at a concentration of 2 x 10^6 conidia/ml and kept at 37°C. To study the effects of culture medium, the same settings were applied except that the fungus was cultivated on Malt (1.5% w/v malt extract, 0.05% w/v chloramphenicol) or YPD agar and then conidia were resuspended in Malt or YPD liquid media which were incubated at 37°C. Finally, for the incubation temperature, conidia taken from cultures on YPD agar at 37°C were resuspended in YPD liquid medium which was incubated at 20°C, 25°C, or 37°C. In all cases, germination in liquid media was monitored over 8 h and five pictures were taken every 2 h, the presence of mycelia was also checked after 16 h. The percentage of germination was determined after counting at least 100 cells from each picture.

Scanning and transmission electron microscopy

Conidia or germ tubes were washed twice in Milli-Q™ water and once in cacodylate buffer (0.1 M), and then incubated in the fixative solution (2.5% (w/v) glutaraldehyde, 2% (w/v) paraformaldehyde, 0.1M cacodylate buffer) for 24 h at room temperature under vacuum. After washing with cacodylate buffer, samples were incubated for 24 h in 2% $KMnO_4$ in cacodylate buffer at 4°C, washed and post-fixed for 2 h at room temperature in 2% osmium tetroxide. Then samples were washed in Milli-Q™ water and finally dehydrated through a series of ethanol-water solutions (50, 70, 95% ethanol, 2 x 30 min each) and then 100% ethanol (3 x 20 min).

For scanning electron microscopy (SEM), samples underwent two baths of graded ethanol-hexamethyldisilazane (HDMS) solutions (50/50, then 25/70 proportions, 45 min each) followed by immersion in pure HMDS baths (3 x 45 min). Processed samples were mounted on aluminium stubs, coated with carbon, and stored in a desiccator until studied. Observations were made on a JSM 6301F scanning electron microscope (Jeol, Paris, France) operating at 3 kV and equipped with digital imaging.

For transmission electron microscopy (TEM), ethanol was replaced by propylene oxide (3 x 20 min) and samples were impregnated overnight in a propylene oxide-Epon mixture

(1:1 v/v) and then in pure Epon for 16 h and 8 h. After polymerization (24 h at 37°C, 24 h at 45°C and then 48 h at 60°C), thin sections were directly examined on a JEM-1400 transmission electron microscope (Jeol, Paris, France; 120 kV) except for life cycle studies of *S. boydii* where thin sections were contrasted with uranyl acetate and lead citrate prior examination.

Ferritin labeling

Cationized ferritin is a positively charged ligand that allows visualization of anionic sites at the cell surface under physiological pH and ionic strength **[12]**. *Scedosporium boydii* germ tubes were examined by TEM after labeling with cationized ferritin, and controls consisted in incubation of fungal elements with native ferritin (lacking a positive charge) and in pretreatment of germ tubes with neuraminidase (type X) in order to remove sialic acids (all products purchased from Sigma-Aldrich, St Quentin Fallaviers, France). To do this, *S. boydii* germ tubes were washed 3 times with MilliQ^{TM} water, centrifuged and then incubated with cationized or native ferritin (1 mg/ml in phosphate buffered saline 150 mM) for 1 h at room temperature with agitation. To remove sialic acids, cells were first incubated with neuraminidase (1 U/ml in 0.1 M acetate buffer pH 5, supplemented with 40 mM $CaCl_2$) for 30 min at room temperature with shaking, washed twice and then incubated with cationized ferritin as described above. Cells in the three conditions were finally washed twice in MilliQ^{TM} water and treated as described earlier for transmission electron microscopy.

Cell surface charge and hydrophobicity measurement

Cell surface charge and hydrophobicity were evaluated by microelectrophoresis and two-phase partitioning as previously described **[8]**. Briefly, resting or germinating conidia were washed and resuspended in Milli-Q^{TM} water containing 1 mM NaCl, then their electrophoretic mobility was measured with the Zetasizer Nano ZS (Malvern Instruments Ltd, Malvern, UK) and zeta potential was calculated using the Smoluchowski equation. Experiments were performed at 25°C and repeated three times (ten to thirty cycles for each measurement). The cell surface hydrophobicity (CSH) was determined using the water/hexadecane system. Briefly, germ tube suspensions (2.5 ml) prepared in PBS were topped or not (in case of control samples) with hexadecane (0.5 ml), and vortexed for 2 min, then allowed to stand at room temperature for 3 min and finally 1 ml of the aqueous phase (bottom) was transferred into a new tube. After repeating the same procedure, samples were homogenized and the optical density (OD) was read at 405 nm on three 200-µl aliquots for each sample. The percentage difference in optical density readings between test samples and controls was considered as the hydrophobic index. Experiments were performed in triplicate.

Lectin labeling

Germ tubes were washed with Tris buffer (0.5 mM Tris, 100 mM NaCl, 1 mM $CaCl_2$, 1 mM $MgCl_2$, pH 7.0) and then incubated with gold-conjugated concanavalin A (Con A-gold 5 nm from Biovalley, Marne la Vallée, France; 1:50 dilution in Tris buffer) or with FITC-conjugated Con A, peanut agglutinin (PNA) or wheat germ agglutinin (WGA) at a final concentration of 100 µg/ml (all fluorescent lectins from Sigma-Aldrich), for 30 min at 37°C with continuous rotatory mixing **[8]**. Control samples consisted in incubation of fungal elements together with the lectins and a large excess (0.2 M) of the lectin-specific carbohydrates (α-methyl D mannopyranoside for Con A, N-acetyl glucosamine for WGA, and galactose for PNA) added immediately before lectins. Finally, samples were washed three times in Tris buffer, and observed under fluorescence microscope (Leica DMR, Leipzig, Germany) for FITC-conjugated lectins or processed as described earlier for TEM without contrasting with uranyl acetate and lead citrate.

Chemical force spectroscopy (CFS) measurements

The surface of *S. boydii* resting or germinated conidia was imaged using a NanoWizard® atomic force microscope (JPK Instruments AG, Berlin, Germany) operating in intermittent contact mode under ambient conditions. A standard rectangular cantilever (Nanosensors NCL-W) was used for imaging, with a free resonance frequency of 165 kHz and a typical spring constant of about 40 N/m. The radius curvature of the tip was ~10 nm. The detailed analysis of chemical force spectroscopy images was performed using JPK Data Processing software (JPK Instruments AG). Hydrophilic and hydrophobic adhesions were obtained in ultrapure water from force-distance curves measured on the surface of both conidia and germ tubes using functionalized cantilevers. Gold-coated cantilevers (Olympus, Hambourg, Germany) with spring constants of 0.01 N/m were immersed either in 1 mM solutions of 1-dodecanethiol or in 11-mercapto-1-undecanol (Sigma-Aldrich) in ethanol for 14 h and then rinsed with ethanol prior their use. From force-curve measurements (2048 measurements), the mean hydrophilic and hydrophobic adhesions were extracted from gaussian fits performed on the histograms. Before probing the conidial or germ tube surface, the cantilevers functionality was tested by measuring their adhesion to hydrophobic or hydrophilic flat surfaces.

Protein extraction, identification and analysis

Protein extraction. Extraction was performed according to Damveld *et al.* **[13]** with modifications. Frozen conidia or germ tubes were ground with a mortar and pestle in liquid nitrogen, then crushed in a cell homogenizer (Braun Melsungen model MSK, Melsungen, Germany) for 1.5 min for conidia or 1 min for germ tubes (150 mg dry material) under a

current of CO_2 cooling in the presence of a protease inhibitor cocktail (15ml; 1X in MilliQ water, cOmplete, EDTA-free, Roche, Meylan, France) and a mix of 1 mm and 0.25 mm diameter glass beads. Glass beads were removed by filtration through 41-µm-pore size sterile nylon filters and cell breakage was confirmed by phase-contrast microscopy (> 95%). Suspensions were centrifuged at 13500 X g for 10 min at 4°C. After lyophilization, cell debris (500-900 mg) were washed 5 times with 50 mM Tris-HCl buffer pH 7.8 (25 µl per mg dry weight) and pelleted at 18000 X g for 10 min at 4°C. Cytosolic contaminants, membrane proteins and disulfide-linked cell wall proteins were removed by boiling five times (2 min each) with SDS-extraction buffer (50 mM Tris-HCl pH 7.8, 2% w/v SDS, 0.1 M Na-EDTA, and 1.6 µl β-mercaptoethanol; 25 µl per mg dry weight). Then cell wall debris were washed six times with MilliQ^{TM} water, lyophilized and weighed. To extract cell wall GPI-anchored proteins, freeze-dried cell wall debris were incubated with HF-pyridine (10 µl per mg dry weight) for 3 h at 0°C **[14]**. Then the suspension was centrifuged at 18000 X g for 10 min at 4°C and proteins were precipitated from the supernatant by the addition of 9 volumes of 100% methanol-Tris buffer (100% v/v methanol, 50 mM Tris-HCl pH 7.8) followed by incubation for 2 h at 0°C. After centrifugation, the pellet was washed twice with 90% methanol-Tris buffer (90% v/v methanol, 50 mM Tris-HCl pH 7.8) and lyophilized. The resulting extracts represented 10.0% and 10.2% of the initial dry weight of cell wall debris after removal of cytosolic contaminants in conidia and germ tubes, respectively. Finally, proteins were deglycosylated with peptide-N-glycosidase F (PNGase glycerol free, New England Biolabs, Evry, France) according to the manufacturer's recommendation. Deglycosylation was performed in glass vials by the addition of 5000 units PNGase F to 50-100 mg protein extract, followed by incubation for 3h at 37°C. Proteins were precipitated and washed as described earlier using the methanol-Tris buffer and finally lyophilized.

Trypsin digestion. Lyophilized samples were suspended in 50 mM ammonium bicarbonate and incubated with 7.2 mM dithiothreitol (DTT) during 15 min at 37°C. They were next incubated with 13.5 mM iodoacetamide during 15 min at room temperature in the dark. Samples were then digested overnight with 4 ng/µl of sequencing grade modified trypsin (Promega, Madison, WI, USA) at 37°C.

Mass spectrometry (MS). MS measurements were done with a nanoflow high-performance liquid chromatography (HPLC) system (Dionex, Villebon sur Yvette, France; LC Packings Ultimate 3000) connected to a hybrid LTQ-OrbiTrap XL (Thermo Fisher Scientific, Villebon sur Yvette, France) equipped with a nanoelectrospray ion source (New Objective, Wil, Switzerland). Peptides from tryptic digestion were injected onto a trapping precolumn (5 mm x 300 µm i.d., 300 Å pore size, Pepmap C18, 5 µm) for 3 min in 2% buffer B (acetonitrile, 0.1% formic acid) at a flow rate of 25 µl/min. This step was followed by

reverse-phase separations at a flow rate of 0.25 µl/min using an analytical column (15 cm x 300 µm i.d., 300 Å pore size, Pepmap C18, 5 µm, Dionex, LC Packings). The gradient ranged from 2% to 35% buffer B for the first 30 min, increased to 60% buffer B until minute 40, and to 90% buffer B in minute 43. Finally, the column was washed with 90% buffer B for 9 min, and equilibrated with 2% buffer B for 21 min prior to loading of the next sample.

The peptides were detected by directly eluting them from the HPLC column into the electrospray ion source of the mass spectrometer. An electrospray ionization (ESI) voltage of 1.5 kV was applied to the HPLC buffer using the liquid junction provided by the nanoelectrospray ion source and the ion transfer tube temperature was set to 200° C. The MS instrument was operated in its data-dependent mode by automatically switching between full survey scan MS and consecutive MS/MS acquisition. Survey full scan MS spectra (mass range 400-2000) were acquired in the OrbiTrap section of the instrument with a resolution of R = 60000 at m/z 400; ion injection times were calculated for each spectrum to allow the accumulation of 10^6 ions in the OrbiTrap. The ten most intense peptide ions in each survey scan with an intensity > 2000 counts (to avoid triggering fragmentation too early during the peptide elution profile) and a charge state = 2 were sequentially isolated at a target value of 10000 and fragmented in the linear ion trap by collision induced dissociation (CID). Normalized collision energy was set to 35% with an activation time of 30 ms. Peaks selected for fragmentation were automatically put on a dynamic exclusion list for 60 s with a mass tolerance of ± 10 ppm. The maximum injection time was set to 500 ms and 300 ms for full MS and MS/MS scan events respectively, and for an optimal duty cycle the fragment ion spectra were recorded in the LTQ mass spectrometer in parallel with the OrbiTrap full scan detection. For OrbiTrap measurements, an external calibration was used before each injection series ensuring an overall error mass accuracy below 5 ppm for the detected peptides. MS data were saved in RAW format files using XCalibur software version 2.0.7 (Thermo Fisher Scientific) with tune 2.5.5 SP1.

Protein identification. The Proteome Discoverer 1.2 software was used to submit MS/MS data to the translated genome of *S. apiospermum* IHEM 14462 (previously *Pseudallescheria apiospermum*) completed with *Sus scrofa* trypsin and *Elizabethkingia miricola* PNGase F (10829 sequences) using the Mascot search engine (Mascot server v2.2; http://www.matrixscience.com). Parameters were set as follows: trypsin as enzyme with one allowed miscleavage, carbamidomethylation of cysteins as fixed modification and methionine oxidation as variable modifications. Mass tolerance for MS and MS/MS was set at 10 ppm and 0.5 Dalton, respectively. Identified rank 1 peptides were filtered based on Xcorr values and the Mascot score to obtain a false discovery rate of 1%.

Protein analysis. Sequences of the identified proteins were analyzed for the presence of GPI anchor using Big PI fungal predictor (http://mendel.imp.ac.at/gpi/fungi_server.html), signal peptide using Signal P (http://www.cbs.dtu.dk/services/SignalP/), transmembrane helices using TMHMM server (http://www.cbs.dtu.dk/services/TMHMM/), N- and O-glycosylation sites using NetNGlyc and NetOGlyc services (http://www.cbs.dtu.dk/services/), pI using ProtPararm (http://web.expasy.org/protparam/) and grand average of hydropathy values (GRAVY) to evaluate the hydrophilic or hydrophobic character of a protein along its amino acid sequence (http://www.bioinformatics.org/sms2/protein_gravy.html). For pipeline filtering of proteins the new web tool proFasta was also used (http://www.bioinformatics.nl/tools/profasta/). Functional domain analysis was performed using Interpro (http://www.ebi.ac.uk/interpro/). Protein sequence similarities were searched by using Blastp in NCBI website (http://blast.ncbi.nlm.nih.gov) against all the non-redundant protein sequences and then against species-specific databases *Aspergillus fumigatus*, *Neurospora crassa*, *Magnaporthe oryzae* and *Saccharomyces cerevisiae*. Specific websites were also used to perform Blastp analysis against *Candida albicans* (http://www.candidagenome.org), *Colletotrichum graminicola* and *Colletotrichum higginsianum* genomes (http://www.broadinstitute.org/annotation/genome/colletotrichum_group/Blast.html).

Statistical analysis.

For studies of the kinetics of germination, two-way analysis of variance (ANOVA) was used with the Bonferroni post-hoc test. For cell surface charge and hydrophobicity studies, results were analyzed using the Student *t*-test. *P*-values less than 0.05 were considered significant.

II.4. Results

Germination and life cycle of *S. boydii*

In order to define the best conditions for germination of *S. boydii*, three different parameters were first investigated: the age of culture, the culture medium and incubation temperature. Tracking germination during 8 h showed significant differences ($P < 0.01$ at 4 h and $P < 0.001$ at 6 and 8 h) in the percentages of germination between conidia isolated from 5-, 9-, and 14-day old cultures (**Figure E.19.A**). Germination started after 4 h of incubation and conidia recovered from 9-day old cultures showed highest rates of germination as well as more homogeneity in terms of size of germ tubes. After 16 h of incubation all cultures showed mycelial agglomerations and the percentage of ungerminated conidia could no more be determined. Germination was also affected by the culture medium. Higher germination rates were observed for conidia recovered from 9-day old cultures and incubated in YPD

liquid medium compared to malt liquid medium (**Figure E.19.B;** $P < 0.001$). Finally, incubation temperature greatly affected the kinetics of germination since the number and length of germ tubes progressively increased with the increase in incubation temperature from 20°C to 25°C and 37°C with the presence of long branched intermixed hyphae after 16 h of incubation at 37°C (**Figure E.19.C**). Therefore germination was performed by incubation of conidia from 9-day old cultures in YPD liquid medium at 37°C for all subsequent experiments.

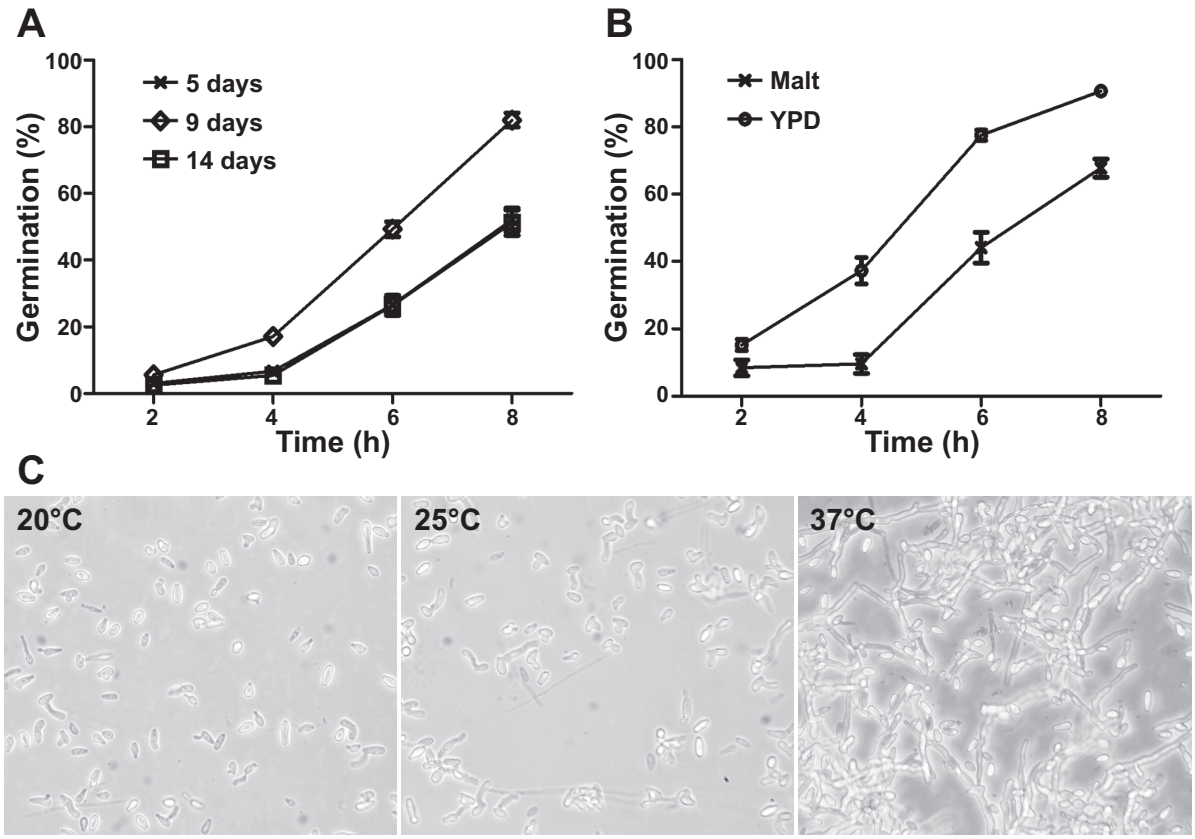

Figure E.19. Kinetics of germination of *S. boydii* in various conditions.

A: conidia isolated from 5-, 9- and 14-day-old cultures on yeast peptone dextrose (YPD) agar were incubated in YPD liquid medium over 8 h at 37°C. B: conidia isolated from 9-day-old cultures on Malt or YPD agar were incubated in Malt or YPD liquid media over 8 h at 37°C. C: conidia isolated from 9-day-old cultures on YPD agar were incubated in YPD liquid medium for 16 h at 20°C, 25°C or 37°C (200X).

The process of germination in *S. boydii* starts by the protrusion of a germ tube from the mother cell without significant differences in the conidial size before and after initiation of the germination process. As illustrated in **Figure E.20.A,** resting conidia measured 5.31 ± 0.92 x 2.74 ± 0.57 µm (7 conidia studied), a size which remains essentially the same after germination (**Figure E.20.B**, 4.79 ± 0.36 x 2.13 ± 0.34 µm; 7 conidia measured). Most

germination events occurred laterally rather than along the axis of the mother cell: Among 111 germinated cells only 29 cells (26.1%) germinated along the axis whereas the rest of conidia (73.9%) germinated laterally as shown in **Figures E.20.B** and **C**. With the progression of germination, branching occured and the first branching site was seen very close to the mother cell (**Figure E.20.D** and **E,** arrow). Finally, more branching appeared along the filaments, at the subapical region of the articles (**Figure E.20.F**, arrowheads), and filaments elongated until the mother cell was no more distinguished.

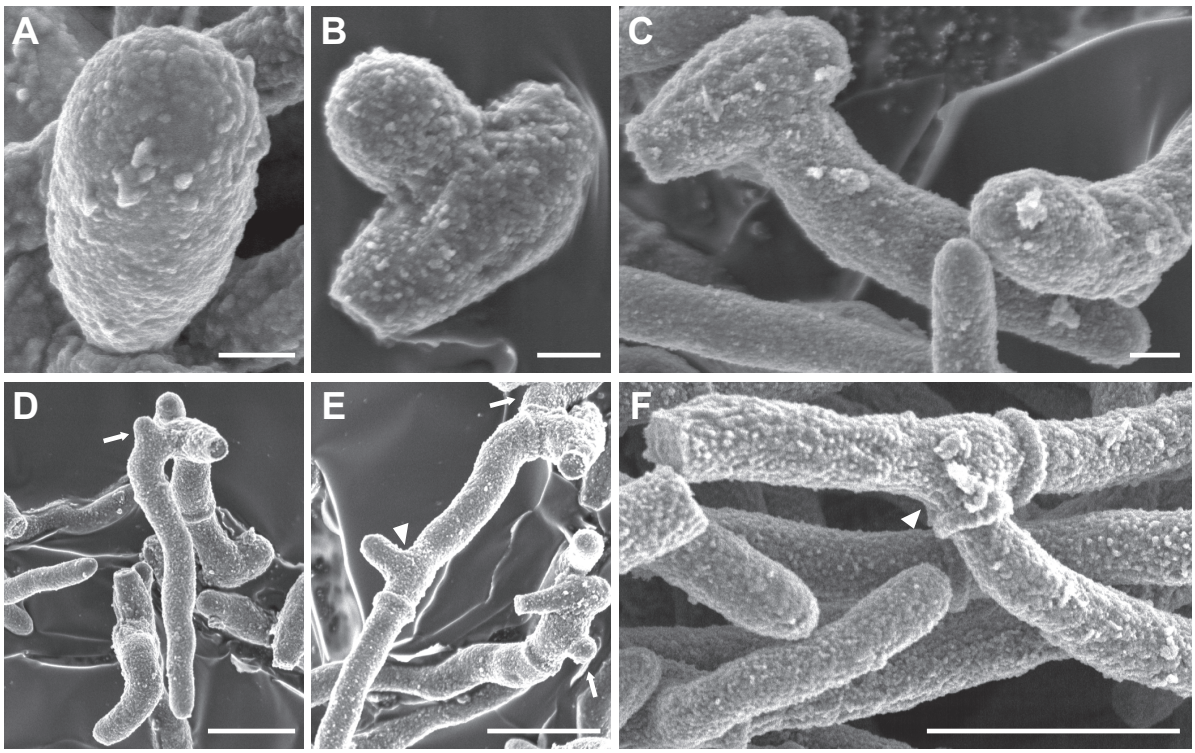

Figure E.20. The life cycle of *S. boydii* under scanning electron microscopy.
After release from phialides, conidia (A) germinate (B) and the hyphal part of germ tubes elongates (C) until a first branch emerges near the mother cell (D). Both hyphae grow and more branching sites appear on filaments at the subapical region of the articles (E) until the mother cell can no more be distinguished (F). Arrows indicate sites of first branching, and later branching are indicated by arrowheads. Bars: 1 µm in A, B and C; 0.5 µm in D; and 5 µm in E and F.

TEM examination of the different morphological stages of the fungus showed important ultrastructural changes in the cell wall during with germination (**Figure E.21**). The fungal cell wall appeared to be composed of two layers, a large electrontransparent inner layer and a thinner electron dense outer layer. Comparing the cell wall of hyphae (**Figure E.21.A**) to that of conidia (**Figure E.21.B**) showed a homogeneous thickness of the outer cell wall layer in resting conidia and mother cells of germ tubes, whereas its thickness greatly varied in hyphae. The outer cell wall layer of the filament was thin or even absent in some places. Of

note, the cell wall surface of the mother cell seemed to be covered by a thin electrondense film which was totally lacking at the surface of the hyphal part of germ tubes, allowing plasticity and elongation of the filament (**Figure E.21.C** and **D**).

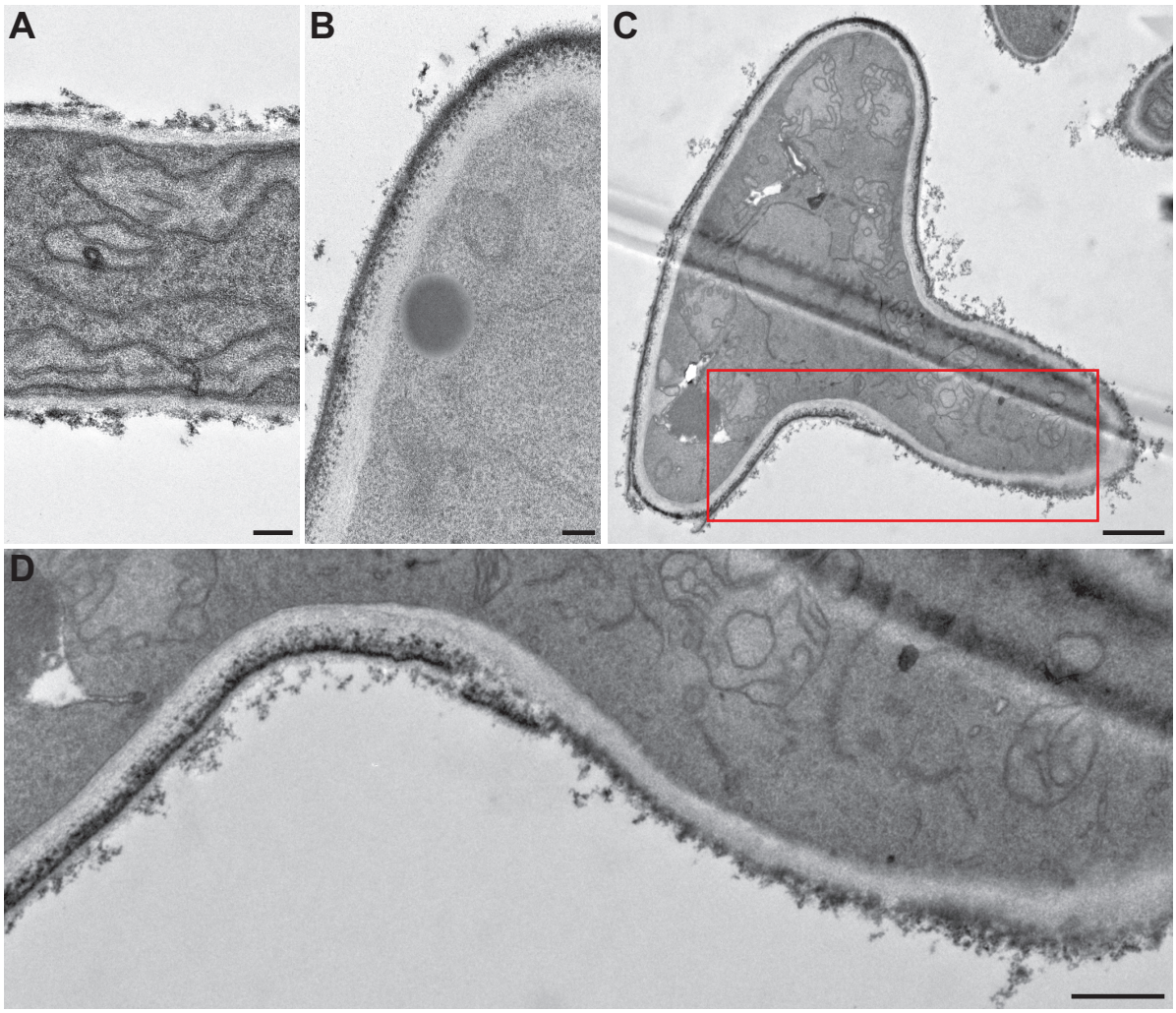

Figure E.21. Cell wall modifications during germination of *S. boydii* under transmission electron microscopy.

A: hyphal cell wall; B: conidial cell wall; and C: cell wall of a germinating conidium. D: enlarged part of C highlighting the cell wall structural modifications during germination and the loss of the electron dense film covering the surface of conidia. Bars: 0.2 µm in A and B; 1 µm in C; and 0.5 µm in D.

Changes in cell surface physical properties during germination

The differences in the biochemical composition of the cell wall between conidia and hyphae reflected by the ultrastructural changes were also revealed by modifications of the surface physical properties as can be seen in **Figure E.22.A**. TEM after cationized ferritin

labeling showed a greater density of negatively charged areas at the surface of mother cells of germ tubes compared to their hyphal part. Neuraminidase pretreatment of germ tubes before incubation with cationized ferritin showed that the surface negative charge was not related to the presence of sialic acids on the mother cell or the hyphal surface (**Figure E.22.B**). The use of native ferritin confirmed that binding of cationized ferritin was related to its electrostatic charge and not to the ferritin molecule itself (**Figure E.22.C**). Zeta potential measurements also provided evidence for the difference in the surface electronegative charge between resting (-40.50 ± 0.15 mV) and germinated (- 16.10 ± 2.42) conidia as seen in **Figure E.22.D** (P = 0.0005).

Similarly, the cell surface hydrophobicity was also shown to decrease after germination (**Figure E.23**, P < 0.0001).

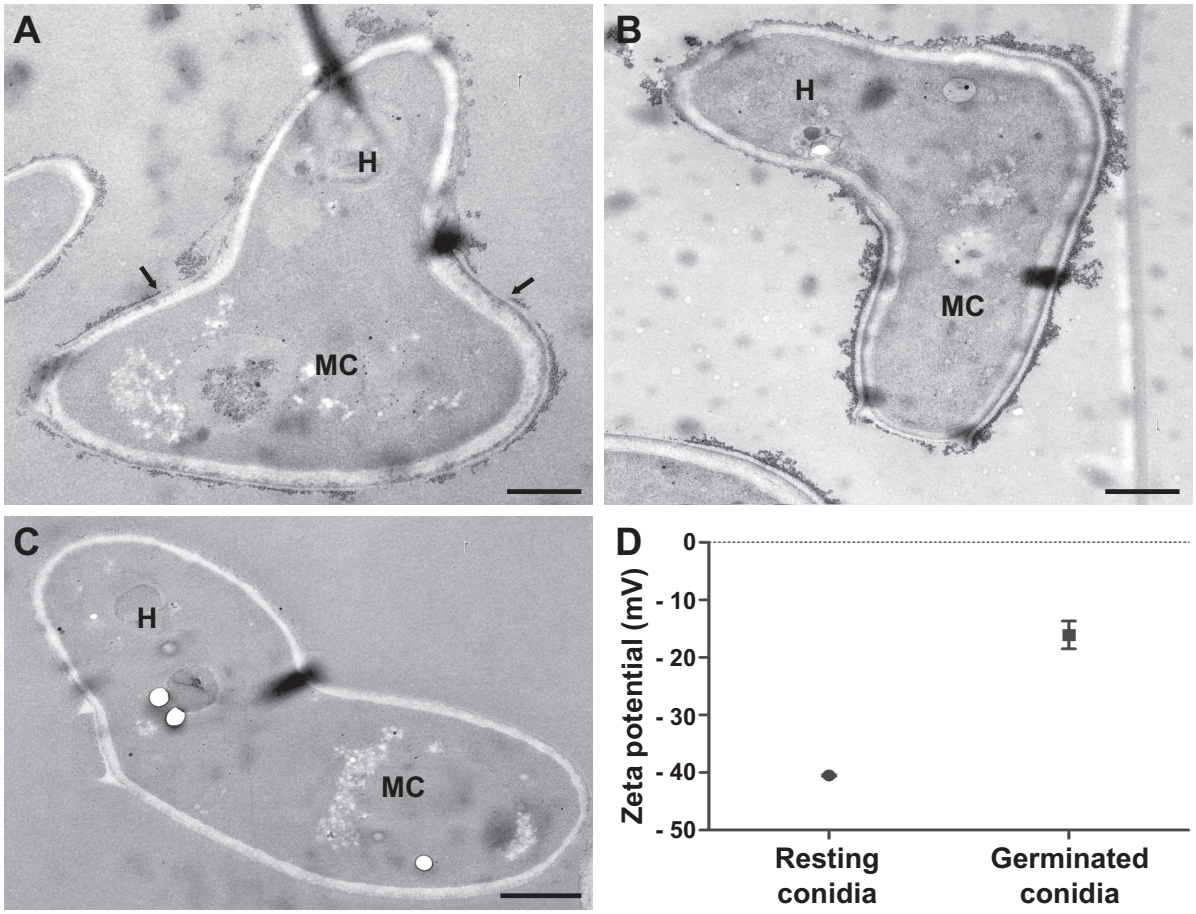

Figure E.22. Detection of surface charge modifications during germination of *S. boydii* by ferritin labeling and zetapotential measurements.

TEM images of germ tubes labeled with cationized ferritin (A), treated with neuraminidase prior cationised ferritin labeling (B) or incubated with native ferritin (C). D: Comparison of the surface electrostatic charge of resting and germinated conidia (P = 0.0005). H: hyphal part of germ tube; MC: mother cell of germ tube. Bars: 1 µm.

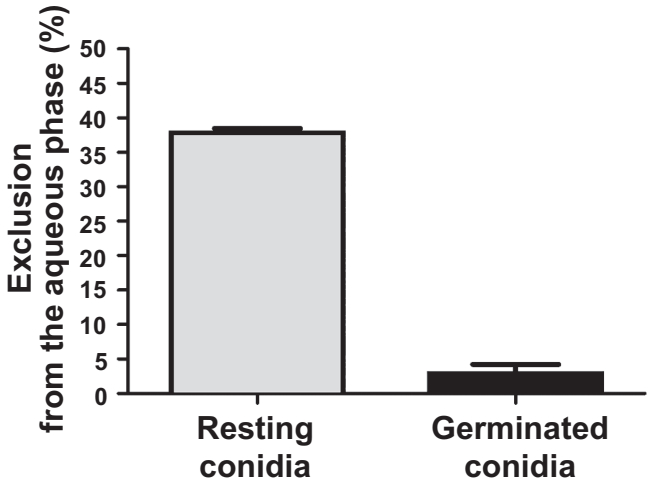

Figure E.23. Change in the cell surface hydrophobicity following germination.
Significant difference in the cell surface hydrophobicity between resting and germinated conidia revealed by two-phase partitioning using the water/hexadecane system ($P < 0.0001$).

Changes in the cell surface composition during germination

Lectin binding to cell wall carbohydates. The accessibility of cell wall carbohydrates to mannose-binding, chitin-binding **[15]** and galactose-binding **[16]** lectins (Con A, WGA and PNA, respectively) was investigated during germination of *S. boydii*. While most of the mother cells were not labeled with Con A, as previously shown for resting conidia **[8]**, the hyphal part of almost all germ tubes was intensely labeled (**Figure E.24.A**, **E.24.D** and **E.25**), suggesting unmasking of the mannose-containing glycoconjugates by the loss of the surface electron dense film seen on the mother cells. A similar binding pattern was also seen for WGA (**Figure E.24.B** and **E.24.E**), whereas no fluorescence was observed after incubation with PNA either on the mother cell or the hyphal part of germ tubes (**Figure E.24.C** and **E.24.F**).

Detection of hydrophobic/hydrophilic adhesions at high spatial resolution in conidia and hyphae. AFM images presented on **Figure E.26.A** and **B** revealed that the surface of *S. boydii* conidia is smooth, devoid of any peculiar organization, conversely to that of *A. fumigatus* conidia which is totally covered by rodlets **[17]**. To investigate the chemical nature of *S. boydii* cell surface, non-specific force-curves were measured with OH- or CH_3-modified tips (**Figure E.26.C**). CFS using CH_3-modified probes (to measure hydrophobic adhesion forces) revealed the presence of hydrophobic components, such as glycoproteins, while the use of OH-modified probes revealed hydrophilic adhesion forces mainly due to the presence of polysaccharides. Force-curves recorded on the surface of nongerminated conidia with CH_3 tips showed large adhesion forces of 1.8 ± 0.3 nN, whereas a lower value of 0.85 ± 0.15 nN was obtained on the surface of the hyphae (**Figure E.26.C**), which was in

agreement with the diminished cell surface hydrophobicity measured by two-phase partitioning. The values for CH3/CH3 interactions measured at the surface of the germ tube and its apex were similar (0.8 to 0.9 nN) suggesting that the same hydrophobic glycoproteins covered the whole hyphal surface.

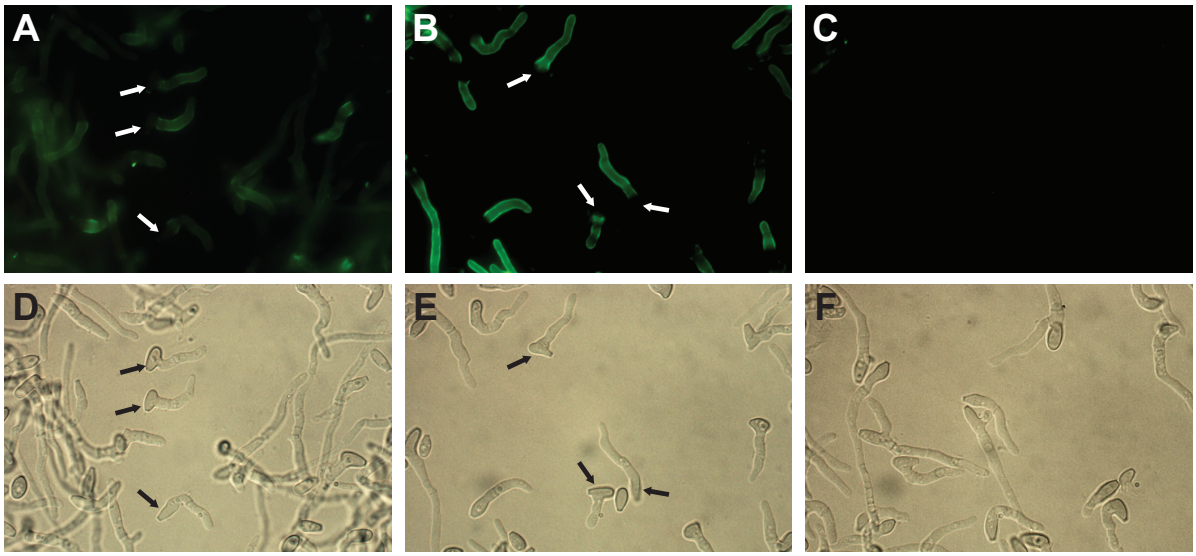

Figure E.24. Fluorescence labeling of *S. boydii* surface carbohydrates with FITC-conjugated lectins.

Germ tubes after labeling with mannose-binding Concanavalin A (A and D), chitin-binding wheat germ agglutinin (B and E), and galactose-binding peanut agglutinin (C and F) lectins. The same fields are presented under fluorescence and phase contrast microscopy respectively. Arrows indicate mother cells.

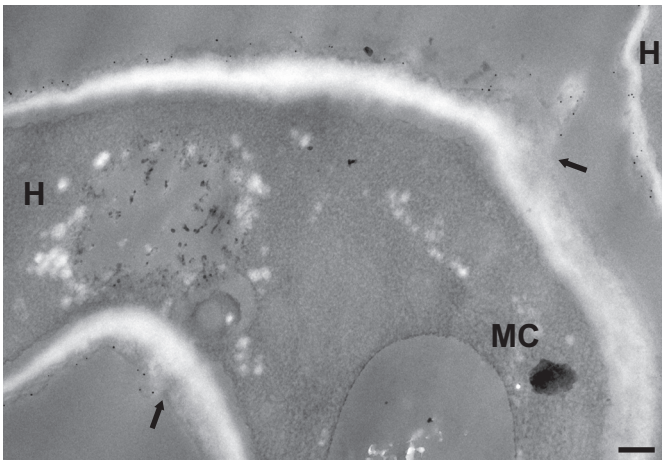

Figure E.25. Gold labeling of cell wall mannan groups in *S. boydii* germ tubes as observed by trasmission electron microscopy.

Germ tubes labeled with gold-conjugated concanavalin A (Con A; 5-nm gold particles) showing higher affinity of gold particles to the hyphal part (H) of germ tubes compared to the mother cell (MC). Arrows indicate the limits of the outer cell wall layer of the mother cell. Bar: 0.5 µm.

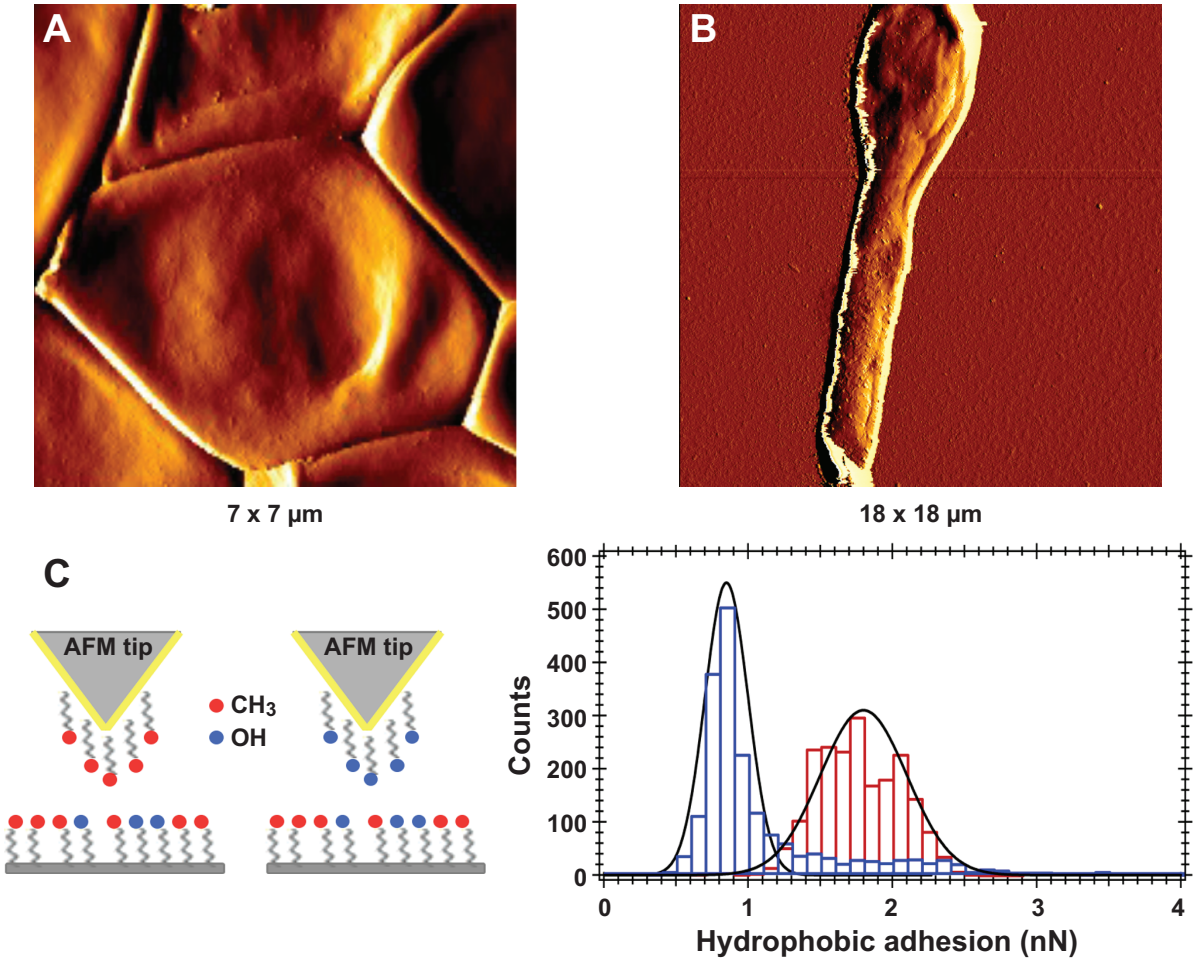

Figure E.26. High resolution imaging and chemical force spectroscopy analysis of *S. boydii* conidia and germ tubes.

AFM amplitude images of a resting (A) or germinated (B) *S. boydii* conidium. C left: Scheme for chemical functionalization of AFM tips. Gold-coated tips were modified with CH3-terminated alkanethiols or OH-terminated alkanethiols. C right: Histograms of hydrophobic adhesion forces measured on the surface of a resting conidium (1.8 ± 0.3 nN, in red) and the hyphal part of a germinated conidium (0.85 ± 0.15 nN, in blue).

On the contrary, no significant difference in OH/OH interactions (hydrophilic adhesions) was observed between resting (1.2 ± 0.4 nN) and germinated conidia (1.0 ± 0.2 nN). Likewise, the same adhesion values (1.0 nN) were calculated for the surface of the basis and the apex of the hyphal part of germ tubes.

Characteristics of the identified surface proteins

Two hundred and fifty proteins were detected from both the conidial and germ tube extracts taken together, and among them 32 had a signal peptide. Analysis with BigPI software identified 20 different GPI-anchored proteins (**Table E.5**). Seven of out of the 20 GPI-anchored proteins were detected in both conidial and germ tube extracts, 12 only in the

germ tube extracts and one only in the conidial extract. Analyzing the 20 identified GPI proteins showed that all proteins were extensively glycosylated (**Table E.6)**, had a signal peptide and all but one had no transmembrane helices after excluding 45-N-terminal and 35 C-terminal amino acids. One transmembranal helix was found for the glycine-rich protein (accession number KEZ42341.1). All 20 proteins had a pI < 5 except for the glycine-rich protein whose pI was 6.89. To analyze the serine-threonine (S/T) content of our proteins, we first considered the overall S/T content of proteins (results indicated in **Table E.6**), then we analyzed them with proFasta with additional filters (S/T content >10%, *Start position of scan* 26 and *End position of scan* -26) to exclude the S/T content of N- and C-terminal signal sequences. With this analysis all 20 proteins had an S/T content higher than 10%.

Analysis of *S. apiospermum* proteome also revealed the presence of 100 gene sequences coding for GPI anchored proteins (**Figure E.27**), which meant that 20% of GPI anchored proteins was extracted in our conditions.

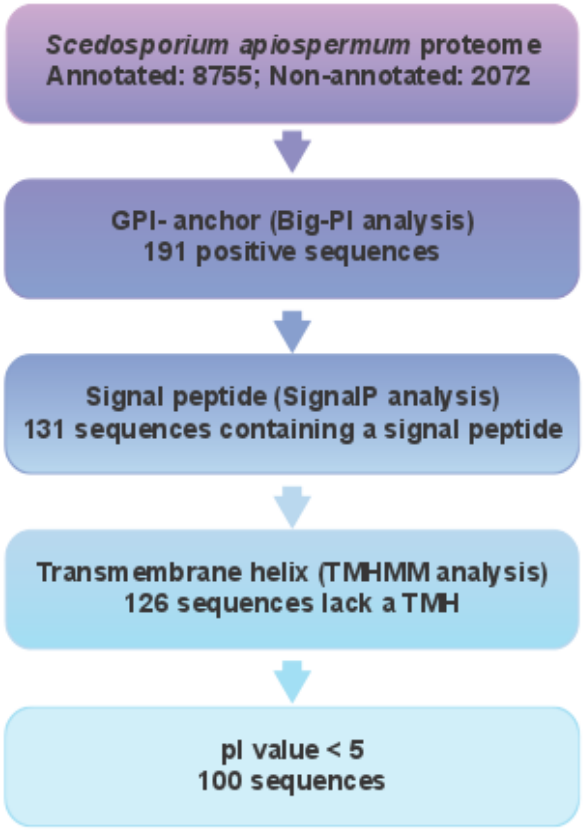

Figure E.27. Flowchart showing the analysis of *S. apiospermum* IHEM 14462 proteome sequences in search for putative GPI-anchored proteins.

Protein sequences used for analysis were generated from internal laboratory sequencing (refer to Experimantal part: Section III). Accession numbers for most protein sequences are available on NCBI database.

Table E.5. Identified GPI-anchored protein sequences in conidial and germ tube extracts

Protein (Accession number) [a]	**Fungal extract**[b]	**Sequence**	**Charge ; m/z [Da]**	**Ion score**	**Modification**[c]	**Coverage**
Glucan endo-1,3-beta-D-glucosidase (KEZ41172.1)	RC	AAQGLDGTNGAFNSAR	2 ; 775.37518	95		3.06
	GC	ISPTGIANKEFAGANPDTLVGYIK	3 ; 826.11169	43		9.58
		EFAGANPDTLVGYIK	2 ; 797.91400	32		
		AAQGLDGTNGAFNSAR	2 ; 775.37335	30		
		SQSDFEAEFKAAQGLDGTNGAFNSAR	3 ; 906.75531	29		
CFEM domain (KEZ46909.1)	RC	AGEFGcQSTDVAcLcR	2 ; 915.88647	76	C6, C13 and C15	12.38
		SRDFVYGIR	2 ; 556.79877	43		
	GC	AGEFGcQSTDVAcLcR	2 ; 915.88623	72	C6, C13 and C15	12.38
		SRDFVYGIR	2 ; 556.79712	36		
		DFVYGIR	2 ; 435.23141	24		
CFEM domain (KEZ46627.1)	RC	QGDWYcGcQPDNmSK	2 ; 931.35608	64	C6, C8 and M13	8.02
	GC	QGDWYcGcQPDNMSK	2 ; 923.35590	59	C6 and C8	26.74
		IQGAATNcVIEAcGGAAGALAVITEVQGIcEEALK	3 ; 1182.26111	55	C8, C13 and C30	
CFEM domain (KEZ44163.1)	RC	IPEcANScVTQATSGNK	2 ; 918.92078	24	C4 and C8	9.83

	GC	IPEcANScVTQATSGNK	2 ; 918.91559	67	C4 and C8	15.61
		IAGcNQGDIK	2 ; 538.26495	33	C4	
GDSL_like lipase (KEZ43142.1)	RC	SQKVVLVDFR	2 ; 595.85217	34		2.83
	GC	MAALLFDGINNAASR	2 ; 782.40625	26		4.25
Glycine-rich protein (KEZ42341.1)	RC	GGSSSSSSSSSRPGSPGFAGSGAPR	3 ; 737.67633	37		8.68
	GC	GGSSSSSSSSSRPGSPGFAGSGAPR	3 ; 737.67267	60		8.68
Unknown function (KEZ44256.1)	RC	NTcEALcPGAAK	2 ; 646.29688	62	C3 and C7	6.32
	GC	YYSASLYSFVcQEAFK	2 ; 981.95807	75	C11	14.74
		NTcEALcPGAAK	2 ; 646.29364	31	C3 and C7	
CRH1_transglycosylase	GC	GAVFSIANEK	2 ; 518.27850	60		13.14
(KEZ42985.1)		LGSWVAGR	2 ; 423.23560	37		
		GGKTYPQTPMQVK	2 ; 717.87677	30		
		TYPQTPMQVK	2 ; 596.80658	28		
		DcPADPAIGGDFTVDFTK	2 ; 963.43573	18	C2	
GH17 family protein (8171 (ANA))	GC	DSNPDNKMQFAITK	2 ; 804.89087	62		10.82
		NAPGKFNAVR	2 ; 537.29724	42		
		AGIGADPSVLVGFIGDYR	2 ; 903.97845	21		
Unknown function (KEZ45212.1)	GC	AcGATDYDcQcAAQQAISTcYNNcPGDSRK	3 ; 1148.13013	29	C2, C9, C11, C20 and C24	19.23
		AcGATDYDcQcAAQQAISTcYNNcPGDSR	3 ; 1105.43347	25	C2, C9, C11, C20 and C24	

1,3-beta-glucanosyltransferase gel4 (KEZ46619.1)	GC	GIAYQQNTGAAGAGVQDAK FFYENGTQFYIK	2 ; 910.45422 2 ; 778.87817	101 21		6.00
Unknown function (KEZ45428.1)	GC	QGLLGVVANAEDGVLYAcSQVK	2 ; 1146.09692	47	C18	9.28
Unknown function (KEZ43031.1)	GC	cVVDGITAIGcTVEDTAcAcTTENLAK	2 ; 1465.16699	44	C1, C11, C18 and C20	13.50
Unknown function (KEZ44206.1)	GC	TPTKDELVPAGK	2 ; 628.34967	48		5.43
Glucanosyltransferase; Glyco_hydro_72 (KEZ46098.1)	GC	ILSAGVKPAPSGK	2 ; 612.87158	33		2.74
Unknown function (KEZ43170.1)	GC	cDQGDGSESATLAYSNcLQK cINScPATDVNcLAHcTPVPSPNEDNLNKLHDcAAK	2 ; 1102.46899 5 ; 819.36963	89 16	C1 and C17 C1, C5, C12, C16 and C33	30.77
Unknown function (941 (ANA))	GC	GLTSMQTSIQQNcANVR	2 ; 954.45905	56	C13	7.11
Unknown function (3034 (ANA))	GC	SGIcGGEGVVSLYKK	2 ; 777.40729	43	C14	2.35
Unknown function (6337 (ANA))	GC	VLTDAPVYNVQYGSGK	2 ; 855.94086	76		3.86
Cu/Zn superoxide dismutase (KEZ44265.1)	RC	TLAHLDPFIR	2 ; 591.83844	23		3.79

[a] ANA= Accession number Not Available yet

[b] RC: resting conidia; GC: germinated conidia.

[c] For amino acid modifications, C «number » corresponds to carbamidomethyl modification at the indicated amino acid number, and M «number » to oxidation modification at the indicated amino acid number.

Raw data containing all details can be found in Annexes 1 and 2 (**Table A.7. and A.8.**). For proteins identified with a single peptide refer to the MS/MS spectra in Annexes 3 (**Figure A.30)**.

Table E.6. Characteristics of the identified GPI-anchored proteins.

Proteins. (Accession number)[a]	**Protein family (fungal extract)**[b]	**S/T**[c] **(%)**	**pI**	**Omega site (ω-5 to ω+5)**[d]	**GRAVY value**[e]	***N*- and *O*-glycosylation**
Glucan endo-1,3-beta-D-glucosidase (KEZ41172.1)	Bglp/Bgtp (Bgt2p); GH 17; (RC/GC)	22.0	4.41	QQAAPSAGSSNN	-0.413	7 N + 68 O
CFEM protein (KEZ46909.1)	CFEM domain; (RC/GC)	26.2	4.01	TQGPGNTGGAQQS	-0.062	0 N + 40 O
CFEM protein (KEZ46627.1)	CFEM domain; (RC/GC)	17.6	4.37	SSFPTAGAGSIA	-0.242	2 N + 24 O
CFEM protein (KEZ44163.1)	CFEM domain; (RC/GC)	22.5	4.24	SAPTSSGAAGVV	0.453	1 N + 25 O
GDSL_like lipase (KEZ43142.1)	?; (RC/GC)	19	4.45	KAGDQGSGAVRV	-0.031	2 N +18 O
Glycine-rich protein (KEZ42341.1)	?; (RC/GC)	20.1	6.89	VPADESGARSV	-0.160	5 N + 4 O
Unknown function (KEZ44256.1)	?; (RC/GC)	21.6	4.25	GSEDSSSGDNKEGAAASV	-0.205	2 N + 9 O
CRH1_transglycosylase (KEZ42985.1)	Crhp (Crh1p); GH16;(GC)	23.3	4.69	TGSQDSGASLVQ	-0.270	2 N + 31 O
GH17 family protein (8171 (ANA))	Bglp/Bgtp (Bgt2p); GH17; (GC)	20.3	4.78	ATGADSSASGYT	-0.222	1 N + 32 O
Unknown function (KEZ45212.1)	?; (GC)	16.1	4.40	SETSKGGAAELA	-0.035	1 N + 14 O
1,3-beta-glucanosyl transferase ; gel4 (KEZ46619.1)	Gelp/Gasp (AfGel5p); GH72; (GC)	13.2	4.70	NKKEDDSSAVRF	-0.275	6 N + 13 O
Unknown function (KEZ45428.1)	? (GC)	19.8	4.19	GSGDEGGAAALA	0.086	3 N + 20 O
CFEM protein (KEZ43031.1)	CFEM domain; (GC)	23.5	3.90	GDDNGNGSGTSGAVVN	0.144	3 N + 30 O
Unknown function (KEZ44206.1)	? (GC)	19.9	4.69	SPVPTNGAARSA	0.090	2 N + 27 O
Glucanosyl transferase Glyco-hydro 72	Gelp/Gasp (AfGel2p);	11.6	4.81	STSKEDAGAFLR	-0.222	3 N + 7 O

(KEZ46098.1)	GH 72; (GC)					
Unknown function (KEZ43170.1)	?; (GC)	25.2	4.20	ATGTGSSASATE	-0.112	0 N + 30 O
Unknown function (941 (ANA))	?; (GC)	20.5	4.72	FDIVASPSAHL	-0.243	0 N + 18 O
Unknown function (3034 (ANA))	?; (GC)	21	3.40	GPVEVSAAGRNT	-1.021	0 N + 120 O
Unknown function (6337 (ANA))	?; (GC)	30.2	4.35	VTAAQSAGRRQ	-0.213	0 N + 94 O
Cu/Zn superoxide dismutase (KEZ44265.1)	Cu/Zn SOD; (RC)	14.1	4.47	TNLPEGSAAVSS	-0.314	4 N + 10 O

[a] ANA: Accession number Not Available yet

[b] RC: resting conidia; GC: germinated conidia.

[c] S: serine; T: threonine.

[d] Red: best predicted ω site. Orange: alternative ω site (second best). Green: basic amino acids.

[e] GRAVY index > 0: hydrophobic; GRAVY index < 0: hydrophilic.

II.5. Discussion

Germination and invasiveness are tightly interwound in fungal infections since the presence of hyphae in tissue sections represents a major indicator of fungal burden **[18**, **29**, **30]**. In filamentous fungi, the conidia-to-hyphae transition is accompanied by cell wall modifications to allow adaptation to new environments. As a matter of fact, in *A. fumigatus*, the cell wall of resting conidia is composed of three layers; during germination, the outer hydrophobin/melanin-rich cell wall layer is shed, leading to major changes in the cell wall ultrastructure and physical properties **[17**, **23**, **31**, **32]**. Other major changes during germination of *A. fumigatus* include the emergence of beta-1,3-glucans to the cell surface leading to selective recognition of hyphae by Dectin-1 and the decrease in laminin receptors that mediate the adherence to the basement membranes **[23**, **24]**. In *C. albicans*, Castillo *et al.* **[10]** also showed that hyphae produced additional GPI-anchored CWPs, Als3 and Rbt1, that are not detected in the cell wall of blastospores. In another study, hyphal induction in *C. albicans* was shown to modulate a larger number of GPI-anchored CWPs such as the Als3, Hwp2, Hyr1, Plb5, Sod5, Rhd3, Sod4 and Ywp1 proteins **[25]**.

In this study, we first showed that the cell wall of *S. boydii,* which is composed of two layers, underwent ultrastructural modifications during germination, demonstrated by the transition from a compact electron dense outer cell wall layer in resting conidia and mother cells of germ tubes to a more diffuse and irregular outer layer in hyphae. However, unlike *A. fumigatus* that passes by the swelling step during germination*,* no major changes in the cell size were observed nor any cytoplasm vacuolization, and the outer cell wall layer of the mother cell remained attached to the electron transparent inner layer after germination. Physical properties of the cell surface were also affected by the germination process: conidia and mother cells of germ tubes were more electronegatively charged than hyphae, as attested by electrophoretic mobility measurements and cationized ferritin binding. Consequently, the presence of the negatively charged sialic acids was investigated since it could affect the surface charge and was previously correlated to fungal pathogenesis **[26]** and adhesion of *A. fumigatus* conidia to the host basal lamina **[27]**. In *S. boydii,* the removal of these sialic acid molecules did not reduce the binding of cationized ferritin to mother cells suggesting that they were not connected to the surface electronegative charge. On the contrary, the inhibition of DHN-melanin synthesis in *S. boydii* **[8]** significantly reduced the surface electronegative charge of conidia suggesting an important effect of melanin on the surface electronegative charge, which is corroborated by the reduction of the electronegative charge upon germination and production of hyaline hyphae.

In a previous study we demonstrated that the cell wall content in mannose-containing glycoconjugates increased with the maturation of conidia **[8]**, but the accessibility of these molecules to Con A was hampered by the accumulation of melanin **[8]**. As conidia germinate, these mannose-containing glycoconjugates as well as the chitin molecules became unmasked in the hyaline hyphal part of *S. boydii* germ tubes, thus markedly increasing the binding to Con A and WGA.

The hydrophobic adhesion forces recorded on the conidial surface of *S. boydii* (1.8 ± 0.3 nN) were significantly lower than those recorded by Dague *et al* **[17]** for *A. fumigatus* conidia (3 ± 0.4 nN). *Scedosporium boydii* conidia lacked any peculiar structures formed by rodlet-forming hydrophobins that render the aspergillar surface homogeneously hydrophobic **[28]**. However, the measurement of CH_3/CH_3 (hydrophobic) and OH/OH (hydrophilic) interactions at the surface of conidia and germ tubes showed non-zero values indicating that the whole surface of the conidial and hyphal structures are composed of a mixture of hydrophobic and hydrophilic components. After germination, CH_3/CH_3 interactions diminished suggesting a decrease in the content of some glycoproteins. The inhibition of DHN-melanin synthesis in conidia did not affect these hydrophobic adhesion forces, which meant that these interactions were not linked to melanin (data not shown). On the other hand, the OH/OH interactions remained the same before and after germination reflecting no change in some polysaccharide components.

Changes in the cell wall during germination were also illustrated by the analysis of GPI-anchored CWPs. The analysis of *S. boydii* cell wall protein extracts revealed 250 proteins, among them only 20 had a GPI-anchor. The presence of non-GPI anchored proteins or atypical proteins was in agreement with numerous studies on *C. albicans* **[10**, **29**, **30]** where such proteins were consistently found in cell wall extracts even after varying the methodologies of extraction except for studies from de Groot *et al* **[14**, **31]** who did not find atypical proteins in the cell wall extracts.

In yeasts and filamentous fungi, GPI-anchored proteins may have two different terminal localizations: the plasma membrane (GPI-PMP) and/or the cell wall (GPI-CWP). Cell wall proteins have abundant *N*- and/or *O*-linked glycosylation sites, a signal peptide **[32]**, and no transmembrane helixes, which was the case for 19 out of the 20 extracted GPI-anchored proteins. Moreover, Pittet and Conzelmann **[33]** reported that GPI-CWPs had pIs of 4.87± 0.22 whereas PMPs had significantly higher pIs of 6.67 ± 0.95. However, a recent study on *Pichia pastoris* showed that proteins in the cell wall or in the plasma membrane did not have different pIs **[34]**. In our case, all the 19 GPI-anchored proteins had a pI value less than 5.

There is growing evidence that the proximal and distal sequences to the GPI-attachment site (called the ω site), found close to the C-terminus of the protein, exert a major effect on the final localization of a GPI-anchored protein. The presence of a high S/T content (or stretches of ST) upstream the ω-proximal region has been greatly recognised as a marking feature for CWPs **[35, 36]** since it can override ω-proximal signals like dibasic amino acid signals (arginine (R), histindine (H) and lysine (K)) at ω-1 and ω-2 sites that direct GPI-containing proteins to the plasma membrane **[37]**. For the 20 extracted proteins and even after the exclusion of N- and C-terminal sequences, the ST content remained higher than 10%. Moreover, no dibasic amino acids were found at the ω-1 and ω-2 sites (**Table E.6**). Ouyang *et al.* **[38]** mentioned that a monobasic amino acid can be sufficient for retaining a GPI-anchored protein in the plasma membrane, as was the case for 3 of our extracted proteins, but again the ST rich regions can override such signal. Add to this, the presence of valine (V), isoleucine (I) or leucine (L) at ω-4 and ω-5 as well as tyrosine (Y) or asparagine (N) at ω-2 was also suggested to act positively for the cell wall localization of proteins according to Hamada *et al.* **[39]** but these conditions did not apply to our protein sequences neither did they apply to some cell wall proteins in *A. fumigatus* like the *Af*Mp1p **[38]**. All these data taken together would suggest a cell wall localization for at least 19 of the extracted proteins. However, the ω-proximal signals and cell wall or membrane localization of proteins remain a matter of debate, especially that the same GPI-anchored protein might be present in both the cell wall and the membrane compartments.

The different families to which these proteins belonged to were also analyzed and compared to other fungi. Among the 20 identified GPI-anchored proteins identified, one was found only in conidial extracts, whereas 12 were found only in the germ tube extracts and 7 proteins were present in both extracts. The protein identified only in conidial extracts (KEZ44265.1) carried a Cu/Zn superoxide dismutase domain. Superoxide dismutases (SOD) are antioxidant enzymes involved in the degradation of superoxide anions. The identified protein in *S. boydii* belonged to a particular class of extracellular SODs containing a signal peptide and predicted to have a GPI anchor. These SODs were first described in the opportunistic fungal pathogen *C. albicans* that expressed three GPI-anchored SOD1-related proteins: CaSod4p, CaSod5p and CaSod6p **[40]**. Strains lacking CaSod5p were more susceptible to killing by macrophages and neutrophils and exhibited a decreased virulence in mouse models **[40]**. Sod5p was suggested to be involved in removal of superoxides produced by the hosts **[41]**. In *S. apiospermum* genome, seven sequences were predicted to have a superoxide dismutase domain (3 of them were Cu/Zn SOD). Among them, only two had a signal peptide, both being Cu/Zn SODs, but only one had a predicted GPI anchor. To be noted, the extracted protein in this study was different from the one previously

identified by Lima *et al.* **[42]** in *S. apiospermum* (KEZ41328.1) that did not contain a signal peptide, a transmembrane helix, or a GPI anchor.

Twelve GPI-anchored proteins were only found in germ tube extracts and among these 4 proteins belonged to known GPI-anchored protein families implicated in cell wall biosynthesis activities, one to CFEM (Common in Fungal Extracellular Membrane)-domain containing proteins while the rest had no known functions. The first group of proteins contained a protein similar to Crhp proteins (KEZ42985.1) that are suggested to be involved in the linkage between the cell wall polysaccharides β(1-6)glucan and chitin **[43**, **44**, **45]**. Crhp proteins are classified in the glycoside hydrolases 16 family (GH16) of the CAZy Database (http://www.cazy.org/). They were originally studied in the yeast *S. cerevisiae*, but their biochemical function in the fungus remains unknown and single deletions of these genes in *A. fumigatus* were not associated to any phenotype changes **[46]**. Two proteins similar to proteins to the Gel/Gas family were also detected in this study in the germ tube cell wall extract (KEZ466191.1, KEZ46098.1). Proteins of this family were particularly well studied in *A. fumigatus, N. crassa, S. cerevisiae* and *C. albicans* **[46]**. Gelp/Gasp proteins belong to the glycoside hydrolase family 72 (GH72) and were shown to perform elongation of β(1-3)glucan chains. To date, only *Af*Gel1p, AfGel2p and *Af*Gel4p in *A. fumigatus* have been studied and *Af*Gel2p was shown to be important for cell wall morphogenesis and virulence in a mouse model of invasive aspergillosis while *Af*GEL4 was shown to be an essential gene for cell wall remodeling **[9**, **47**, **48**, **49]**. In *S. boydii* germ tube extract, a protein (8171(ANA)) similar to proteins of the Bgtp/Bglp family was also identified. These proteins belong to the glycoside hydrolase 17 family (GH17) and were studied in *S. cerevisiae* and *A. fumigatus*. AfBgt2p displays a branching activity in the cell wall by cleaving two residues of a β(1-3)glucan chain and transferring them to another chain of β(1-3) glucan with a β(1-6) linkage **[48]**. This was the first time that a branching activity, which is a key activity for cell wall morphogenesis, was described in fungi. However the single *Afbgt2* mutant strain did not display a differential phenotype with respect to the wild-type strain, thus suggesting that there were other proteins with β(1-3) glucan branching activity in the cell wall **[48**, **49]**.

One protein with a predicted CFEM domain was also detected in the hyphal extract. This domain contains around 60 amino acids, predominantly hydrophobic, and eight cysteine residues with a conserved spacing **[51]**. These domains are found mainly in GPI-CWPs and most CFEM-containing proteins studied to date are involved in host-pathogen interaction and virulence. In *M. grisea,* Pth11p, which contains a CFEM domain, is required for plant infection **[52]**. Likewise, three proteins with a CFEM domain were shown to be involved in the cell wall stabilization in *A. fumigatus,* but they did not play a role in cell wall morphogenesis or

as virulence factors **[53]**. In *C. albicans* proteins containing CFEM domains have been suggested to play a role in biofilm structure **[54]**.

We identified 7 proteins present in both conidial and germ tube extracts of which 3 had no known function or domain, 3 had CFEM domains and one was similar to AfBgt2p (KEZ41172.1) and shared 31.4% homology with its *S. boydii* paralogue (8171 (ANA)) detected in germ tube extracts mentioned earlier. Both proteins (KEZ41172.1 and 8171 (ANA)) contained the two conserved glutamic acid residues of the catalytic site described for proteins of GH17 family **[55]**.

Finally, no hydrophobins could be identified in our extracts using the hydrophobin conserved eight-cystein pattern in proFasta. In *A. fumigatus*, Dague *et al* **[28]** showed that the presence of the hydrophobin RodAp accounted for the high CH3/CH3 interactions measured on the conidial surface. RodAp is a moderately hydrophobic protein with a GRAVY value of 0.245 (*A. fumigatus* Af293, protein accession P41746.2) and a suggested GPI-anchor **[56]**. After analyzing the GRAVY values of our extracted GPI-anchored proteins, only one protein in the conidial extract presented a hydrophobic character (GRAVY > 0, **Table E.6**). Interestingly, this protein was twice more hydrophobic than RodAp (GRAVY = 0.453) and had a CFEM domain (KEZ44163.1). CFEM domains, as previously mentioned, have a conserved eight-cysteine pattern that is distinct from that of hydrophobins; they are commonly identified in GPI-anchored cell wall proteins extracts and have predominant hydrophobic amino acid residues in their sequences (32% to 45% of the total amino acids) **[51]**. The identified CFEM (KEZ44163.1) was present in both conidial and germ tube extracts, but its relative amount with respect to the extracted conidial or hyphal GPI-anchored proteins (calculated after analyzing the average intensity of the strongest peptides) was twice higher in the conidial extract (2.054 %) than in the germ tube extract (1.055 %). Even though this remains speculative, this may account for the higher cell surface hydrophobicity and CH3/CH3 interactions observed on the conidial surface and suggests a hypothesis for future investigations on the conidial surface of fungi having high hydrophobic adhesions and no rodlet layer as *S. boydii*.

The analysis of the genome of *S. apiospermum* also revealed the presence of 100 gene sequences coding for GPI-anchored proteins which is similar to the number identified in other fungal genomes like *A. fumigatus* strains Af293 and A1163 containing 91 and 85 sequences respectively **[36]**. The extraction of only 20% of these proteins suggests that in our conditions only 20 proteins are expressed. Other culture conditions should be tested to investigate the expression of the other coding sequences.

Together these data demonstrate that, similarly to other fungi, the cell wall in *S. boydii* is a highly dynamic structure composed of a mixture of molecules that give, when taken

together, the physical, chemical and molecular fungal cell wall imprint. Today, mapping interactions at the surface of *S. boydii* cells at high spatial resolution and correlating such information to molecular data is highly valuable to our understanding of the pathogenesis of this fungus.

II.6. Acknowledgments

This work was supported by Région Pays de la Loire as part of the Myco-AFM research program.

The authors would like to thank Dr. Emmanuelle Com and the Proteomics Core Facility Biogenouest, IRSET-Inserm U1085, UMS 6480 Biosit (Rennes, France) for the assistance to identify proteins in our extracts and the thoughtful discussions for the protein analysis. The authors also acknowledge Dr. Patrick Saulnier (L'UNAM Université, Université d'Angers, INSERM U646, France) for the use of the Zetasizer Nano ZS.

II.7. References

1. **Cortez KJ, Roilides E, Quiroz-Telles F, Meletiadis J, Antachopoulos C, Knudsen T, Buchanan W, Milanovich J, Sutton DA, Fothergill A, Rinaldi MG, Shea YR, Zaoutis T, Kottilil S, Walsh TJ.** 2008. Infections caused by *Scedosporium* spp. Clin. Microbiol. Rev. 21:157–197.

2. **Latgé J-P**. 2007. The cell wall: a carbohydrate armour for the fungal cell. Mol. Microbiol. **66**:279–290.

3. **Latgé J-P, Beauvais A**. 2014. Functional duality of the cell wall. Curr. Opin. Microbiol. **20**:111–117.

4. **Lopes LCL, da Silva MID, Bittencourt VCB, Figueiredo RT, Rollin-Pinheiro R, Sassaki GL, Bozza MT, Gorin PAJ, Barreto-Bergter E**. 2011. Glycoconjugates and polysaccharides from the *Scedosporium*/*Pseudallescheria boydii* complex: structural characterisation, involvement in cell differentiation, cell recognition and virulence. Mycoses **54**:28–36.

5. **Bittencourt VCB, Figueiredo RT, Silva RB da, Mourão-Sá DS, Fernandez PL, Sassaki GL, Mulloy B, Bozza MT, Barreto-Bergter E**. 2006. An α-glucan of *Pseudallescheria boydii* is involved in fungal phagocytosis and toll-like receptor activation. J. Biol. Chem. **281**:22614–22623.

6. **Pinto MR, Rodrigues ML, Travassos LR, Haido RMT, Wait R, Barreto-Bergter E**. 2002. Characterization of glucosylceramides in *Pseudallescheria boydii* and their involvement in fungal differentiation. Glycobiology **12**:251–260.

7. **Rollin-Pinheiro R, Liporagi-Lopes LC, de Meirelles JV, Souza LM de, Barreto-Bergter E**. 2014. Characterization of *Scedosporium apiospermum* glucosylceramides and their involvement in fungal development and macrophage functions. PLoS ONE **9**:e98149.

8. **Ghamrawi S, Renier G, Saulnier P, Cuenot S, Zykwinska A, Dutilh BE, Thornton C, Faure S, Bouchara J-P**. 2014. Cell wall modifications during conidial maturation of the human pathogenic fungus *Pseudallescheria boydii*. PLoS ONE **9**:e100290.

9. **Mouyna I, Fontaine T, Vai M, Monod M, Fonzi WA, Diaquin M, Popolo L, Hartland RP, Latgé J-P**. 2000. Glycosylphosphatidylinositol-anchored glucanosyltransferases play an active role in the biosynthesis of the fungal cell wall. J. Biol. Chem. **275**:14882–14889.

10. **Castillo L, Calvo E, Martínez AI, Ruiz-Herrera J, Valentín E, Lopez JA, Sentandreu R**. 2008. A study of the *Candida albicans* cell wall proteome. Proteomics **8**:3871–3881.

11. **Free SJ**. 2013. Fungal cell wall organization and biosynthesis, p. 33–82. *In* T Friedmann, JC Dunalp and SF Goodwin (eds.), Advances in Genetics, Vol. 81. Academic Press.

12. **Bouchara JP, Sanchez M, Esnault K, Tronchin G**. 1999. Interactions between *Aspergillus fumigatus* and host matrix proteins. Contrib Microbiol **2**:167–181.

13. **Damveld RA, Arentshorst M, VanKuyk PA, Klis FM, van den Hondel CAMJJ, Ram AFJ**. 2005. Characterisation of CwpA, a putative glycosylphosphatidylinositol-anchored cell wall mannoprotein in the filamentous fungus *Aspergillus niger*. Fungal Genet. Biol. **42**:873–885.

14. **De Groot PWJ, de Boer AD, Cunningham J, Dekker HL, de Jong L, Hellingwerf KJ, de Koster C, Klis FM**. 2004. Proteomic analysis of *Candida albicans* cell walls reveals covalently bound carbohydrate-active enzymes and adhesins. Eukaryot Cell **3**:955–965.

15. **Bloch R, Burger MM**. 1974. Purification of wheat germ agglutinin using affinity chromatography on chitin. Biochem. Biophys. Res. Commun. **58**:13–19.

16. **Lotan R, Skutelsky E, Danon D, Sharon N**. 1975. The purification, composition, and specificity of the anti-T lectin from peanut (*Arachis hypogaea*). J. Biol. Chem. **250**:8518–8523.

17. **Dague E, Alsteens D, Latgé J-P, Dufrene YF**. 2008. High-resolution cell surface dynamics of germinating *Aspergillus fumigatus* conidia. Biophys. J. **94**:656–660.

18. **Jabado N, Casanova J-L, Haddad E, Dulieu F, Fournet J-C, Dupont B, Fischer A, Hennequin C, Blanche S**. 1998. Invasive pulmonary infection due to *Scedosporium apiospermum* in two children with chronic granulomatous disease. Clin. Infect. Dis. **27**:1437–1441.

19. **Kepez Yildiz B, Hasanreisoglu M, Aktas Z, Aksu G, Kocak BC, Akata F**. 2014. Fungal keratitis secondary to *Scedosporium apiospermum* infection and successful treatment with surgical and medical intervention. Int. Ophthalmol. **34**:305–308.

20. **Sundaram C, Shantveer Gu, Umabala P, Lakshmi V**. 2014. Diagnostic utility of melanin production by fungi: Study on tissue sections and culture smears with Masson-Fontana stain. Ind. J. Pathol. Microbiol. **57**:217.

21. **Tronchin G, Bouchara J-P, Ferron M, Larcher G, Chabasse D**. 1995. Cell surface properties of *Aspergillus fumigatus* conidia: correlation between adherence, agglutination, and rearrangements of the cell wall. Can. J. Microbiol. **41**:714–721.

22. **Pihet M, Vandeputte P, Tronchin G, Renier G, Saulnier P, Georgeault S, Mallet R, Chabasse D, Symoens F, Bouchara J-P**. 2009. Melanin is an essential component for the integrity of the cell wall of *Aspergillus fumigatus* conidia. BMC Microbiol **9**.

23. **Tronchin G, Esnault K, Renier G, Filmon R, Chabasse D, Bouchara JP**. 1997. Expression and identification of a laminin-binding protein in *Aspergillus fumigatus* conidia. Infect. Immun. **65**:9–15.

24. **Gersuk GM, Underhill DM, Zhu L, Marr KA**. 2006. Dectin-1 and TLRs permit macrophages to distinguish between different *Aspergillus fumigatus* cellular states. J Immunol **176**:3717–3724.

25. **Heilmann CJ, Sorgo AG, Siliakus AR, Dekker HL, Brul S, Koster CG de, Koning LJ de, Klis FM**. 2011. Hyphal induction in the human fungal pathogen *Candida albicans* reveals a characteristic wall protein profile. Microbiology **157**:2297–2307.

26. **Wasylnka JA, Simmer MI, Moore MM**. 2001. Differences in sialic acid density in pathogenic and non-pathogenic *Aspergillus* species. Microbiology **147**:869–877.

27. **Wasylnka JA, Moore MM**. 2000. Adhesion of *Aspergillus* species to extracellular matrix proteins: evidence for involvement of negatively charged carbohydrates on the conidial surface. Infect. Immun. **68**:3377–3384.

28. **Dague E, Alsteens D, Latgé J-P, Verbelen C, Raze D, Baulard AR, Dufrêne YF**. 2007. Chemical force microscopy of single live cells. Nano Lett. **7**:3026–3030.

29. **Ebanks RO, Chisholm K, McKinnon S, Whiteway M, Pinto DM**. 2006. Proteomic analysis of *Candida albicans* yeast and hyphal cell wall and associated proteins. Proteomics **6**:2147–2156.

30. **Nombela C, Gil C, Chaffin WL**. 2006. Non-conventional protein secretionin yeast. Trends Microbiol. **14**:15–21.

31. **De Groot PWJ, Brandt BW, Horiuchi H, Ram AFJ, de Koster CG, Klis FM**. 2009. Comprehensive genomic analysis of cell wall genes in *Aspergillus nidulans*. Fungal Genet. Biol. **46 Suppl 1**:S72–81.

32. **Bowman SM, Free SJ** (2006) The structure and synthesis of the fungal cell wall. BioEssays 28: 799–808.

33. **Pittet M, Conzelmann A**. 2007. Biosynthesis and function of GPI proteins in the yeast *Saccharomyces cerevisiae*. Biochim. Biophys. Acta **1771**:405–420.

34. **Zhang L, Liang S, Zhou X, Jin Z, Jiang F, Han S, Zheng S, Lin Y**. 2013. Screening for glycosylphosphatidylinositol-modified cell wall proteins in *Pichia pastoris* and their recombinant expression on the cell surface. Appl. Environ. Microbiol. **79**:5519–5526.

35. **Frieman MB, Cormack BP**. 2004. Multiple sequence signals determine the distribution of glycosylphosphatidylinositol proteins between the plasma membrane and cell wall in *Saccharomyces cerevisiae*. Microbiology **150**:3105–3114.

36. **De Groot PWJ, Brandt BW**. 2012. ProFASTA: A pipeline web server for fungal protein scanning with integration of cell surface prediction software. Fungal Genet. Biol. **49**:173–179.

37. **Eisenhaber B, Schneider G, Wildpaner M, Eisenhaber F**. 2004. A sensitive predictor for potential GPI lipid modification sites in fungal protein sequences and its application to genome-wide studies for *Aspergillus nidulans, Candida albicans Neurospora crassa*, *Saccharomyces cerevisiae* and *Schizosaccharomyces pombe*. J. Mol. Biol. **337**:243–253.

38. **Ouyang H, Chen X, Lu Y, Wilson IBH, Tang G, Wang A, Jin C**. 2013. One single basic amino acid at the ω-1 or ω-2 site is a signal that retains glycosylphosphatidylinositol-anchored protein in the plasma membrane of *Aspergillus fumigatus*. Eukaryot. Cell **12**:889–899.

39. **Hamada K, Terashima H, Arisawa M, Yabuki N, Kitada K**. 1999. Amino acid residues in the ω-minus region participate in cellular localization of yeast glycosylphosphatidylinositol-attached proteins. J. Bacteriol. **181**:3886–3889.

40. **Frohner IE, Bourgeois C, Yatsyk K, Majer O, Kuchler K**. 2009. *Candida albicans* cell surface superoxide dismutases degrade host-derived reactive oxygen species to escape innate immune surveillance. Mol. Microbiol. **71**:240–252.

41. **Gleason JE, Galaleldeen A, Peterson RL, Taylor AB, Holloway SP, Waninger-Saroni J, Cormack BP, Cabelli DE, Hart PJ, Culotta VC**. 2014. *Candida albicans* SOD5 represents the prototype of an unprecedented class of Cu-only superoxide dismutases required for pathogen defense. Proc. Natl. Acad. Sci. USA **111**:5866–5871.

42. **Lima OC, Larcher G, Vandeputte P, Lebouil A, Chabasse D, Simoneau P, Bouchara J-P**. 2007. Molecular cloning and biochemical characterization of a Cu,Zn-superoxide dismutase from *Scedosporium apiospermu*m. Microbes Infect. **9**:558–565.

43. **Cabib E, Blanco N, Grau C, Rodriguez-Pena JM, Arroyo J**. 2007. Crh1p and Crh2p are required for the cross-linking of chitin to beta(1-6)glucan in the *Saccharomyces cerevisiae* cell wall. Mol Microbiol **63**:921–935.

44. **Cabib E, Farkas V, Kosik O, Blanco N, Arroyo J, McPhie P**. 2008. Assembly of the yeast cell wall. Crh1p and Crh2p act as transglycosylases *in vivo* and *in vitro*. J. Biol. Chem. **283**:29859–29872.

45. **Cabib E**. 2009. Two novel techniques for determination of polysaccharide cross-links show that Crh1p and Crh2p attach chitin to both beta(1-6)- and beta(1-3)glucan in the *Saccharomyces cerevisiae* cell wall. Eukaryot Cell **8**:1626–1636.

46. **Mouyna I, Hartl L, Latgé J-P**. 2013. β-1,3-glucan modifying enzymes in *Aspergillus fumigatus*. Front. Microbiol. **4**.

47. **Mouyna I, Morelle W, Vai M, Monod M, Lechenne B, Fontaine T, Beauvais A, Sarfati J, Prevost M-C, Henry C, Latgé J-P**. 2005. Deletion of *GEL2* encoding for a beta(1-3)glucanosyltransferase affects morphogenesis and virulence in *Aspergillus fumigatus*. Mol. Microbiol. **56**:1675–1688.

48. **Gastebois A, Mouyna I, Simenel C, Clavaud C, Coddeville B, Delepierre M, Latgé J-P, Fontaine T**. 2010. Characterization of a new beta(1-3)-glucan branching activity of *Aspergillus fumigatus*. J. Biol. Chem. **285**:2386–2396.

49. **Gastebois A, Fontaine T, Latgé J-P, Mouyna I**. 2010. beta(1-3)Glucanosyltransferase Gel4p is essential for *Aspergillus fumigatus.* Eukaryot. Cell **9**:1294–1298.

50. **Mouyna I, Hartland RP, Fontaine T, Diaquin M, Simenel C, Delepierre M, Henrissat B, Latgé J-P**. 1998. A 1,3-beta-glucanosyltransferase isolated from the cell wall of *Aspergillus fumigatus* is a homologue of the yeast Bgl2p. Microbiology **144**:3171–3180.

51. **Kulkarni RD, Kelkar HS, Dean RA**. 2003. An eight-cysteine-containing CFEM domain unique to a group of fungal membrane proteins. Trends Biochem. Sci. **28**:118–121.

52. **DeZwaan TM, Carroll AM, Valent B, Sweigard JA**. 1999. *Magnaporthe grisea* pth11p is a novel plasma membrane protein that mediates appressorium differentiation in response to inductive substrate cues. Plant Cell **11**:2013–2030.

53. **Vaknin Y, Shadkchan Y, Levdansky E, Morozov M, Romano J, Osherov N**. 2014. The three *Aspergillus fumigatus* CFEM-domain GPI-anchored proteins (CfmA-C) affect cell-wall stability but do not play a role in fungal virulence. Fungal Genet. Biol. **63**:55–64.

54. **Perez A, Pedros B, Murgui A, Casanova M, Lopez-Ribot JL, Martinez JP**. 2006. Biofilm formation by *Candida albicans* mutants for genes coding fungal proteins exhibiting the eight-cysteine-containing CFEM domain. FEMS Yeast Res **6**:1074–1084.

55. **Mouyna I, Monod M, Fontaine T, Henrissat B, Lechenne B, Latgé JP**. 2000. Identification of the catalytic residues of the first family of beta(1-3)glucanosyltransferases identified in fungi. Biochem. J. **347**:741–747.

56. **Aimanianda V, Bayry J, Bozza S, Kniemeyer O, Perruccio K, Elluru SR, Clavaud C, Paris S, Brakhage AA, Kaveri SV, Romani L, Latgé J-P.** (2009) Surface hydrophobin prevents immune recognition of airborne fungal spores. Nature **460**: 1117–1121.

III. Study III: The genome of *S. apiospermum*

Draft genome sequence of the pathogenic fungus *Scedosporium apiospermum*

Patrick Vandeputte[1,2], Sarah Ghamrawi[1], Mathias Rechenmann[3], Agnès Iltis[3], Sandrine Giraud[1], Maxime Fleury[1], Christopher Thornton[4], Laurence Delhaès[5], Wieland Meyer[6], Nicolas Papon[7] and Jean-Philippe Bouchara[1,2].

1. L'UNAM Université, Université d'Angers, Groupe d'Etude des Interactions Hôte-Pathogène, EA 3142, Angers, France
2. Laboratoire de Parasitologie-Mycologie, Centre Hospitalier Universitaire, Angers, France
3. Genostar, Montbonnot, France
4. Hybridoma, Exeter, United Kingdom
5. Université de Lille II, Biologie et Diversité des Pathogènes Eucaryotes Emergents, EA 4547, Lille, France
6. Molecular Mycology Research Laboratory, Centre for Infectious Diseases and Microbiology, Sydney Medical School – Westmead Hospital, Marie Bashir Institute foe Infectious Diseases and Biosecurity, The University of Sydney, Westmead Millenium Institute for Medical Research, Westmead, NSW 2145, Australia
7. Université de Tours, Biomolécules et Biotechnologie Végétales, EA2106, Faculté de Pharmacie, Tours, France

III.1. Abstract

The first genome of one species of the *S. apiospermum* complex, responsible for localized to severe disseminated infections according to the immune status of the host, will contribute to a better understanding of the pathogenicity of these fungi, but also to the discovery of the mechanisms underlying their low susceptibility to current antifungals.

III.2. *Scedosporium apiospermum* genome sequencing

Pseudallescheria apiosperma, also known as *Scedosporium apiospermum*, is a soil-borne opportunistic pathogen, responsible for cutaneous or sub-cutaneous mycetomas following traumatic inoculation of fungal elements, and for respiratory tract infections. Moreover, it becomes a redoubtable pathogen in immuno-compromised patients, where it may cause disseminated infections with skin, eye, bones, joints, and deep organs involvement such as the heart and central nervous system **[1]**. Besides, species of the *S. apiospermum* complex are the second most frequent molds, after *A. fumigatus*, colonizing the respiratory tract of cystic fibrosis patients, causing in this clinical context respiratory infections such as bronchiitis and allergic broncho-pulmonary mycoses, or disseminated life-threatening infections in case of immunodeficiency like cortico-steroid induced diabetes or after lung transplantation. Here we report the sequencing and annotation of the genome of one of the major species within this closely related species complex.

The genome sequence of *Scedosporium apiospermum* strain IHEM 14462, isolated in 1998 from a sputum sample from a cystic fibrosis patient in Tours, France, was resolved by two distinct high throughput Illumina sequencing technologies, on a HiSeq2000: a paired-end run, sequencing on average 50 bp at each extremity of approximately 120.3 millions of 250-bp inserts, and a mate-pairs run, sequencing on average 50 bp at each extremity of approximately 82.2 millions of 4-kb inserts. *D*e *novo* assembly was achieved by an additional single molecule real-time sequencing on a PacBio RSII instrument (Pacific Biosciences), thus fully sequencing 273,000 inserts with a mean size of 2.3 kb. After trimming bad quality Illumina runs, the sequences were assembled by Genostar (Montbonnot, France) in 3,744 contigs with the CLC Genomics Workbench v6.0.2 (http://www.clcbio.com/products/clc-genomics-workbench/). PacBio RSII reads were then used to generate scaffolds from the contigs using the softwares BLASR **[2]** and SSPACE Premium scaffolder v2.3 **[3]**. Subsequently, gaps were closed with GapFiller v1.10 **[4]**. Finally, 176 scaffolds were obtained with a mean size of 246,804 bp representing a total length of 43.4 Mbp.

The genome annotation was performed by Genostar: coding sequences (CDS) prediction was performed with Augustus v2.5.5 **[5]**, trained on an algorithm optimized for

Neurospora crassa. The 10,919 putative CDS identified were annotated by BlastP **[6]** against the TrEmbl database **[7]**. A function was inferred for a given CDS when the deduced protein sequence shared at least 80% similarity and 40% identity with a protein of known function in the TrEmbl database. A putative function was attributed to the remaining CDS by functional domain searches through the Pfam database **[8]**. Thus, a function was assigned to 8,818 out of the 10,919 CDS (80.75%). For 813 CDS, the functional annotation was refined by attribution of enzyme classification (EC) numbers.

Genomic data will greatly improve the comprehension of the pathogenic mechanisms underlying pseudallescheriosis, and will help at understanding the low susceptibility of *Pseudallescheria apiosperma* to currently available antifungal drugs **[9]**.

Nucleotide sequence accession number. This Whole Genome Shotgun project has been deposited at DDBJ/EMBL/GenBank under the accession JOWA00000000. The version described in this paper is the first version, JOWA01000000.

III.3. Acknowledgements

This work was supported by a Grant (RF20120600725) from the association Vaincre la Mucoviscidose (France), which is gratefully acknowledged.

III.4. References

1. **Guarro J, Kantarcioglu AS, Horré R, Rodriguez-Tudela JL, Cuenca Estrella M, Berenguer J, de Hoog GS**. 2006. *Scedosporium apiospermum*: changing clinical spectrum of a therapy-refractory opportunist. Med. Mycol. **44**:295–327.

2. **Chaisson MJ, Tesler G**. 2012. Mapping single molecule sequencing reads using basic local alignment with successive refinement (BLASR): application and theory. BMC Bioinformatics **13**:238.

3. **Boetzer M, Henkel CV, Jansen HJ, Butler D, Pirovano W**. 2011. Scaffolding pre-assembled contigs using SSPACE. Bioinforma. Oxf. Engl. **27**:578–579.

4. **Boetzer M, Pirovano W**. 2012. Toward almost closed genomes with GapFiller. Genome Biol. **13**:R56.

5. **Stanke M, Steinkamp R, Waack S, Morgenstern B**. 2004. AUGUSTUS: a web server for gene finding in eukaryotes. Nucleic Acids Res. **32**:W309–W312.

6. **Altschul SF, Gish W, Miller W, Myers EW, Lipman DJ**. 1990. Basic local alignment search tool. J. Mol. Biol. **215**:403–410.

7. **Magrane M, Consortium U**. 2011. UniProt Knowledgebase: a hub of integrated protein data. Database **2011**:bar009–bar009.

8. **Punta M, Coggill PC, Eberhardt RY, Mistry J, Tate J, Boursnell C, Pang N, Forslund K, Ceric G, Clements J, Heger A, Holm L, Sonnhammer ELL, Eddy SR, Bateman A, Finn RD.** 2012. The Pfam protein families database. Nucleic Acids Res.

40:D290–301.

9. **Lackner M, de Hoog GS, Verweij PE, Najafzadeh MJ, Curfs-Breuker I, Klaassen CH, Meis JF**. 2012. Species-specific antifungal susceptibility patterns of *Scedosporium* and *Pseudallescheria* species. Antimicrob. Agents Chemother. **56**:2635–2642.

GENERAL DISCUSSION

The recognition of *Scedosporium* species as human pathogens came a 100 years after their discovery in 1889 **[6]**. Ever since then, the number of case reports related to these fungi was on the rise. Today, infections of immunocompetent individuals by *Scedosporium* species are no more restricted to mycetoma and these fungi are increasingly recognized as major causal agents of deep infections after near-drowning **[63]** and respiratory infections in patients with underlying diseases like cystic fibrosis **[28]**. Recent studies have focused on providing diagnostic tools for a better identification of *Scedosporium* species in fungal infections and one of the interesting tools, developed by Thornton **[63]**, targeted a carbohydrate component of the cell wall.

The fungal cell wall components (like ergosterol, chitin, β 1,3 and β 1,6-glucan) have been major targets for antifungal treatments **[94]**. Most of the cell wall components are absent in mammalian cells and its unique biochemistry and structural organization make it an interesting structure to study **[167]**.

Our understanding of the role of the cell wall in maintaining fungal life has radically changed in the last century. It is now viewed as a dynamic structure that changes in various fungal growth states and in response to surrounding conditions. It maintains a protective role in adverse conditions and plays an aggressive role during pathogenesis. However, cell wall remodeling is not restricted to the fungal kingdom; it is also known in other life forms like bacteria and plants.

In bacteria, a large number of enzymes are involved in the cell wall synthesis and maintenance. In *Escerichia coli* enzymes for precursor synthesis, peptidoglycan synthesis and regulation, cell wall stability, peptidoglycan hydrolysis, cell wall elongation and division were well studied **[168]**. Peptidoglycan is an essential and specific constituent of the bacterial cell wall. It is a polymer formed by alternating residues of N-acetylglucosamine (GlcNAc) and N-acetylmuramic acid (MurNAc). During bacterial cell growth and division, the peptidoglycan mesh is constantly cleaved by hydrolases that allow remodelling of the cell wall including the insertion of new glycan chains, control of cross-linking, cell separation, etc. Although the main function of the bacterial cell wall is to preserve internal osmotic pressure and maintain the shape, recent evidence demonstrate that the cell wall synthesis directly affects the movement of filamental gram positive and gram negative bacteria **[168]**. Moreover, the cell wall differs in exponentially growing bacteria; the average glycan chain length decreases by 30% as bacteria reach the stationary phase **[168]**. The crosslinking and covalent attachment of outer membrane lipoproteins also increases which reflects a cell wall maturation event **[168]**.

In plants, if we take the outer epidermal wall in the juvenile plant axis (hypocotyl) that is composed of pectic substances, hemicellulose, cellulose, glycoproteins and phenolic substances, the thickness of the wall differs depending on the age and culture conditions (light or dark) **[169]**. The epidermal outer wall has a composition similar to that of secondary walls yet it is still capable of elongation **[170]**. As the plant grows, certain cells reach their final size and start depositing lignified secondary wall that may contain up to 80% cellulose per dry mass **[169]**. Eventhough plants are multicellular systems, some cells do undergo changes in their wall composition and thickness before and after reaching their final size.

In our study we have first seen major changes in the conidial cell wall properties and composition with the ageing culture. Modifications in the cell surface hydrophobicity, in the electronegative charge as well as in melanin and mannose residue content provided evidence for conidial maturation. This maturation process probably occurs after reaching final conidial size but before the detachment of conidia from the filament or conidiogenous cell. This means that that the interruption of the maturation process at day 5 results in harvesting conidia with less resistance capacities and more immunogenic properties since the quantity of melanin does not yet reach its maximum level. At day 9, the majority of conidia underwent maturion, despite the continued increase in the quantity of mannan containing polysaccharides as shown by flow cytometry; later on, our study about the cell wall changes associated with germination revealed that the capacity of conidia to germinate decreases at day 14, thus indicating conidial ageing. Therefore we concluded that the increase in immunogenic molecules like mannose containing polysaccharides is progressively masked by the accumulation of melanin, which is reflected in the surface physical properties. Melanin is known to allow the fungal escape from the host immune defenses, it physically shields the fungal cells and quenches toxic free radicals produced by the host. Evidently, these scavenging capacities depend on a higher antioxidant state of melanin; in other terms a higher degree of polymerization or a higher molecular weight of the melanin polymer. This was demonstrated in conidia by UV-visible spectrophotometry which revealed the increase in the quantity of extracted melanin with age of cultures and the decrease in EPR signals indicating a decrease in the quantity of synthesis intermediates.

Cell wall modifications were also tracked during germination. The absence of melanin in *S. boydii* hyphae, which are hyaline, renders mannose containing polysaccharides and chitin more accessible to their specific lectins ConA and WGA, respectively. These changes were also seen after examining the cell wall ultrastructure under transmission electron microscopy. The cell wall of *S. boydii* is composed of two layers; the inner electron transparent cell wall layer was continuous from the mother cell to the germ tube whereas

the outer electron-dense layer that was compact and of uniform thickness in the mother cell but totally different in the hyphal wall of germ tubes since it was irregular and diffuse. Nevertheless, the outer compact cell wall layer of the resting conidia remained attached to the inner layer for mother cells of germ tubes contrary to what is seen in *A. fumigatus* after germination with the progressive shedding of the outer cell wall layer during swelling.

Changes during germination were also confirmed using other approaches. Studying the surface physical properties revealed a more hydrophobic and more electronegative surface in conidia compared to hyphae. Unlike inhibition of melanin synthesis, removal of cell wall sialic acids did not affect the electronegative surface charge. Conversely to chemical interactions with OH-containing molecules, interactions with CH_3-containing molecules decreased after germination reflecting a change in some cell wall glycoprotein content or accessibility.

Extracting GPI-anchored glycoproteins allowed the identification of 8 proteins in conidial extracts and 20 proteins in germ tube extracts, 7 of which were common between both extracts. The protein families to which these proteins belonged was explained earlier in study II and this revealed a number of proteins potentially implicated in virulence as seen in other fungal models. Our contribution to the general understanding of *Scedosporium* virulence factors or molecules with potential role in virulence is summed up in **Figure D.28**.

During the course of this work, genome sequencing was deemed indispensable since in the first study the sequencing of *PKS1* (≈7000 bp) and *4HNR* (≈1000 bp), to elucidate the genetic basis of DHN melanin synthesis, was not an easy task. Moreover, the identification of cell wall GPI-anchored proteins was impossible without the availability of the genome since no sufficiently close fungi were sequenced so far and primary analyses using the closest fungal genomes like that of *Colletotrichum* allowed the identification of only 8 proteins instead of the 250 identified using *S. apiospermum*'s genome.

The complete genome sequence of *S. apiosperma* strain IHEM14462 was finally published and almost 80% of the predicted coding sequences were annotated. Analysis of *S. apiospermum* genome revealed interesting metabolic pathways involved in bioremediation. Bioinformatic analysis of the genome unravelled an important number of enzymes involved in the degradation pathways of various environmental pollutants, the activity of some was previously investigated while other enzymes were identified for the first time.

Scedosporium species, are ubiquitous ascomycetes known for their ability to adapt to various human-impacted ecological niches, including highly polluted soils and water **[25]**. These fungi were reported to use phenyl benzoate and crude oil as sole carbon sources **[172**, **173]** and to degrade gaseous saturated hydrocarbons **[92]**, phenol and *p*-cresol **[173]** and more recently dioxin **[175**, **176]**. Because of these particular properties, they were proposed for bioremediation.

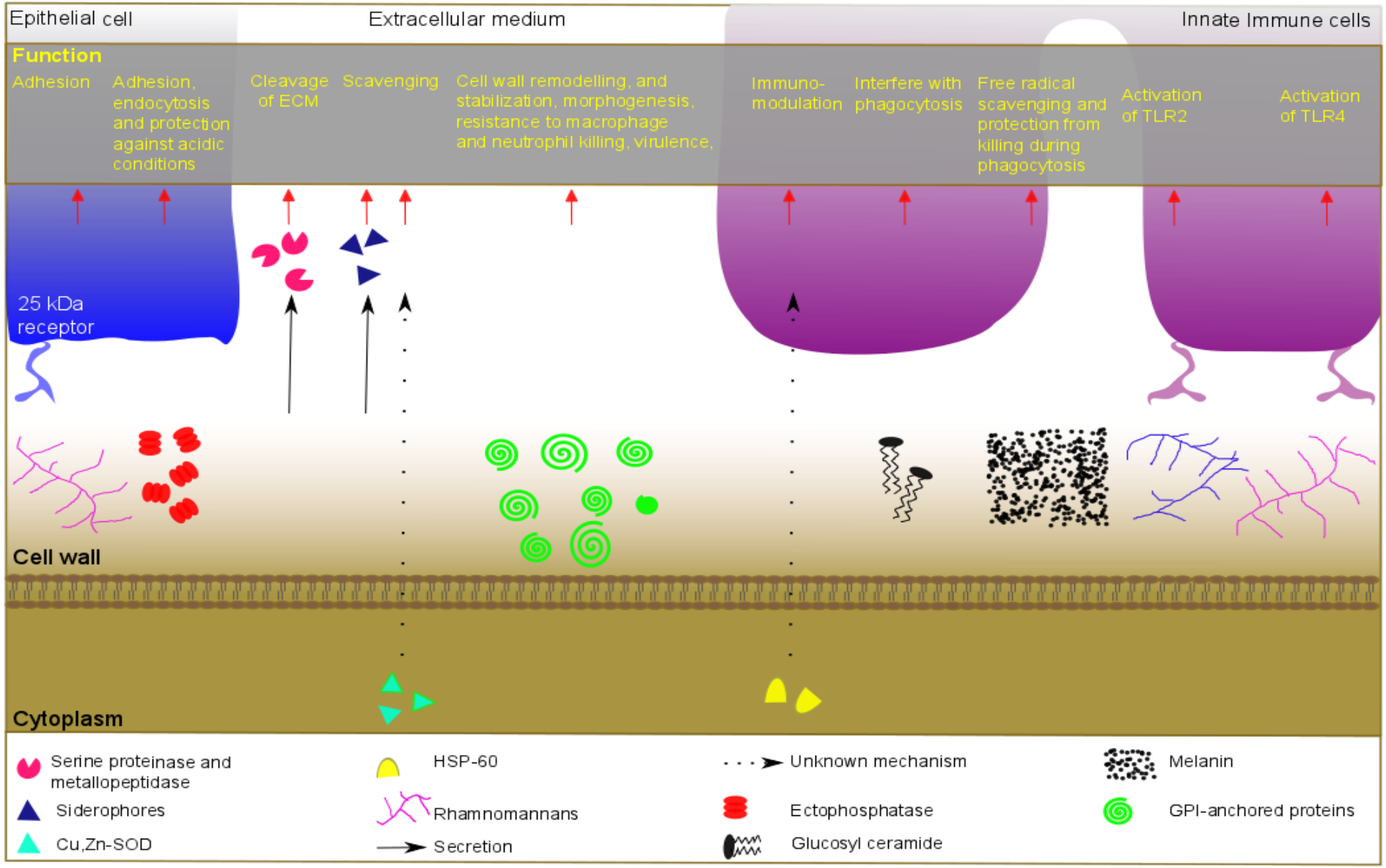

Figure D.28. Virulence factors identified in species of the *S. apiospermum* complex and possible pathogenic mechanisms as compared to other fungal models

Analysis of the predicted metabolic pathways in *S. apiospermum* genome using KEGG pathway database (http://www.genome.jp/kegg/) unraveled an important number of enzymes implicated in the degradation of various pollutants. Our data indicated that 23, 22 and 3 open reading frames (ORFs) encode enzymes involved in the degradation pathways of benzoate, aminobenzoate and fluorobenzoate respectively. Thirty-four ORFs were identified for methane metabolism (gaseous hydrocarbon), 13 ORFs for toluene degradation (**Figure D.29**), 2 ORFs for xylene degradation, 11 ORFs for styrene degradation, 13 ORFs for chlorohexane and chlorobenzene degradation and 2 ORFs for polychlorinated biphenyls degradation.

Claussen and Schmidt **[173]** previously demonstrated that phenol degradation in *S. apiospermum* proceeded via two distinct pathways, the catechol and the hydroquinone pathways, by measuring the corresponding enzyme activities. In the genome sequence, we identified the ORFs encoding enzymes belonging to each pathway. Regarding the catechol pathway, we found 3 ORFs encoding catechol 1,2-dioxygenases (Enzyme Commission number (EC) 1.13.11.1) and for the hydroquinone pathway we found 3 ORFs coding for hydroxyquinol 1,2-dioxygenases (EC 1.13.11.37) and 2 ORFS coding for maleylacetate reductases (EC 1.3.1.32). In addition, two genes encoding phenol 2-monooxygenases (EC 1.14.13.7) were found, these enzymes are predicted to mediate the hydroxylation step common to both pathways **[176]**.

Moreover, we investigated major classes of fungal enzymes known to catabolize organic pollutants, but lacking substrate specificity **[177]**. For instance, we found 2 genes encoding laccases (EC 1.10.3.2), one encoding a tyrosinase (EC 1.14.18.1), a chloride peroxidase (EC 1.11.1.10), a putative nitroreductase and a quinone reductase (EC 1.6.5.2). Likewise, within 98 genes coding for P450 cytochromes, we searched for families that were reported to degrade pollutants like CYP52, CYP53 and CYP504 **[178]**. Two genes belonging to the CYP53 family, known to degrade benzoate and its derivatives, were found in *S. apiospermum* genome (EC 1.14.13.12 and EC 1.14.14.1).

Together these data provide a molecular support for running efforts to use these fungi or attenuated strains of these fungi in bioremediation, and open the way to genetic engineering experiments to overexpress certain desired enzymes.

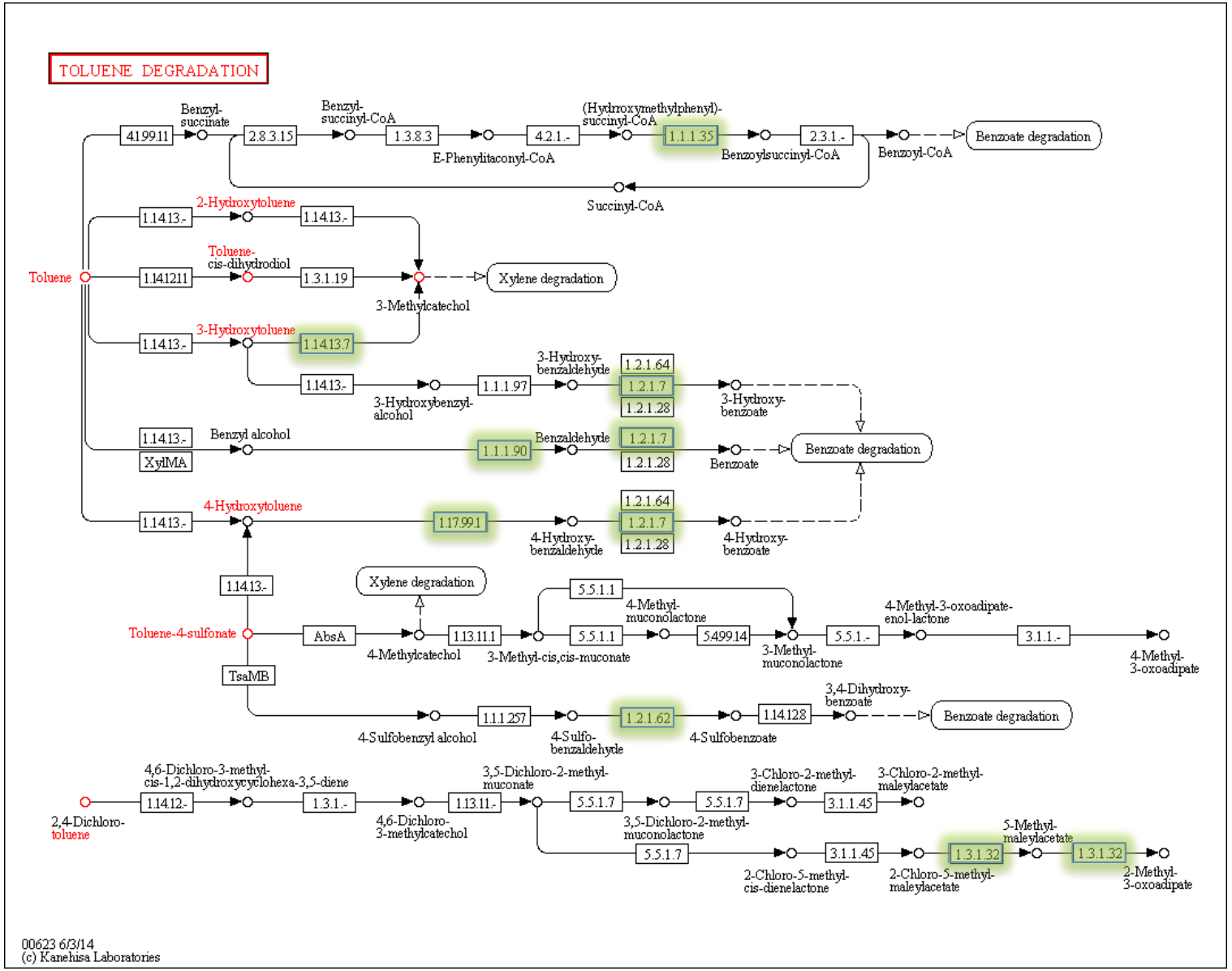

Figure D.29. Toluene degradation.

Enzymes identified in *S. apiospermum* genome are highlighted in green.

CONCLUSIONS AND PERSPECTIVES

This work highlights the cell wall remodeling in *S. boydii* during maturation and germination of conidia. A number of potential virulence factors were identified providing a basis for future studies on the role of each of these molecules in the host-pathogen interactions. Eventhough no rodlet-forming hydrophobins were observed in atomic force microscopy for conidia, a CFEM domain-containing protein (KEZ44163.1) seemed to be interesting for further studies since it was twice more hydrophobic that RodAp, has a conserved spacing of 8 cysteine residues close to that of hydrophobins, and it might justify the higher hydrophobicity and higher CH_3/CH_3 interactions seen on the conidial cell wall.

Genome analysis of *S. apiospermum* also provided molecular evidence for ongoing research in the domain of bioremediation and would also provide support for other studies concerning pathogenesis and biotechnological applications.

The fungal cell wall is a highly dynamic structure that is composed of a mixture of molecules that ensure various surface interactions. Combining our knowledge on surface properties, interactions and molecular data would provide valuable explanations for fungal pathogenesis, particularly for the adherence of the fungus to the host tissues and its evasion from the host immune response.

REFERENCES

1. **Hawksworth DL** (1991) The fungal dimension of biodiversity: magnitude, significance, and conservation. Mycol Res **95**: 641–655.

2. **O'Brien HE, Parrent JL, Jackson JA, Moncalvo J-M, Vilgalys R** (2005) Fungal community analysis by large-scale sequencing of environmental samples. Appl Environ Microbiol **71**: 5544–5550.

3. **Blackwell M** (2011) The fungi: 1, 2, 3 … 5.1 million species? Am J Bot **98**: 426–438.

4. Types of Fungal Diseases | Fungal | CDC (n.d.). Available: http://www.cdc.gov/fungal/diseases/index.html/. Accessed 21 August 2014.

5. **Garcia-Solache MA, Casadevall A** (2010) Global warming will bring new fungal diseases for mammals. mBio **1**: e00061–10.

6. **Cortez KJ, Roilides E, Quiroz-Telles F, Meletiadis J, Antachopoulos C, *et al*.** (2008) Infections caused by *Scedosporium* spp. Clin Microbiol Rev **21**: 157–197.

7. **Havlickova B, Czaika VA, Friedrich M** (2008) Epidemiological trends in skin mycoses worldwide. Mycoses **51** Suppl 4: 2–15.

8. **Brown GD, Denning DW, Gow NAR, Levitz SM, Netea MG,** *et al.* (2012) Hidden killers: human fungal infections. Sci Transl Med **4**: 165rv13–rv165rv13.

9. Global Plague : How 150 people die every hour from fungal infection while the world turns a blind eye | Gaffi - Global Action Fund for Fungal Infections (n.d.). Available: http://www.gaffi.org/global-plague-how-150-people-die-every-hour-from-fungal-infection-while-the-world-turns-a-blind-eye/. Accessed 21 August 2014.

10. **Maertens J, Vrebos M, Boogaerts M** (2001) Assessing risk factors for systemic fungal infections. Eur J Cancer Care **10**: 56–62.

11. **Cornely OA, Böhme A, Reichert D, Reuter S, Maschmeyer G, *et al.*** (2008) Risk factors for breakthrough invasive fungal infection during secondary prophylaxis. J Antimicrob Chemother **61**: 939–946.

12. **Puel A, Cypowyj S, Bustamante J, Wright JF, Liu L, *et al.*** (2011) Chronic mucocutaneous candidiasis in humans with inborn errors of interleukin-17 immunity. Science **332**: 65–68.

13. **Ferwerda B, Ferwerda G, Plantinga TS, Willment JA, van Spriel AB,** *et al.* (2009) Human dectin-1 deficiency and mucocutaneous fungal infections. New Engl J Med **361**: 1760–1767.

14. **Guarro J, Kantarcioglu AS, Horré R, Luis Rodriguez-Tudela J, Cuenca Estrella M, *et al.*** (2006) *Scedosporium apiospermum*: changing clinical spectrum of a therapy-refractory opportunist. Med Mycol **44**: 295–327.

15. **Gilgado F, Cano J, Gené J, Guarro J** (2005) Molecular phylogeny of the *Pseudallescheria boydii* species complex: proposal of two new species. J Clin Microbiol **43**: 4930–4942.

16. **Gilgado F, Cano J, Gené J, Sutton DA, Guarro J** (2008) Molecular and phenotypic data supporting distinct species statuses for *Scedosporium apiospermum* and *Pseudallescheria boydii* and the proposed new species *Scedosporium dehoogii*. J Clin Microbiol **46**: 766–771.

17. **Lackner M, de Hoog SG, Yang L, Ferreira Moreno L, Ahmed SA, *et al.*** (2014) Proposed nomenclature for *Pseudallescheria*, *Scedosporium* and related genera. Fungal diversity doi:10.1007/s13225-014-0295-4.

18. **Hawksworth DL** (2011) A new dawn for the naming of fungi: impacts of decisions made in Melbourne in July 2011 on the future publication and regulation of fungal names1. IMA Fungus **2**: 155–162.

19. **Ghamrawi S, Renier G, Saulnier P, Cuenot S, Zykwinska A, *et al.*** (2014) Cell wall modifications during conidial maturation of the human pathogenic fungus *Pseudallescheria boydii*. PLoS One **9**: e100290.

20. **De Hoog GS, Marvin-Sikkema FD, Lahpoor GA, Gottschall JC, Prins RA, *et al.*** (1994) Ecology and physiology of the emerging opportunistic fungi *Pseudallescheria boydii* and *Scedosporium prolificans*. Mycoses **37**: 71–78.

21. **Beguin H, Nolard N** (1994) Mould biodiversity in homes I. Air and surface analysis of 130 dwellings. Aerobiologia **10**: 157–166.

22. **Summerbell RC, Krajden S, Kane J** (1989) Potted plants in hospitals as reservoirs of pathogenic fungi. Mycopathologia **106**: 13–22.

23. **Kaltseis J, Rainer J, De Hoog GS** (2009) Ecology of *Pseudallescheria* and *Scedosporium* species in human-dominated and natural environments and their distribution in clinical samples. Med Mycol **47**: 398–405.

24. **Harun A, Gilgado F, Chen SC-A, Meyer W** (2010) Abundance of *Pseudallescheria*/*Scedosporium* species in the Australian urban environment suggests a possible source for scedosporiosis including the colonization of airways in cystic fibrosis. Med Mycol **48**: S70–S76.

25. **Rougeron A, Schuliar G, Leto J, Sitterle E, Landry D, *et al.*** (2014) Human-impacted areas of France are environmental reservoirs of the *Pseudallescheria boydii* / *Scedosporium apiospermum* species complex. Environ Microbiol doi:10.1111/1462-2920.12472.

26. **Lackner M, Najafzadeh MJ, Sun J, Lu Q, de Hoog GS** (2012) Rapid Identification of *Pseudallescheria* and *Scedosporium* strains by using rolling circle amplification. Appl Environ Microbiol **78**: 126–133.

27. **Cimon B, Carrère J, Chazalette J-P, Ginies J-L, Six P, *et al.*** (1995) Fungal colonization and immune response to fungi in cystic fibrosis. J Mycol Méd **5**: 211–216.

28. **Cimon B, Carrère J, Vinatier J-F, Chazalette J-P, Chabasse D, *et al.*** (2000) Clinical significance of *Scedosporium apiospermum* in patients with cystic fibrosis. Eur J Clin Microbiol Infect Dis **19**: 53–56.

29. **Blyth CC, Harun A, Middleton PG, Sleiman S, Lee O, *et al.*** (2010) Detection of occult *Scedosporium* species in respiratory tract specimens from patients with cystic fibrosis by use of selective media. J Clin Microbiol **48**: 314–316.

30. **Zouhair R, Rougeron A, Razafimandimby B, Kobi A, Bouchara J-P, *et al.*** (2013) Distribution of the different species of the *Pseudallescheria boydii/Scedosporium apiospermum* complex in French patients with cystic fibrosis. Med Mycol **51**: 603–613.

31. **Gilgado F, Cano J, Gené J, Serena C, Guarro J** (2009) Different virulence of the species of the *Pseudallescheria boydii* complex. Med Mycol **47**: 371–374.

32. **Jimenez AL, Salvo NL** (2011) Mycetoma or synovial sarcoma? A case report with review of the ilterature. J. Foot Ankle Surg **50**: 569–576.

33. **Castro LG, Belda Júnior W, Salebian A, Cucé LC** (1993) Mycetoma: a retrospective study of 41 cases seen in São Paulo, Brazil, from 1978 to 1989. Mycoses **36**: 89–95.

34. **Guarro J, Kantarcioglu AS, Horré R, Luis Rodriguez-Tudela J, Cuenca Estrella M, *et al.*** (2006) *Scedosporium apiospermum*: changing clinical spectrum of a therapy-refractory opportunist. Med Mycol **44**: 295–327.

35. **Serda Kantarcioglu A, Sybren de Hoog G, Guarro J** (2012) Clinical characteristics and epidemiology of pulmonary pseudallescheriasis. Rev Iberoamer Micol **29**: 1–13.

36. **Boyle MP, De Boeck K** (2013) A new era in the treatment of cystic fibrosis: correction of the underlying CFTR defect. Lancet Respir Med **1**: 158–163.

37. **Parize P, Billaud S, Bienvenu A-L, Bourdy S, le Pogam M-A, *et al.*** (In Press) Impact of *Scedosporium apiospermum* complex seroprevalence in patients with cystic fibrosis. Journal of Cystic Fibrosis. Available: http://www.sciencedirect.com/science/article/pii/S1569199314000368. Accessed 25 August 2014.

38. **Tintelnot K, Wagner N, Seibold M, de Hoog GS, Horré R** (2008) Re-identification of clinical isolates of the *Pseudallescheria boydii* complex involved in near-drowning. Mycoses **51**: 11–16.

39. **WHO** | Drowning (n.d.). WHO. Available: http://www.who.int/mediacentre/factsheets/fs347/en/. Accessed 24 August 2014.

40. **Ender PT, Dolan MJ** (1997) Pneumonia associated with near-drowning. Clin Infect Dis **25**: 896–907.

41. **Leroy P, Smismans A, Seute T** (2006) Invasive pulmonary and central nervous system aspergillosis after near-drowning of a child: case report and review of the literature. Pediatrics **118**: e509–e513.

42. **Buzina W, Feierl G, Haas D, Reinthaler FF, Holl A,** *et al.* (2006) Lethal brain abscess due to the fungus *Scedosporium apiospermum* (teleomorph *Pseudallescheria boydii*) after a near-drowning incident: case report and review of the literature. Med Mycol **44**: 473–477.

43. **Mursch K, Trnovec S, Ratz H, Hammer D, Horré R, *et al.*** (2006) Successful treatment of multiple *Pseudallescheria boydii* brain abscesses and ventriculitis/ependymitis in a 2-year-old child after a near-drowning episode. Childs Nerv Syst **22**:189-192.

44. **Kantarcioglu AS, Guarro J, De Hoog GS** (2008) Central nervous system infections by members of the *Pseudallescheria boydii* species complex in healthy and

immunocompromised hosts: epidemiology, clinical characteristics and outcome. Mycoses **51**: 275–290.

45. **Rolfe NE, Haddad TJ, Wills TS** (2013) Management of *Scedosporium apiospermum* in a pre- and post-lung transplant patient with cystic fibrosis. Med Mycol Case Reports **2**: 37–39.

46. **Symoens F, Knoop C, Schrooyen M, Denis O, Estenne M, *et al.*** (2006) Disseminated *Scedosporium apiospermum* infection in a cystic fibrosis patient after double-lung transplantation. J Heart Lung Transplant **25**: 603–607

47. **Tammer I, Tintelnot K, Braun-Dullaeus RC, Mawrin C, Scherlach C, *et al.*** (2011) Infections due to *Pseudallescheria/Scedosporium* species in patients with advanced HIV disease — a diagnostic and therapeutic challenge. Int J Infect Dis **15**: e422–e429.

48. **Pinto MR, de Sá ACM, Limongi CL, Rozental S, Santos ALS, *et al.*** (2004) Involvement of peptidorhamnomannan in the interaction of *Pseudallescheria boydii* and HEp2 cells. Microbes Infect **6**: 1259–1267.

49. **Larcher G, Cimon B, Symoens F, Tronchin G, Chabasse D, *et al.*** (1996) A 33 kDa serine proteinase from *Scedosporium apiospermum*. Biochem J **315**: 119–126.

50. **Silva BA, Pinto MR, Soares RMA, Barreto-Bergter E, Santos ALS** (2006) *Pseudallescheria boydii* releases metallopeptidases capable of cleaving several proteinaceous compounds. Res Microbiol **157**: 425–432.

51. **Gil-Lamaignere C, Roilides E, Lyman CA, Simitsopoulou M, Stergiopoulou T, *et al.*** *(*2003) Human phagocytic cell responses to *Scedosporium apiospermum* (*Pseudallescheria boydi*i): variable susceptibility to oxidative injury. Infect Immun **71**: 6472–6478.

52. **Winn RM, Gil-Lamaignere C, Roilides E, Simitsopoulou M, Lyman CA, *et al.*** (2005) Effects of interleukin-15 on antifungal responses of human polymorphonuclear leukocytes against *Fusarium* spp. and *Scedosporium* spp. Cytokine **31**: 1–8.

53. **Lima OC, Larcher G, Vandeputte P, Lebouil A, Chabasse D,** *et al.* (2007) Molecular cloning and biochemical characterization of a Cu,Zn-superoxide dismutase from *Scedosporium apiospermum*. Microbes Infect **9**: 558–565.

54. **Bittencourt VCB, Figueiredo RT, Silva RB da, Mourão-Sá DS, Fernandez PL, *et al.*** (2006) An α-glucan of *Pseudallescheria boydii* is involved in fungal phagocytosis and toll-like receptor activation. J Biol Chem **281**: 22614–22623.

55. **Santos ALS, Santos ALS, Bittencourt VCB, Pinto MR, Silva BA, *et al.*** (2009) Biochemical characterization of potential virulence markers in the human fungal pathogen *Pseudallescheria boydii*. Med Mycol **47**: 375–386.

56. **Lopes LCL, da Silva MID, Bittencourt VCB, Figueiredo RT, Rollin-Pinheiro R, *et al.*** (2011) Glycoconjugates and polysaccharides from the *Scedosporium/Pseudallescheria boydii* complex: structural characterisation, involvement in cell differentiation, cell recognition and virulence. Mycoses **54**: 28–36.

57. **Figueiredo RT, Bittencourt VCB, Lopes LCL, Sassaki G, Barreto-Bergter E** (2012) Toll-like receptors (TLR2 and TLR4) recognize polysaccharides of *Pseudallescheria boydii* cell wall. Carbohydrate Res **356**: 260–264.

58. **Rollin-Pinheiro R, Liporagi-Lopes LC, de Meirelles JV, Souza LM de, Barreto-Bergter E** (2014) Characterization of *Scedosporium apiospermum* glucosylceramides and their involvement in fungal development and macrophage functions. PLoS One **9**: e98149.

59. **Kiffer-Moreira T, Pinheiro AAS, Pinto MR, Esteves FF, Souto-Padrón T, *et al.*** (2007) Mycelial forms of *Pseudallescheria boydii* present ectophosphatase activities. Arch Microbiol **188**: 159–166.

60. **Bertrand S, Larcher G, Landreau A, Richomme P, Duval O, *et al.*** (2009) Hydroxamate siderophores of *Scedosporium apiospermum*. Biometals **22**: 1019–1029.

61. **Raggam RB, Salzer HJF, Marth E, Heiling B, Paulitsch AH,** *et al.* (2011) Molecular detection and characterisation of fungal heat shock protein 60. Mycoses **54**: e394–e399.

62. **Rainer J, Kaltseis J, Hoog SG de, Summerbell RC** (2008) Efficacy of a selective isolation procedure for members of the *Pseudallescheria boydii* complex. Antonie van Leeuwenhoek **93**: 315–322.

63. **Thornton CR** (2009) Tracking the emerging human pathogen *Pseudallescheria boydii* by using highly specific monoclonal antibodies. Clin Vaccine Immunol **16**: 756–764.

64. **Pinto MR, Mulloy B, Haido RMT, Travassos LR, Barreto-Bergter E** (2001) A peptidorhamnomannan from the mycelium of *Pseudallescheria boydii* is a potential diagnostic antigen of this emerging human pathogen. Microbiology **147**: 1499–1506.

65. **Pavlaskova K, Nedved J, Kuzma M, Zabka M, Sulc M,** *et al.* (2010) Characterization of pseudacyclins A–E, a suite of cyclic peptides produced by *Pseudallescheria boydii*. J Nat Prod **73**: 1027–1032.

66. **Havlicek V, Kuzma M, Sklenar J, Zabka M, Nevded J,** *et al.* (2011) Pseudacyclin and method of indication of a fungus *Pseudallescheria boydii*. Available: http://www.google.com/patents/EP2303915A2. Accessed 27 August 2014.

67. **Bertrand S, Bouchara J-P, Venier M-C, Richomme P, Duval O,** *et al.* (2010) N(α)-methyl coprogen B, a potential marker of the airway colonization by *Scedosporium apiospermum* in patients with cystic fibrosis. Med Mycol **48** Suppl 1: S98–S107.

68. **Harun A, Blyth CC, Gilgado F, Middleton P, Chen SC-A, *et al.*** (2011) Development and validation of a multiplex PCR for detection of *Scedosporium* spp. in respiratory tract specimens from patients with cystic fibrosis. J Clin Microbiol **49**: 1508–1512.

69. **Lu Q, van den Ende AHGG, de Hoog GS, Li R, Accoceberry I, *et al.*** (2011) Reverse line blot hybridisation screening of *Pseudallescheria/Scedosporium* species in patients with cystic fibrosis. Mycoses **54**: 5–11.

70. **Bouchara J-P, Hsieh HY, Croquefer S, Barton R, Marchais V, *et al.*** (2009) Development of an oligonucleotide array for direct detection of fungi in sputum samples from patients with cystic fibrosis. J Clin Microbiol **47**: 142–152.

71. **Meletiadis J, Meis JFGM, Mouton JW, Rodriquez-Tudela JL, Donnelly JP, *et al.*** (2002) *In vitro* ativities of new and conventional antifungal agents against clinical *Scedosporium* isolates. Antimicrob. Agents Chemother **46**: 62–68.

72. **Lackner M, Hoog GS de, Verweij PE, Najafzadeh MJ, Curfs-Breuker I, *et al.*** (2012) Species-specific antifungal susceptibility patterns of *Scedosporium* and *Pseudallescheria* species. Antimicrob Agents Chemother **56**: 2635–2642.

73. **Troke P, Aguirrebengoa K, Arteaga C, Ellis D, Heath CH, *et al.*** (2008) Treatment of scedosporiosis with voriconazole: clinical experience with 107 patients. Antimicrob Agents Chemother **52**: 1743–1750.

74. **Perfect JR, Marr KA, Walsh TJ, Greenberg RN, Dupont B,** *et al.* (2003) Voriconazole treatment for less-common, emerging, or refractory fungal infections. Clin Infect Dis **36**: 1122–1131.

75. **Walsh TJ, Lutsar I, Driscoll T, Dupont B, Roden M, *et al.*** (2002) Voriconazole in the treatment of aspergillosis, scedosporiosis and other invasive fungal infections in children. Pediatr Infect Dis 2002 **21**: 240–248.

76. **Pfaller MA, Hata K, Jones RN, Messer SA, Moet GJ, *et al.*** (2011) *In vitro* activity of a novel broad-spectrum antifungal, E1210, tested against *Candida* spp. as determined by CLSI broth microdilution method. Diagn Microbiol Infect Dis **71**: 167–170.

77. **Hata K, Horii T, Miyazaki M, Watanabe N, Okubo M, *et al.*** (2011) Efficacy of oral E1210, a new broad-spectrum antifungal with a novel mechanism of action, in murine models of candidiasis, aspergillosis, and fusariosis. Antimicrob Agents Chemother **55**: 4543–4551.

78. **McLellan CA, Whitesell L, King OD, Lancaster AK, Mazitschek R, *et al.*** (2012) Inhibiting GPI anchor biosynthesis in fungi stresses the endoplasmic reticulum and enhances immunogenicity. ACS Chem Biol **7**: 1520–1528.

79. **Maebayashi Y, Horie Y, Satoh Y, Yamazaki M** (1985) Isolation of pseurotin A and a new pyrazine from *Pseudallescheria boydii.* Mycotoxins **1985**: 33–34.

80. Pseurotin A (CAS 58523-30-1) || Cayman Chemical | Supplier (n.d.). Available: https://www.caymanchem.com/app/template/Product.vm/catalog/14441;jsessionid=01633BB01E9010E4EEC1F94ECE1134B8. Accessed 26 August 2014.

81. **Kuroda K, Yoshida M, Uosaki Y, Ando K, Kawamoto I, *et al.*** (1993) AS-183, a novel inhibitor of acyl-CoA: cholesterol acyltransferase produced by *Scedosporium* sp. SPC-15549. J Antibiot **46**: 1196–1202.

82. **Hayakawa Y, Yamashita T, Mori T, Nagai K, Shin-Ya K,** *et al.* (2004) Structure of tyroscherin, an antitumor antibiotic against IGF-1-dependent cells from *Pseudallescheria* sp. J Antibiot **57**: 634–638.

83. **Kamigiri K, Tanaka K, Matsumoto H, Nagai K, Watanabe M, *et al.*** (2004) YM-193221, a novel antifungal antibiotic produced by *Pseudallescheria ellipsoidea.* J Antibiot **57**: 569–572.

84. **Katsuta R, Yajima A, Ishigami K, Nukada T, Watanabe H** (2010) Synthesis of (2RS,8R,10R)-YM-193221 and an improved approach to tyroscherin, bioactive natural compounds from *Pseudallescheria* sp. Biosci Biotechnol Biochem **74**: 2056–2059.

85. **Nirma C, Eparvier V, Stien D** (2013) Antifungal agents from *Pseudallescheria boydii* SNB-CN73 isolated from a *Nasutitermes* sp. termite. J Nat Prod **76**: 988–991.

86. **Li X, Kim S-K, Nam KW, Kang JS, Choi HD, *et al.*** (2006) A new antibacterial dioxopiperazine alkaloid related to gliotoxin from a marine isolate of the fungus *Pseudallescheria*. J Antibiot **59**: 248–250.

87. **Ko W-H, Tsou Y-J, Ju Y-M, Hsieh H-M, Ann P-J** (2010) Production of a fungistatic substance by *Pseudallescheria boydii* isolated from soil amended with vegetable tissues and its significance. Mycopathologia **169**: 125–131.

88. **Su H-J, Lin M-J, Tsou Y-J, Ko W-H** (2012) Pseudallin, a new antibiotic produced by the human pathogenic fungus *Pseudallescheria boydii*, with ecological significance. Botanical Studies **53**: 239–242.

89. **Guisado G, Lopez MJ, Vargas-García MC, Suárez-Estrella F, Moreno J** (2011) *Pseudallescheria angusta*, a ligninolytic microorganism for wood fibers biomodification. BioResources **7**: 0464–0474.

90. **Chang Y-C, Deng T-S, Pang K-L, Hsiao C-J, Chen Y-Y, *et al.*** (2013) Polyketides from the littoral plant associated fungus *Pseudallescheria boydii*. J Nat Prod **76**: 1796–1800.

91. **Lan W-J, Liu W, Liang W-L, Xu Z, Le X, *et al.*** (2014) Pseudaboydins A and B: novel isobenzofuranone derivatives from marine fungus *Pseudallescheria boydii* associated with starfish acanthaster planci. Mar Drugs **12**: 4188–4199.

92. **Onodera M, Endo Y, Ogasawara N** (1989) Utilization of short-chain hydrocarbons and accumulation of methylketones by a gaseous hydrocarbon assimilating mold, *Scedosporium* sp. A-4. Agricultur Biol Chem **53**: 1431–1432.

93. **Feofilova EP** (2010) The fungal cell wall: Modern concepts of its composition and biological function. Microbiology **79**: 711–720.

94. **Woods M, Redmond A, Dancer C** (2007) Fungal infections of the central nervous system: A review of fungal pathogens and treatment. Neurology India **55**: 251.

95. **Ruiz-Herrera J** (2012) Fungal cell wall: structure, synthesis, and assembly, Second Edition. CRC Press. 207 p.

96. **Gastebois A, Clavaud C, Aimanianda V, Latgé J-P** (2009) *Aspergillus fumigatus*: cell wall polysaccharides, their biosynthesis and organization. Future Microbiol **4**: 583–595.

97. **Lesage G, Bussey H** (2006) Cell wall assembly in *Saccharomyces cerevisiae.* Microbiol Mol Biol Rev **70**: 317–343.

98. **Latgé J-P, Mouyna I, Tekaia F, Beauvais A, Debeaupuis J-P, *et al.*** (2005) Specific molecular features in the organization and biosynthesis of the cell wall of *Aspergillus fumigatus.* Med Mycol **43** Suppl 1: S15–S22.

99. **Free SJ** (2013) Chapter Two - Fungal Cell Wall Organization and Biosynthesis. In: Theodore Friedmann JCD and SFG, editor. Advances in Genetics. Academic Press, Vol. Volume **81**. pp. 33–82.

100. **Maddi A, Free SJ** (2010) α-1,6-Mannosylation of N-linked oligosaccharide present on cell wall proteins is required for their incorporation into the cell wall in the filamentous fungus *Neurospora crassa*. Eukaryot Cell **9**: 1766–1775.

101. **Abad A, Fernández-Molina JV, Bikandi J, Ramírez A, Margareto J, *et al.*** (2010) What makes *Aspergillus fumigatus* a successful pathogen? Genes and molecules involved in invasive aspergillosis. Rev Iberoam Micol **27**: 155–182.

102. **Mouyna I, Hartl L, Latgé J-P** (2013) beta-1,3-glucan modifying enzymes in *Aspergillus fumigatus*. Front Microbiol **4**: 81

103. **Reid DM, Gow NA, Brown GD** (2009) Pattern recognition: recent insights from Dectin-1. Curr Opin Immunol **21**: 30–37.

104. **Ruiz-Herrera J, Victoria Elorza M, Valentín E, Sentandreu R** (2006) Molecular organization of the cell wall of *Candida albicans* and its relation to pathogenicity. FEMS Yeast Res **6**: 14–29.

105. **Herrero AB, Magnelli P, Mansour MK, Levitz SM, Bussey H,** *et al.* (2004) *KRE5* gene null mutant strains of *Candida albicans* are avirulent and have altered cell wall composition and hypha formation properties. Eukaryot Cell **3**: 1423–1432.

106. **Fontaine T, Simenel C, Dubreucq G, Adam O, Delepierre M,** *et al.* (2000) Molecular organization of the alkali-insoluble fraction of *Aspergillus fumigatus* cell wall. J Biol Chem **275**: 27594-27607.

107. **Maubon D, Park S, Tanguy M, Huerre M, Schmitt C, *et al.*** (2006) AGS3, an α(1–3)glucan synthase gene family member of *Aspergillus fumigatus*, modulates mycelium growth in the lung of experimentally infected mice. Fungal Genet Biol **43**: 366–375.

108. **Barreto-Bergter E, Sassaki GL, Wagner R, Souza LM, Souza MVAR, *et al.*** (2008) The opportunistic fungal pathogen *Scedosporium prolificans*: carbohydrate epitopes of its glycoproteins. Int J Biol Macromol **42**: 93–102.

109. **Hall RA, Gow NAR** (2013) Mannosylation in *Candida albicans*: role in cell wall function and immune recognition. Mol Microbiol **90**: 1147–1161.

110. **Martinez JP, Gil ML, Lopez-Ribot JL, Chaffin WL** (1998) Serologic response to cell wall mannoproteins and proteins of *Candida albicans.* Clin Microbiol Rev **11**: 121–141.

111. **Heilmann CJ, Sorgo AG, Klis FM** (2012) News from the fungal front: wall proteome dynamics and host–pathogen interplay. PLoS Pathog **8**: e1003050.

112. **Fabre E, Hurtaux T, Fradin C** (2014) Mannosylation of fungal glycoconjugates in the Golgi apparatus. Curr Opin Microbiol **20**: 103–110.

113. **Ruiz-Herrera J** (1991) Fungal cell wall: structure, synthesis, and assembly. CRC Press. 260 p.

114. **Lenardon MD, Munro CA, Gow NA** (2010) Chitin synthesis and fungal pathogenesis. Curr Opin Microbiol **13**: 416–423.

115. **Baker LG, Specht CA, Donlin MJ, Lodge JK** (2007) Chitosan, the deacetylated form of chitin, is necessary for cell wall integrity in *Cryptococcus neoformans*. Eukaryot Cell **6**: 855–867.

116. **Bartnicki-Garcia S** (1968) Cell wall chemistry, morphogenesis, and taxonomy of fungi. Annu Rev Microbiol **22**: 87–108.

117. **Doering TL** (2009) How sweet it is! Cell wall biogenesis and polysaccharide capsule formation in *Cryptococcus neoformans*. Annu Rev Microbiol **63**: 223–247.

118. **Villiers C, Chevallet M, Diemer H, Couderc R, Freitas H, *et al.*** (2009) From secretome analysis to immunology. Mol Cell Proteomics **8**: 1252–1264.

119. **Bowman SM, Free SJ** (2006) The structure and synthesis of the fungal cell wall. BioEssays **28**: 799–808.

120. **Linder MB, Szilvay GR, Nakari-Setälä T, Penttilä ME** (2005) Hydrophobins: the protein-amphiphiles of filamentous fungi. FEMS Microbiol Rev **29**: 877–896.

121. **Wessels JG** (1997) Hydrophobins: proteins that change the nature of the fungal surface. Adv Microb Physiol **38**: 1–45.

122. **Jensen BG, Andersen MR, Pedersen MH, Frisvad JC, Søndergaard I** (2010) Hydrophobins from *Aspergillus* species cannot be clearly divided into two classes. BMC Research Notes **3**: 344.

123. **Kershaw MJ, Talbot NJ** (1998) Hydrophobins and repellents: proteins with fundamental roles in fungal morphogenesis. Fungal Genet Biol **23**: 18–33.

124. **Kwan AHY, Winefield RD, Sunde M, Matthews JM, Haverkamp RG,** *et al.* (2006) Structural basis for rodlet assembly in fungal hydrophobins. PNAS **103**: 3621–3626.

125. **Talbot NJ, Kershaw MJ, Wakley GE, Vries OD, Wessels J, *et al.*** (1996) *MPG1* encodes a fungal hydrophobin involved in surface interactions during infection-related development of *Magnaporthe grisea*. Plant Cell **8**: 985–999.

126. **Bowden CG, Smalley E, Guries RP, Hubbes M, Temple B, *et al.*** (1996) Lack of association between cerato-ulmin production and virulence in *Ophiostoma novo-ulmi*. Mol Plant Microbe Interact **9**: 556–564.

127. **De Groot PWJ, Brandt BW** (2012) ProFASTA: A pipeline web server for fungal protein scanning with integration of cell surface prediction software. Fungal Genet Biol **49**: 173–179.

128. **Beauvais A, Schmidt C, Guadagnini S, Roux P, Perret E, *et al.*** (2007) An extracellular matrix glues together the aerial-grown hyphae of *Aspergillus fumigatus*. Cell Microbiol **9**: 1588–1600.

129. **Aimanianda V, Bayry J, Bozza S, Kniemeyer O, Perruccio K, *et al.*** (2009) Surface hydrophobin prevents immune recognition of airborne fungal spores. Nature **460**: 1117–1121.

130. **Ouyang H, Chen X, Lu Y, Wilson IBH, Tang G, *et al.*** (2013) One single basic amino acid at the ω-1 or ω-2 site Is a signal that retains glycosylphosphatidylinositol-anchored protein in the plasma membrane of *Aspergillus fumigatus*. Eukaryot Cell **12**: 889–899.

131. **Müller G** (2011) Novel applications for glycosylphosphatidylinositol-anchored proteins in pharmaceutical and industrial biotechnology. Mol Membr Biol **28**: 187–205.

132. **Eisenhaber B, Schneider G, Wildpaner M, Eisenhaber F** (2004) A sensitive predictor for potential GPI lipid modification sites in fungal protein sequences and its application to genome-wide studies for *Aspergillus nidulans*, *Candida albicans,*

Neurospora crassa, *Saccharomyces cerevisiae* and *Schizosaccharomyces pombe*. J Mol Biol **337**: 243–253.

133. **De Groot PWJ, Hellingwerf KJ, Klis FM** (2003) Genome-wide identification of fungal GPI proteins. Yeast **20**: 781–796.

134. **Caro LHP, Tettelin H, Vossen JH, Ram AFJ, Van Den Ende H, *et al.*** (1997) *In silicio* identification of glycosyl-phosphatidylinositol-anchored plasma-membrane and cell wall proteins of *Saccharomyces cerevisiae*. Yeast **13**: 1477–1489.

135. **Klis FM, de Koster CG, Brul S** (2011) A mass spectrometric view of the fungal wall proteome. Future Microbiol **6**: 941–951.

136. **De Groot PWJ, Ram AF, Klis FM** (2005) Features and functions of covalently linked proteins in fungal cell walls. Fungal Genet Biol **42**: 657–675.

137. **Chaffin WL** (2008) *Candida albicans* cell wall proteins. Microbiol Mol Biol Rev **72**: 495–544.

138. **Castillo L, Calvo E, Martínez AI, Ruiz-Herrera J, Valentín E, *et al.*** (2008) A study of the *Candida albicans* cell wall proteome. Proteomics **8**: 3871–3881.

139. **Ebanks RO, Chisholm K, McKinnon S, Whiteway M, Pinto DM** (2006) Proteomic analysis of *Candida albicans* yeast and hyphal cell wall and associated proteins. Proteomics **6**: 2147–2156.

140. **Maddi A, Bowman SM, Free SJ** (2009) Trifluoromethanesulfonic acid-based proteomic analysis of cell wall and secreted proteins of the ascomycetous fungi *Neurospora crassa* and *Candida albicans*. Fungal Genet Biol **46**: 768–781.

141. **Pardo M, Ward M, Bains S, Molina M, Blackstock W,** *et al.* (2000) A proteomic approach for the study of *Saccharomyces cerevisiae* cell wall biogenesis. Electrophoresis **21**: 3396–3410.

142. **Casadevall A, Rosas AL, Nosanchuk JD** (2000) Melanin and virulence in *Cryptococcus neoformans*. Curr Opin Microbiol **3**: 354–358.

143. **Wakamatsu K, Ito S** (2002) Advanced chemical methods in melanin determination. Pigment Cell Research **15**: 174–183.

144. **Beltran-Garcia MJ, Prado FM, Oliveira MS, Ortiz-Mendoza D, Scalfo AC, *et al.*** (2014) Singlet molecular oxygen generation by light-activated DHN-melanin of the fungal pathogen *Mycosphaerella fijiensis* in black Sigatoka disease of bananas. PLoS One **9**: e91616.

145. **Eisenman HC, Nosanchuk JD, Webber JBW, Emerson RJ, Camesano TA, *et al.*** (2005) Microstructure of cell wall-associated melanin in the human pathogenic fungus *Cryptococcus neoformans*. Biochemistry **44**: 3683–3693.

146. **Williamson PR** (1994) Biochemical and molecular characterization of the diphenol oxidase of *Cryptococcus neoformans*: identification as a laccase. J Bacteriol **176**: 656–664.

147. **Chang T-S** (2009) An updated review of tyrosinase inhibitors. Intern J Mol Sci **10**: 2440–2475.

148. **Nosanchuk JD, Ovalle R, Casadevall A** (2001) Glyphosate inhibits melanization of *Cryptococcus neoformans* and prolongs survival of mice after systemic infection. J Infect Dis **183**: 1093–1099.

149. **Pihet M, Vandeputte P, Tronchin G, Renier G, Saulnier P, *et al.*** (2009) Melanin is an essential component for the integrity of the cell wall of *Aspergillus fumigatus* conidia. BMC Microbiol **9**: 177.

150. **Kimura N, Tsuge T** (1993) Gene cluster involved in melanin biosynthesis of the filamentous fungus *Alternaria alternata*. J Bacteriol **175**: 4427–4435.

151. **Singh S, Malhotra AG, Pandey A, Pandey KM** (2013) Computational model for pathway reconstruction to unravel the evolutionary significance of melanin synthesis. Bioinformation **9**: 94–100.

152. **Sono K, Lye D, Moore CA, Boyd WC, Gorlin TA,** *et al.* (2012) Melanin-based coatings as lead-binding agents. Bioinorg Chem Appl **2012**: e361803.

153. **Khajo A, Bryan RA, Friedman M, Burger RM, Levitsky Y, *et al.*** (2011) Protection of melanized *Cryptococcus neoformans* from lethal dose gamma irradiation involves changes in melanin's chemical structure and paramagnetism. PLoS One **6**: e25092

154. **Nosanchuk JD, Casadevall A** (2006) Impact of melanin on microbial virulence and clinical resistance to antimicrobial compounds. Antimicrob Agents Chemother **50**: 3519–3528.

155. **Jacobson ES** (2000) Pathogenic roles for fungal melanins. Clin Microbiol Rev **13**: 708–717.

156. **Romero-Martinez R, Wheeler M, Guerrero-Plata A, Rico G, Torres-Guerrero H** (2000) Biosynthesis and Functions of Melanin in Sporothrix schenckii. Infect Immun **68**: 3696–3703.

157. **Woo PCY, Tam EWT, Chong KTK, Cai JJ, Tung ETK, *et al.*** (2010) High diversity of polyketide synthase genes and the melanin biosynthesis gene cluster in *Penicillium marneffei*. FEBS J **277**: 3750–3758.

158. **Tsai H-F, Chang YC, Washburn RG, Wheeler MH, Kwon-Chung KJ** (1998) The developmentally regulated *alb1* gene of *Aspergillus fumigatus*: Its role in modulation of conidial morphology and virulence. J Bacteriol **180**: 3031.

159. **Sarangarajan R, Apte SP** (2006) The polymerization of melanin: a poorly understood phenomenon with egregious biological implications. Melanoma Res **16**: 3–10.

160. **Tavares PM, Thevissen K, Cammue BPA, Francois IEJA, Barreto-Bergter E, *et al.*** (2008) *In vitro* activity of the antifungal plant defensin RsAFP2 against *Candida* isolates and its *in vivo* efficacy in prophylactic murine models of candidiasis. Antimicrob Agents Chemother **52**: 4522–4525.

161. **Barreto-Bergter E, Sassaki GL, Souza L** (2011) Structural analysis of fungal cerebrosides. Front Microbiol **2**: 239.

162. **Barreto-Bergter E, Pinto MR, Rodrigues ML** (2004) Structure and biological functions of fungal cerebrosides. Anais da Academia Brasileira de Ciências **76**: 67–84.

163. **Rollin-Pinheiro R, Liporagi-Lopes LC, de Meirelles JV, Souza LM de, Barreto-Bergter E** (2014) Characterization of *Scedosporium apiospermum* glucosylceramides and their involvement in fungal development and macrophage functions. PLoS One **9**: e98149.

164. **Lopes-Bezerra LM** (2011) *Sporothrix schenckii* cell wall peptidorhamnomannans. Front Microbiol **2**.

165. **Leitão EA, Bittencourt VCB, Haido RMT, Valente AP, Peter-Katalinic J,** *et al.* (2003) β-Galactofuranose-containing O-linked oligosaccharides present in the cell wall peptidogalactomannan of *Aspergillus fumigatus* contain immunodominant epitopes. Glycobiology **13**: 681–692.

166. **Pinto MR, Rodrigues ML, Travassos LR, Haido RMT, Wait R, *et al.*** (2002) Characterization of glucosylceramides in *Pseudallescheria boydii* and their involvement in fungal differentiation. Glycobiology **12**: 251–260.

167. **Latgé J-P** (2007) The cell wall: a carbohydrate armour for the fungal cell. Molecular Microbiology **66**: 279–290.

168. **Typas A, Banzhaf M, Gross CA, Vollmer W** (2012) From the regulation of peptidoglycan synthesis to bacterial growth and morphology. Nat Rev Micro **10**: 123–136.

169. **Kutschera U** (2008) The growing outer epidermal wall: design and physiological role of a composite structure. Ann Bot **101**: 615–621.

170. **Bret-Harte MS, Talbott LD** (1993) Changes in composition of the outer epidermal cell wall of pea stems during auxin-induced growth. Planta **190**: 369–378.

171. **April TM, Abbott SP, Foght JM, Currah RS** (1998) Degradation of hydrocarbons in crude oil by the ascomycete *Pseudallescheria boydii* (Microascaceae). Can J Microbiol **44**: 270–278.

172. **Clauβen M, Schmidt S** (1999) Biodegradation of phenylbenzoate and some of its derivatives by *Scedosporium apiospermum*. Res Microbiol **150**: 413–420.

173. **Claußen M, Schmidt S** (1998) Biodegradation of phenol and *p*-cresol by the hyphomycete *Scedosporium apiospermum*. Res Microbiol **149**: 399–406.

174. **Ishii K, Furuichi T** (2007) Development of bioreactor system for treatment of dioxin-contaminated soil using *Pseudallescheria boydii.* J Hazard Mater **148**: 693–700.

175. **Ishii K, Furuichi T, Tanikawa N, Kuboshima M** (2009) Estimation of the biodegradation rate of 2,3,7,8-tetrachlorodibenzo-*p*-dioxin by using dioxin-degrading fungus, *Pseudallescheria boydii*. J Hazard Mater **162**: 328–332.

176. **Enguita FJ, Leitã**o AL (2013) Hydroquinone: environmental pollution, toxicity, and microbial answers. BioMed Res Int **2013**: e542168.

177. **Harms H, Schlosser D, Wick LY** (2011) Untapped potential: exploiting fungi in bioremediation of hazardous chemicals. Nat Rev Micro **9**: 177–192.

178. **Črešnar B, Petrič Š** (2011) Cytochrome P450 enzymes in the fungal kingdom. Biochimica et Biophysica Acta (BBA) - Proteins and Proteomics **1814**: 29–35.

ANNEXES

Annex I

Raw MS data for conidial cell wall extracts

Annex II

Raw MS data for mycelial cell wall extracts

Annex III

MS/MS spectra from proteins identified with a single-peptide from mycelial and conidial extracts.

I. Annex 1

Table A.7. Raw MS data for conidial cell wall extracts. Protein sequences with predicted GPI-anchor are shaded in grey.

Accession	Coverage	# PSMs	# Peptides	# AAs	MW [kDa]	calc. pI	Score	Description
A_P_NEUCRA_SCA_CDS_9909	36.48	18	11	307	32.5	9.55	530.63	CDS 1024675 1026580 Direct (translation)
A_P_NEUCRA_SCA_CDS_5086	31.36	13	10	338	36.3	6.95	403.53	CDS 164130 165831 Reverse (translation)
A_P_NEUCRA_SCA_CDS_6775	29.86	11	10	355	37.4	7.02	294.87	CDS 1275054 1276728 Direct (translation)
A_P_NEUCRA_SCA_CDS_720	41.98	10	9	212	23.6	11.14	287.32	CDS 1438411 1439493 Reverse (translation)
A_P_NEUCRA_SCA_CDS_3537	21.99	10	9	391	44.4	10.20	223.55	CDS 854001 855532 Reverse (translation)
A_P_NEUCRA_SCA_CDS_5972	36.19	12	9	257	27.9	10.40	354.10	CDS 463869 464893 Direct (translation)
A_P_NEUCRA_SCA_CDS_1688	41.61	13	9	161	18.0	11.37	348.57	CDS 546288 547203 Reverse (translation)
A_P_NEUCRA_SCA_CDS_10475	14.42	10	9	652	71.0	5.22	309.48	CDS 608324 610529 Direct (translation)
A_P_NEUCRA_SCA_CDS_1515	31.30	10	8	262	29.4	10.37	268.73	CDS 1187524 1188738 Reverse (translation)
A_P_NEUCRA_SCA_CDS_9538	19.53	11	8	553	59.5	9.14	281.34	CDS 2192317 2194572 Direct (translation)
A_P_NEUCRA_SCA_CDS_7198	49.51	11	8	103	11.3	11.36	291.89	CDS 2840263 2840773 Direct (translation)
A_P_NEUCRA_SCA_CDS_4128	49.26	39	8	136	14.7	10.13	1284.25	CDS 598951 599519 Reverse (translation)
A_P_NEUCRA_SCA_CDS_7250	49.33	10	8	150	16.0	10.54	263.39	CDS 3009246 3009995 Direct (translation)
A_P_NEUCRA_SCA_CDS_7341	18.45	12	7	439	47.6	9.07	306.68	CDS 249002 251080 Reverse (translation)

Accession	Coverage	# PSMs	# Peptides	# AAs	MW [kDa]	calc. pI	Score	Description
A_P_NEUCRA_SCA_CDS_9776	46.15	10	7	130	14.9	10.70	259.80	CDS 459394 459933 Reverse (translation)
A_P_NEUCRA_SCA_CDS_6709	8.89	7	7	844	93.3	6.98	202.43	CDS 1023156 1026040 Reverse (translation)
A_P_NEUCRA_SCA_CDS_8164	3.91	9	7	2069	234.3	6.57	260.32	CDS 1226215 1232601 Reverse (translation)
A_P_NEUCRA_SCA_CDS_5869	22.90	7	7	310	34.0	9.51	167.63	CDS 85365 87080 Reverse (translation)
A_P_NEUCRA_SCA_CDS_3357	16.23	8	6	308	33.7	9.85	263.99	CDS 179931 181468 Reverse (translation)
A_P_NEUCRA_SCA_CDS_3189	7.77	6	6	914	98.6	5.26	230.80	CDS 95272 98370 Reverse (translation)
A_P_NEUCRA_SCA_CDS_10806	28.85	6	6	156	17.8	10.77	164.86	CDS 723031 723861 Direct (translation)
A_P_NEUCRA_SCA_CDS_7163	29.13	5	5	254	27.6	11.14	89.19	CDS 2684196 2685276 Direct (translation)
A_P_NEUCRA_SCA_CDS_9624	34.91	7	5	106	11.8	11.69	234.13	CDS 2535074 2535801 Reverse (translation)
A_P_NEUCRA_SCA_CDS_6345	23.50	6	5	200	23.0	10.29	209.45	CDS 1937786 1938849 Reverse (translation)
A_P_NEUCRA_SCA_CDS_8525	18.40	5	5	375	41.6	5.69	159.21	CDS 1090548 1092375 Direct (translation)
A_P_NEUCRA_SCA_CDS_10467	23.01	6	5	239	27.5	10.64	194.98	CDS 571292 572521 Direct (translation)
A_P_NEUCRA_SCA_CDS_1326	21.78	6	5	225	25.6	10.27	145.67	CDS 496028 497064 Direct (translation)
A_P_NEUCRA_SCA_CDS_4712	36.89	6	5	122	14.0	10.32	183.29	CDS 146610 147201 Reverse (translation)
A_P_NEUCRA_SCA_CDS_5046	22.06	5	4	136	15.4	11.15	119.83	CDS 29127 29648 Direct (translation)
A_P_NEUCRA_SCA_CDS_4692	24.22	5	4	161	18.6	10.74	104.75	CDS 86340 87050 Direct (translation)
A_P_NEUCRA_SCA_CDS_1000	20.39	4	4	152	16.9	8.38	152.30	CDS 433450 434368 Reverse (translation)

Accession	Coverage	# PSMs	# Peptides	# AAs	MW [kDa]	calc. pI	Score	Description
A_P_NEUCRA_SCA_CDS_7719	6.27	5	4	702	80.0	5.00	149.51	CDS 771188 773356 Reverse (translation)
A_P_NEUCRA_SCA_CDS_5104	8.36	4	4	586	61.5	5.72	155.60	CDS 230142 232077 Reverse (translation)
A_P_NEUCRA_SCA_CDS_9198	29.14	4	4	151	16.9	10.61	149.46	CDS 891285 892014 Direct (translation)
A_P_NEUCRA_SCA_CDS_973	7.18	7	4	529	58.6	8.60	262.26	CDS 325614 328603 Reverse (translation)
A_P_NEUCRA_SCA_CDS_9938	17.20	5	4	157	17.4	10.29	191.80	CDS 1151322 1152074 Direct (translation)
A_P_NEUCRA_SCA_CDS_1189	22.45	6	4	196	21.5	5.48	208.89	CDS 353654 354241 Reverse (translation)
A_P_NEUCRA_SCA_CDS_7766	23.12	6	4	186	20.8	10.81	136.15	CDS 1018601 1019576 Direct (translation)
A_P_NEUCRA_SCA_CDS_9673	32.77	5	4	119	12.9	10.70	125.44	CDS 43430 44381 Reverse (translation)
A_P_NEUCRA_SCA_CDS_996	14.71	5	4	238	26.8	9.82	76.29	CDS 420676 422469 Reverse (translation)
A_P_NEUCRA_SCA_CDS_9088	16.72	4	4	287	31.5	10.23	165.30	CDS 394712 395755 Reverse (translation)
A_P_NEUCRA_SCA_CDS_9294	13.89	4	4	396	44.7	5.17	79.25	CDS 1264789 1266546 Direct (translation)
A_P_NEUCRA_SCA_CDS_10804	5.93	4	4	928	103.9	5.95	118.64	CDS 716700 719483 Direct (translation)
A_P_NEUCRA_SCA_CDS_6580	6.42	4	4	670	72.4	6.13	131.87	CDS 459371 461529 Reverse (translation)
A_P_NEUCRA_SCA_CDS_9929	41.06	4	4	151	16.4	10.71	101.69	CDS 1123121 1123923 Reverse (translation)
A_P_NEUCRA_SCA_CDS_9756	10.51	4	4	514	55.3	5.50	122.87	CDS 390259 392448 Reverse (translation)
A_P_NEUCRA_SCA_CDS_9175	16.99	5	4	153	17.6	10.02	156.72	CDS 771674 772565 Direct (translation)
A_P_NEUCRA_SCA_CDS_6759	18.58	4	4	226	24.9	9.66	127.22	CDS 1188946 1189912 Reverse (translation)

Accession	Coverage	# PSMs	# Peptides	# AAs	MW [kDa]	calc. pI	Score	Description
A_P_NEUCRA_SCA_CDS_1325	39.09	5	3	110	11.7	9.95	143.20	CDS 494888 495601 Reverse (translation)
A_P_NEUCRA_SCA_CDS_2888	18.58	4	3	183	20.7	11.71	63.39	CDS 1737995 1739028 Reverse (translation)
A_P_NEUCRA_SCA_CDS_4129	27.21	3	3	136	14.2	10.71	59.63	CDS 600516 601038 Direct (translation)
A_P_NEUCRA_SCA_CDS_3432	20.95	4	3	105	11.4	9.19	65.57	CDS 441669 442608 Reverse (translation)
A_P_NEUCRA_SCA_CDS_3192	8.46	3	3	473	52.0	8.16	149.10	CDS 116556 118313 Reverse (translation)
A_P_NEUCRA_SCA_CDS_2275	30.15	4	3	136	15.5	10.83	128.87	CDS 1197945 1198666 Direct (translation)
A_P_NEUCRA_SCA_CDS_7189	6.83	3	3	410	44.7	8.28	74.75	CDS 2800829 2802494 Direct (translation)
A_P_NEUCRA_SCA_CDS_1887	7.50	3	3	480	52.7	8.38	65.59	CDS 1378282 1379954 Reverse (translation)
A_P_NEUCRA_SCA_CDS_6299	11.97	3	3	259	28.4	8.97	116.43	CDS 1748300 1749286 Reverse (translation)
A_P_NEUCRA_SCA_CDS_10073	6.11	3	3	785	85.4	6.84	65.44	CDS 490962 493583 Reverse (translation)
A_P_NEUCRA_SCA_CDS_6011	20.69	3	3	174	20.5	10.35	99.09	CDS 639501 640596 Reverse (translation)
A_P_NEUCRA_SCA_CDS_8471	11.11	3	3	351	37.7	11.05	126.31	CDS 887110 888540 Direct (translation)
A_P_NEUCRA_SCA_CDS_3358	31.25	5	3	96	10.7	9.99	170.41	CDS 183973 184599 Reverse (translation)
A_P_NEUCRA_SCA_CDS_5073	16.36	4	3	165	18.8	9.70	110.43	CDS 126434 127128 Reverse (translation)
A_P_NEUCRA_SCA_CDS_10350	12.23	3	3	417	44.4	6.48	124.50	CDS 102013 103753 Reverse (translation)
A_P_NEUCRA_SCA_CDS_3359	13.62	3	3	213	23.6	8.81	127.60	CDS 185105 185935 Direct (translation)
A_P_NEUCRA_SCA_CDS_6778	13.18	3	3	258	27.7	8.76	71.68	CDS 1283772 1284925 Reverse (translation)

Accession	Coverage	# PSMs	# Peptides	# AAs	MW [kDa]	calc. pI	Score	Description
A_P_NEUCRA_SCA_CDS_9108	6.38	3	3	549	56.7	5.21	86.40	CDS 463865 465645 Direct (translation)
A_P_NEUCRA_SCA_CDS_10679	20.65	4	3	92	10.5	11.65	92.99	CDS 207679 208336 Reverse (translation)
A_P_NEUCRA_SCA_CDS_3343	20.29	5	3	207	23.3	10.73	119.14	CDS 95015 95746 Direct (translation)
A_P_NEUCRA_SCA_CDS_5144	16.33	3	3	251	26.2	10.33	127.27	CDS 396804 398661 Direct (translation)
A_P_NEUCRA_SCA_CDS_3910	9.51	3	3	263	28.4	6.54	123.73	CDS 207748 208694 Direct (translation)
A_P_NEUCRA_SCA_CDS_9322	7.36	3	3	530	58.0	6.95	135.96	CDS 1368868 1370956 Reverse (translation)
A_P_NEUCRA_SCA_CDS_1031	6.69	3	3	583	63.5	9.13	93.50	CDS 559039 561306 Direct (translation)
A_P_NEUCRA_SCA_CDS_6886	4.24	3	3	849	94.3	4.58	89.11	CDS 1703813 1706916 Reverse (translation)
A_P_NEUCRA_SCA_CDS_1005	4.80	3	3	1001	112.5	9.23	131.29	CDS 452883 456037 Reverse (translation)
A_P_NEUCRA_SCA_CDS_1787	5.07	3	3	808	86.6	5.58	107.43	CDS 988309 990992 Direct (translation)
NA_P_NEUCRA_SCA_CDS_1559	25.55	3	3	137	15.4	9.00	116.80	CDS 1376605 1377302 Direct (translation)
A_P_NEUCRA_SCA_CDS_1469	3.92	2	2	689	74.5	6.27	91.55	CDS 1008742 1011330 Direct (translation)
A_P_NEUCRA_SCA_CDS_10684	11.88	2	2	160	18.3	10.62	46.46	CDS 226013 226888 Reverse (translation)
A_P_NEUCRA_SCA_CDS_3404	2.57	2	2	662	72.4	8.44	35.86	CDS 347023 349090 Direct (translation)
A_P_NEUCRA_SCA_CDS_6477	3.52	2	2	711	79.2	5.21	73.33	CDS 30182 32898 Direct (translation)
A_P_NEUCRA_SCA_CDS_2877	0.63	2	2	2866	312.2	7.21	75.85	CDS 1696403 1706483 Direct (translation)
A_P_NEUCRA_SCA_CDS_7637	4.46	2	2	202	23.0	10.46	56.61	CDS 410256 411590 Reverse (translation)

Accession	Coverage	# PSMs	# Peptides	# AAs	MW [kDa]	calc. pI	Score	Description
A_P_NEUCRA_SCA_CDS_7765	6.94	2	2	317	33.2	10.08	54.27	CDS 1015713 1016914 Reverse (translation)
A_P_NEUCRA_SCA_CDS_2300	8.49	2	2	106	12.0	10.48	49.89	CDS 1318160 1318947 Reverse (translation)
A_P_NEUCRA_SCA_CDS_8155	26.25	2	2	80	9.1	10.11	64.00	CDS 1203536 1204076 Direct (translation)
A_P_NEUCRA_SCA_CDS_6593	23.08	2	2	104	11.2	9.13	31.87	CDS 528076 528731 Direct (translation)
A_P_NEUCRA_SCA_CDS_988	11.56	2	2	199	22.4	9.99	27.47	CDS 399776 400725 Reverse (translation)
KEZ46909.1	12.38	3	2	202	19.9	4.12	115.50	CDS 972008 972906 Reverse (translation)
A_P_NEUCRA_SCA_CDS_9455	17.60	2	2	125	14.6	11.55	38.21	CDS 1882988 1883811 Reverse (translation)
A_P_NEUCRA_SCA_CDS_8488	6.28	2	2	414	46.5	6.24	63.24	CDS 942260 943901 Direct (translation)
A_P_NEUCRA_SCA_CDS_9537	12.72	2	2	173	20.0	10.33	55.61	CDS 2190536 2191200 Direct (translation)
A_P_NEUCRA_SCA_CDS_9928	9.61	2	2	333	34.6	6.15	58.37	CDS 1119505 1120898 Reverse (translation)
A_P_NEUCRA_SCA_CDS_3199	8.62	2	2	290	31.3	4.93	75.06	CDS 139597 140674 Direct (translation)
A_P_NEUCRA_SCA_CDS_1449	9.19	2	2	283	30.1	8.92	56.95	CDS 958207 959804 Reverse (translation)
A_P_NEUCRA_SCA_CDS_9166	16.50	3	2	103	11.6	9.48	125.76	CDS 729467 729952 Direct (translation)
A_P_NEUCRA_SCA_CDS_9287	5.11	2	2	313	33.7	4.96	57.36	CDS 1237017 1238212 Direct (translation)
A_P_NEUCRA_SCA_CDS_1242	6.98	2	2	401	44.8	8.72	55.52	CDS 154701 156291 Direct (translation)
A_P_NEUCRA_SCA_CDS_9417	7.53	2	2	438	47.4	5.34	107.05	CDS 1726222 1727829 Direct (translation)
A_P_NEUCRA_SCA_CDS_8101	4.27	2	2	445	49.3	6.38	75.91	CDS 944933 946391 Reverse (translation)

Accession	Coverage	# PSMs	# Peptides	# AAs	MW [kDa]	calc. pI	Score	Description
A_P_NEUCRA_SCA_CDS_6573	7.55	2	2	384	41.6	7.55	71.41	CDS 421496 423212 Reverse (translation)
A_P_NEUCRA_SCA_CDS_1767	4.80	3	2	542	61.0	7.94	117.62	CDS 885430 887670 Reverse (translation)
A_P_NEUCRA_SCA_CDS_6143	14.62	3	2	130	14.8	9.94	120.54	CDS 1121022 1121736 Reverse (translation)
A_P_NEUCRA_SCA_CDS_1025	6.02	2	2	465	53.0	6.73	58.76	CDS 532079 533473 Direct (translation)
A_P_NEUCRA_SCA_CDS_8689	5.28	2	2	417	45.6	6.70	72.60	CDS 1687747 1689671 Reverse (translation)
A_P_NEUCRA_SCA_CDS_6701	25.98	3	2	127	13.7	9.98	105.38	CDS 992827 993541 Direct (translation)
A_P_NEUCRA_SCA_CDS_1547	4.53	2	2	574	64.1	5.83	70.39	CDS 1332432 1335096 Reverse (translation)
NA_P_NEUCRA_SCA_CDS_8322	8.63	2	2	278	29.3	4.48	65.15	CDS 379477 380310 Reverse (translation)
A_P_NEUCRA_SCA_CDS_5984	4.42	2	2	634	68.0	4.93	93.56	CDS 536425 538326 Reverse (translation)
A_P_NEUCRA_SCA_CDS_7876	17.24	2	2	116	13.1	9.80	47.88	CDS 130930 131423 Direct (translation)
A_P_NEUCRA_SCA_CDS_2408	7.73	3	2	362	38.9	5.10	99.96	CDS 1740861 1741946 Direct (translation)
A_P_NEUCRA_SCA_CDS_6956	4.60	1	1	261	29.3	10.26	50.49	CDS 1966228 1967418 Reverse (translation)
A_P_NEUCRA_SCA_CDS_5568	2.36	1	1	381	41.6	7.58	28.72	CDS 707892 709250 Direct (translation)
A_P_NEUCRA_SCA_CDS_1408	3.25	1	1	277	30.5	9.06	66.31	CDS 844551 845499 Reverse (translation)
A_P_NEUCRA_SCA_CDS_3622	4.93	1	1	142	15.2	10.45	34.06	CDS 1198629 1199577 Reverse (translation)
A_P_NEUCRA_SCA_CDS_8966	4.96	1	1	141	15.5	10.37	46.47	CDS 248941 249471 Reverse (translation)
A_P_NEUCRA_SCA_CDS_1185	6.25	1	1	192	21.5	9.51	33.03	CDS 343939 344986 Reverse (translation)

Accession	Coverage	# PSMs	# Peptides	# AAs	MW [kDa]	calc. pI	Score	Description
A_P_NEUCRA_SCA_CDS_3196	1.97	1	1	608	67.0	7.64	63.46	CDS 133885 135872 Reverse (translation)
A_P_NEUCRA_SCA_CDS_438	6.25	1	1	272	29.7	8.00	53.56	CDS 313359 314643 Direct (translation)
A_P_NEUCRA_SCA_CDS_7354	8.15	1	1	135	15.7	10.64	42.49	CDS 341208 341945 Reverse (translation)
A_P_NEUCRA_SCA_CDS_5900	2.44	1	1	614	66.6	5.50	44.06	CDS 206553 208910 Reverse (translation)
A_P_NEUCRA_SCA_CDS_10423	2.79	1	1	394	43.7	7.43	30.36	CDS 401791 403400 Direct (translation)
A_P_NEUCRA_SCA_CDS_4285	5.71	1	1	333	34.9	7.83	28.26	CDS 573029 574264 Direct (translation)
A_P_NEUCRA_SCA_CDS_10369	3.12	1	1	449	48.9	6.16	36.91	CDS 172591 174092 Reverse (translation)
A_P_NEUCRA_SCA_CDS_10685	5.79	1	1	190	22.0	10.29	28.20	CDS 227326 228207 Direct (translation)
A_P_NEUCRA_SCA_CDS_6483	3.53	1	1	255	28.6	7.96	51.42	CDS 53328 54936 Direct (translation)
A_P_NEUCRA_SCA_CDS_2495	11.80	1	1	305	34.3	7.59	51.42	CDS 309886 310999 Direct (translation)
A_P_NEUCRA_SCA_CDS_7864	5.88	1	1	153	17.6	9.73	51.42	CDS 93117 93640 Reverse (translation)
A_P_NEUCRA_SCA_CDS_3337	1.56	1	1	959	99.0	5.90	36.27	CDS 64157 67308 Direct (translation)
A_P_NEUCRA_SCA_CDS_1158	2.28	1	1	483	53.0	7.27	47.73	CDS 234952 236623 Direct (translation)
A_P_NEUCRA_SCA_CDS_9558	1.91	1	1	577	63.2	9.10	39.73	CDS 2251576 2255495 Reverse (translation)
A_P_NEUCRA_SCA_CDS_3403	2.04	1	1	489	53.4	5.87	35.83	CDS 341774 343860 Reverse (translation)
NA_P_NEUCRA_SCA_CDS_2301	4.69	1	1	341	37.1	8.66	53.68	CDS 1320256 1321699 Reverse (translation)
A_P_NEUCRA_SCA_CDS_10469	3.23	1	1	310	34.4	9.79	31.08	CDS 589601 590699 Direct (translation)

Accession	Coverage	# PSMs	# Peptides	# AAs	MW [kDa]	calc. pI	Score	Description
A_P_NEUCRA_SCA_CDS_10746	9.78	1	1	92	10.2	10.99	34.21	CDS 490702 491262 Reverse (translation)
A_P_NEUCRA_SCA_CDS_7325	8.97	1	1	145	16.8	10.62	79.26	CDS 181988 182558 Direct (translation)
A_P_NEUCRA_SCA_CDS_2479	1.66	1	1	664	72.2	5.05	37.81	CDS 197423 199735 Reverse (translation)
A_P_NEUCRA_SCA_CDS_1358	2.99	1	1	301	34.5	8.90	44.06	CDS 669635 670835 Reverse (translation)
A_P_NEUCRA_SCA_CDS_6916	4.01	1	1	324	35.0	5.92	80.31	CDS 1808555 1810173 Direct (translation)
A_P_NEUCRA_SCA_CDS_6489	6.85	1	1	146	16.9	9.88	33.98	CDS 67851 68436 Direct (translation)
A_P_NEUCRA_SCA_CDS_5882	2.53	1	1	475	52.8	5.87	42.55	CDS 138137 139888 Reverse (translation)
A_P_NEUCRA_SCA_CDS_2890	3.91	1	1	256	30.2	10.48	38.48	CDS 1743282 1744636 Reverse (translation)
A_P_NEUCRA_SCA_CDS_7180	3.88	1	1	309	33.7	9.03	53.14	CDS 2753313 2754434 Reverse (translation)
A_P_NEUCRA_SCA_CDS_7862	2.52	1	1	516	55.9	8.92	31.24	CDS 87352 89008 Reverse (translation)
A_P_NEUCRA_SCA_CDS_9759	7.51	1	1	173	19.2	9.70	51.42	CDS 400519 401450 Reverse (translation)
A_P_NEUCRA_SCA_CDS_9543	4.94	1	1	243	26.5	8.81	32.25	CDS 2218233 2219226 Direct (translation)
A_P_NEUCRA_SCA_CDS_7793	1.35	3	1	889	98.3	7.01	140.20	CDS 1096982 1100780 Reverse (translation)
A_P_NEUCRA_SCA_CDS_5571	3.04	2	1	395	43.3	9.16	89.49	CDS 714176 715579 Direct (translation)
A_P_NEUCRA_SCA_CDS_8988	1.90	1	1	684	72.3	8.79	38.20	CDS 17277 19328 Direct (translation)
A_P_NEUCRA_SCA_CDS_8520	3.95	1	1	354	38.6	6.25	30.30	CDS 1072534 1073743 Reverse (translation)
A_P_NEUCRA_SCA_CDS_9265	2.14	1	1	653	71.8	6.83	66.73	CDS 1153114 1155451 Direct (translation)

Accession	Coverage	# PSMs	# Peptides	# AAs	MW [kDa]	calc. pI	Score	Description
A_P_NEUCRA_SCA_CDS_5560	3.90	1	1	385	41.8	6.24	27.08	CDS 669277 670603 Reverse (translation)
A_P_NEUCRA_SCA_CDS_301	2.29	1	1	611	66.0	6.87	37.48	CDS 651809 653941 Reverse (translation)
A_P_NEUCRA_SCA_CDS_5212	2.41	1	1	622	65.4	6.62	33.98	CDS 743883 745818 Direct (translation)
A_P_NEUCRA_SCA_CDS_1265	10.88	1	1	147	15.8	10.13	35.98	CDS 260283 260815 Direct (translation)
NA_P_NEUCRA_SCA_CDS_2332	1.47	1	1	614	62.0	4.59	40.14	CDS 1456020 1457861 Reverse (translation)
A_P_NEUCRA_SCA_CDS_8038	10.43	2	1	211	21.4	10.59	79.75	CDS 686263 687185 Direct (translation)
A_P_NEUCRA_SCA_CDS_6915	1.58	1	1	888	97.9	7.59	48.71	CDS 1803081 1805744 Direct (translation)
A_P_NEUCRA_SCA_CDS_7707	10.75	1	1	186	21.0	9.41	48.92	CDS 726521 727078 Reverse (translation)
A_P_NEUCRA_SCA_CDS_6833	2.94	1	1	884	100.1	5.97	21.85	CDS 1486978 1490262 Reverse (translation)
KEZ46627.1	8.02	2	1	187	18.7	4.45	90.28	CDS 531513 532142 Direct (translation)
A_P_NEUCRA_SCA_CDS_6821	0.12	1	1	4339	491.6	6.11	27.67	CDS 1426280 1439442 Reverse (translation)
A_P_NEUCRA_SCA_CDS_2997	4.86	1	1	288	30.4	6.67	46.67	CDS 2180458 2181412 Direct (translation)
A_P_NEUCRA_SCA_CDS_6681	1.35	1	1	891	95.6	8.56	45.45	CDS 900934 904482 Reverse (translation)
A_P_NEUCRA_SCA_CDS_335	7.11	1	1	197	20.5	10.29	33.11	CDS 779672 780610 Direct (translation)
KEZ44163.1	9.83	1	1	173	16.2	4.42	24.28	CDS 215154 215800 Direct (translation)
A_P_NEUCRA_SCA_CDS_4105	1.93	1	1	571	63.3	7.94	41.89	CDS 518893 520863 Direct (translation)
A_P_NEUCRA_SCA_CDS_1411	6.67	2	1	150	15.8	9.31	59.45	CDS 848773 849485 Reverse (translation)

Accession	Coverage	# PSMs	# Peptides	# AAs	MW [kDa]	calc. pI	Score	Description
KEZ41172.1	3.06	1	1	523	50.9	4.64	94.97	CDS 1101340 1103048 Direct (translation)
A_P_NEUCRA_SCA_CDS_501	4.94	1	1	243	26.3	4.93	39.25	CDS 576440 577509 Direct (translation)
A_P_NEUCRA_SCA_CDS_2762	5.24	1	1	286	31.8	10.05	26.25	CDS 1300250 1301607 Reverse (translation)
KEZ44256.1	6.32	1	1	190	19.7	4.41	62.17	CDS 695902 696649 Direct (translation)
A_P_NEUCRA_SCA_CDS_9719	15.33	1	1	137	14.6	9.69	39.30	CDS 232082 232564 Reverse (translation)
NA_P_NEUCRA_SCA_CDS_8085	12.26	1	1	155	15.7	9.58	29.04	CDS 867806 868270 Reverse (translation)
A_P_NEUCRA_SCA_CDS_1741	0.86	1	1	1398	152.8	9.20	37.34	CDS 753335 760327 Direct (translation)
A_P_NEUCRA_SCA_CDS_1727	9.76	1	1	82	8.9	9.26	40.22	CDS 709839 710466 Direct (translation)
A_P_NEUCRA_SCA_CDS_5076	9.64	1	1	83	9.0	10.11	31.06	CDS 130129 130698 Direct (translation)
A_P_NEUCRA_SCA_CDS_9463	1.76	1	1	794	87.1	6.73	73.68	CDS 1905440 1907821 Direct (translation)
A_P_NEUCRA_SCA_CDS_5580	4.66	1	1	193	20.8	5.22	45.90	CDS 752980 754655 Direct (translation)
A_P_NEUCRA_SCA_CDS_6507	0.48	1	1	2521	279.9	9.41	49.77	CDS 141521 149223 Reverse (translation)
A_P_NEUCRA_SCA_CDS_2944	2.68	1	1	448	48.5	6.23	28.31	CDS 1973155 1974890 Direct (translation)
KEZ44265.1	3.79	1	1	264	27.6	4.60	23.38	CDS 733621 734543 Direct (translation)
KEZ43142.1	2.83	1	1	353	35.7	4.60	33.95	CDS 262747 263972 Direct (translation)
A_P_NEUCRA_SCA_CDS_2433	2.33	1	1	429	44.6	7.99	40.50	CDS 2715 4204 Direct (translation)
A_P_NEUCRA_SCA_CDS_3548	13.33	1	1	90	10.3	10.29	25.97	CDS 900297 900726 Direct (translation)

Accession	Coverage	# PSMs	# Peptides	# AAs	MW [kDa]	calc. pI	Score	Description
A_P_NEUCRA_SCA_CDS_8709	9.90	1	1	101	11.3	10.33	32.28	CDS 1741580 1742281 Direct (translation)
A_P_NEUCRA_SCA_CDS_2826	3.08	1	1	389	42.4	5.54	33.04	CDS 1509155 1510409 Direct (translation)
A_P_NEUCRA_SCA_CDS_3163	2.42	1	1	454	51.7	6.15	31.00	CDS 69868 71767 Direct (translation)
A_P_NEUCRA_SCA_CDS_2691	1.28	1	1	1015	106.4	7.77	34.93	CDS 1002245 1006207 Reverse (translation)
A_P_NEUCRA_SCA_CDS_10076	8.96	1	1	134	15.0	6.71	48.33	CDS 500103 500821 Reverse (translation)
A_P_NEUCRA_SCA_CDS_6241	1.88	1	1	691	76.8	5.59	21.05	CDS 1520961 1523302 Direct (translation)
A_P_NEUCRA_SCA_CDS_500	3.28	1	1	366	39.5	9.29	53.45	CDS 569253 570680 Direct (translation)
A_P_NEUCRA_SCA_CDS_2345	3.47	1	1	375	41.2	6.76	47.28	CDS 1512170 1513363 Reverse (translation)
A_P_NEUCRA_SCA_CDS_349	1.62	1	1	862	94.6	7.06	29.64	CDS 850990 855630 Reverse (translation)
A_P_NEUCRA_SCA_CDS_7122	5.74	1	1	244	26.8	9.22	45.39	CDS 2531054 2531989 Reverse (translation)
A_P_NEUCRA_SCA_CDS_1737	14.71	1	1	102	11.8	10.13	32.94	CDS 740065 740476 Direct (translation)
A_P_NEUCRA_SCA_CDS_3697	7.45	1	1	188	20.8	9.33	33.06	CDS 93925 94563 Reverse (translation)
A_P_NEUCRA_SCA_CDS_2554	4.45	1	1	292	32.9	8.37	64.00	CDS 522452 523429 Direct (translation)
A_P_NEUCRA_SCA_CDS_3591	2.76	1	1	508	56.7	5.33	22.08	CDS 1078032 1080066 Direct (translation)
A_P_NEUCRA_SCA_CDS_411	14.56	1	1	103	10.6	9.09	69.15	CDS 206030 206397 Reverse (translation)
A_P_NEUCRA_SCA_CDS_2706	4.01	1	1	374	39.9	7.62	33.30	CDS 1081521 1082812 Reverse (translation)
A_P_NEUCRA_SCA_CDS_347	1.17	1	1	1363	147.0	6.52	35.54	CDS 844110 849022 Direct (translation)

Accession	Coverage	# PSMs	# Peptides	# AAs	MW [kDa]	calc. pI	Score	Description
A_P_NEUCRA_SCA_CDS_6925	9.77	1	1	174	19.3	5.99	30.89	CDS 1834380 1835131 Reverse (translation)
KEZ42341.1	8.68	1	1	288	28.6	7.37	36.93	CDS 163008 164053 Reverse (translation)
A_P_NEUCRA_SCA_CDS_7148	22.94	1	1	109	11.2	11.66	30.54	CDS 2637746 2638366 Reverse (translation)
A_P_NEUCRA_SCA_CDS_3289	11.50	1	1	200	22.6	10.11	20.30	CDS 203749 204348 Direct (translation)

#= number; PSM= peptide spectrum match; AA= amino acid

II. Annex 2

Table A.8. Raw MS data for mycelial cell wall extracts. Protein sequences with predicted GPI-anchor are shaded in grey.

Accession	Coverage	# PSMs	# Peptides	# AAs	MW [kDa]	calc. pI	Score	Description
A_P_NEUCRA_SCA_CDS_9909	46.91	18	14	307	32.5	9.55	554.91	CDS 1024675 1026580 Direct (translation)
A_P_NEUCRA_SCA_CDS_6775	40.56	12	11	355	37.4	7.02	499.05	CDS 1275054 1276728 Direct (translation)
A_P_NEUCRA_SCA_CDS_4128	53.68	79	10	136	14.7	10.13	1728.14	CDS 598951 599519 Reverse (translation)
A_P_NEUCRA_SCA_CDS_3357	29.55	10	8	308	33.7	9.85	261.72	CDS 179931 181468 Reverse (translation)
A_P_NEUCRA_SCA_CDS_7765	32.49	11	8	317	33.2	10.08	331.67	CDS 1015713 1016914 Reverse (translation)
A_P_NEUCRA_SCA_CDS_3432	43.81	10	7	105	11.4	9.19	281.43	CDS 441669 442608 Reverse (translation)
A_P_NEUCRA_SCA_CDS_5972	31.91	7	7	257	27.9	10.40	256.54	CDS 463869 464893 Direct (translation)
A_P_NEUCRA_SCA_CDS_7862	14.53	8	7	516	55.9	8.92	134.72	CDS 87352 89008 Reverse (translation)
A_P_NEUCRA_SCA_CDS_5869	20.97	7	7	310	34.0	9.51	237.96	CDS 85365 87080 Reverse (translation)
A_P_NEUCRA_SCA_CDS_6593	63.46	9	6	104	11.2	9.13	174.34	CDS 528076 528731 Direct (translation)
KEZ42985.1	13.14	6	5	373	38.5	4.89	114.93	CDS 1076497 1077781 Reverse (translation)
A_P_NEUCRA_SCA_CDS_7341	18.45	9	5	439	47.6	9.07	219.48	CDS 249002 251080 Reverse (translation)
A_P_NEUCRA_SCA_CDS_3196	13.65	5	5	608	67.0	7.64	174.46	CDS 133885 135872 Reverse (translation)
A_P_NEUCRA_SCA_CDS_1688	26.71	6	5	161	18.0	11.37	210.52	CDS 546288 547203 Reverse (translation)
A_P_NEUCRA_SCA_CDS_5046	25.00	5	4	136	15.4	11.15	133.18	CDS 29127 29648 Direct (translation)

Accession	Coverage	# PSMs	# Peptides	# AAs	MW [kDa]	calc. pI	Score	Description
A_P_NEUCRA_SCA_CDS_10806	24.36	5	4	156	17.8	10.77	90.94	CDS 723031 723861 Direct (translation)
A_P_NEUCRA_SCA_CDS_973	7.18	5	4	529	58.6	8.60	129.85	CDS 325614 328603 Reverse (translation)
A_P_NEUCRA_SCA_CDS_9538	10.13	4	4	553	59.5	9.14	149.46	CDS 2192317 2194572 Direct (translation)
A_P_NEUCRA_SCA_CDS_7198	36.89	5	4	103	11.3	11.36	137.40	CDS 2840263 2840773 Direct (translation)
A_P_NEUCRA_SCA_CDS_2275	27.21	6	4	136	15.5	10.83	185.05	CDS 1197945 1198666 Direct (translation)
A_P_NEUCRA_SCA_CDS_6709	7.23	4	4	844	93.3	6.98	92.21	CDS 1023156 1026040 Reverse (translation)
A_P_NEUCRA_SCA_CDS_7250	22.00	6	4	150	16.0	10.54	199.44	CDS 3009246 3009995 Direct (translation)
A_P_NEUCRA_SCA_CDS_9175	29.41	6	4	153	17.6	10.02	187.28	CDS 771674 772565 Direct (translation)
A_P_NEUCRA_SCA_CDS_1031	12.86	4	4	583	63.5	9.13	114.62	CDS 559039 561306 Direct (translation)
KEZ41172.1	9.56	4	4	523	50.9	4.64	85.34	CDS 1101340 1103048 Direct (translation)
A_P_NEUCRA_SCA_CDS_1000	15.79	4	3	152	16.9	8.38	148.97	CDS 433450 434368 Reverse (translation)
A_P_NEUCRA_SCA_CDS_5086	10.95	3	3	338	36.3	6.95	84.14	CDS 164130 165831 Reverse (translation)
A_P_NEUCRA_SCA_CDS_5104	8.19	3	3	586	61.5	5.72	107.98	CDS 230142 232077 Reverse (translation)
A_P_NEUCRA_SCA_CDS_9198	21.85	4	3	151	16.9	10.61	87.99	CDS 891285 892014 Direct (translation)
A_P_NEUCRA_SCA_CDS_9624	28.30	4	3	106	11.8	11.69	158.30	CDS 2535074 2535801 Reverse (translation)
A_P_NEUCRA_SCA_CDS_9776	32.31	4	3	130	14.9	10.70	84.55	CDS 459394 459933 Reverse (translation)
A_P_NEUCRA_SCA_CDS_6345	25.50	3	3	200	23.0	10.29	54.87	CDS 1937786 1938849 Reverse (translation)

Accession	Coverage	# PSMs	# Peptides	# AAs	MW [kDa]	calc. pI	Score	Description
A_P_NEUCRA_SCA_CDS_9938	22.29	4	3	157	17.4	10.29	104.18	CDS 1151322 1152074 Direct (translation)
A_P_NEUCRA_SCA_CDS_2300	15.09	3	3	106	12.0	10.48	62.27	CDS 1318160 1318947 Reverse (translation)
A_P_NEUCRA_SCA_CDS_8155	45.00	3	3	80	9.1	10.11	112.07	CDS 1203536 1204076 Direct (translation)
A_P_NEUCRA_SCA_CDS_6483	11.37	4	3	255	28.6	7.96	56.99	CDS 53328 54936 Direct (translation)
A_P_NEUCRA_SCA_CDS_3358	31.25	4	3	96	10.7	9.99	123.15	CDS 183973 184599 Reverse (translation)
KEZ46909.1	12.38	3	3	202	19.9	4.12	102.12	CDS 972008 972906 Reverse (translation)
A_P_NEUCRA_SCA_CDS_9108	6.38	3	3	549	56.7	5.21	79.34	CDS 463865 465645 Direct (translation)
A_P_NEUCRA_SCA_CDS_10679	33.70	3	3	92	10.5	11.65	93.40	CDS 207679 208336 Reverse (translation)
A_P_NEUCRA_SCA_CDS_9928	12.01	3	3	333	34.6	6.15	118.38	CDS 1119505 1120898 Reverse (translation)
A_P_NEUCRA_SCA_CDS_9756	10.12	4	3	514	55.3	5.50	127.95	CDS 390259 392448 Reverse (translation)
A_P_NEUCRA_SCA_CDS_8038	25.12	4	3	211	21.4	10.59	129.93	CDS 686263 687185 Direct (translation)
8171 (ANA)	10.82	3	3	388	41.1	4.97	88.22	CDS 1254213 1255376 Reverse (translation)
A_P_NEUCRA_SCA_CDS_347	1.98	3	3	1363	147.0	6.52	47.17	CDS 844110 849022 Direct (translation)
A_P_NEUCRA_SCA_CDS_2531	7.06	3	3	439	46.0	4.82	66.52	CDS 434965 436281 Reverse (translation)
A_P_NEUCRA_SCA_CDS_720	16.51	2	2	212	23.6	11.14	48.86	CDS 1438411 1439493 Reverse (translation)
A_P_NEUCRA_SCA_CDS_4129	27.21	2	2	136	14.2	10.71	56.47	CDS 600516 601038 Direct (translation)
A_P_NEUCRA_SCA_CDS_8966	12.77	2	2	141	15.5	10.37	31.76	CDS 248941 249471 Reverse (translation)

Accession	Coverage	# PSMs	# Peptides	# AAs	MW [kDa]	calc. pI	Score	Description
A_P_NEUCRA_SCA_CDS_7189	6.10	2	2	410	44.7	8.28	55.50	CDS 2800829 2802494 Direct (translation)
A_P_NEUCRA_SCA_CDS_8471	9.69	2	2	351	37.7	11.05	134.08	CDS 887110 888540 Direct (translation)
A_P_NEUCRA_SCA_CDS_10746	29.35	2	2	92	10.2	10.99	61.79	CDS 490702 491262 Reverse (translation)
A_P_NEUCRA_SCA_CDS_6225	3.51	2	2	1055	120.1	9.50	49.87	CDS 1447562 1451004 Direct (translation)
A_P_NEUCRA_SCA_CDS_6489	23.29	2	2	146	16.9	9.88	58.80	CDS 67851 68436 Direct (translation)
A_P_NEUCRA_SCA_CDS_2890	9.77	2	2	256	30.2	10.48	72.05	CDS 1743282 1744636 Reverse (translation)
A_P_NEUCRA_SCA_CDS_7793	2.14	2	2	889	98.3	7.01	78.33	CDS 1096982 1100780 Reverse (translation)
A_P_NEUCRA_SCA_CDS_9166	30.10	2	2	103	11.6	9.48	122.78	CDS 729467 729952 Direct (translation)
A_P_NEUCRA_SCA_CDS_10406	39.71	2	2	68	7.2	10.05	87.27	CDS 349762 350115 Direct (translation)
A_P_NEUCRA_SCA_CDS_1265	24.49	3	2	147	15.8	10.13	102.93	CDS 260283 260815 Direct (translation)
KEZ46627.1	26.74	3	2	187	18.7	4.45	125.58	CDS 531513 532142 Direct (translation)
KEZ44163.1	15.61	2	2	173	16.2	4.42	84.22	CDS 215154 215800 Direct (translation)
KEZ44256.1	14.74	2	2	190	19.7	4.41	89.89	CDS 695902 696649 Direct (translation)
KEZ43170.1	30.77	3	2	182	17.7	4.36	138.55	CDS 395583 396264 Reverse (translation)
NA_P_NEUCRA_SCA_CDS_8085	14.84	3	2	155	15.7	9.58	62.46	CDS 867806 868270 Reverse (translation)
KEZ45212.1	19.23	2	2	156	15.6	4.53	41.08	CDS 1611962 1612506 Reverse (translation)
NA_P_NEUCRA_SCA_CDS_1559	17.52	2	2	137	15.4	9.00	44.66	CDS 1376605 1377302 Direct (translation)

Accession	Coverage	# PSMs	# Peptides	# AAs	MW [kDa]	calc. pI	Score	Description
A_P_NEUCRA_SCA_CDS_351	4.33	3	2	508	53.5	4.94	48.01	CDS 863690 865271 Reverse (translation)
A_P_NEUCRA_SCA_CDS_4090	11.59	2	2	207	21.1	11.49	77.41	CDS 460621 461368 Direct (translation)
KEZ46619.1	6.00	2	2	517	56.3	4.88	103.31	CDS 494030 495765 Direct (translation)
A_P_NEUCRA_SCA_CDS_3189	1.42	1	1	914	98.6	5.26	62.41	CDS 95272 98370 Reverse (translation)
A_P_NEUCRA_SCA_CDS_1408	3.25	1	1	277	30.5	9.06	26.63	CDS 844551 845499 Reverse (translation)
A_P_NEUCRA_SCA_CDS_3622	4.93	1	1	142	15.2	10.45	27.20	CDS 1198629 1199577 Reverse (translation)
A_P_NEUCRA_SCA_CDS_1185	4.17	1	1	192	21.5	9.51	55.40	CDS 343939 344986 Reverse (translation)
A_P_NEUCRA_SCA_CDS_3192	2.75	1	1	473	52.0	8.16	27.35	CDS 116556 118313 Reverse (translation)
A_P_NEUCRA_SCA_CDS_7637	6.44	1	1	202	23.0	10.46	31.51	CDS 410256 411590 Reverse (translation)
A_P_NEUCRA_SCA_CDS_7865	13.56	2	1	118	13.4	10.68	41.87	CDS 94397 95212 Direct (translation)
A_P_NEUCRA_SCA_CDS_5900	2.28	1	1	614	66.6	5.50	48.21	CDS 206553 208910 Reverse (translation)
A_P_NEUCRA_SCA_CDS_1887	2.29	1	1	480	52.7	8.38	25.88	CDS 1378282 1379954 Reverse (translation)
A_P_NEUCRA_SCA_CDS_1326	3.56	1	1	225	25.6	10.27	27.41	CDS 496028 497064 Direct (translation)
A_P_NEUCRA_SCA_CDS_9652	11.01	2	1	109	12.1	10.73	25.30	CDS 2685790 2686587 Direct (translation)
A_P_NEUCRA_SCA_CDS_1189	7.14	1	1	196	21.5	5.48	101.21	CDS 353654 354241 Reverse (translation)
A_P_NEUCRA_SCA_CDS_10685	4.74	1	1	190	22.0	10.29	39.33	CDS 227326 228207 Direct (translation)
A_P_NEUCRA_SCA_CDS_9673	9.24	1	1	119	12.9	10.70	40.00	CDS 43430 44381 Reverse (translation)

Accession	Coverage	# PSMs	# Peptides	# AAs	MW [kDa]	calc. pI	Score	Description
A_P_NEUCRA_SCA_CDS_6011	6.32	1	1	174	20.5	10.35	66.49	CDS 639501 640596 Reverse (translation)
A_P_NEUCRA_SCA_CDS_996	4.20	1	1	238	26.8	9.82	36.86	CDS 420676 422469 Reverse (translation)
A_P_NEUCRA_SCA_CDS_1673	2.24	1	1	446	50.8	8.12	30.35	CDS 487745 490088 Reverse (translation)
A_P_NEUCRA_SCA_CDS_2495	11.80	1	1	305	34.3	7.59	29.98	CDS 309886 310999 Direct (translation)
A_P_NEUCRA_SCA_CDS_7864	5.88	1	1	153	17.6	9.73	29.98	CDS 93117 93640 Reverse (translation)
A_P_NEUCRA_SCA_CDS_3337	0.94	1	1	959	99.0	5.90	26.99	CDS 64157 67308 Direct (translation)
A_P_NEUCRA_SCA_CDS_1158	1.45	1	1	483	53.0	7.27	25.76	CDS 234952 236623 Direct (translation)
A_P_NEUCRA_SCA_CDS_9088	6.27	1	1	287	31.5	10.23	108.43	CDS 394712 395755 Reverse (translation)
A_P_NEUCRA_SCA_CDS_9294	4.04	1	1	396	44.7	5.17	36.58	CDS 1264789 1266546 Direct (translation)
A_P_NEUCRA_SCA_CDS_9558	1.73	1	1	577	63.2	9.10	37.50	CDS 2251576 2255495 Reverse (translation)
A_P_NEUCRA_SCA_CDS_5073	11.52	2	1	165	18.8	9.70	67.52	CDS 126434 127128 Reverse (translation)
A_P_NEUCRA_SCA_CDS_6778	5.81	1	1	258	27.7	8.76	46.11	CDS 1283772 1284925 Reverse (translation)
NA_P_NEUCRA_SCA_CDS_8978	12.99	1	1	77	8.4	7.99	29.07	CDS 277450 277770 Reverse (translation)
A_P_NEUCRA_SCA_CDS_9033	5.40	1	1	352	39.8	8.70	33.51	CDS 177625 178847 Reverse (translation)
A_P_NEUCRA_SCA_CDS_4712	9.84	1	1	122	14.0	10.32	24.68	CDS 146610 147201 Reverse (translation)
A_P_NEUCRA_SCA_CDS_2878	1.31	1	1	535	58.8	8.95	25.76	CDS 1709634 1711585 Direct (translation)
A_P_NEUCRA_SCA_CDS_6580	2.09	1	1	670	72.4	6.13	32.59	CDS 459371 461529 Reverse (translation)

Accession	Coverage	# PSMs	# Peptides	# AAs	MW [kDa]	calc. pI	Score	Description
A_P_NEUCRA_SCA_CDS_3343	6.76	1	1	207	23.3	10.73	24.88	CDS 95015 95746 Direct (translation)
A_P_NEUCRA_SCA_CDS_9929	7.95	1	1	151	16.4	10.71	31.62	CDS 1123121 1123923 Reverse (translation)
A_P_NEUCRA_SCA_CDS_8988	1.02	1	1	684	72.3	8.79	27.51	CDS 17277 19328 Direct (translation)
A_P_NEUCRA_SCA_CDS_9287	5.11	1	1	313	33.7	4.96	52.63	CDS 1237017 1238212 Direct (translation)
NA_P_NEUCRA_SCA_CDS_6217	4.88	1	1	328	36.6	10.35	53.67	CDS 1405168 1406151 Direct (translation)
A_P_NEUCRA_SCA_CDS_5784	1.99	1	1	705	78.8	9.82	82.15	CDS 384336 386450 Direct (translation)
A_P_NEUCRA_SCA_CDS_9265	2.14	1	1	653	71.8	6.83	68.31	CDS 1153114 1155451 Direct (translation)
A_P_NEUCRA_SCA_CDS_7247	2.08	1	1	864	97.7	5.19	78.37	CDS 3002645 3005319 Reverse (translation)
A_P_NEUCRA_SCA_CDS_5144	6.77	1	1	251	26.2	10.33	58.98	CDS 396804 398661 Direct (translation)
A_P_NEUCRA_SCA_CDS_3910	5.32	1	1	263	28.4	6.54	24.94	CDS 207748 208694 Direct (translation)
A_P_NEUCRA_SCA_CDS_1767	2.95	1	1	542	61.0	7.94	91.43	CDS 885430 887670 Reverse (translation)
941 (ANA)	7.11	1	1	239	25.3	4.88	56.15	CDS 184022 184738 Reverse (translation)
NA_P_NEUCRA_SCA_CDS_2332	1.79	1	1	614	62.0	4.59	38.46	CDS 1456020 1457861 Reverse (translation)
A_P_NEUCRA_SCA_CDS_6143	13.85	1	1	130	14.8	9.94	127.08	CDS 1121022 1121736 Reverse (translation)
KEZ45428.1	9.28	2	1	237	23.4	4.37	68.47	CDS 225338 226130 Direct (translation)
A_P_NEUCRA_SCA_CDS_9208	10.74	1	1	121	13.3	11.41	21.36	CDS 935189 935788 Reverse (translation)
KEZ43031.1	13.50	1	1	200	18.5	4.09	43.81	CDS 142127 142835 Reverse (translation)

Accession	Coverage	# PSMs	# Peptides	# AAs	MW [kDa]	calc. pI	Score	Description
A_P_NEUCRA_SCA_CDS_3265	1.38	1	1	506	55.4	8.79	25.76	CDS 123037 124730 Direct (translation)
A_P_NEUCRA_SCA_CDS_6701	10.24	1	1	127	13.7	9.98	59.50	CDS 992827 993541 Direct (translation)
KEZ44206.1	5.43	2	1	221	22.0	4.82	68.74	CDS 428360 429175 Reverse (translation)
NA_P_NEUCRA_SCA_CDS_8322	4.32	1	1	278	29.3	4.48	49.86	CDS 379477 380310 Reverse (translation)
A_P_NEUCRA_SCA_CDS_8558	1.48	1	1	948	103.0	5.30	22.09	CDS 1238077 1241585 Direct (translation)
A_P_NEUCRA_SCA_CDS_1727	19.51	1	1	82	8.9	9.26	29.48	CDS 709839 710466 Direct (translation)
A_P_NEUCRA_SCA_CDS_7876	6.90	1	1	116	13.1	9.80	25.57	CDS 130930 131423 Direct (translation)
A_P_NEUCRA_SCA_CDS_5580	5.70	1	1	193	20.8	5.22	22.61	CDS 752980 754655 Direct (translation)
KEZ43142.1	4.25	1	1	353	35.7	4.60	25.64	CDS 262747 263972 Direct (translation)
A_P_NEUCRA_SCA_CDS_8709	9.90	2	1	101	11.3	10.33	39.85	CDS 1741580 1742281 Direct (translation)
A_P_NEUCRA_SCA_CDS_6759	4.42	1	1	226	24.9	9.66	23.98	CDS 1188946 1189912 Reverse (translation)
A_P_NEUCRA_SCA_CDS_2574	2.34	1	1	599	62.9	9.38	79.05	CDS 592656 594669 Direct (translation)
A_P_NEUCRA_SCA_CDS_2345	3.47	1	1	375	41.2	6.76	29.61	CDS 1512170 1513363 Reverse (translation)
A_P_NEUCRA_SCA_CDS_1737	14.71	1	1	102	11.8	10.13	85.46	CDS 740065 740476 Direct (translation)
A_P_NEUCRA_SCA_CDS_1417	6.72	1	1	253	26.6	7.74	77.88	CDS 866084 867005 Direct (translation)
A_P_NEUCRA_SCA_CDS_6925	16.09	2	1	174	19.3	5.99	29.21	CDS 1834380 1835131 Reverse (translation)
KEZ42341.1	8.68	1	1	288	28.6	7.37	60.39	CDS 163008 164053 Reverse (translation)

Accession	Coverage	# PSMs	# Peptides	# AAs	MW [kDa]	calc. pI	Score	Description
A_P_NEUCRA_SCA_CDS_7148	22.94	1	1	109	11.2	11.66	21.02	CDS 2637746 2638366 Reverse (translation)
A_P_NEUCRA_SCA_CDS_7630	0.56	1	1	1063	116.4	4.93	24.14	CDS 392366 395554 Direct (translation)
NA_P_NEUCRA_SCA_CDS_1330	7.87	1	1	127	13.4	9.03	26.08	CDS 516405 517031 Reverse (translation)
A_P_NEUCRA_SCA_CDS_3383	11.11	1	1	72	8.0	10.71	29.19	CDS 283134 283447 Reverse (translation)
A_P_NEUCRA_SCA_CDS_5917	0.36	1	1	2490	276.0	6.95	26.29	CDS 281769 289304 Direct (translation)
A_P_NEUCRA_SCA_CDS_2753	3.23	1	1	434	47.9	9.26	85.51	CDS 1261410 1262893 Direct (translation)
KEZ46098.1	2.74	2	1	475	51.9	5.01	35.44	CDS 339111 340928 Direct (translation)
A_P_NEUCRA_SCA_CDS_685	1.12	1	1	1156	122.6	4.96	65.00	CDS 1324742 1328559 Reverse (translation)
A_P_NEUCRA_SCA_CDS_2675	1.21	1	1	910	106.9	9.88	45.43	CDS 961702 964704 Reverse (translation)
A_P_NEUCRA_SCA_CDS_2516	2.64	1	1	492	53.9	10.45	42.61	CDS 386434 388007 Reverse (translation)
A_P_NEUCRA_SCA_CDS_5438	1.73	1	1	751	81.2	7.43	36.28	CDS 226631 229033 Reverse (translation)
A_P_NEUCRA_SCA_CDS_10547	1.44	1	1	905	104.1	9.91	25.17	CDS 893901 896615 Direct (translation)
3034 (ANA)	2.35	1	1	638	64.5	3.56	42.93	CDS 2371122 2373035 Reverse (translation)
A_P_NEUCRA_SCA_CDS_8867	1.29	1	1	1164	126.2	5.16	35.26	CDS 465465 469189 Reverse (translation)
A_P_NEUCRA_SCA_CDS_9613	2.59	1	1	540	56.6	4.65	75.89	CDS 2475697 2477578 Direct (translation)
6337 (ANA)	3.86	1	1	415	41.8	4.51	76.07	CDS 1907638 1908882 Reverse (translation)
NA_P_NEUCRA_SCA_CDS_1805	16.82	1	1	107	11.5	9.82	36.85	CDS 1043012 1043637 Direct (translation)

Accession	Coverage	# PSMs	# Peptides	# AAs	MW [kDa]	calc. pI	Score	Description
NA_P_NEUCRA_SCA_CDS_8894	3.12	1	1	609	63.5	9.44	39.19	CDS 562329 564275 Direct (translation)
A_P_NEUCRA_SCA_CDS_1717	10.19	1	1	157	17.7	5.07	54.36	CDS 678688 679395 Direct (translation)
A_P_NEUCRA_SCA_CDS_3488	3.56	1	1	533	57.2	5.40	35.93	CDS 661703 663436 Direct (translation)
A_P_NEUCRA_SCA_CDS_5167	8.89	1	1	225	23.8	9.47	30.82	CDS 508995 510046 Reverse (translation)
A_P_NEUCRA_SCA_CDS_10364	6.51	1	1	307	33.8	7.84	35.95	CDS 158303 159939 Direct (translation)

#= number; PSM= peptide spectrum match; AA= amino acid; ANA= Accession number Not Available yet

III. Annex 3

a

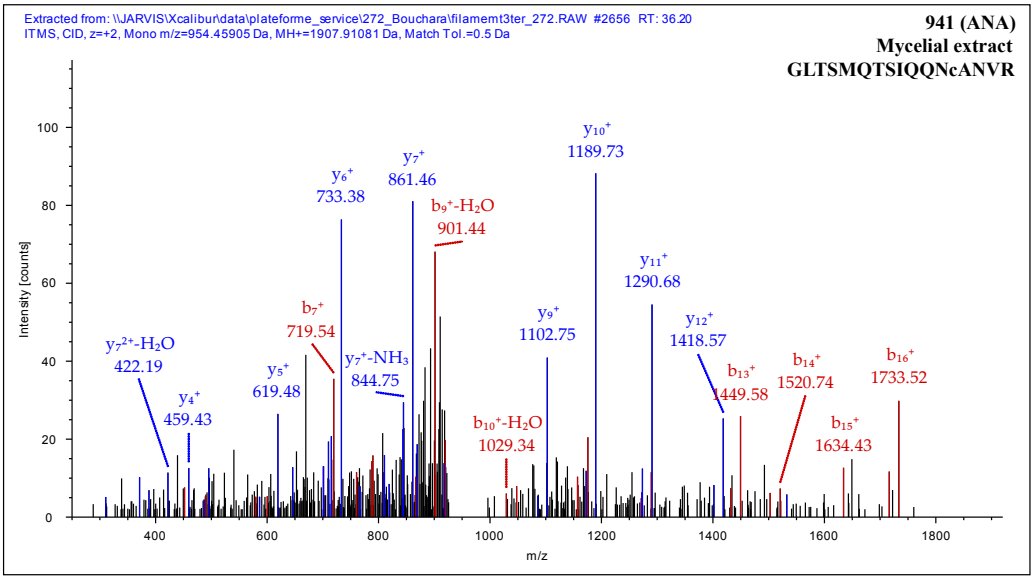

b

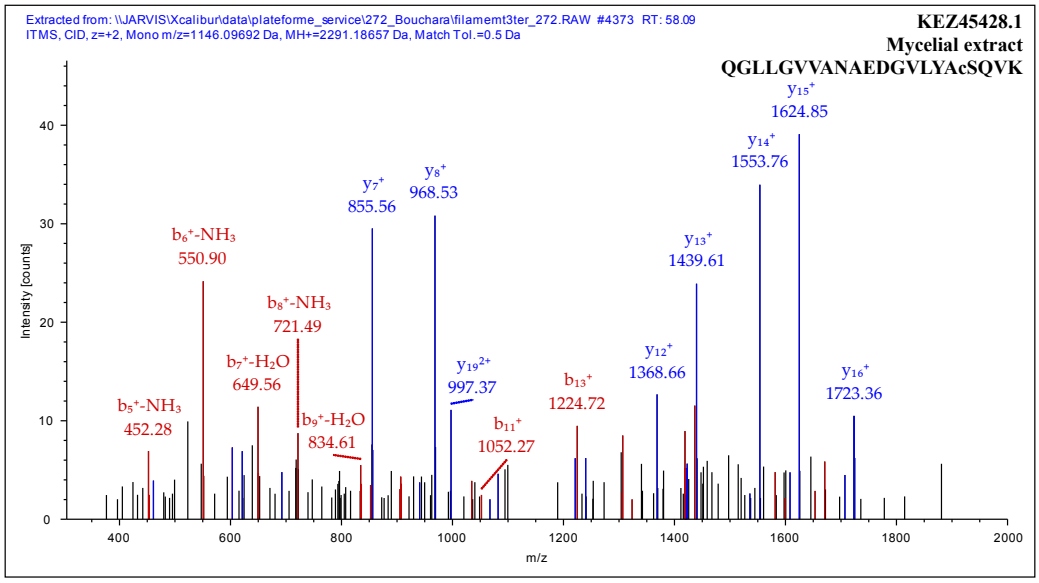

c

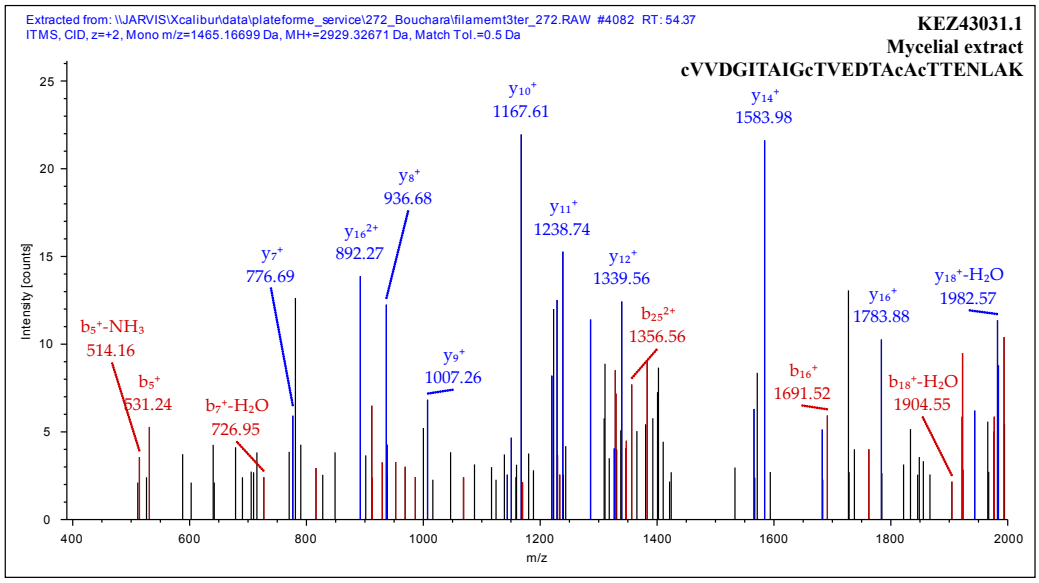
Extracted from: \\JARVIS\Xcalibur\data\plateforme_service\272_Bouchara\filamemt3ter_272.RAW #4082 RT: 54.37
ITMS, CID, z=+2, Mono m/z=1465.16699 Da, MH+=2929.32671 Da, Match Tol.=0.5 Da
KEZ43031.1
Mycelial extract
cVVDGITAIGcTVEDTAcAcTTENLAK
y10+ 1167.61
y14+ 1583.98
y8+ 936.68
y11+ 1238.74
y16 2+ 892.27
y7+ 776.69
y12+ 1339.56
y18+-H2O 1982.57
y16+ 1783.88
b25 2+ 1356.56
b5+-NH3 514.16
y9+ 1007.26
b16+ 1691.52
b5+ 531.24
b18+-H2O 1904.55
b7+-H2O 726.95
Intensity [counts]
m/z

d

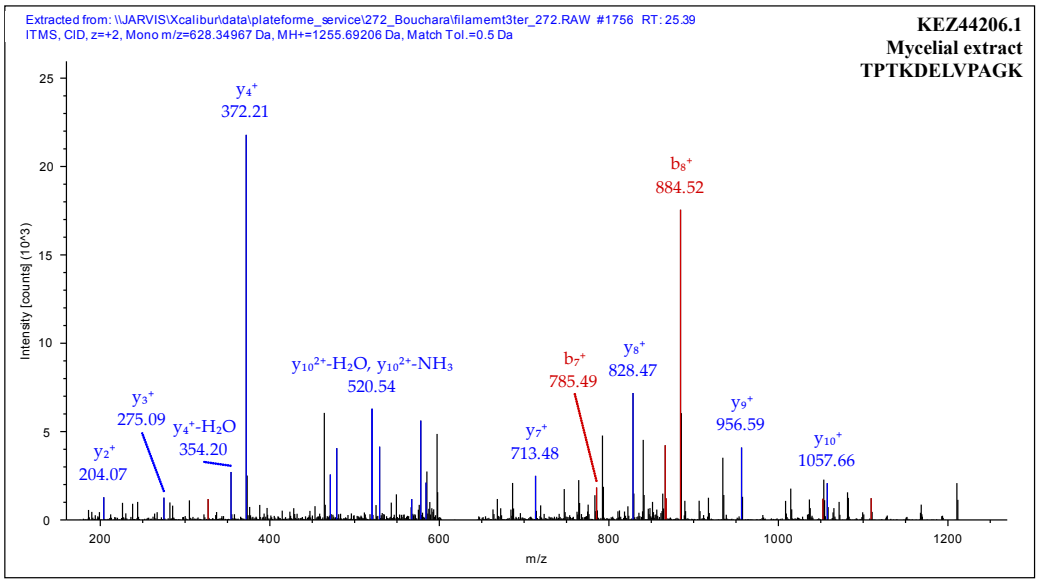
Extracted from: \\JARVIS\Xcalibur\data\plateforme_service\272_Bouchara\filamemt3ter_272.RAW #1756 RT: 25.39
ITMS, CID, z=+2, Mono m/z=628.34967 Da, MH+=1255.69206 Da, Match Tol.=0.5 Da
KEZ44206.1
Mycelial extract
TPTKDELVPAGK
y4+ 372.21
b8+ 884.52
y10 2+-H2O, y10 2+-NH3 520.54
b7+ 785.49
y8+ 828.47
y3+ 275.09
y4+-H2O 354.20
y9+ 956.59
y7+ 713.48
y10+ 1057.66
y2+ 204.07
Intensity [counts] (10^3)
m/z

e

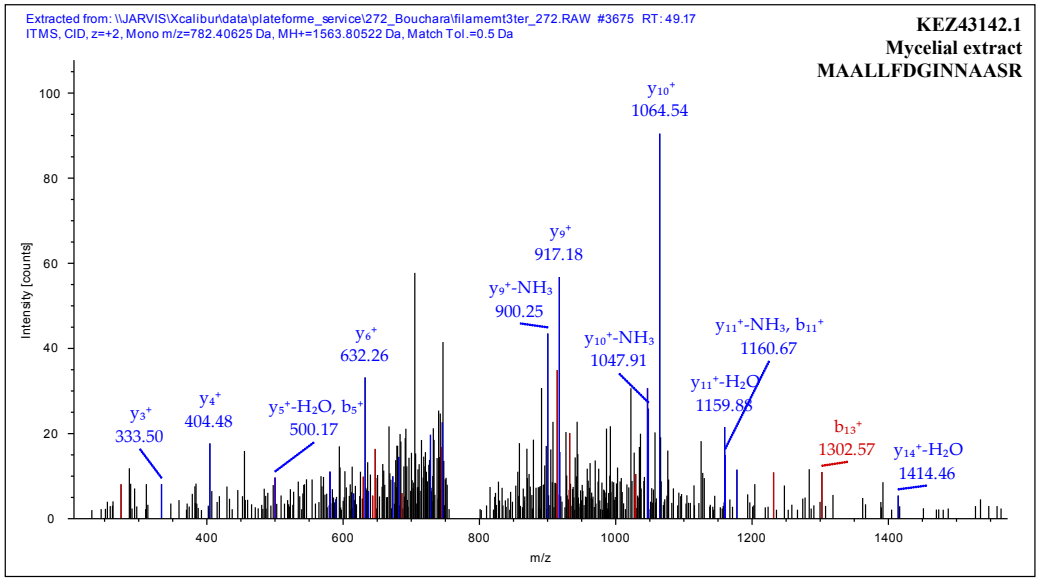
Extracted from: \\JARVIS\Xcalibur\data\plateforme_service\272_Bouchara\filamemt3ter_272.RAW #3675 RT: 49.17
ITMS, CID, z=+2, Mono m/z=782.40625 Da, MH+=1563.80522 Da, Match Tol.=0.5 Da
KEZ43142.1
Mycelial extract
MAALLFDGINNAASR
y10+ 1064.54
y9+ 917.18
y9+-NH3 900.25
y6+ 632.26
y10+-NH3 1047.91
y11+-NH3, b11+ 1160.67
y11+-H2O 1159.88
y3+ 333.50
y4+ 404.48
y5+-H2O, b5+ 500.17
b13+ 1302.57
y14+-H2O 1414.46
Intensity [counts]
m/z

f

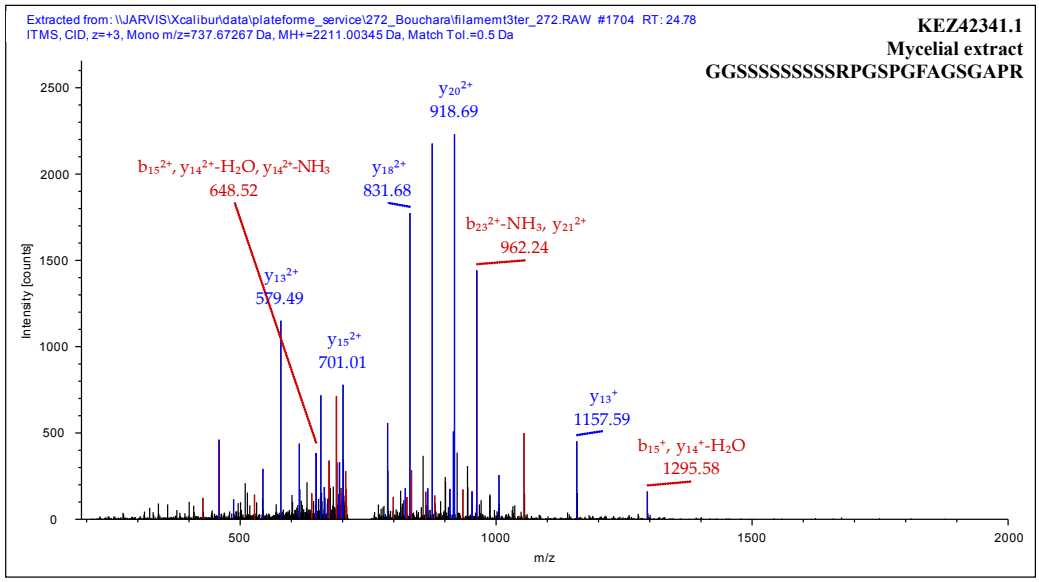
Extracted from: \\JARVIS\Xcalibur\data\plateforme_service\272_Bouchara\filamemt3ter_272.RAW #1704 RT: 24.78
ITMS, CID, z=+3, Mono m/z=737.67267 Da, MH+=2211.00345 Da, Match Tol.=0.5 Da
KEZ42341.1
Mycelial extract
GGSSSSSSSSSRPGSPGFAGSGAPR
y20 2+ 918.69
b15 2+, y14 2+-H2O, y14 2+-NH3 648.52
y18 2+ 831.68
b23 2+-NH3, y21 2+ 962.24
y13 2+ 579.49
y15 2+ 701.01
y13+ 1157.59
b15+, y14+-H2O 1295.58
Intensity [counts]
m/z

g

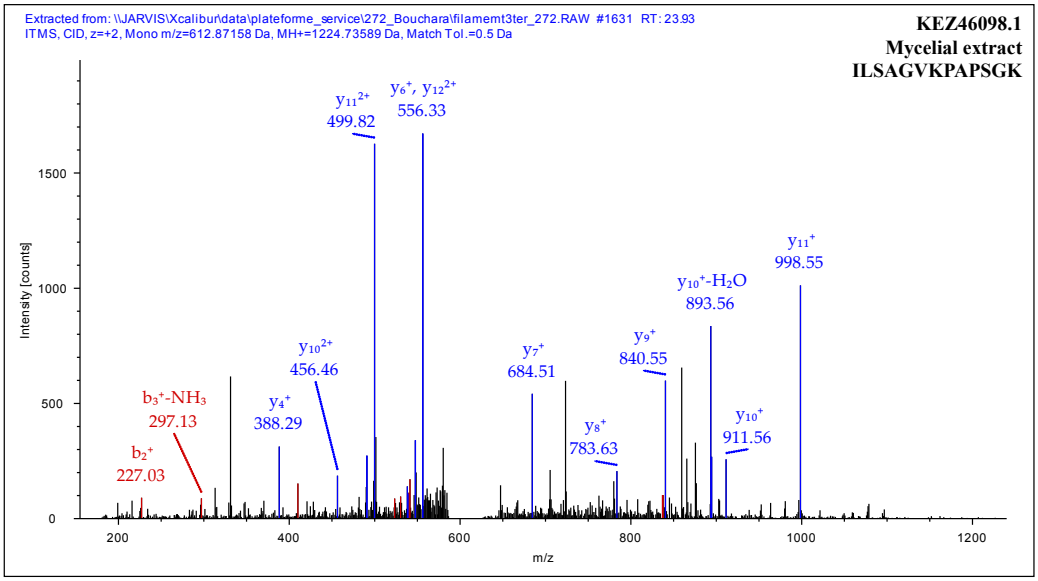
Extracted from: \\JARVIS\Xcalibur\data\plateforme_service\272_Bouchara\filamemt3ter_272.RAW #1631 RT: 23.93
ITMS, CID, z=+2, Mono m/z=612.87158 Da, MH+=1224.73589 Da, Match Tol.=0.5 Da
KEZ46098.1
Mycelial extract
ILSAGVKPAPSGK
Intensity [counts]
m/z
y11 2+ 499.82
y6+, y12 2+ 556.33
y11+ 998.55
y10+-H2O 893.56
y9+ 840.55
y10 2+ 456.46
y7+ 684.51
b3+-NH3 297.13
y4+ 388.29
y8+ 783.63
y10+ 911.56
b2+ 227.03

h

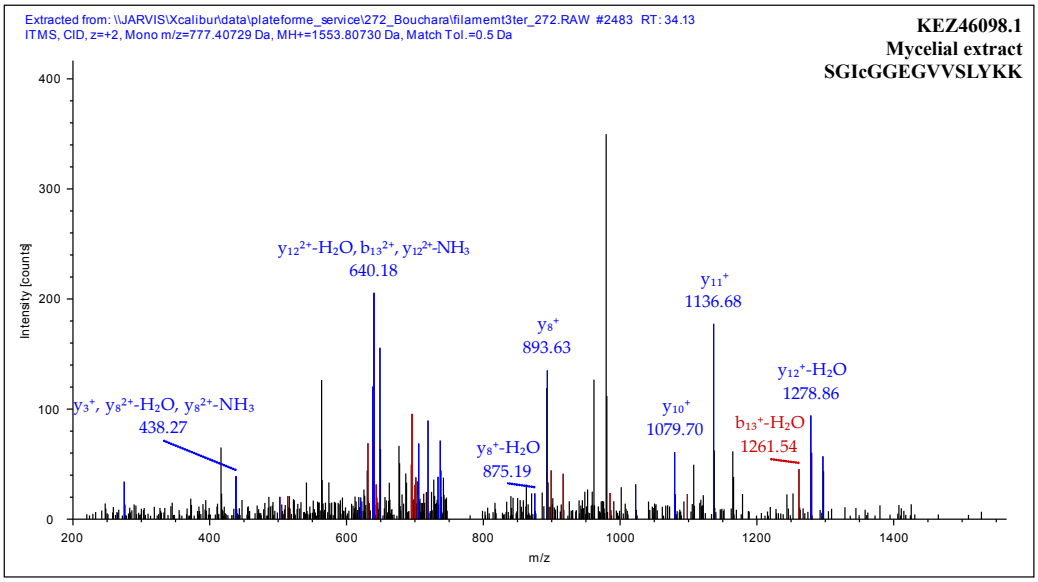
Extracted from: \\JARVIS\Xcalibur\data\plateforme_service\272_Bouchara\filamemt3ter_272.RAW #2483 RT: 34.13
ITMS, CID, z=+2, Mono m/z=777.40729 Da, MH+=1553.80730 Da, Match Tol.=0.5 Da
KEZ46098.1
Mycelial extract
SGIcGGEGVVSLYKK
Intensity [counts]
m/z
y12 2+-H2O, b13 2+, y12 2+-NH3 640.18
y11+ 1136.68
y8+ 893.63
y12+-H2O 1278.86
y3+, y8 2+-H2O, y8 2+-NH3 438.27
y10+ 1079.70
b13+-H2O 1261.54
y8+-H2O 875.19

i

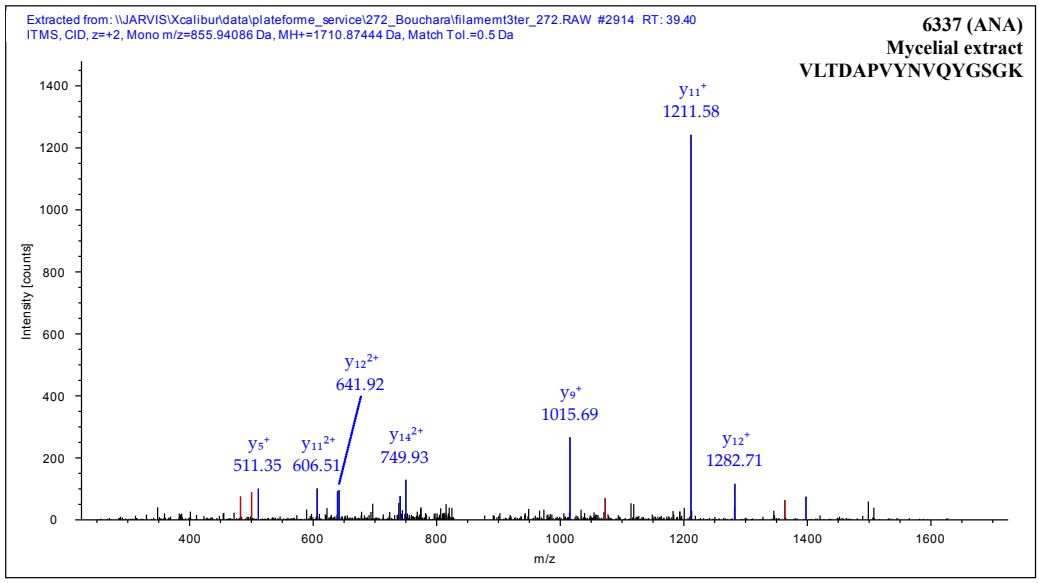
Extracted from: \\JARVIS\Xcalibur\data\plateforme_service\272_Bouchara\filamemt3ter_272.RAW #2914 RT: 39.40
ITMS, CID, z=+2, Mono m/z=855.94086 Da, MH+=1710.87444 Da, Match Tol.=0.5 Da
6337 (ANA)
Mycelial extract
VLTDAPVYNVQYGSGK
y11+ 1211.58
y122+ 641.92
y9+ 1015.69
y142+ 749.93
y5+ 511.35
y112+ 606.51
y12+ 1282.71
Intensity [counts]
m/z

j

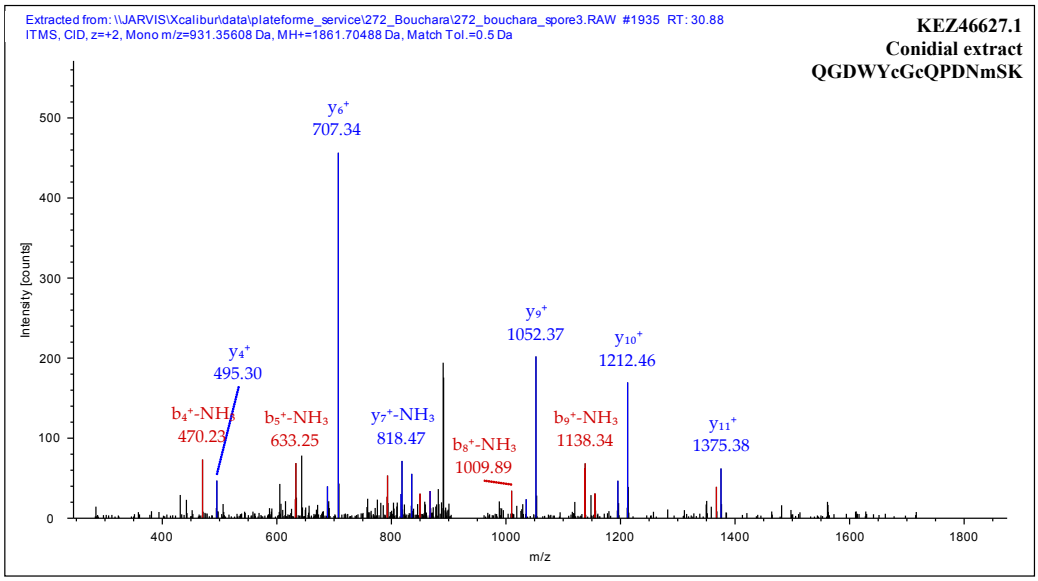
Extracted from: \\JARVIS\Xcalibur\data\plateforme_service\272_Bouchara\272_bouchara_spore3.RAW #1935 RT: 30.88
ITMS, CID, z=+2, Mono m/z=931.35608 Da, MH+=1861.70488 Da, Match Tol.=0.5 Da
KEZ46627.1
Conidial extract
QGDWYcGcQPDNmSK
y6+ 707.34
y9+ 1052.37
y10+ 1212.46
y4+ 495.30
b4+-NH3 470.23
b5+-NH3 633.25
y7+-NH3 818.47
b8+-NH3 1009.89
b9+-NH3 1138.34
y11+ 1375.38
Intensity [counts]
m/z

k

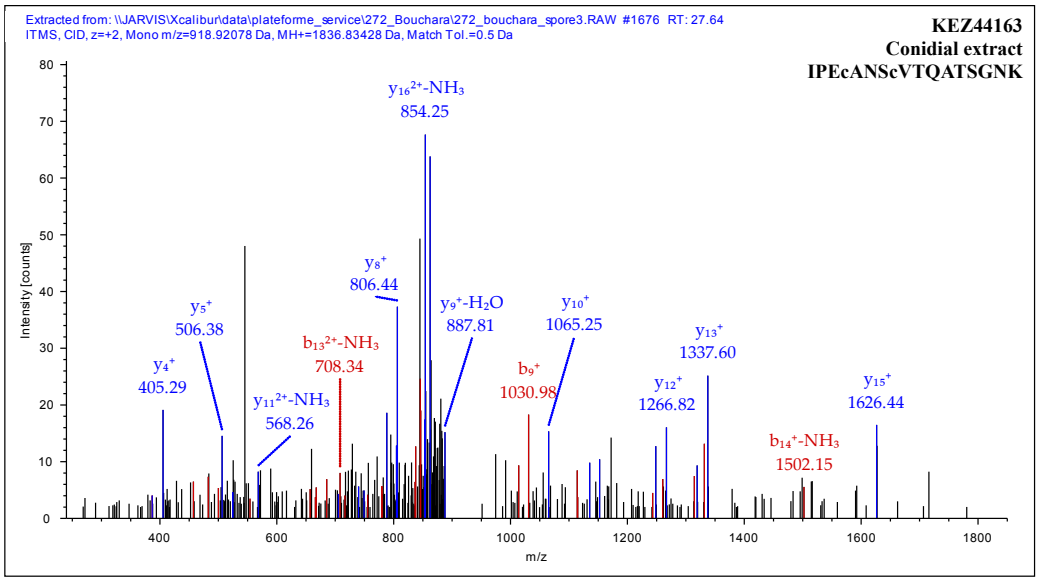
Extracted from: \\JARVIS\Xcalibur\data\plateforme_service\272_Bouchara\272_bouchara_spore3.RAW #1676 RT: 27.64
ITMS, CID, z=+2, Mono m/z=918.92078 Da, MH+=1836.83428 Da, Match Tol.=0.5 Da
KEZ44163
Conidial extract
IPEcANScVTQATSGNK
y16 2+-NH3 854.25
y8+ 806.44
y5+ 506.38
y9+-H2O 887.81
y10+ 1065.25
y13+ 1337.60
b13 2+-NH3 708.34
y4+ 405.29
b9+ 1030.98
y12+ 1266.82
y15+ 1626.44
y11 2+-NH3 568.26
b14+-NH3 1502.15
Intensity [counts]
m/z

l

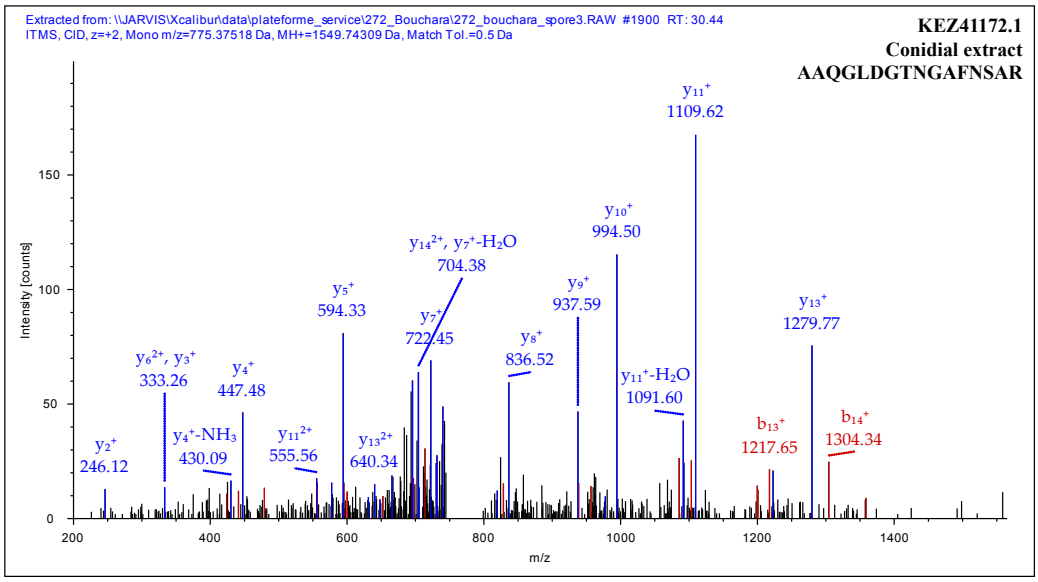
Extracted from: \\JARVIS\Xcalibur\data\plateforme_service\272_Bouchara\272_bouchara_spore3.RAW #1900 RT: 30.44
ITMS, CID, z=+2, Mono m/z=775.37518 Da, MH+=1549.74309 Da, Match Tol.=0.5 Da
KEZ41172.1
Conidial extract
AAQGLDGTNGAFNSAR
y11+ 1109.62
y10+ 994.50
y14 2+, y7+-H2O 704.38
y5+ 594.33
y9+ 937.59
y7+ 722.45
y13+ 1279.77
y8+ 836.52
y6 2+, y3+ 333.26
y4+ 447.48
y11+-H2O 1091.60
b13+ 1217.65
b14+ 1304.34
y4+-NH3 430.09
y11 2+ 555.56
y13 2+ 640.34
y2+ 246.12
Intensity [counts]
m/z

m

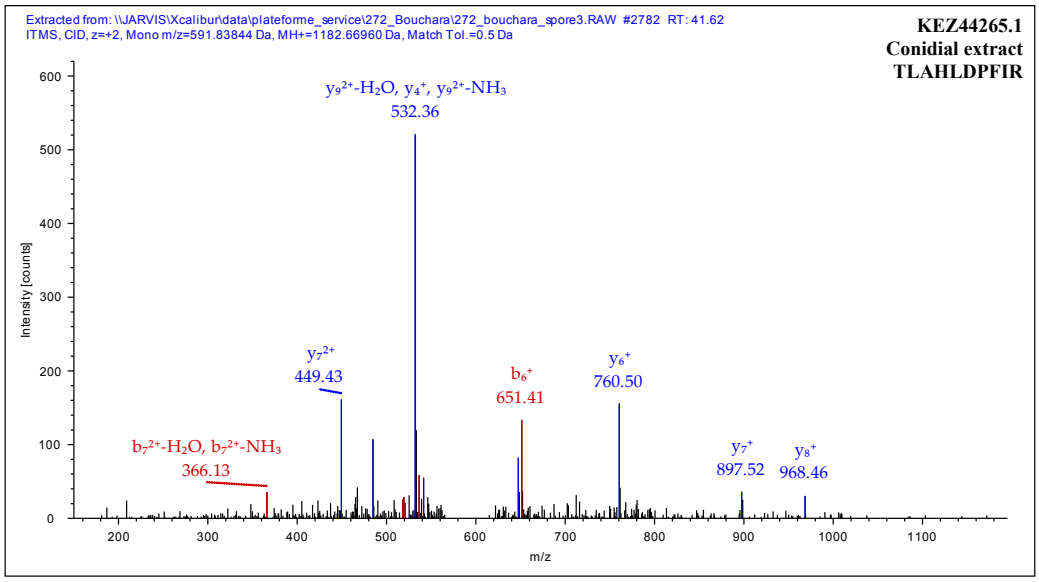
Extracted from: \\JARVIS\Xcalibur\data\plateforme_service\272_Bouchara\272_bouchara_spore3.RAW #2782 RT: 41.62
ITMS, CID, z=+2, Mono m/z=591.83844 Da, MH+=1182.66960 Da, Match Tol.=0.5 Da
KEZ44265.1
Conidial extract
TLAHLDPFIR
y9 2+-H2O, y4+, y9 2+-NH3
532.36
y7 2+
449.43
b6+
651.41
y6+
760.50
b7 2+-H2O, b7 2+-NH3
366.13
y7+
897.52
y8+
968.46
Intensity [counts]
m/z

n

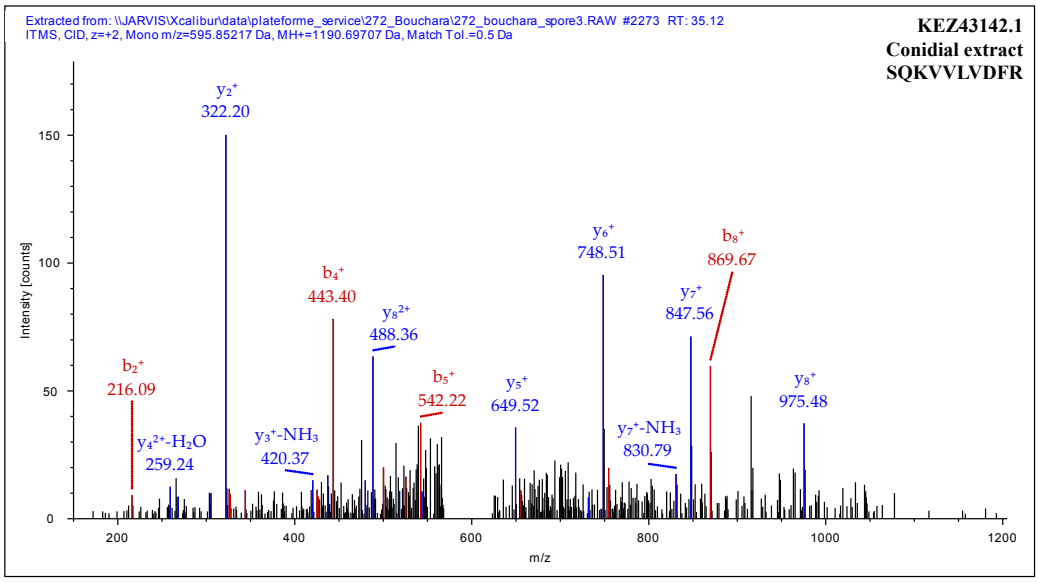
Extracted from: \\JARVIS\Xcalibur\data\plateforme_service\272_Bouchara\272_bouchara_spore3.RAW #2273 RT: 35.12
ITMS, CID, z=+2, Mono m/z=595.85217 Da, MH+=1190.69707 Da, Match Tol.=0.5 Da
KEZ43142.1
Conidial extract
SQKVVLVDFR
y2+
322.20
y6+
748.51
b8+
869.67
b4+
443.40
y7+
847.56
y8 2+
488.36
b2+
216.09
b5+
542.22
y5+
649.52
y8+
975.48
y4 2+-H2O
259.24
y3+-NH3
420.37
y7+-NH3
830.79
Intensity [counts]
m/z

o

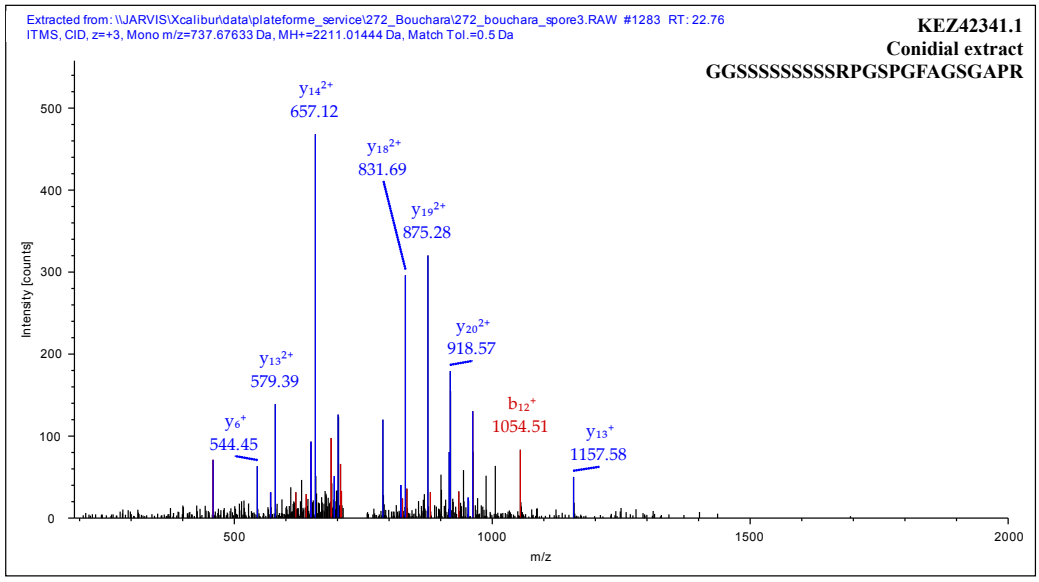

p

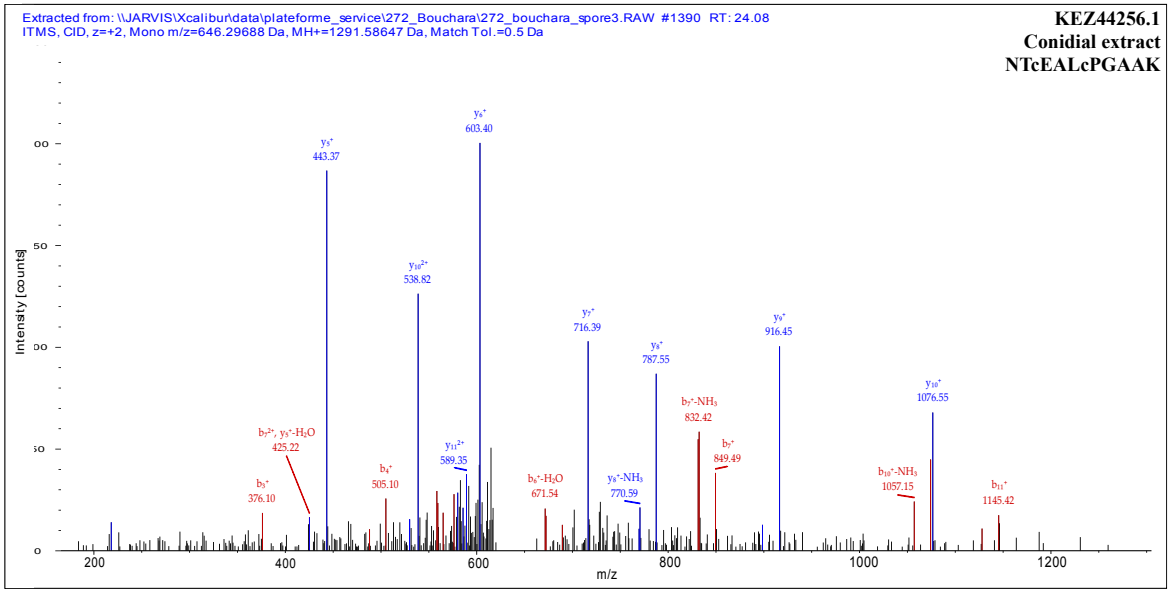

Figure A.30. MS/MS spectra from proteins identified with a single-peptide from mycelial (a - i) and conidial extracts (j - p).

The major fragmentation series (y-carboxy and b-amino) are annotated; the deduced sequence, m/z value and charge state from the precursor ion are indicated. ANA indicates that Accession number is Not yet Available and that the numbers are from the internal laboratory annotation system.

ENGAGEMENT DE NON PLAGIAT

Je, soussignée Sarah Ghamrawi El Ali
déclare être pleinement consciente que le plagiat de documents ou d'une partie d'un document publiée sur toutes formes de support, y compris l'internet, constitue une violation des droits d'auteur ainsi qu'une fraude caractérisée.
En conséquence, je m'engage à citer toutes les sources que j'ai utilisées pour écrire ce rapport ou mémoire.

signé par l'étudiant(e) le **17** / **09** / **2014**

Présidence de l'université
40 rue de rennes – BP 73532
49035 Angers cedex
Tél. 02 41 96 23 23 | Fax 02 41 96

université angers

RÉSUMÉ

Les espèces du complexe *Scedosporium apiospermum* sont des agents pathogènes émergents qui se situent au deuxième rang parmi les champignons filamenteux isolés des voies respiratoires des patients atteints de mucoviscidose. Ils sont omniprésents et particulièrement rencontrés dans les zones polluées. Malgré leur notoriété, nos connaissances sur leur biologie moléculaire et leur physiologie restent limitées.

Chez les champignons, la paroi cellulaire constitue un bouclier protecteur face à des conditions environnementales défavorables ainsi qu'une structure bien contrôler pour la pathogénicité des champignons. Ici, nous avons étudié les changements dynamiques de la paroi des conidies de *S. boydii*, l'une des deux espèces majeures de ce complexe avec *S. apiospermum*, avec pour objectif d'identifier des facteurs de virulence potentiels. En utilisant une large variété de techniques, allant de la microscopie électronique à balayage ou à transmission à l'analyse protéomique des protéines à ancre glycosylphosphatidylinositol (GPI) en passant par la microélectrophorèse et la partition de phase, la cytométrie en flux, la microscopie de force atomique, la résonance paramagnétique électronique, ou encore des techniques moléculaires, nous avons mis en évidence diverses modifications qui se produisent dans la paroi pendant la maturation et la germination des conidies de *S. boydii* et nous avons identifié la DHN-mélanine ainsi qu'un nombre important de protéines à ancre GPI.

Enfin, nous avons fourni la première séquence complète du génome de *S. apiospermum* qui appuierait les différents domaines de la recherche sur ces champignons que ce soit pour l'étude des mécanismes pathogènes ou pour des applications biotechnologiques.

Mots-clés : *Scedosporium boydii*, *S. apiospermum*, champignons filamenteux, paroi, germination, maturation, génome, biotechnologie, protéines à ancre GPI, mélanine, virulence.

ABSTRACT

Species of the *Scedosporium apiospermum* complex are emerging human pathogens that rank the second, after *Aspergillus fumigatus*, among the filamentous fungi colonizing the airways of patients with cystic fibrosis. These fungi are ubiquitous in nature and particularly encountered in polluted areas. Despite their clinical notoriety, our knowledge about their molecular biology and physiology remains rather limited.

In fungi, the cell wall forms a protective shield against adverse environmental conditions as well as a well-regulated structure for fungal pathogenesis, which makes it an interesting target for antifungal drug development. Here, in an attempt to identify potential virulence factors, we investigated the dynamic changes of the cell wall of conidia in *S. boydii*, one of the main pathogenic species within this species complex with *Scedosporium apiospermum*. Using various techniques, ranging from scanning and transmission electron microscopy to proteomic analysis of glycosylphosphatidylinositol (GPI)-anchored proteins, passing through two-phase partitioning and microelectrophoresis, atomic force microscopy and chemical force spectroscopy, flow cytometry, electron paramagnetic resonance and molecular techniques. We highlighted various modifications occurring in the cell wall during maturation and germination of *S. boydii* and we identified DHN-melanin as well as a substantial number of GPI-anchored proteins in the cell wall.

Finally, we provided the first publicly available genome sequence of *S. apiospermum* that would support various research fields on these fungi whether for the understanding of their pathogenic mechanisms or for various biotechnological applications.

Keywords : *Scedosporium boydii*, *S. apiospermum*, filamentous fungi, cell wall, germination, maturation, genome, biotechnology, GPI-anchored proteins, melanin, virulence.

Présidence de l'université
40 rue de rennes – BP 73532
49035 Angers cedex
Tél. 02 41 96 23 23 | Fax 02 41 96

l'université nantes angers le mans
PÔLE DE RECHERCHE ET D'ENSEIGNEMENT SUPÉRIEUR

université angers

Thèse de Doctorat

Sarah GHAMRAWI

Modifications de la paroi au cours de la maturation et de la germination des conidies de *Scedosporium boydii*

A multifaceted study of the cell wall changes during maturation and germination of the conidia in *Scedosporium boydii*

Résumé

Les espèces du complexe *Scedosporium apiospermum* sont des agents pathogènes émergents qui se situent au deuxième rang parmi les champignons filamenteux rencontrés au cours de la mucoviscidose. Ils sont omniprésents et particulièrement rencontrés dans les zones polluées. En dépit de leur importance clinique, nos connaissances sur leur biologie moléculaire et leur physiologie restent limitées.

Chez les champignons, la paroi constitue un bouclier protecteur face à des conditions environnementales défavorables, et joue un rôle essentiel dans la pathogénicité. Ici, nous avons étudié les changements dynamiques de la paroi des conidies de *S. boydii*, l'une des deux espèces majeures de ce complexe avec *S. apiospermum*, avec pour objectif d'identifier des facteurs de virulence potentiels. En utilisant une large variété de techniques, allant de la microscopie électronique à balayage ou à transmission à l'analyse protéomique des protéines à ancre glycosylphosphatidylinositol (GPI) en passant par la microélectrophorèse et la partition de phase, la cytométrie en flux, la microscopie de force atomique, la résonance paramagnétique électronique, ou encore des techniques moléculaires, nous avons mis en évidence diverses modifications qui se produisent dans la paroi pendant la maturation et la germination des conidies de *S. boydii* et nous avons identifié la DHN-mélanine ainsi qu'un nombre important de protéines à ancre GPI.

Enfin, nous avons fourni la première séquence complète du génome de *S. apiospermum* qui appuierait les différents domaines de la recherche sur ces champignons que ce soit pour l'étude des mécanismes pathogènes ou pour des applications biotechnologiques.

Mots clés

Scedosporium boydii, *S. apiospermum*, champignons filamenteux, paroi, germination, maturation, génome, biotechnologie, protéines à ancre GPI, mélanine, virulence.

Abstract

Species of the *Scedosporium apiospermum* complex are emerging human pathogens which rank the second, after *Aspergillus fumigatus,* among the filamentous fungi colonizing the airways of patients with cystic fibrosis. These fungi are ubiquitous in nature and particularly encountered in polluted areas. Despite their clinical relevance, our knowledge about their molecular biology and physiology remains rather limited.

In fungi, the cell wall forms a protective shield against adverse environmental conditions, and therefore plays a key role in pathogenesis, which makes it an interesting target for antifungal drug development. Here, in an attempt to identify potential virulence factors, we investigated the dynamic changes of the cell wall of conidia in *S. boydii,* one of the main pathogenic species within this species complex with *Scedosporium apiospermum*. Using various techniques, ranging from scanning and transmission electron microscopy to proteomic analysis of glycosylphosphatidylinositol (GPI)-anchored proteins, through two-phase partitioning and microelectrophoresis, atomic force microscopy and chemical force spectroscopy, flow cytometry, electron paramagnetic resonance and molecular techniques, we highlighted various modifications occurring in the cell wall during maturation and germination of *S. boydii* and we identified DHN-melanin as well as a substantial number of GPI-anchored proteins in the cell wall.

Finally, we provided the first publicly available genome sequence of *S. apiospermum* that would support various research fields on these fungi whether for understanding their pathogenic mechanisms or for various biotechnological applications.

Key Words

Scedosporium boydii, *S. apiospermum*, filamentous fungi, cell wall, germination, maturation, genome, biotechnology, GPI-anchored proteins, melanin, virulence.